Reference neutron activation library

INTERNATIONAL ATOMIC ENERGY AGENCY **IAEA**

REFERENCE NEUTRON ACTIVATION LIBRARY
IAEA, VIENNA, 2002
IAEA-TECDOC-1285
ISSN 1011–4289

FOREWORD

A major objective of the IAEA nuclear data programme is to promote improvement of the quality of nuclear data used in science and technology and to provide users with high quality and easily available libraries. For many years various national projects around the world have engaged in the compilation and evaluation of neutron activation cross-sections. Generally these evaluation efforts were carried out independently and arrived at different values for the same quantities. Therefore, a user in need of evaluated data has to search through the national libraries for the necessary evaluations and decide which one of those available is the best. While interrogating various libraries is time consuming (and not always possible) the selection of the most suitable data set presents a major challenge. It requires understanding of the evaluation procedures, comparisons against experimental data and results of the systematics and judicious use of various nuclear models. In practice, it can only be done by a professional evaluator.

To facilitate users' access to the high quality activation data, the IAEA established in 1994 a Co-ordinated Research Project (CRP) with the objective of providing a universal, internationally recognized library of neutron activation cross-sections for the reactions which are most important for practical applications. The CRP accomplished this task, producing the Reference Neutron Activation Library (RNAL), containing cross-sections for the 255 neutron induced reactions relevant to a wide range of applications. This report describes the contents of the RNAL library. It also includes graphical comparison of recommended cross-sections against available experimental data.

The RNAL library can be conveniently accessed using the Web interface
(**http://www-nds.iaea.org/ndspub/rnal/www/**):
or via anonymous FTP at:
(**iaeand.iaea.org/**)
in the directory **rnal**. In addition, the library is available cost-free from the IAEA Nuclear Data Section on a CD-ROM upon request.

The IAEA wishes to thank all the participants of the CRP for their contribution to the library development. Particular recognition goes to J. Kopecky and S. Hlavac for the assessment of the library. The IAEA staff member responsible for this report was M. Herman of the Division of Physical and Chemical Sciences.

Contents

INTRODUCTION

Many scientific endeavors require accurate nuclear data. Examples include studies of environmental protection connected with the running of a nuclear installation, the conceptual designs of fusion energy producing devices, astrophysics and the production of medical isotopes. In response to this need, many national and international data libraries have evolved over the years. Initially nuclear data work concentrated on materials relevant to the commercial power industry which is based on the fission of actinides, but recently the topic of activation has become of increasing importance. Activation of materials occurs in fission devices, but is generally overshadowed by the primary fission process. In fusion devices, high energy (14 MeV) neutrons produced in the D-T fusion reaction cause activation of the structure, and (with the exception of the tritium fuel) is the dominant source of activity. Astrophysics requires cross-sections (generally describing neutron capture) for its studies of nucleosynthesis. Many analytical techniques require activation analysis. For example, borehole logging uses the detection of gamma rays from irradiated materials to determine the various components of rocks.

To provide data for these applications, various specialized data libraries have been produced. The most comprehensive of these have been developed for fusion studies, since it has been appreciated that impurities are of the greatest importance in determining the overall activity, and thus data on all elements are required. These libraries contain information on a wide range of reactions: (n,γ), (n,2n), (n,α), (n,p), (n,d), (n,t), (n,^{3}He) and (n,n') over the energy range from 10^{-5} eV to 15 or 20 MeV. It should be noted that the production of various isomeric states have to be treated in detail in these libraries, and that the range of targets must include long-lived radioactive nuclides in addition to stable nuclides. These comprehensive libraries thus contain almost all the reactions of interest to the other applications mentioned above. However, because these fusion activation libraries are so large (more than 10,000 reactions are common), there are cases where specialized libraries contain or require more accurate information. For this reason the IAEA felt that research in these areas could be helped by developing a library of particularly important activation reactions which would be of benefit to a broad range of applications, some of which are mentioned above.

1. Description of the Reference Neutron Activation Library

1.1. Progression of the Co-ordinated Research Project

The initial aims of the Co-ordinated Research Project (CRP) were to provide a universal database of neutron and charged particle activation cross-sections that would satisfy the following requirements:

- be of use to many applications.

- contain data on a set of reactions judged to be of the highest importance.

- cover the energy range up to 20 MeV, with possible extension to higher energies later.

- include cross-section uncertainty estimates if possible.

- tested against experiments.

At the first Research Co-ordination Meeting (RCM) at Debrecen in October 1994, the aims were revised. The main points agreed were:

1. The range of applications that should be covered by the library should contain:

   - Magnetic confinement fusion
   - Inertial confinement fusion
   - Fission reactors
   - Geophysical and borehole logging
   - Dosimetry
   - Astrophysics

2. For the neutron induced library it was agreed to produce a master list of reactions appropriate for all selected applications, and to produce plots of the various evaluated files with the available experimental data. From such plots a choice from the candidate evaluations could be made and a starter file in an agreed format could be produced. A full covariance description of uncertainties is required only for the dosimetry reactions. Any less complete uncertainty data available for other reactions will be included in the starter file.

3. For the charged particle library it was agreed to consider a very restricted set of reactions most commonly used for production of medical radioisotopes.

The second RCM held in Madrid in May 1996 modified some of the aims of the library. It was recognised that a new IAEA CRP on charged particle data was a more appropriate place to consider the development of a charged particle library. Therefore all work on charged particles was transferred to the new CRP. The second meeting concentrated on the questions of changes to the master list of reactions, the choice of candidate for each reaction and the format of the starter file.

Later sections of this report describe assembling of the library and contain a detailed description and plot for each of the reactions. Readers can judge from these the quality of the data contained in the **R**eference **N**eutron **A**ctivation **L**ibrary (RNAL), and appreciate the benefit in having such data available in the concise format used here.

1.2. Selected reactions and their applications

Reactions selected for the RNAL are listed below. For each reaction one or more applications which justify the selection are given. In most cases applications are followed by a more specific description of the reaction usage.

^{1}H(n,γ)^{2}H	Borehole logging
^{10}B(n,α)^{7}Li	Borehole logging
^{12}C(n,2n)^{11}C	Dosimetry - high energies
^{12}C(n,γ)^{13}C	Borehole logging
^{13}C(n,γ)^{14}C	Fission Reactors - decommissioning
^{14}N(n,p)^{14}C	Inertial Fusion - waste, Magnetic Fusion - waste
^{16}O(n,n'α)^{12}C	Borehole logging - interfering
^{16}O(n,p)^{16}N	Borehole logging
^{19}F(n,2n)^{18}F	Dosimetry, Magnetic Fusion - safety/maintenance
^{23}Na(n,2n)^{22}Na	Magnetic Fusion - safety/maintenance, Borehole logging
^{23}Na(n,γ)^{24}Na	Geophysical - detector, Magnetic Fusion - safety/maintenance, Dosimetry
^{24}Mg(n,p)^{24}Na	Geophysical - interfering, Magnetic Fusion - safety/maintenance, Dosimetry
^{26}Mg(n,γ)^{27}Mg	Geophysical - detector, Astrophysics
^{27}Al(n,2n)^{26}Al	Magnetic Fusion - waste, Inertial Fusion - waste
^{27}Al(n,nα)^{23}Na	Magnetic Fusion - safety/maintenance
^{27}Al(n,γ)^{28}Al	Geophysical - detector
^{27}Al(n,p)^{27}Mg	Dosimetry, Magnetic Fusion - safety, Geophysical - interfering
^{27}Al(n,α)^{24}Na	Geophysical - interfering, Magnetic Fusion - safety/maintenance, Inertial Fusion - safety (Na-22 from Si)
^{28}Si(n,p)^{28}Al	Dosimetry - fusion, Borehole logging
^{28}Si(n,d+np)^{27}Al	Magnetic Fusion - waste, Inertial Fusion - safety (Na-22 from Si)
^{29}Si(n,p)^{29}Al	Borehole logging
^{29}Si(n,t)^{27}Al	Magnetic Fusion - tritium from SiC
^{29}Si(n,d+np)^{28}Al	Geophysical -interfering
^{30}Si(n,α)^{27}Mg	Geophysical - interfering
^{30}Si(n,γ)^{31}Si	Inertial Fusion - safety, Magnetic Fusion - safety, Borehole logging, Astrophysics
^{31}P(n,γ)^{32}P	Inertial Fusion - safety, Magnetic Fusion - safety, Astrophysics - s-process
^{31}P(n,p)^{31}Si	Dosimetry
^{31}P(n,α)^{28}Al	Geophysical - interfering
^{32}S(n,p)^{32}P	Dosimetry
^{34}S(n,γ)^{35}S	Astrophysics s-process, origin of
^{34}S(n,p)^{34}P	Borehole logging
^{36}S(n,γ)^{37}S	Borehole logging
^{35}Cl(n,2n)^{34m}Cl	Borehole logging
^{35}Cl(n,γ)^{36}Cl	Fission Reactors - decommissioning
^{37}Cl(n,γ)^{38}Cl	Borehole logging, Astrophysics - s-process (origin of S-36)

^{37}Cl(n,p)^{37}S	Borehole logging - interfering
^{37}Cl(n,α)^{34}P	Borehole logging - interfering
^{36}Ar(n,γ)^{37}Ar	Astrophysics - s-process (origin of S-36)
^{38}Ar(n,γ)^{39}Ar	Astrophysics - s-process (origin of S-36)
^{40}Ar(n,γ)^{41}Ar	Magnetic Fusion - safety/maintenance
^{39}K(n,p)^{39}Ar	Magnetic Fusion - waste
^{41}K(n,γ)^{42}K	Astrophysics - s-process (Ca isotopes)
^{41}K(n,α)^{38}Cl	Borehole logging - interfering
^{40}Ca(n,γ)^{41}Ca	Fission Reactors - decommissioning
^{44}Ca(n,p)^{44}K	Borehole logging
^{45}Ca(n,α)^{42}Ar	Magnetic Fusion - waste
^{48}Ca(n,γ)^{49}Ca	Borehole logging
^{45}Sc(n,γ)^{46}Sc	Dosimetry, Astrophysics - s-process (Ti isotopes)
^{46}Ti(n,2n)^{45}Ti	Dosimetry
^{46}Ti(n,p)^{46}Sc	Dosimetry - PWR, Magnetic Fusion - safety/maintenance, Inertial Fusion - safety
^{47}Ti(n,p)^{47}Sc	Magnetic Fusion - safety/maintenance
^{47}Ti(n,d+np)^{46}Sc	Dosimetry
^{48}Ti(n,p)^{48}Sc	Magnetic Fusion - safety/maintenance
^{48}Ti(n,d+np)^{47}Sc	Dosimetry
^{48}Ti(n,α)^{45}Ca	Magnetic Fusion - waste, Inertial Fusion - waste
^{50}Ti(n,α)^{47}Ca	Magnetic Fusion - safety
^{50}Ti(n,γ)^{51}Ti	Borehole logging Interfering
^{50}V(n,2n)^{49}V	Magnetic Fusion - waste
^{51}V(n,γ)^{52}V	Geophysical - detector, Magnetic Fusion -safety, Astrophysics - s-process (Cr isotopes)
^{51}V(n,p)^{51}Ti	Borehole logging - interfering
^{51}V(n,α)^{48}Sc	Magnetic Fusion - safety/maintenance, Dosimetry
^{50}Cr(n,γ)^{51}Cr	Magnetic Fusion - safety/maintenance, Inertial Fusion - safety, Borehole logging, Astrophysics - s-process (Cr isotopes)
^{52}Cr(n,2n)^{51}Cr	Dosimetry, Magnetic Fusion - safety/maintenance
^{52}Cr(n,p)^{52}V	Geophysical - interfering
^{53}Cr(n,d+np)^{52}V	Geophysical - interfering
^{54}Cr(n,γ^{55})Cr	Astrophysics - s-process (Cr isotopes)
^{54}Cr(n,α)^{51}Ti	Borehole logging - interfering
^{53}Mn(n,γ)^{54}Mn	Geophysical - detector
^{55}Mn(n,2n)^{54}Mn	Magnetic Fusion- safety/maintenance, Fission Reactors - decommissioning, Borehole logging, Dosimetry
^{55}Mn(n,γ)^{56}Mn	Magnetic Fusion - safety/maintenance, Inertial Fusion - safety, Astrophysics - s-process, Borehole logging - interfering, Dosimetry
^{55}Mn(n,α)^{52}V	Geophysical - interfering
^{54}Fe(n,2n)^{53}Fe	Dosimetry - fusion
^{54}Fe(n,γ)^{55}Fe	Fission Reactors - decommissioning
^{54}Fe(n,p)^{54}Mn	Magnetic Fusion - safety/maintenance, Fission Reactors - decommissioning, Dosimetry
^{56}Fe(n,2n)^{55}Fe	Magnetic Fusion - safety, Inertial Fusion - safety, Fission Reactors - decommissioning

4

$^{56}Fe(n,\gamma)^{57}Fe$	Inertial Fusion - safety/maintenance (Co-60 from Fe), Magnetic Fusion - safety/maintenance (Co-60 from Fe)
$^{56}Fe(n,p)^{56}Mn$	Geophysical - interfering, Magnetic Fusion - safety/maintenance, Dosimetry
$^{57}Fe(n,\gamma)^{58}Fe$	Inertial Fusion - safety/maintenance (Co-60 from Fe), Magnetic Fusion - safety/maintenance (Co-60 from Fe)
$^{58}Fe(n,\gamma)^{59}Fe$	Inertial Fusion - safety/maintenance (Co-60 from Fe), Magnetic Fusion - safety/maintenance (Co-60 from Fe), Astrophysics - s-process (anomalies), Dosimetry
$^{60}Fe(n,\gamma)^{61}Fe$	Astrophysics - s-process (anomalies)
$^{59}Co(n,2n)^{58}Co$	Dosimetry
$^{59}Co(n,\gamma)^{60}Co$	Magnetic Fusion - safety/maintenance, Inertial Fusion - safety/maintenance, Astrophysics - s-process, Fission Reactors - decommissioning, Dosimetry
$^{59}Co(n,\alpha)^{56}Mn$	Geophysical - interfering, Dosimetry
$^{60}Co(n,\gamma)^{61}Co$	Magnetic Fusion - waste (Ni-63 from Co), Inertial Fusion - waste (Ni-63 from Co)
$^{60}Co(n,p)^{60}Fe$	Inertial Fusion - waste, Magnetic Fusion - waste
$^{58}Ni(n,2n)^{57}Ni$	Dosimetry
$^{58}Ni(n,\gamma)^{59}Ni$	Magnetic Fusion - waste, Inertial Fusion - waste, Fission Reactors - decommissioning
$^{58}Ni(n,p)^{58}Co$	Dosimetry, Magnetic Fusion - safety/maintenance, Fission Reactors - decommissioning
$^{58}Ni(n,d+np)^{57}Co$	Magnetic Fusion - safety/maintenance, Fission Reactors - decommissioning
$^{60}Ni(n,2n)^{59}Ni$	Magnetic Fusion - waste
$^{60}Ni(n,p)^{60}Co$	Magnetic Fusion - safety/maintenance, Inertial Fusion - safety/maintenance, Fission Reactors - decommissioning, Dosimetry
$^{61}Ni(n,\gamma)^{62}Ni$	Magnetic Fusion - waste (Ni-63 from Ni & Co), Inertial Fusion - waste (Ni-63 from Co)
$^{62}Ni(n,\gamma)^{63}Ni$	Magnetic Fusion - waste, Inertial Fusion - waste, Fission Reactors - decommissioning
$^{64}Ni(n,2n)^{63}Ni$	Magnetic Fusion - waste
$^{64}Ni(n,\gamma)^{65}Ni$	Astrophysics - s-process
$^{63}Cu(n,2n)^{62}Cu$	Dosimetry
$^{63}Cu(n,\gamma)^{64}Cu$	Magnetic Fusion - safety, Astrophysics - s-process (branching to Zn-64), Dosimetry
$^{63}Cu(n,p)^{63}Ni$	Magnetic Fusion - waste
$^{63}Cu(n,\alpha)^{60}Co$	Magnetic Fusion - safety/maintenance, Inertial Fusion - safety/maintenance, Dosimetry
$^{65}Cu(n,2n)^{64}Cu$	Magnetic Fusion - safety, Dosimetry
$^{65}Cu(n,\gamma)^{66}Cu$	Geophysical - detector, Magnetic Fusion - safety, Astrophysics - s-process (branching)
$^{64}Zn(n,\gamma)^{65}Zn$	Fission Reactors - decommissioning, Astrophysics - s-process (branching to Zn-64)
$^{64}Zn(n,p)^{64}Cu$	Dosimetry

Reaction	Application
^{66}Zn(n,p)^{66}Cu	Geophysical - interfering
^{68}Zn(n,γ)^{69}Zn	Astrophysics - s-process
^{70}Zn(n,γ)^{71}Zn	Astrophysics - s-process
^{69}Ga(n,γ)^{70}Ga	Astrophysics - s-process
^{69}Ga(n,α)^{66}Cu	Geophysical - interfering
^{71}Ga(n,γ)^{71}Ga	Astrophysics
^{74}Se(n,γ)^{75}Se	Astrophysics - p-process
^{78}Se(n,γ)^{79}Se	Inertial Fusion - waste
^{79}Se(n,γ)^{80}Se	Fission Reactors
^{80}Se(n,γ)^{81}Se	Astrophysics - s-process (branching)
^{82}Se(n,γ)^{83}Se	Astrophysics - s-process (branching)
^{80}Kr(n,γ)^{81}Kr	Astrophysics
^{84}Kr(n,γ)^{85}Kr	Astrophysics
^{86}Kr(n,γ)^{87}Kr	Astrophysics
^{85}Rb(n,γ)^{85}Rb	Astrophysics
^{84}Sr(n,γ)^{85}Sr	Astrophysics - p-process
^{89}Sr(n,γ)^{90}Sr	Fission Reactors - decommissioning
^{90}Sr(n,γ)^{91}Sr	Fission Reactors
^{90}Zr(n,2n)^{89}Zr	Magnetic Fusion -safety/maintenance, Dosimetry
^{93}Zr(n,γ)^{94}Zr	Fission Reactors
^{94}Zr(n,γ)^{95}Zr	Magnetic Fusion - safety/maintenance
^{96}Zr(n,2n)^{95}Zr	Magnetic Fusion - safety/maintenance
^{93}Nb(n,n')^{93m}Nb	Dosimetry - fission reactors, Magnetic Fusion - safety/maintenance, Fission Reactors - decommissioning
^{93}Nb(n,2n)^{92}Nb	Magnetic Fusion - waste
^{93}Nb(n,γ)^{94}Nb	Magnetic Fusion - waste, Inertial Fusion - waste, Fission Reactors - decommissioning
^{92}Mo(n,γ)^{93}Mo	Magnetic Fusion - waste
^{92}Mo(n,p)^{92}Nb	Magnetic Fusion - waste
^{92}Mo(n,d+np)^{91}Nb	Magnetic Fusion - waste, Inertial Fusion - waste
^{93}Mo(n,d+np)^{92}Nb	Magnetic Fusion - waste
^{94}Mo(n,2n)^{93}Mo	Magnetic Fusion - waste
^{94}Mo(n,p)^{94}Nb	Magnetic Fusion - waste, Inertial Fusion - waste
^{94}Mo(n,d+np)^{93m}Nb	Magnetic Fusion - safety/maintenance, Inertial Fusion - safety/maintenance
^{95}Mo(n,p)^{95}Nb	Magnetic Fusion - safety/maintenance
^{95}Mo(n,d+np)^{94}Nb	Magnetic Fusion - waste, Inertial Fusion - waste
^{98}Mo(n,γ)^{99}Mo	Magnetic Fusion - safety/waste (Tc-99 from Mo), Inertial Fusion - safety/waste (Tc-99 from Mo), Astrophysics, Fission Reactors - decommissioning (Tc-99 from Mo)
^{100}Mo(n,2n)^{99}Mo	Magnetic Fusion - safety/waste (Tc-99 from Mo)
^{100}Mo(n,γ)^{101}Mo	Astrophysics - cross-section systematics in Mo
^{99}Tc(n,2n)^{98}Tc	Magnetic Fusion - waste
^{96}Ru(n,γ)^{97}Ru	Astrophysics - p-process
^{102}Ru(n,γ)^{103}Ru	Astrophysics
^{104}Ru(n,γ)^{105}Ru	Astrophysics
^{103}Rh(n,n')^{103m}Rh	Dosimetry

^{103}Rh(n,γ)^{104}Rh	Astrophysics - comparison with differential data
^{102}Pd(n,γ)^{103}Pd	Astrophysics - p-process
^{108}Pd(n,γ)^{109}Pd	Astrophysics - s-process (Pd isotopes)
^{110}Pd(n,γ)^{111}Pd	Astrophysics - s-process (Pd isotopes)
^{107}Ag(n,γ)^{108m}Ag	Magnetic Fusion - waste, Inertial Fusion - waste, Fission Reactors - decommissioning
^{108m}Ag(n,γ)^{109}Ag	Magnetic Fusion - waste, Inertial Fusion - waste
^{109}Ag(n,2n)^{108m}Ag	Magnetic Fusion - waste, Fission Reactors - decommissioning, Inertial Fusion - waste
^{109}Ag(n,γ)^{110m}Ag	Fission Reactors - decommissioning, Dosimetry
^{106}Cd(n,γ)^{107}Cd	Astrophysics - p-process
^{108}Cd(n,γ)^{109}Cd	Astrophysics - p-process
^{114}Cd(n,γ)^{115}Cd	Astrophysics
^{113}In(n,γ)^{114}In	Astrophysics - s-process branchings at A=113, 115
^{115}In(n,n')^{115m}In	Dosimetry - D-D diagnostics, Inertial Fusion
^{115}In(n,γ)^{116m}In	Dosimetry, Astrophysics - s-process branchings at A=113, 115
^{120}Sn(n,γ)^{121m}Sn	Magnetic Fusion - waste
^{121}Sn(n,γ)^{122}Sn	Astrophysics
^{122}Sn(n,2n)^{121m}Sn	Magnetic Fusion - waste
^{125}Sn(n,γ)^{126}Sn	Magnetic Fusion - waste
^{126}Sn(n,γ)^{127}Sn	Fission Reactors
^{123}Sb(n,γ)^{124}Sb	Astrophysics, Fission Reactors - decommissioning (production of Sb-125)
^{124}Sb(n,γ)^{125}Sb	Fission Reactors - decommissioning
^{120}Te(n,γ)^{121}Te	Astrophysics - p-process
^{128}Te(n,γ)^{129}Te	Astrophysics
^{130}Te(n,γ)^{131}Te	Astrophysics
^{127}I(n,2n)^{126}I	Dosimetry
^{127}I(n,γ)^{128}I	Astrophysics
^{128}I(n,γ)^{129}I	Fission Reactors - decommissioning
^{134}Xe(n,γ)^{135}Xe	Astrophysics
^{136}Xe(n,γ)^{137}Xe	Astrophysics
^{133}Cs(n,γ)^{134}Cs	Astrophysics, Fission Reactors - decommissioning
^{135}Cs(n,γ)^{136}Cs	Fission Reactors
^{136}Cs(n,γ)^{137}Cs	Fission Reactors Decommissioning
^{137}Cs(n,γ)^{138}Cs	Fission Reactors
^{130}Ba(n,γ)^{131}Ba	Astrophysics
^{132}Ba(n,γ)^{133}Ba	Fission Reactors -decommissioning, Astrophysics - p-process
^{137}Ba(n,p)^{137}Cs	Magnetic Fusion - waste
^{138}Ba(n,α)^{135}Xe	Magnetic Fusion - waste (Cs-135 from Ba), Astrophysics
^{138}La(n,γ)^{139}La	Astrophysics - s-process
^{139}La(n,γ)^{140}La	Astrophysics, Dosimetry
^{143}Ce(n,γ)^{144}Ce	Fission Reactors - decommissioning
^{146}Nd(n,γ)^{147}Nd	Astrophysics
^{148}Nd(n,γ)^{149}Nd	Astrophysics
^{150}Nd(n,γ)^{151}Nd	Astrophysics
^{144}Sm(n,γ)^{145}Sm	Astrophysics - p-process

^{152}Sm(n,γ)^{153}Sm	Astrophysics
^{154}Sm(n,γ)^{155}Sm	Astrophysics
^{151}Eu(n,2n)^{150}Eu	Magnetic Fusion - waste
^{151}Eu(n,γ)^{152}Eu	Astrophysics, Fission Reactors - decommissioning
^{153}Eu(n,2n)^{152}Eu	Magnetic Fusion - waste
^{153}Eu(n,γ)^{154}Eu	Fission Reactors - decommissioning
^{154}Eu(n,γ)^{155}Eu	Fission Reactors - decommissioning
^{159}Tb(n,2n)^{158}Tb	Magnetic Fusion - waste
^{159}Tb(n,γ)^{160}Tb	Astrophysics - s-process (lanthanides)
^{158}Dy(n,γ)^{159}Dy	Astrophysics - p-process
^{158}Dy(n,p)^{158}Tb	Magnetic Fusion - waste
^{164}Dy(n,γ)^{165}Dy	Astrophysics - s-process (lanthanides)
^{165}Ho(n,γ)^{166}Ho	Astrophysics, Magnetic Fusion - waste
^{162}Er(n,γ)^{163}Er	Astrophysics
^{164}Er(n,γ)^{165}Er	Astrophysics
^{168}Er(n,γ)^{169}Er	Astrophysics s-process (lanthanides)
^{170}Er(n,γ)^{171}Er	Astrophysics
^{169}Tm(n,γ)^{170}Tm	Astrophysics - s-process (lanthanides)
^{168}Yb(n,γ)^{169}Yb	Astrophysics - p-process
^{174}Yb(n,γ)^{175}Yb	Astrophysics - s-process (lanthanides)
^{176}Yb(n,γ)^{177}Yb	Astrophysics
^{175}Lu(n,γ)^{176}Lu	Astrophysics
^{176}Lu(n,γ)^{177}Lu	Astrophysics
^{174}Hf(n,γ)^{175}Hf	Astrophysics - p-process
^{179}Hf(n,2n)^{178n}Hf	Magnetic Fusion - waste
^{181}Ta(n,3n)^{179}Ta	Magnetic Fusion -safety (Hf-178^{n} from Ta)
^{181}Ta(n,γ)^{182}Ta	Magnetic Fusion - safety
^{182}W(n,2n)^{181}W	Magnetic Fusion - safety/maintenance
^{182}W(n,nα)^{178n}Hf	Magnetic Fusion - waste
^{183}W(n,γ)^{184}W	Inertial Fusion - waste (Re-186m from W), Magnetic Fusion - waste (Re-186m from W)
^{184}W(n,γ)^{185}W	Magnetic Fusion - safety, Inertial Fusion - waste, Astrophysics - s-process
^{186}W(n,2n)^{185}W	Magnetic Fusion - safety
^{186}W(n,nα)^{182}Hf	Magnetic Fusion - waste
^{186}W(n,γ)^{187}W	Geophysical - detector, Magnetic Fusion - safety, Inertial Fusion - safety, Dosimetry
^{185}Re(n,2n)^{184}Re	Magnetic Fusion - maintenance
^{185}Re(n,γ)^{186m}Re	Magnetic Fusion - waste, Inertial Fusion - waste
^{187}Re(n,2n)^{186m}Re	Magnetic Fusion - waste
^{187}Re(n,γ)^{188}Re	Inertial Fusion -safety, Magnetic Fusion - safety
^{187}Re(n,p)^{187}W	Geophysical - interfering, Magnetic Fusion - maintenance
^{184}Os(n,γ)^{185}Os	Astrophysics - p-process
^{188}Os(n,γ)^{189}Os	Inertial Fusion - waste, Magnetic Fusion - waste
^{190}Os(n,γ)^{191}Os	Inertial Fusion - safety, Magnetic Fusion - safety, Astrophysics - s-process (branchings at A=191, 192)
^{190}Os(n,α)^{187}W	Geophysical - interfering

^{192}Os(n,γ)^{193}Os	Astrophysics - s-process (branchings at A=191, 192)
^{191}Ir(n,γ)^{192n}Ir	Inertial Fusion - waste, Magnetic Fusion - waste
^{192}Ir(n,n')^{192n}Ir	Inertial Fusion - waste, Magnetic Fusion - waste
^{192n}Ir(n,γ)^{193}Ir	Inertial Fusion - waste
^{193}Ir(n,2n)^{192n}Ir	Magnetic Fusion - waste, Inertial Fusion - waste
^{190}Pt(n,γ)^{191}Pt	Astrophysics - p-process
^{192}Pt(n,γ)^{193}Pt	Inertial Fusion - waste, Magnetic Fusion - waste, Astrophysics - s-process (branchings)
^{194}Pt(n,γ)^{195}Pt	Astrophysics
^{196}Pt(n,γ)^{197}Pt	Astrophysics
^{198}Pt(n,γ)^{198}Pt	Astrophysics
^{197}Au(n,2n)^{196}Au	Dosimetry
^{197}Au(n,γ)^{198}Au	Astrophysics, Borehole logging, Dosimetry
^{196}Hg(n,γ)^{197}Hg	Astrophysics - p-process
^{202}Hg(n,γ)^{203}Hg	Astrophysics - s-process (branchings at A=203, 204)
^{204}Hg(n,γ)^{205}Hg	Astrophysics - s-process (branchings at A=203, 204)
^{203}Tl(n,γ)^{204}Tl	Astrophysics - s-process (branchings at A=203, 204)
^{205}Tl(n,γ)^{206}Tl	Astrophysics - s-process (branchings at A=203, 204)
^{204}Pb(n,2n)^{203}Pb	Magnetic Fusion - safety/maintenance
^{206}Pb(n,2n)^{205}Pb	Magnetic Fusion - waste
^{206}Pb(n,α)^{203}Hg	Magnetic Fusion - safety/maintenance
^{208}Pb(n,γ)^{209}Pb	Magnetic Fusion - safety
^{209}Bi(n,2n)^{208}Bi	Magnetic Fusion - waste, Inertial Fusion - waste
^{209}Bi(n,γ)^{210m}Bi	Magnetic Fusion - waste, Inertial Fusion -waste

1.3. Development of the library

This section describes how the data for the RNAL library have been selected. As potential data candidates the following activation libraries have been considered: EAF-4.1, FENDL/A-1, FENDL/A-2.0, JENDL-Act96 and ADL-3. Among these libraries, only two libraries (JENDL-Act96 [1] and ADL-3 [2]) are exclusively based on their original evaluations. The EAF-4.1 library [3] is a combination of adopted data from other libraries with the original evaluations (primarily of the (n,γ) reactions). Both FENDL activation libraries are based purely on data adopted from other libraries. FENDL/A-1 is a combination of EAF-3, as a basic data library, with about 250 important reactions adopted from other sources (for details see Ref. [4]). FENDL/A-2.0 [5], the follow-up of FENDL/A-1, used EAF-4.1 as the basic library together with 398 reactions important for fusion applications.

A special procedure for the selection of the best available data for these reactions in FENDL has been applied. An international panel of 8 members used graphical intercomparisons of all recently available evaluations for these reactions against the EXFOR experimental data base (for details see Ref. [5]) to choose the best evaluation. The selected data represent the state of the art evaluations for these reactions and therefore these selections have also been almost in all cases adopted in the RNAL library

ADL-3 EAF Eval. ENDF/B-VI IRDF-90.2 JENDL-3.1/3.2 JENDL-Act96 FENDL/A-1	EAF-4.1	
	CRP EAF-99 EFF-2.4 FEI-98 FENDL/A-1 IPPE IRK JEF-2.2 JENDL-FF LANL LANL-96 RNAL original RRDF-98	RNAL LIBRARY

FIG. 1. The chronological development of the RNAL library

The data selection for the RNAL library has been done in parallel with the FENDL/A-2.0 assembling taking advantage of the FENDL important reaction choices. However, in some cases, some new (and better) data have been adopted within this CRP. In two cases original RNAL evaluations were developed. The flow of the selection steps of the RNAL library is shown in Fig.1.

The master list of the RNAL reference reactions with their data sources is given in Table 1. The column 'Reaction' defines the reaction. All selected (n,d) reactions are activation reactions and they represent the sum of (n,d) and (n,np) reaction channels. For all reactions, the initial state (IS) is the ground state, except reactions Ag-108(n,γ) and Ir-192(n, γ) with the initial states being the first and the second metastable states, respectively. Further, the status of the data to different final states, as stored in the RNAL data base, is given in the column FS employing symbols 99 (for total cross-section), 0 (for ground state), 1 (for the first metastable state) and 2 (for the second metastable state). The metastable states are in the reaction nomenclature described by 'm' and 'n' for the FS=1 or 2. Note, that FS flags are only used in the text of the present document and not in the files. The latter conform to the ENDF-6 standard and use MF=10 to describe partial cross-sections.

In the column 'Data source' the library or evaluation is given, at the assembling level of the FENDL/A-2.0 library. In other words, the data source is given as chosen for the FENDL/A-2.0 library, except a number of new selections made within this CRP

(see Ref. [6] and this report) selection procedure and recommendations. Remaining data are automatically based on EAF-4.1. The original data, as adopted in EAF-4.1 and FENDL/A-1 libraries, are given in brackets. The original EAF evaluations are denoted with EAF-4.1 without any data source in brackets. The references to the national/regional projects that contributed to RNAL are given in Table 2. A total of 255 reactions have been included in the Master list (see Table 1).

Table 1. List of RNAL reactions with their data sources.

#	Reaction	FS	Data
1	H-1(n,γ) H-2	99	EAF-4.1(JEF-2.2)
2	B-10(n,α) Li-7	99	EAF-4.1(IRDF-90.2)
3	C-12(n,2n) C-11	99	RRDF-98
4	C-12(n,γ) C-13	99	JENDL-FF
5	C-13(n,γ) C-14	99	EAF-4.1
6	N-14(n,p) C-14	99	ENDF/B-VI
7	O-16(n,n'α)C-12	99	JENDL-Act96
8	O-16(n,p) N-16	99	FENDL/A-1 (ENDF/B-VI)
9	F-19(n,2n) F-18	99	FENDL/A-1 (IRDF-90.2)
10	Na-23 (n,2n) Na-22	99	ADL-3
11	Na-23 (n,γ) Na-24	0,1	EAF-4.1 (JEF-2.2)
12	Mg-24 (n,p) Na-24	0,1	IRDF-90.2
13	Mg-26 (n,γ) Mg-27	99	EAF-4.1 (JENDL-3.1)
14	Al-27 (n,2n) Al-26	0,1	ADL-3
15	Al-27 (n,nα) Na-23	99	ADL-3
16	Al-27 (n,γ) Al-28	99	EAF-4.1 (JEF-2.2)
17	Al-27 (n,p) Mg-27	99	RRDF-98
18	Al-27 (n,α) Na-24	0,1	IRDF-90.2
19	Si-28 (n,p) Al-28	99	JENDL-Act96
20	Si-28 (n,d+np) Al-27	99	JENDL-Act96
21	Si-29 (n,p) Al-29	99	JENDL-Act96
22	Si-29 (n,d+np) Al-28	99	JENDL-3.1 [(n,np)], ADL-3 [(n,d)]
23	Si-29 (n,t) Al-27	99	ADL-3
24	Si-30 (n,α) Mg-27	99	JENDL-3.1
25	Si-30 (n,γ) Si-31	99	EAF-4.1 (JENDL-3.1)
26	P-31 (n,γ) P-32	99	EAF-4.1 (JEF-2.2)
27	P-31 (n,p) Si-31	99	EAF-4.1 (IRDF-90.2)
28	P-31 (n,α) Al-28	99	JENDL-Act96
29	S-32 (n,p) P-32	99	IRDF-90.2
30	S-34 (n,γ) S-35	99	EAF-4.1 (JEF-2.2)
31	S-34 (n,p) P-34	99	ADL-3
32	S-36 (n,γ) S-37	99	EAF-4.1 (JEF-2.2)
33	Cl-35 (n,2n) Cl-34m	0,1	EAF-4.1
34	Cl-35 (n,γ) Cl-36	99	EAF-4.1
35	Cl-37 (n,γ) Cl-38	0,1	JENDL-3.2
36	Cl-37 (n,p) S-37	99	JENDL-Act96
37	Cl-37 (n,α) P-34	99	ADL-3
38	Ar-36 (n,γ) Ar-37	99	EAF-4.1 (JEF-2.2)
39	Ar-38 (n,γ) Ar-39	99	EAF-4.1 (JEF-2.2)
40	Ar-40 (n,γ) Ar-41	99	EAF-4.1 (JEF-2.2)
41	K-39 (n,p) Ar-39	99	ADL-3
42	K-41 (n,γ) K-42	99	EAF-4.1 (JENDL-3.1)
43	K-41 (n,α) Cl-38	0,1	ADL-3

Table 1. Cont.

#	Reaction	FS	Data
44	Ca-40 (n,γ) Ca-41	99	EAF-4.1 (JENDL-3.1)
45	Ca-44 (n,p) K-44	99	ADL-3
46	Ca-45 (n,α) Ar-42	99	ADL-3
47	Ca-48 (n,γ) Ca-49	99	EAF-4.1 (JENDL-3.1)
48	Sc-45 (n,γ) Sc-46	0,1	EAF-4.1 (ENDF/B-VI)
49	Ti-46 (n,2n) Ti-45	99	RRDF-98
50	Ti-46 (n,p) Sc-46	0,1	ADL-3
51	Ti-47 (n,p) Sc-47	99	JENDL-Act96
52	Ti-47 (n,d+np) Sc-46	99	RNAL
53	Ti-48 (n,p) Sc-48	99	IRK
54	Ti-48 (n,d+np) Sc-47	99	FENDL/A-1 [(n,d)], IRDF-90.2 [(n,np)]
55	Ti-48 (n,α) Ca-45	99	IPPE
56	Ti-50 (n,α) Ca-47	99	JENDL-Act96
57	Ti-50 (n,γ) Ti-51	99	EAF-4.1 (JENDL-3.1)
58	V-50 (n,2n) V-49	99	JENDL-Act96
59	V-51 (n,γ) V-52	99	EAF-4.1 (JENDL-3.1)
60	V-51 (n,p) Ti-51	99	JENDL-Act96
61	V-51 (n,α) Sc-48	99	EAF-4.1 (IRDF-90.2)
62	Cr-50 (n,γ) Cr-51	99	EAF-4.1 (EFF-2.4)
63	Cr-52 (n,2n) Cr-51	99	IRDF-90.2
64	Cr-52 (n,p) V-52	99	ADL-3
65	Cr-53 (n,d+np) V-52	99	EFF-2.4
66	Cr-54 (n,γ) Cr-55	99	EAF-4.1 (EFF-2.4)
67	Cr-54 (n,α) Ti-51	99	IPPE
68	Mn-53 (n,γ) Mn-54	99	EAF-4.1
69	Mn-55 (n,2n) Mn-54	99	ADL-3
70	Mn-55 (n,γ) Mn-56	99	EAF-4.1 (JEF-2.2)
71	Mn-55 (n,α) V-52	99	IPPE
72	Fe-54 (n,2n) Fe-53	0,1	RRDF-98
73	Fe-54 (n,γ) Fe-55	99	EAF-4.1 (ENDF/B-VI)
74	Fe-54 (n,p) Mn-54	99	JENDL-Act96
75	Fe-56 (n,2n) Fe-55	99	ADL-3
76	Fe-56 (n,γ) Fe-57	99	EAF-4.1 (ENDF/B-VI)
77	Fe-56 (n,p) Mn-56	99	EAF-4.1 (IRDF-90.2)
78	Fe-57 (n,γ) Fe-58	99	EAF-4.1 (ENDF/B-VI)
79	Fe-58 (n,γ) Fe-59	99	EAF-4.1 (ENDF/B-VI)
80	Fe-60 (n,γ) Fe-61	99	EAF-4.1
81	Co-59 (n,2n) Co-58	99	IRDF-90.2
82	Co-59 (n,γ) Co-60	0,1	EAF-4.1 (JEF-2.2)
83	Co-59 (n,α) Mn-56	99	EAF-4.1 (IRDF-90.2)
84	Co-60 (n,γ) Co-61	99	EAF-4.1
85	Co-60 (n,p) Fe-60	99	ADL-3
86	Ni-58 (n,2n) Ni-57	99	EAF-4.1 (IRDF-90.2)
87	Ni-58 (n,γ) Ni-59	99	EAF-4.1 (EFF-2.4)

Table 1. Cont.

#	Reaction	FS	Data
88	Ni-58 (n,p) Co-58	99	IPPE
89	Ni-58 (n,d+np) Co-57	99	EAF-4.1 (JEF-2.2)
90	Ni-60 (n,2n) Ni-59	99	ADL-3
91	Ni-60 (n,p) Co-60	0,1	ADL-3
92	Ni-61 (n,γ) Ni-62	99	EAF-4.1 (EFF-2.4)
93	Ni-62 (n,γ) Ni-63	99	EAF-4.1 (EFF-2.4)
94	Ni-64 (n,2n) Ni-63	99	ADL-3
95	Ni-64 (n,γ) Ni-65	99	EAF-4.1 (EFF-2.4)
96	Cu-63 (n,2n) Cu-62	99	EAF-4.1 (IRDF-90.2)
97	Cu-63 (n,γ) Cu-64	99	EAF-4.1 (ENDF/B-VI)
98	Cu-63 (n,p) Ni-63	99	ADL-3
99	Cu-63 (n,α) Co-60	99	RRDF-98
100	Cu-65 (n,2n) Cu-64	99	JENDL-Act96
101	Cu-65 (n,γ) Cu-66	99	EAF-4.1 (ENDF/B-VI)
102	Zn-64 (n,γ) Zn-65	99	EAF-4.1 (JEF-2.2)
103	Zn-64 (n,p) Cu-64	99	JENDL-Act96
104	Zn-66 (n,p) Cu-66	99	JENDL-Act96
105	Zn-68 (n,γ) Zn-69	0,1	EAF-4.1
106	Zn-70 (n,γ) Zn-71	0,1	EAF-4.1
107	Ga-69 (n,γ) Ga-70	99	EAF-4.1
108	Ga-69 (n,α) Cu-66	99	JENDL-Act96
109	Ga-71 (n,γ) Ga-72	99	EAF-4.1
110	Se-74 (n,γ) Se-75	99	EAF-4.1 (JEF-2.2)
111	Se-78 (n,γ) Se-79	0,1	EAF-4.1 (JEF-2.2)
112	Se-79 (n,γ) Se-80	99	EAF-4.1
113	Se-80 (n,γ) Se-81	0,1	EAF-4.1 (JEF-2.2)
114	Se-82 (n,γ) Se-83	0,1	EAF-4.1 (JEF-2.2)
115	Kr-80 (n,γ) Kr-81	0,1	EAF-4.1 (JEF-2.2)
116	Kr-84 (n,γ) Kr-85	0,1	EAF-4.1 (JEF-2.2)
117	Kr-86 (n,γ) Kr-87	99	EAF-4.1 (JEF-2.2)
118	Rb-85 (n,γ) Rb-86	0,1	EAF-4.1 (JEF-2.2)
119	Sr-84 (n,γ) Sr-85	0,1	EAF-4.1
120	Sr-89 (n,γ) Sr-90	99	EAF-4.1 (JEF-2.2)
121	Sr-90 (n,γ) Sr-91	99	EAF-4.1 (JEF-2.2)
122	Zr-90 (n,2n) Zr-89	0,1	ADL-3
123	Zr-93 (n,γ) Zr-94	99	EAF-4.1 (JEF-2.2)
124	Zr-94 (n,γ) Zr-95	99	EAF-4.1 (JEF-2.2)
125	Zr-96 (n,2n) Zr-95	99	JENDL-Act96
126	Nb-93 (n,n') Nb-93m	1	RRDF-98
127	Nb-93 (n,2n) Nb-92	0,1	JENDL-Act96
128	Nb-93 (n,γ) Nb-94	0,1	EAF-4.1 (JEF-2.2)
129	Mo-92 (n,γ) Mo-93	0,1	EAF-4.1 (JEF-2.2)
130	Mo-92 (n,p) Nb-92	0,1	ADL-3

Table 1. Cont.

#	Reaction	FS	Data
131	Mo-92 (n,d+np) Nb-91	1	RNAL
132	Mo-93 (n,d+np) Nb-92	0,1	ADL-3
133	Mo-94 (n,2n) Mo-93	0,1	ADL-3
134	Mo-94 (n,p) Nb-94	0,1	CRP
135	Mo-94 (n,d+np)Nb-93m	1	ADL-3
136	Mo-95 (n,p) Nb-95	0,1	ADL-3
137	Mo-95 (n,d+np) Nb-94	0,1	ADL-3
138	Mo-98 (n,γ) Mo-99	99	EAF-4.1 (JEF-2.2)
139	Mo-100(n,2n) Mo-99	99	JENDL-Act96
140	Mo-100(n,γ) Mo-101	99	EAF-4.1 (JEF-2.2)
141	Tc-99 (n,2n) Tc-98	99	ADL-3
142	Ru-96 (n,γ) Ru-97	99	EAF-4.1 (JEF-2.2)
143	Ru-102(n,γ) Ru-103	99	EAF-4.1 (JEF-2.2)
144	Ru-104(n,γ) Ru-105	99	EAF-4.1 (JEF-2.2)
145	Rh-103(n,n') Rh-103m	1	IRK
146	Rh-103(n,γ) Rh-104	0,1	EAF-4.1 (JEF-2.2)
147	Pd-102(n,γ) Pd-103	99	EAF-4.1 (JEF-2.2)
148	Pd-108(n,γ) Pd-109	0,1	EAF-4.1 (JEF-2.2)
149	Pd-110(n,γ) Pd-111	0,1	EAF-4.1 (JEF-2.2)
150	Ag-107(n,γ) Ag-108m	1	EAF-4.1 (JEF-2.2)
151	Ag-108m(n,γ) Ag-109	0,1	EAF-4.1
152	Ag-109(n,2n) Ag-108m	1	CRP
153	Ag-109(n,γ) Ag-110m	1	EAF-4.1 (JEF-2.2)
154	Cd-106(n,γ) Cd-107	99	EAF-4.1 (JEF-2.2)
155	Cd-108(n,γ) Cd-109	99	EAF-4.1 (JENDL-3.1)
156	Cd-114(n,γ) Cd-115	0,1	EAF-4.1 (JEF-2.2)
157	In-113(n,γ) In-114	0,1	EAF-4.1 (JEF-2.2)
158	In-115(n,n') In-115m	1	ENDF/B-VI
159	In-115(n,γ) In-116	0,1	ENDF/B-VI [FS=0], JEF-2.2 [FS=1]
160	Sn-120(n,γ) Sn-121m	1	EAF-4.1 (JEF-2.2)
161	Sn-121(n,γ) Sn-122	99	EAF-4.1
162	Sn-122(n,2n) Sn-121m	1	EAF-4.1 (JEF-2.2)
163	Sn-125(n,γ) Sn-126	99	EAF-4.1 (JEF-2.2)
164	Sn-126(n,γ) Sn-127	99	EAF-4.1 (JEF-2.2)
165	Sb-123(n,γ) Sb-124	0,1,2	EAF-4.1 (JEF-2.2)
166	Sb-124(n,γ) Sb-125	99	EAF-4.1 (JEF-2.2)
167	Te-120(n,γ) Te-121	0,1	EAF-4.1 (JEF-2.2)
168	Te-128(n,γ) Te-129	0,1	EAF-4.1 (JEF-2.2)
169	Te-130(n,γ) Te-131	0,1	EAF-4.1 (JEF-2.2)
170	I-127(n,2n) I-126	99	EAF-4.1 (IRDF-90.2)
171	I-127(n,γ) I-128	99	EAF-4.1 (JEF-2.2)
172	I-128(n,γ) I-129	99	EAF-4.1
173	Xe-134(n,γ) Xe-135	0,1	EAF-4.1 (JEF-2.2)
174	Xe-136(n,γ) Xe-137	99	EAF-4.1 (JEF-2.2)

Table 1. Cont.

#	Reaction	FS	Data
175	Cs-133(n,γ) Cs-134	0,1	EAF-4.1 (JEF-2.2)
176	Cs-135(n,γ) Cs-136	0,1	EAF-4.1 (JEF-2.2)
177	Cs-136(n,γ) Cs-137	99	EAF-4.1 (JEF-2.2)
178	Cs-137(n,γ) Cs-138	0,1	EAF-4.1 (JEF-2.2)
179	Ba-130(n,γ) Ba-131	0,1	EAF-4.1
180	Ba-132(n,γ) Ba-133	0,1	EAF-4.1 (JENDL-3.1)
181	Ba-137(n,p) Cs-137	99	ADL-3
182	Ba-138(n,α) Xe-135	0,1	ADL-3
183	La-138(n,γ) La-139	99	EAF-4.1 (JENDL-3.1)
184	La-139(n,γ) La-140	99	EAF-4.1 (JEF-2.2)
185	Ce-143(n,γ) Ce-144	99	EAF-4.1 (JEF-2.2)
186	Nd-146(n,γ) Nd-147	99	EAF-4.1 (JEF-2.2)
187	Nd-148(n,γ) Nd-149	99	EAF-4.1 (JEF-2.2)
188	Nd-150(n,γ) Nd-151	99	EAF-4.1 (JEF-2.2)
189	Sm-144(n,γ) Sm-145	99	EAF-99
190	Sm-152(n,γ) Sm-153	99	EAF-4.1 (JEF-2.2)
191	Sm-154(n,γ) Sm-155	99	EAF-4.1 (JEF-2.2)
192	Eu-151(n,2n) Eu-150	0,1	CRP [FS=0], ADL-3 [FS=1]
193	Eu-151(n,γ) Eu-152	0,1,2	EAF-4.1 (JEF-2.2)
194	Eu-153(n,2n) Eu-152	0,1,2	CRP [FS=0], EAF-4.1 [FS=1,2]
195	Eu-153(n,γ) Eu-154	0,1	EAF-4.1 (JEF-2.2)
196	Eu-154(n,γ) Eu-155	99	EAF-4.1 (JEF-2.2)
197	Tb-159(n,2n) Tb-158	0,1	CRP [FS=0], ADL-3 [FS=1]
198	Tb-159(n,γ) Tb-160	99	EAF-4.1 (JEF-2.2)
199	Dy-158(n,γ) Dy-159	99	EAF-4.1
200	Dy-158(n,p) Tb-158	0,1	EAF-4.1 (ADL-3)
201	Dy-164(n,γ) Dy-165	0,1	EAF-4.1 (JEF-2.2)
202	Ho-165(n,γ) Ho-166	0,1	EAF-4.1 (JEF-2.2)
203	Er-162(n,γ) Er-163	99	EAF-4.1
204	Er-164(n,γ) Er-165	99	EAF-4.1
205	Er-168(n,γ) Er-169	99	EAF-4.1
206	Er-170(n,γ) Er-171	99	EAF-4.1
207	Tm-169(n,γ) Tm-170	99	EAF-4.1
208	Yb-168(n,γ) Yb-169	0,1	EAF-4.1
209	Yb-174(n,γ) Yb-175	99	EAF-4.1
210	Yb-176(n,γ) Yb-177	0,1	EAF-4.1
211	Lu-175(n,γ) Lu-176	0,1	EAF-4.1 (JEF-2.2)
212	Lu-176(n,γ) Lu-177	0,1	EAF-4.1 (JEF-2.2)
213	Hf-174(n,γ) Hf-175	99	EAF-4.1 (JEF-2.2)
214	Hf-179(n,2n) Hf-178n	2	CRP
215	Ta-181(n,3n) Ta-179	99	ADL-3
216	Ta-181(n,γ) Ta-182	0,1,2	EAF-4.1 (JEF-2.2)
217	W-182(n,2n) W-181	99	ADL-3
218	W-182(n,nα) Hf-178n	2	ADL-3

Table 1. Cont.

#	Reaction	FS	Data
219	W-183(n,γ) W-184	99	EAF-4.1 (JEF-2.2)
220	W-184(n,γ) W-185	99	EAF-4.1 (LANL)
221	W-186(n,2n) W-185	0,1	JENDL-Act96
222	W-186(n,nα) Hf-182	0,1	ADL-3
223	W-186(n,γ) W-187	99	EAF-4.1 (JEF-2.2)
224	Re-185(n,2n) Re-184	0,1	EAF-4.1 (ENDF/B-VI)
225	Re-185(n,γ) Re-186m	1	EAF-4.1 (LANL)
226	Re-187(n,2n) Re-186m	1	CRP
227	Re-187(n,γ) Re-188	0,1	EAF-4.1 (JEF-2.2)
228	Re-187(n,p) W-187	99	ADL-3
229	Os-184(n,γ) Os-185	99	EAF-4.1
230	Os-188(n,γ) Os-189	0,1	EAF-4.1
231	Os-190(n,γ) Os-191	0,1	EAF-4.1
232	Os-190(n,α) W-187	99	EAF-99
233	Os-192(n,γ) Os-193	99	EAF-4.1
234	Ir-191(n,γ) Ir-192n	2	EAF-4.1
235	Ir-192(n,n') Ir-192n	2	EAF-4.1 (ADL-3)
236	Ir-192n(n,γ) Ir-193	0,1	EAF-4.1
237	Ir-193(n,2n) Ir-192n	2	EAF-4.1 (ADL-3)
238	Pt-190(n,γ) Pt-191	99	EAF-4.1
239	Pt-192(n,γ) Pt-193	0,1	EAF-4.1
240	Pt-194(n,γ) Pt-195	99	LANL-96
241	Pt-196(n,γ) Pt-197	99	LANL-96
242	Pt-198(n,γ) Pt-198	99	LANL-96
243	Au-197(n,2n) Au-196	99	EAF-4.1 (IRDF-90.2)
244	Au-197(n,γ) Au-198	0,1	EAF-4.1 (JEF-2.2)
245	Hg-196(n,γ) Hg-197	0,1	EAF-4.1
246	Hg-202(n,γ) Hg-203	99	EAF-4.1
247	Hg-204(n,γ) Hg-205	99	EAF-4.1
248	Tl-203(n,γ) Tl-204	99	EAF-4.1
249	Tl-205(n,γ) Tl-206	0,1	EAF-4.1
250	Pb-204(n,2n) Pb-203	0,1	ADL-3
251	Pb-206(n,2n) Pb-205	99	FENDL/A-1 (ENDF/B-VI)
252	Pb-206(n,α) Hg-203	99	ADL-3
253	Pb-208(n,γ) Pb-209	99	EAF-4.1 (ENDF/B-VI)
254	Bi-209(n,2n) Bi-208	99	IPPE
255	Bi-209(n,γ) Bi-210m	1	EAF-4.1 (JEF-2.2)

Table 2. Sources of adopted evaluations.

Data source	Number
ADL-3 [2]	42
CRP [7]	7
EAF-4.1 [3]	39
EAF-99 [8]	2
EFF-2.4 [9]	7
ENDF/B-VI [10]	14
FENDL/A-1 [4]	1
IPPE [11–13]	5
IRDF-90.2 [14]	16
IRK [15]	2
JEF-2.2 [16]	79
JENDL-3.1 [17]	12
JENDL-3.2 [18]	1
JENDL-Act96 [1]	19
JENDL-FF [19, 20]	1
LANL [21]	2
LANL-96 [22]	3
RNAL	2
RRDF-98 [23]	6
Total	260

Statistics of the evaluation origins and related references are displayed in Table 2. In most cases, all channels (FS=0,1 or (n,np) and (n,d)) contributing to a reaction were taken from the same source. However, for 5 reactions evaluations from two different libraries were accepted for separate channels. This brings the sum in Table 2 to 260.

1.4.   Library format and structure

The strict ENDF-6 format has been adopted without any modifications. The total cross-sections are stored in file MF=3. The partial cross-sections, leading to the ground state or metastable states of the residual nucleus are coded in file MF=10. Within MF=10 the identifiers LIS and LFS are used to indicate states (isomers) of the target and final nuclei, respectively. According to standard ENDF-6 convention LFS is 0 for the ground state, 1 for the first metastable state and 2 for the second metastable state.

The RNAL library is stored in separate files for each reaction and final state (g.s., first metastable and second metastable states if appropriate), unless reaction to the metastable state is the reference reaction. If no metastable state exists in the final nucleus the total cross-sections are given. The total cross-sections are also given for some reactions leading to the nuclei with metastable states if partial cross-sections were not available in the recommended evaluation. In addition, separate evaluations are generally given for the (n,np) and (n,d) reaction channels. Only in the two original RNAL evaluations (^{47}Ti and

18

^{92}Mo calculated with EMPIRE-2.13) the data represent a sum of (n,np) and (n,d) reaction channels. Thus, RNAL contains 342 evaluations which are listed in Table 3. The names of the files consist of 'za' characters followed by Z and A numbers, dot, and MT of the reaction. In the case of a partial cross-section the standard ENDF-6 MT number (in the file name only!) is increased by 300 for the reaction leaving a residue in the first metastable state and by 600 for the second metastable state.

For the convenience of the user a single ENDF-6 file containing all RNAL evaluations is also provided (compressed with GNU gzip, size 6 Mb).

Table 3. List of RNAL files.

#	Reaction	total	g.s.	meta-1	meta-2
1	H- 1(n,γ)	za01001.102			
2	B-10(n,α)	za05010.107			
3	C-12(n,2n)	za06012.016			
4	C-12(n,γ)	za06012.102			
5	C-13(n,γ)	za06013.102			
6	N-14(n,p)	za07014.103			
7	O-16(n,nα)	za08016.022			
8	O-16(n,p)	za08016.103			
9	F-19(n,2n)	za09019.016			
10	Na-23(n,2n)	za11023.016			
11	Na-23(n,γ)		za11023.102	za11023.402	
12	Mg-24(n,p)		za12024.103	za12024.403	
13	Mg-26(n,γ)	za12026.102			
14	Al-27(n,2n)		za13027.016	za13027.316	
15	Al-27(n,nα)	za13027.022			
16	Al-27(n,γ)	za13027.102			
17	Al-27(n,p)	za13027.103			
18	Al-27(n,α)		za13027.107	za13027.407	
19	Si-28(n,p)	za14028.103			
20	Si-28(n,np)	za14028.028			
	Si-28(n,d)	za14028.104			
21	Si-29(n,p)	za14029.103			
22	Si-29(n,np)	za14029.028			
	Si-29(n,d)	za14029.104			
23	Si-29(n,t)	za14029.105			
24	Si-30(n,α)	za14030.107			
25	Si-30(n,γ)	za14030.102			
26	P-31(n,γ)	za15031.102			
27	P-31(n,p)	za15031.103			
28	P-31(n,α)	za15031.107			
29	S-32(n,p)	za16032.103			
30	S-34(n,γ)	za16034.102			
31	S-34(n,p)	za16034.103			
32	S-36(n,γ)	za16036.102			
33	Cl-35(n,2n)		za17035.016	za17035.316	
34	Cl-35(n,γ)	za17035.102			
35	Cl-37(n,γ)		za17037.102	za17037.402	
36	Cl-37(n,p)	za17037.103			
37	Cl-37(n,α)	za17037.107			
38	Ar-36(n,γ)	za18036.102			
39	Ar-38(n,γ)	za18038.102			
40	Ar-40(n,γ)	za18040.102			
41	K-39(n,p)	za19039.103			
42	K-41(n,γ)	za19041.102			

Table 3. Cont.

#	Reaction	total	g.s.	meta-1	meta-2
43	K-41(n,α)		za19041.107	za19041.407	
44	Ca-40(n,γ)	za20040.102			
45	Ca-44(n,p)	za20044.103			
46	Ca-45(n,α)	za20045.107			
47	Ca-48(n,γ)	za20048.102			
48	Sc-45(n,γ)		za21045.102	za21045.402	
49	Ti-46(n,2n)	za22046.016			
50	Ti-46(n,p)		za22046.103	za22046.403	
51	Ti-47(n,p)	za22047.103			
52	Ti-47(n,np+d)	za22047.104			
53	Ti-48(n,p)	za22048.103			
54	Ti-48(n,np)	za22048.028			
	Ti-48(n,d)	za22048.104			
55	Ti-48(n,α)	za22048.107			
56	Ti-50(n,α)	za22050.107			
57	Ti-50(n,γ)	za22050.102			
58	V-50(n,2n)	za23050.016			
59	V-51(n,γ)	za23051.102			
60	V-51(n,p)	za23051.103			
61	V-51(n,α)	za23051.107			
62	Cr-50(n,γ)	za24050.102			
63	Cr-52(n,2n)	za24052.016			
64	Cr-52(n,p)	za24052.103			
65	Cr-53(n,np)	za24053.028			
	Cr-53(n,d)	za24053.104			
66	Cr-54(n,γ)	za24054.102			
67	Cr-54(n,α)	za24054.107			
68	Mn-53(n,γ)	za25053.102			
69	Mn-55(n,2n)	za25055.016			
70	Mn-55(n,γ)	za25055.102			
71	Mn-55(n,α)	za25055.107			
72	Fe-54(n,2n)		za26054.016	za26054.316	
73	Fe-54(n,γ)	za26054.102			
74	Fe-54(n,p)	za26054.103			
75	Fe-56(n,2n)	za26056.016			
76	Fe-56(n,γ)	za26056.102			
77	Fe-56(n,p)	za26056.103			
78	Fe-57(n,γ)	za26057.102			
79	Fe-58(n,γ)	za26058.102			
80	Fe-60(n,γ)	za26060.102			
81	Co-59(n,2n)	za27059.016			
82	Co-59(n,γ)		za27059.102	za27059.402	
83	Co-59(n,α)	za27059.107			
84	Co-60(n,γ)	za27060.102			

Table 3. Cont.

#	Reaction	total	g.s.	meta-1	meta-2
85	Co-60(n,p)	za27060.103			
86	Ni-58(n,2n)	za28058.016			
87	Ni-58(n,γ)	za28058.102			
88	Ni-58(n,p)	za28058.103			
89	Ni-58(n,np)	za28058.028			
	Ni-58(n,d)	za28058.104			
90	Ni-60(n,2n)	za28060.016			
91	Ni-60(n,p)		za28060.103	za28060.403	
92	Ni-61(n,γ)	za28061.102			
93	Ni-62(n,γ)	za28062.102			
94	Ni-64(n,2n)	za28064.016			
95	Ni-64(n,γ)	za28064.102			
96	Cu-63(n,2n)	za29063.016			
97	Cu-63(n,γ)	za29063.102			
98	Cu-63(n,p)	za29063.103			
99	Cu-63(n,α)	za29063.107			
100	Cu-65(n,2n)	za29065.016			
101	Cu-65(n,γ)	za29065.102			
102	Zn-64(n,γ)	za30064.102			
103	Zn-64(n,p)	za30064.103			
104	Zn-66(n,p)	za30066.103			
105	Zn-68(n,γ)		za30068.102	za30068.402	
106	Zn-70(n,γ)		za30070.102	za30070.402	
107	Ga-69(n,γ)	za31069.102			
108	Ga-69(n,α)	za31069.107			
109	Ga-71(n,γ)	za31071.102			
110	Se-74(n,γ)	za34074.102			
111	Se-78(n,γ)		za34078.102	za34078.402	
112	Se-79(n,γ)	za34079.102			
113	Se-80(n,γ)		za34080.102	za34080.402	
114	Se-82(n,γ)		za34082.102	za34082.402	
115	Kr-80(n,γ)		za36080.102	za36080.402	
116	Kr-84(n,γ)		za36084.102	za36084.402	
117	Kr-86(n,γ)	za36086.102			
118	Rb-85(n,γ)		za37085.102	za37085.402	
119	Sr-84(n,γ)		za38084.102	za38084.402	
120	Sr-89(n,γ)	za38089.102			
121	Sr-90(n,γ)	za38090.102			
122	Zr-90(n,2n)		za40090.016	za40090.316	
123	Zr-93(n,γ)	za40093.102			
124	Zr-94(n,γ)	za40094.102			
125	Zr-96(n,2n)	za40096.016			
126	Nb-93(n,n')			za41093.051	
127	Nb-93(n,2n)		za41093.016	za41093.316	

Table 3. Cont.

#	Reaction	total	g.s.	meta-1	meta-2
128	Nb-93(n,γ)		za41093.102	za41093.402	
129	Mo-92(n,γ)		za42092.102	za42092.402	
130	Mo-92(n,p)			za42092.403	
131	Mo-92(n,d+np)			za42092.404	
132	Mo-93(n,np)		za42093.028	za42093.328	
	Mo-93(n,d)		za42093.104	za42093.404	
133	Mo-94(n,2n)		za42094.016	za42094.316	
134	Mo-94(n,p)		za42094.103	za42094.403	
135	Mo-94(n,np)			za42094.328	
	Mo-94(n,d)			za42094.404	
136	Mo-95(n,p)		za42095.103	za42095.403	
137	Mo-95(n,np)		za42095.028	za42095.328	
	Mo-95(n,d)		za42095.104	za42095.404	
138	Mo-98(n,γ)	za42098.102			
139	Mo-100(n,2n)	za42100.016			
140	Mo-100(n,γ)	za42100.102			
141	Tc-99(n,2n)	za43099.016			
142	Ru-96(n,γ)	za44096.102			
143	Ru-102(n,γ)	za44102.102			
144	Ru-104(n,γ)	za44104.102			
145	Rh-103(n,n')			za45103.304	
146	Rh-103(n,γ)		za45103.102	za45103.402	
147	Pd-102(n,γ)	za46102.102			
148	Pd-108(n,γ)		za46108.102	za46108.402	
149	Pd-110(n,γ)		za46110.102	za46110.402	
150	Ag-107(n,γ)			za47107.402	
151	Ag-108m(n,γ)		za47108.102	za47108.402	
152	Ag-109(n,2n)			za47109.316	
153	Ag-109(n,γ)			za47109.402	
154	Cd-106(n,γ)	za48106.102			
155	Cd-108(n,γ)	za48108.102			
156	Cd-114(n,γ)		za48114.102	za48114.402	
157	In-113(n,γ)		za49113.102	za49113.402	
158	In-115(n,n')			za49115.051	
159	In-115(n,γ)		za49115.102	za49115.402	
160	Sn-120(n,γ)			za50120.402	
161	Sn-121(n,γ)	za50121.102			
162	Sn-122(n,2n)			za50122.316	
163	Sn-125(n,γ)	za50125.102			
164	Sn-126(n,γ)	za50126.102			
165	Sb-123(n,γ)		za51123.102	za51123.402	za51123.702
166	Sb-124(n,γ)	za51124.102			
167	Te-120(n,γ)		za52120.102	za52120.402	

Table 3. Cont.

#	Reaction	total	g.s.	meta-1	meta-2
168	Te-128(n,γ)		za52128.102	za52128.402	
169	Te-130(n,γ)		za52130.102	za52130.402	
170	I-127(n,2n)	za53127.016			
171	I-127(n,γ)	za53127.102			
172	I-128(n,γ)	za53128.102			
173	Xe-134(n,γ)		za54134.102	za54134.402	
174	Xe-136(n,γ)	za54136.102			
175	Cs-133(n,γ)		za55133.102	za55133.402	
176	Cs-135(n,γ)		za55135.102	za55135.402	
177	Cs-136(n,γ)	za55136.102			
178	Cs-137(n,γ)		za55137.102	za55137.402	
179	Ba-130(n,γ)		za56130.102	za56130.402	
170	Ba-132(n,γ)		za56132.102	za56132.402	
181	Ba-137(n,p)	za56137.103			
182	Ba-138(n,α)		za56138.107	za56138.407	
183	La-138(n,γ)	za57138.102			
184	La-139(n,γ)	za57139.102			
185	Ce-143(n,γ)	za58143.102			
186	Nd-146(n,γ)	za60146.102			
187	Nd-148(n,γ)	za60148.102			
188	Nd-150(n,γ)	za60150.102			
189	Sm-144(n,γ)	za62144.102			
190	Sm-152(n,γ)	za62152.102			
191	Sm-154(n,γ)	za62154.102			
192	Eu-151(n,2n)		za63151.016	za63151.316	
193	Eu-151(n,γ)		za63151.102	za63151.402	za63151.702
194	Eu-153(n,2n)		za63153.016	za63153.316	za63153.616
195	Eu-153(n,γ)		za63153.102	za63153.402	
196	Eu-154(n,γ)	za63154.102			
197	Tb-159(n,2n)		za65159.016	za65159.316	
198	Tb-159(n,γ)	za65159.102			
199	Dy-158(n,γ)	za66158.102			
200	Dy-158(n,p)		za66158.103	za66158.403	
201	Dy-164(n,γ)		za66164.102	za66164.402	
202	Ho-165(n,γ)		za67165.102	za67165.402	
203	Er-162(n,γ)	za68162.102			
204	Er-164(n,γ)	za68164.102			
205	Er-168(n,γ)	za68168.102			
206	Er-170(n,γ)	za68170.102			
207	Tm-169(n,γ)	za69169.102			
208	Yb-168(n,γ)		za70168.102	za70168.402	
209	Yb-174(n,γ)	za70174.102			
210	Yb-176(n,γ)		za70176.102	za70176.402	
211	Lu-175(n,γ)		za71175.102	za71175.402	

Table 3. Cont.

#	Reaction	total	g.s.	meta-1	meta-2
212	Lu-176(n,γ)		za71176.102	za71176.402	
213	Hf-174(n,γ)	za72174.102			
214	Hf-179(n,2n)				za72179.616
215	Ta-181(n,3n)	za73181.017			
216	Ta-181(n,γ)		za73181.102	za73181.402	za73181.702
217	W-182(n,2n)	za74182.016			
218	W-182(n,nα)				za74182.622
219	W-183(n,γ)	za74183.102			
220	W-184(n,γ)	za74184.102			
221	W-186(n,2n)		za74186.016	za74186.316	
222	W-186(n,nα)		za74186.022	za74186.322	
223	W-186(n,γ)	za74186.102			
224	Re-185(n,2n)		za75185.016	za75185.316	
225	Re-185(n,γ)			za75185.402	
226	Re-187(n,2n)			za75187.316	
227	Re-187(n,γ)		za75187.102	za75187.402	
228	Re-187(n,p)	za75187.103			
229	Os-184(n,γ)	za76184.102			
230	Os-188(n,γ)		za76188.102	za76188.402	
231	Os-190(n,γ)		za76190.102	za76190.402	
232	Os-190(n,α)	za76190.107			
233	Os-192(n,γ)	za76192.102			
234	Ir-191(n,γ)				za77191.702
235	Ir-192n(n,n')				za77192.604
236	Ir-192(n,γ)		za77192.102	za77192.402	
237	Ir-193(n,2n)				za77193.616
238	Pt-190(n,γ)	za78190.102			
239	Pt-192(n,γ)		za78192.102	za78192.402	
240	Pt-194(n,γ)	za78194.102			
241	Pt-196(n,γ)	za78196.102			
242	Pt-198(n,γ)	za78198.102			
243	Au-197(n,2n)	za79197.016			
244	Au-197(n,γ)		za79197.102	za79197.402	
245	Hg-196(n,γ)		za80196.102	za80196.402	
246	Hg-202(n,γ)	za80202.102			
247	Hg-204(n,γ)	za80204.102			
248	Tl-203(n,γ)	za81203.102			
249	Tl-205(n,γ)		za81205.102	za81205.402	
250	Pb-204(n,2n)		za82204.016	za82204.316	
251	Pb-206(n,2n)	za82206.016			
252	Pb-206(n,α)	za82206.107			
253	Pb-208(n,γ)	za82208.102			
254	Bi-209(n,2n)	za83209.016			
255	Bi-209(n,γ)			za83209.402	

1.5. Final remarks

From the description given above it can be seen how the work of the CRP aiming towards the production of the RNAL has developed. Such work is necessarily of a long term nature and in addition to the production of the deliverable — in this case the RNAL library in electronic form and the present report — there is the very valuable by-product of increased international cooperation and information exchange between the relatively small number of groups working on these problems. The overriding initial considerations in the setting up of the CRP were to focus on the encouragement of new relevant experimental measurements that could be used to validate activation libraries, and on innovative work on data uncertainties, intermediate energy data and sequential charged particle interactions. Valuable contributions on these topics were presented at the two meetings, and although some are not directly present in the final library, the results of these studies will be incorporated in the various national and international programmes. This illustrates the IAEA's important role in stimulating and coordinating scientific work as well as making the results available to all in the form of data libraries. Another strand of the IAEA nuclear data programme over the last ten years has led to the production of the FENDL library. This library is targeted at the fusion community and includes many parts, one of which is an activation library. The exchange of information between RNAL and the FENDL activation library has been in both directions and the two libraries have consequently been improved. But the main reason for the production of RNAL in addition to FENDL has been the possibility of concentrating on activation reactions for applications other than fusion, and by providing data in a format appropriate for users of data in many applications. The production of an international library such as RNAL exposes it to wider scrutiny than a regional library and therefore the quality of the data can be significantly improved.

2. Assessment of the library

The RNAL library has been assembled and checked at the IAEA Nuclear Data Section. All individual evaluations were reformatted to conform to the ENDF-6 standard. A number of deviations form the ENDF-6 format were removed. All Q-values and thresholds were consistently recalculated using recent recommended masses [24] and isomer energies taken from NUDAT [25]. Finally, the library was checked using CHECKR, FIZCON and PSYCHE codes, which produced no serious diagnostics.

In the following every reaction will be shortly commented. These comments give information on the following items:

1. The original source of the data (the library) is quoted. This may help the user to look for more details on the data evaluation, if needed, in the corresponding library documentation. If EAF-4.1 is the original source (only for (n,γ) data), the code used in the evaluation is quoted.

2. The basic information on the determination of the branching ratio for the partial cross-sections to the ground state (FS=0), first and second isomeric state (FS=1,2). For reactions with partial cross-sections the redundant total cross-section is not included in the RNAL database.

3. The agreement of the adopted excitation curve with the experimental data, retrieved from the EXFOR data base, is commented on and discussed.

4. In many capture reactions additional experimental information exists (not included in EXFOR), in particular 30 keV and 14.5 MeV cross-sections, as compiled in Refs. [26] and [27]. These data are also used in the discussion of the evaluation agreements with the experimental data. The graphical presentation of many of these data can also be found in Ref. [28].

5. Finally, in cases when the agreement is not satisfactory and a revision or improvement of data is needed, this recommendation is included as a comment.

In the following, comments are given on all evaluations together with their graphical comparison with the experimental data base. This graphical validation section includes 260 figures (in 5 cases, due to the large number of experimental points, two plots are provided for a single reaction).
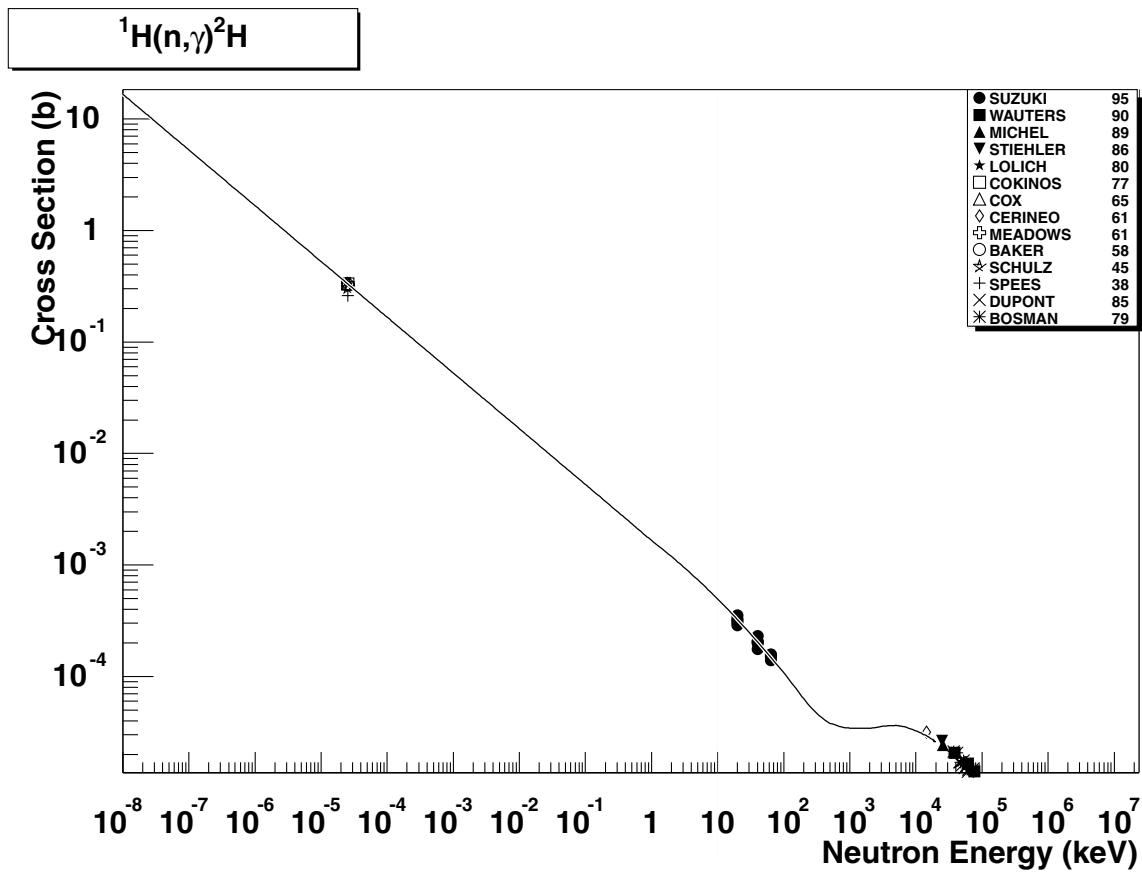
2.1. ^{1}**H (n,γ)** ^{2}**H**

final state: total
source: EAF-4.1 (JEF-2.2)

The adopted evaluation, which originates from ENDF/B-VI, reproduces well all experimental data points. There are recent experimental data obtained by Igashira et al. (private communication) between 1-100 keV, which nicely confirm the adopted ENDF/B-VI in the 1/v region.

^{10}B(n,α)^{7}Li

● FRIESENHAHN	75
■ BOGART	69
▲ MACKLIN	68
▼ COX	67
★ PROSDOCIMI	67
□ MOORING	64
△ BILPUCH	60
◇ BICHSEL	57
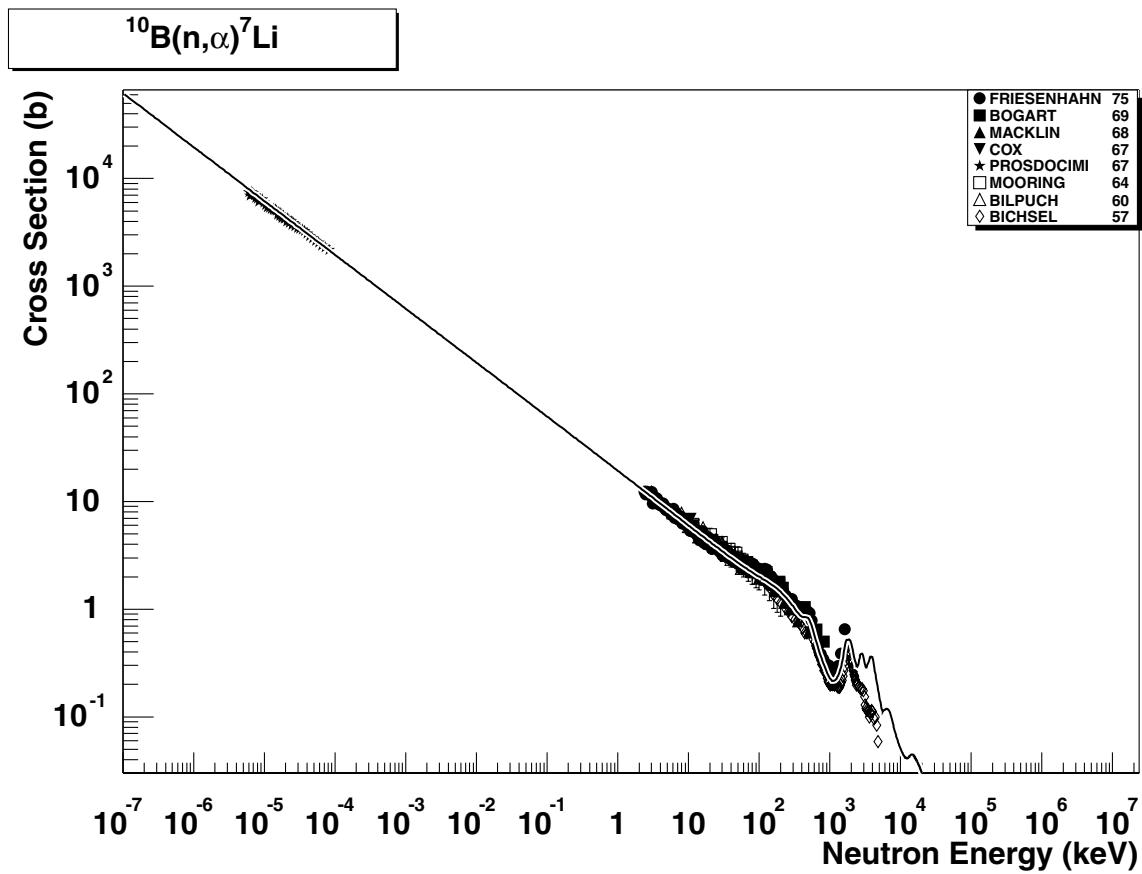
2.2. ^{10}B (n,α) ^{7}Li

final state: total
source: EAF-4.1 (IRDF-90.2)

The recommended evaluation provides for a very good reproduction of the experimental data up to the energy of 2 MeV. Above this energy several d-resonances have been included in the evaluation, which are missing in the EXFOR data.

^{12}C(n,2n)^{11}C

● SOEWARSONO	92
■ ANDERS	81
▲ WELCH	81
▼ BRILL	61
★ BROLLEY JR	52
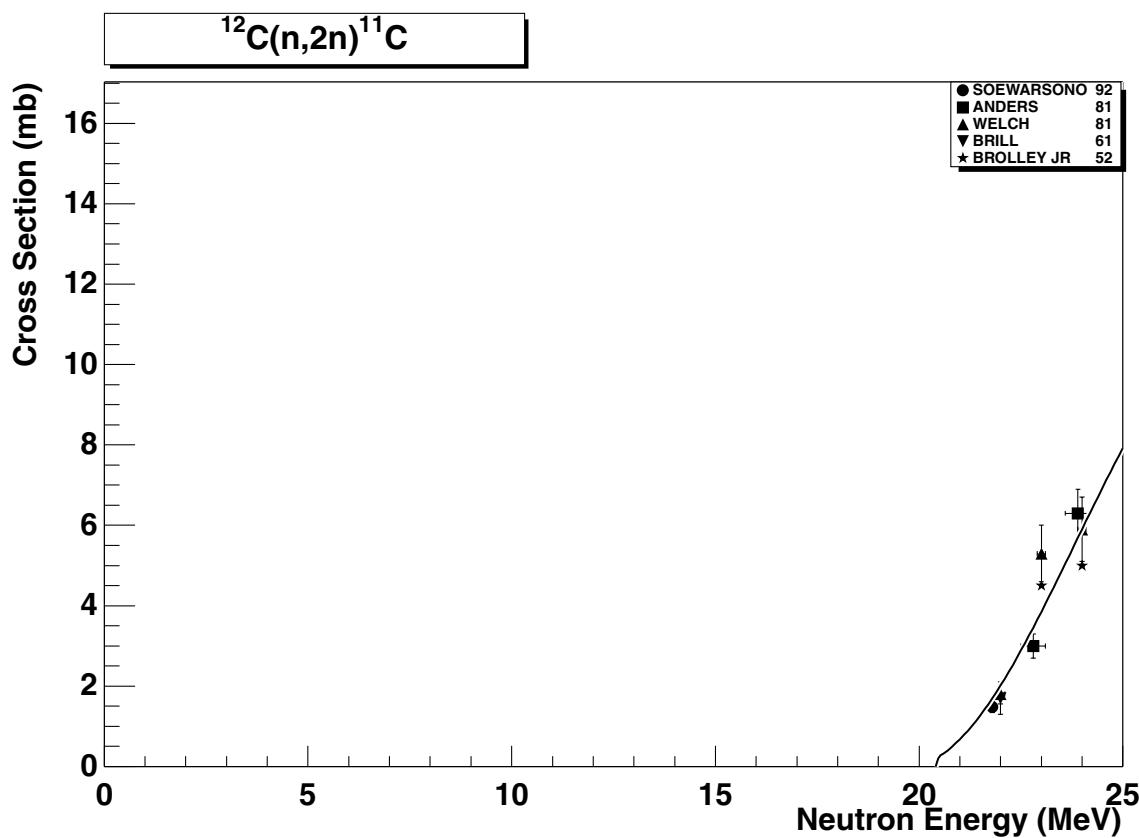
2.3. ^{12}C (n,2n) ^{11}C

final state: total
source: RRDF-98

RRDF-98 evaluation runs satisfactorily through all the experimental data.
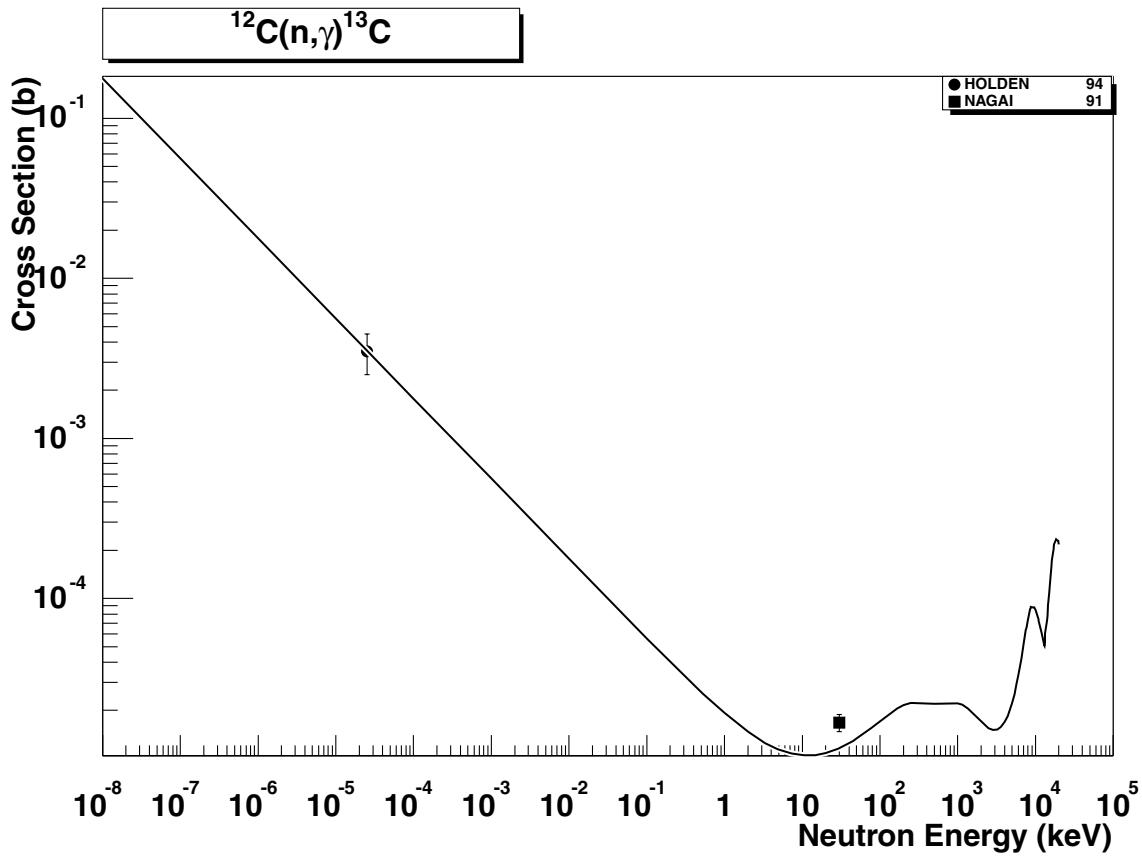
2.4. ^{12}C (n,γ) ^{13}C

final state: total
source: JENDL-FF

A new evaluation, prepared for JENDL-FF, which includes the recent direct radiation capture calculations by Mengoni [29] has been adopted. It reproduces the experimental data of Holden94, Nagai91 and recent data of Oshaki et al. [30] rather well.

2.5. ^{13}C (n,γ) ^{14}C
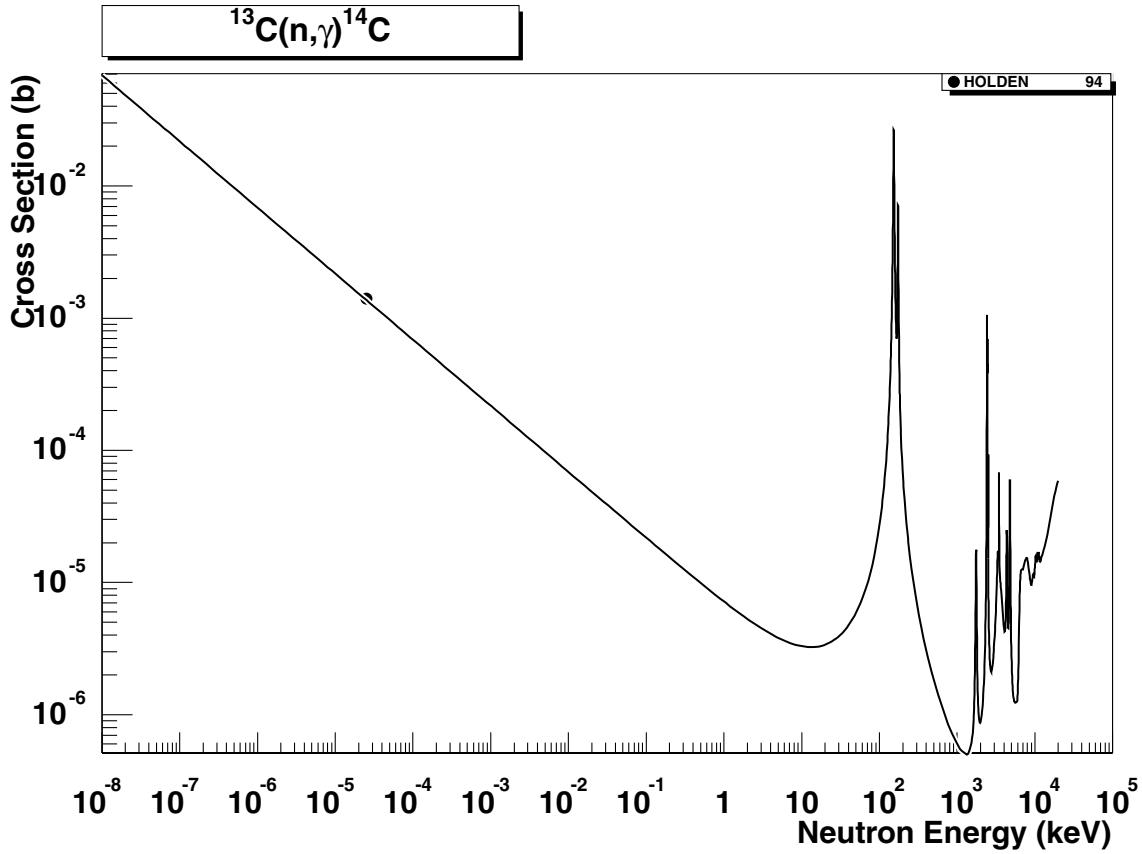
final state: total
source: EAF-4.1

No experimental data are included in EXFOR. The EAF-4.1 evaluation generated cross-sections up to 7 MeV from the resolved resonance parameters of Ref. [31] (MLBW option in NJOY). These were joined smoothly with the high energy component taken over from the ACTL library. The evaluation reproduces well the thermal cross-section of Holden94 [32] (C/E=1.00) but misses the contribution of the p-wave DRC. This contribution may result in a slight increase of the cross-section in the high energy region. However, strong resolved resonance contributions make the p-wave DRC less dominant. No revision is needed at this moment, DRC calculations by Mengoni are in progress.

The figure shows the cross section plot for ^{14}N(n,p)^{14}C. The legend lists:

●	KOEHLER	89
■	MORGAN	79
▲	GABBARD	59
▼	GIBBONS	59
★	BOLLMANN	51
□	JOHNSON	50
△	BALDINGER	39
◇	FELBER	76
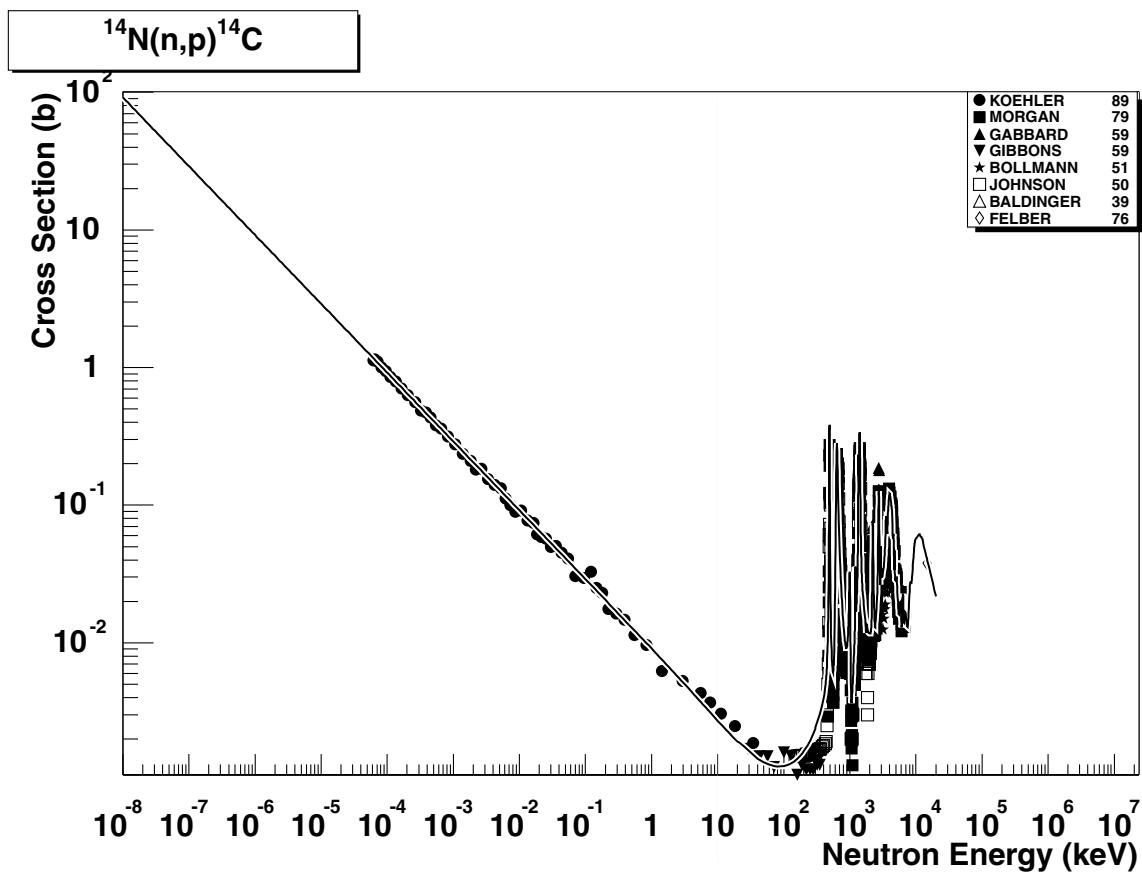
2.6. ^{14}N (n,p) ^{14}C

final state: total
source: ENDF/B-VI

The ENDF/B-VI evaluation is in excellent agreement with all experimental data in the whole energy range. The resolved resonance region is fully included.

^{16}O(n,nα)^{12}C
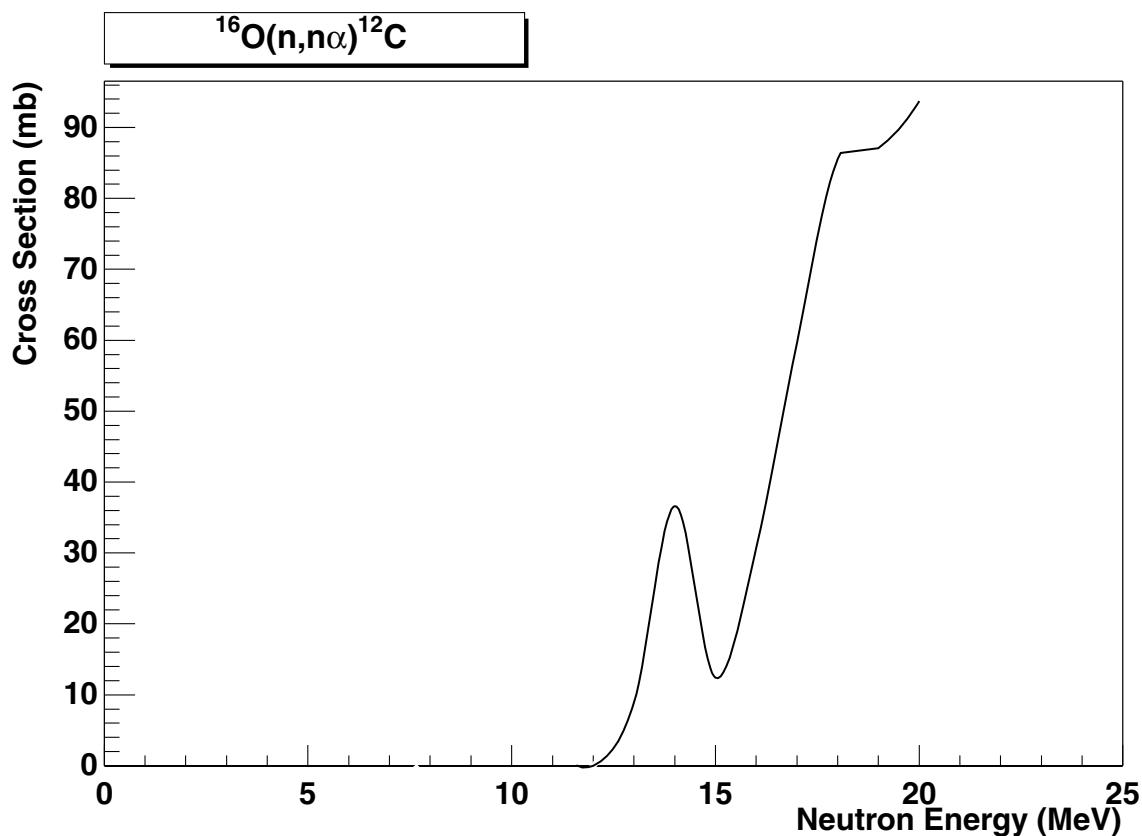
2.7. ^{16}O (n,n'α)^{12}C

final state: total
source: JENDL-Act96

No EXFOR data are available. The evaluation results from the calculation with the SIN-CROSII code, results of which are usually reliable.

The figure shows a plot titled $^{16}O(n,p)^{16}N$ with Cross Section (mb) on the y-axis (0 to 90) and Neutron Energy (MeV) on the x-axis (0 to 25).

Legend:
●	SCHMIDT	72
■	PRASAD	71
▲	SCHANTL	70
▼	BORMANN	67
★	MITRA	66
□	DE JUREN	62
△	KANTELE	62
◇	SEEMAN	62
✛	DE JUREN	60
○	MARTIN	54
☆	PAUL	53
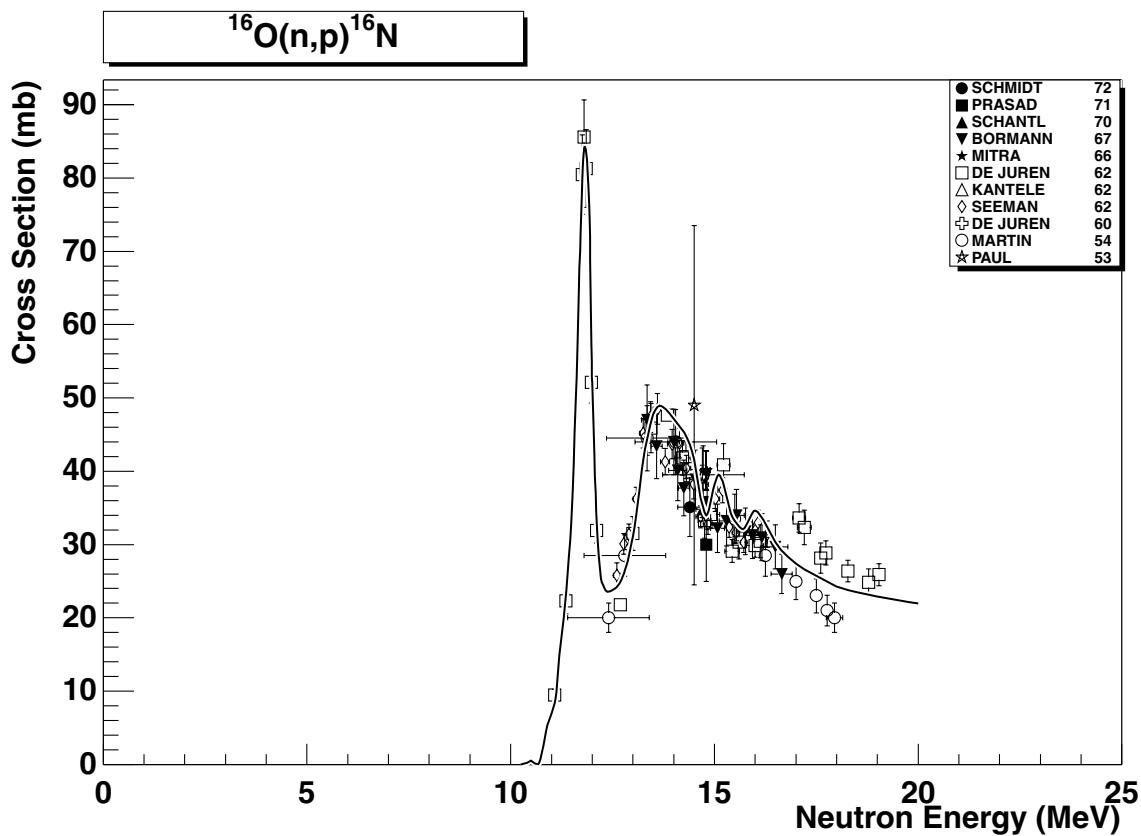
2.8. ^{16}O (n,p) ^{16}N

final state: total
source: FENDL/A-1 (ENDF/B-VI)

ENDF-B-VI reproduces all experimental data including several strong overlapping resonances above 12 MeV.

^{19}F(n,2n)^{18}F

●	HARTMANN	91
■	IKEDA	88
▲	KOBAYASHI	88
▼	RYVES	78
★	SIGG	76
□	ARAMINOWICZ	73
△	ROBERTSON	73
◇	MOGHARRAB	72
⊕	BARRALL	69
○	CHATTERJEE	69
☆	CRUMPTON	69
+	SHIOKAWA	68
×	VONACH	68
✳	CHATTERJEE	67
·	MENLOVE	67
◎	PASQUARELLI	67
⊠	NAGEL	66
△	BORMANN	65
◇	CSIKAI	65
⊕	PICARD	65
★	STRAIN	65
◉	CEVOLANI	62
⊠	RAYBURN	62
⊛	BRILL	61
⊞	RAYBURN	61
△	MC CRARY	60
◈	ASHBY	58
⊕	PAUL	53
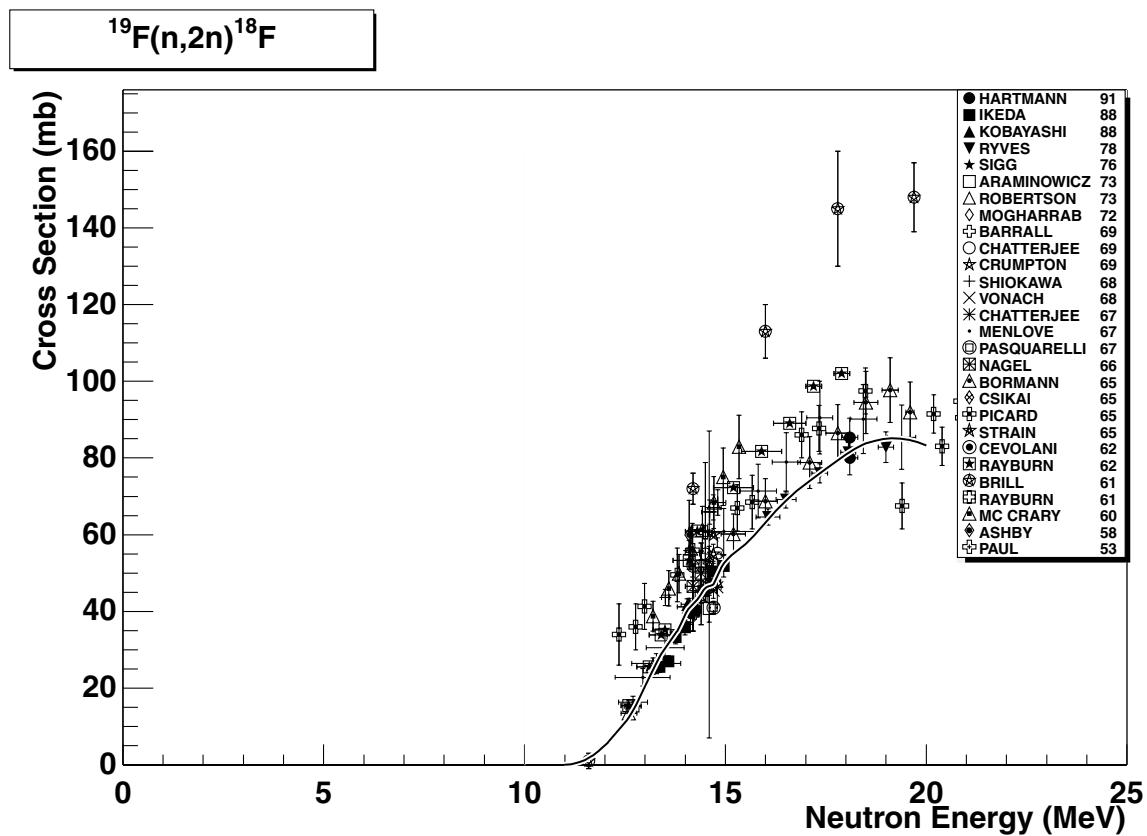
2.9. ^{19}F (n,2n) ^{18}F

final state: total
source: FENDL/A-1 (IRDF-90.2)

IRDF-90.2 evaluation lies at the lower part of the experimental data band, however, it reproduces well the latest and reliable data of Ryves78, Kobayashi88, Ikeda88 and Hartmann91. This may suggest that older data are systematically too large (Brill61 should be definitely disregarded).

^{23}Na(n,2n)^{22}Na

Legend:
- ● FILATENKOV 97
- ■ HANLIN 92
- ▲ SOEWARSONO 92
- ▼ ZHI-ZHENG 91
- ○ IKEDA 88
- □ ADAMSKI 80
- △ SHANI 76
- ◇ SIGG 76
- ✚ ARAMINOWICZ 73
- ★ MASLOV 72
- ☆ BARRALL 69
- + MENLOVE 67
- ✳ LISKIEN 65
- ✕ PICARD 65
- · PRESTWOOD 55
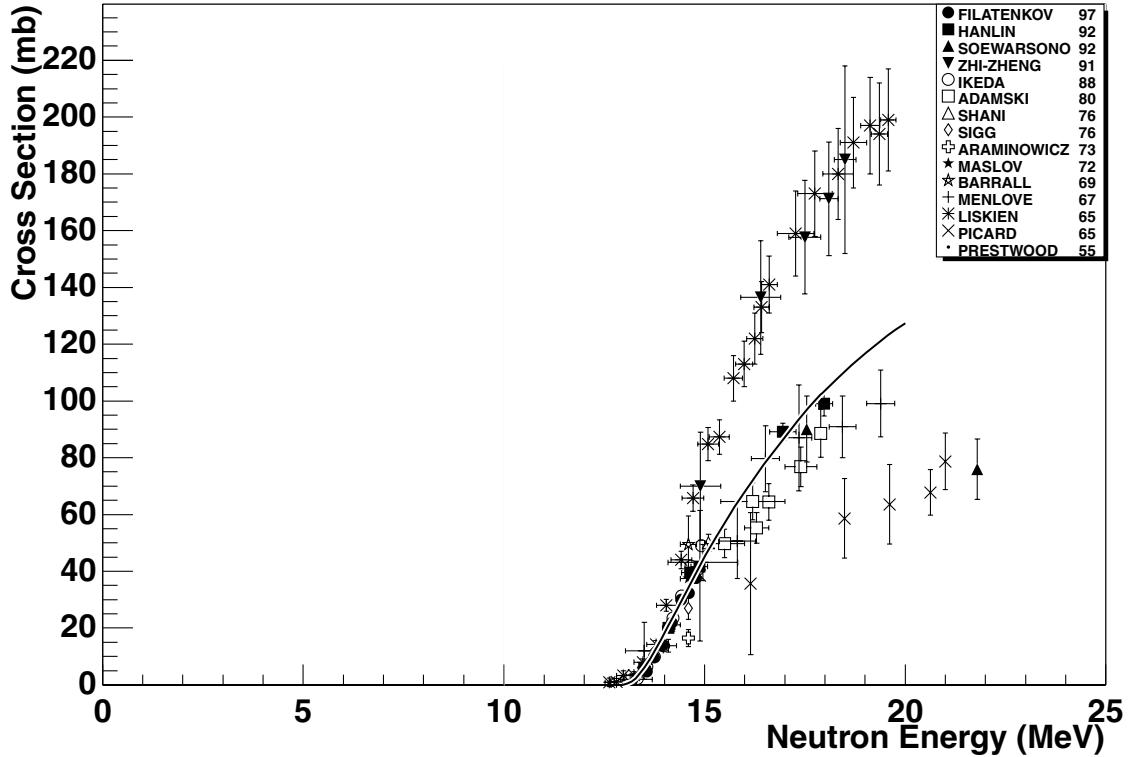
2.10. ^{23}Na (n,2n) ^{22}Na

final state: total
source: ADL-3

ADL-3 reproduces the experimental data below 15 MeV rather well. However, the experimental situation above 15 MeV is inconsistent and the data show three different trends. ADL-3 follows reasonably the intermediate trend, which includes the most recent data, such as Hanlin92, Filatenkov97 and Soerwarsono92. This is also supported by recent measurement of Wagner [33], which gives 115 mb at 19.6 MeV. The higher data set consists of Liskien65 and Zhi-zheng91, while the lower one is due to Picard65. Both these outer trends can be disregarded.

^{23}Na(n,γ)^{24}Na

●	MAGNUSSON	80
■	SIGG	76
▲	HOLUB	72
▼	RYVES	70
★	YAMAMURO	70
□	HASAN	68
△	MENLOVE	67
◇	CSIKAI	66
⊕	LE RIGOLEUR	66
○	MACKLIN	63
✫	MEADOWS	61
+	BAME JR	59
×	JOWITT	59
✳	LYON	59
·	BOOTH	58
⊚	KONONOV	58
⊠	LEIPUNSKIJ	58
⬢	PERKIN	58
◈	COCKING	57
⊞	MACKLIN	57
✭	GROSHEV	55
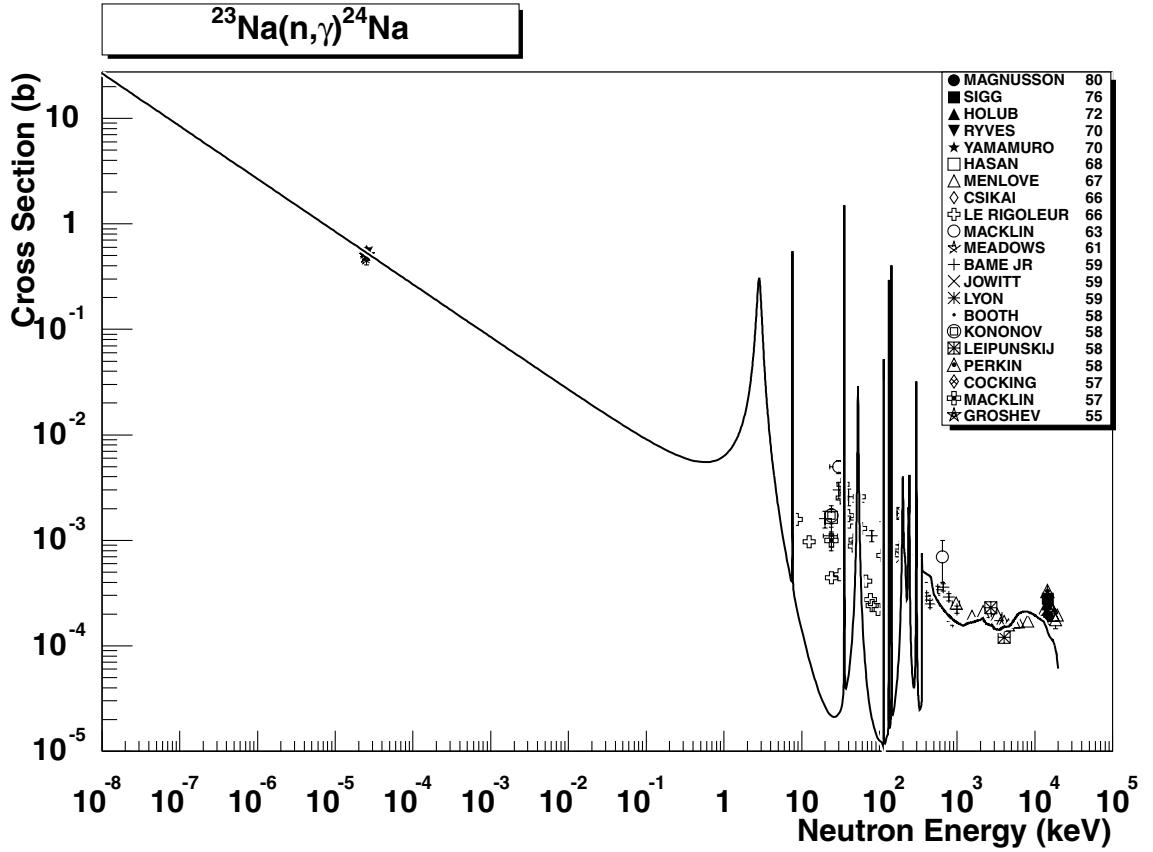
2.11. ^{23}Na (n,γ) ^{24}Na

final states: g.s., meta
source: EAF-4.1 (JEF-2.2)

The JEF-2.2 evaluation has adopted the JENDL-3.2 data. The splitting into g.s. and meta-1 cross-sections is based on the experimental data from Ref. [26] and applied up to the end of the resolved resonance region. The energy dependent branching ratio systematics [2] is applied for the high energy region. The total cross-section reasonably reproduces experimental points at the thermal energy and also the smooth component above 400 keV. The pre-equilibrium region around 15 MeV slightly underestimates the experimental data, probably due to the application of a simplified D-SD model in the calculation.

Figure: ^{24}Mg(n,p)^{24}Na cross section (mb) versus Neutron Energy (MeV), with data from the following references:

● GERALDO	89
■ HANLIN	89
▲ JI-ZHOU	89
▼ KOLKOWSKI	89
★ IKEDA	88
□ JANCZYSZYN	88
△ KOBAYASHI	88
◇ MOLLA	86
✥ GUPTA	85
○ HYVOENEN	78
✬ MOSTAFA	76
＋ MANNHART	75
✕ ROBERTSON	73
✳ PRASAD	71
· BARRALL	69
◎ CLATOR	69
⊠ VONACH	68
◬ FERGUSON	67
◈ PASQUARELLI	67
⊕ LISKIEN	66
✫ PAULSEN	65
◉ STRAIN	65
⊞ IMHOF	64
⊛ BUTLER	63
⊡ GABBARD	62
◭ DEPRAZ	60
◆ TEWES	60
✣ KERN	59
✩ COHEN	56
◎ PAUL	53

2.12. ^{24}Mg (n,p) ^{24}Na

final states: g.s., meta
source: IRDF-90.2

The evaluation from the dosimetry library IRDF-90.2 has been adopted and the branching ratio systematics of Ref. [2] has been applied to generate cross-sections to the ground state and to the metastable state. The total cross-section agrees very well with the experimental data in the whole energy range.
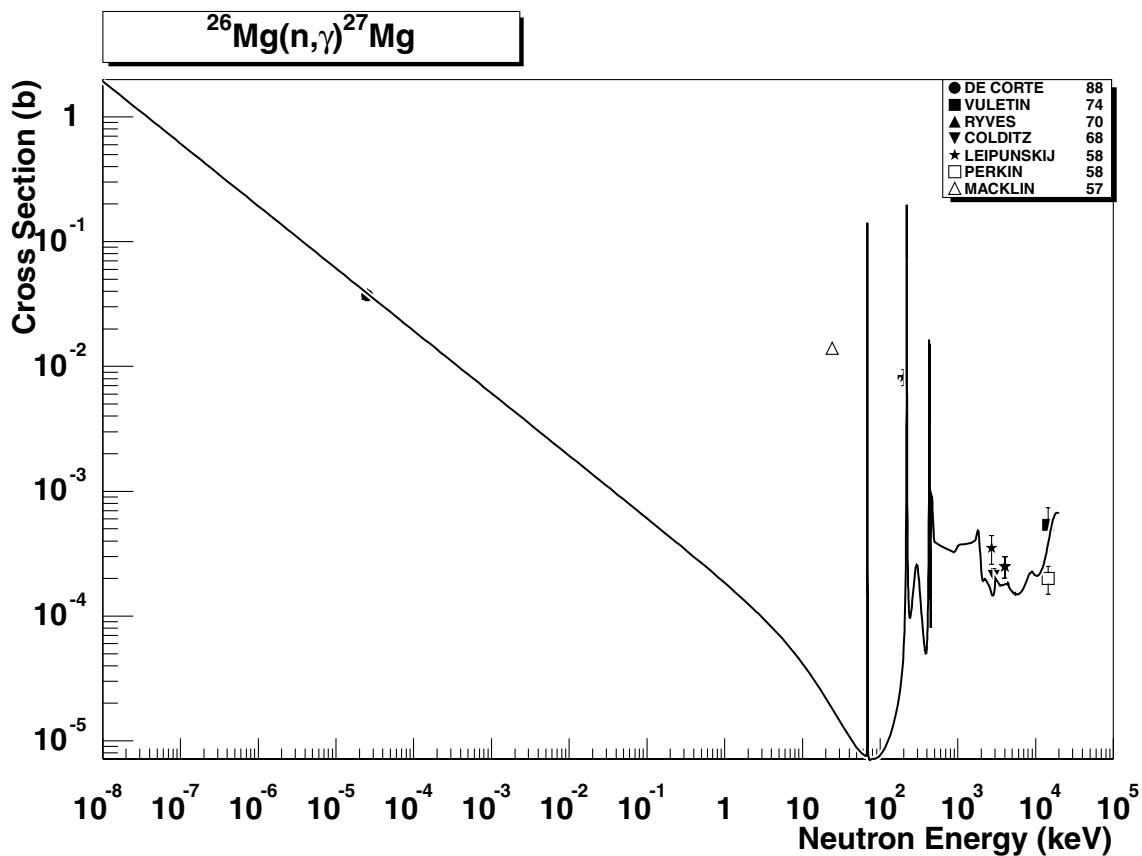
2.13. ^{26}Mg (n,γ) ^{27}Mg

final state: total
source: EAF-4.1 (JENDL-3.1)

The experimental data base is rather small. The JENDL-3.1 evaluation agrees well with the thermal point of De Corte88 and reasonably well with other experimental data except Macklin57 at about 30 keV. The latter one is an averaged value and should not be considered.
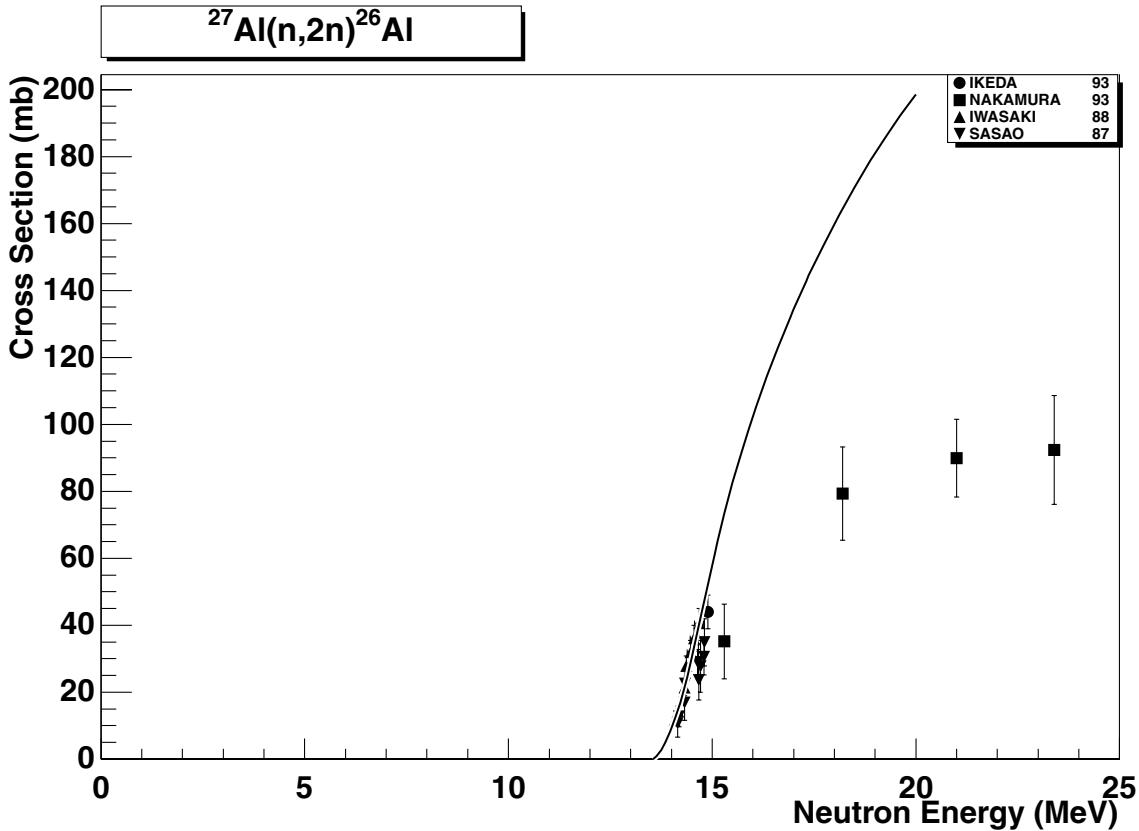
2.14. ^{27}Al (n,2n) ^{26}Al

final states: g.s., meta
source: ADL-3

ADL-3 evaluation follows nicely the experimental points below 15 MeV. The total cross-section is measured by Iwasaki88 only. Sudbrock99, Ikeda93, Nakamura93 and Sasao87 report cross-sections to the g.s.. However, population of the meta state below 15 MeV incident energy is so small that they have been plotted as total. Nakamura93 is by a factor 2 lower than the recommended evaluation. The recent data by Wallner97 [34] (not plotted due to lack of numerical data) partially confirm this trend being 30 to 40% lower than the ADL-3 evaluation. There are indications that the recommended evaluation is too high also above 15 MeV. The sum of the meta state contribution (~40 mb at 18 MeV according to Arnold65) and the ground state cross-section (~80 and 90 mb according to Nakamura93 and Wallner97) is well below the recommended value of about 160 mb. The g.s. and metastable cross sections result from model calculations.

^{27}Al(n,nα)^{23}Na
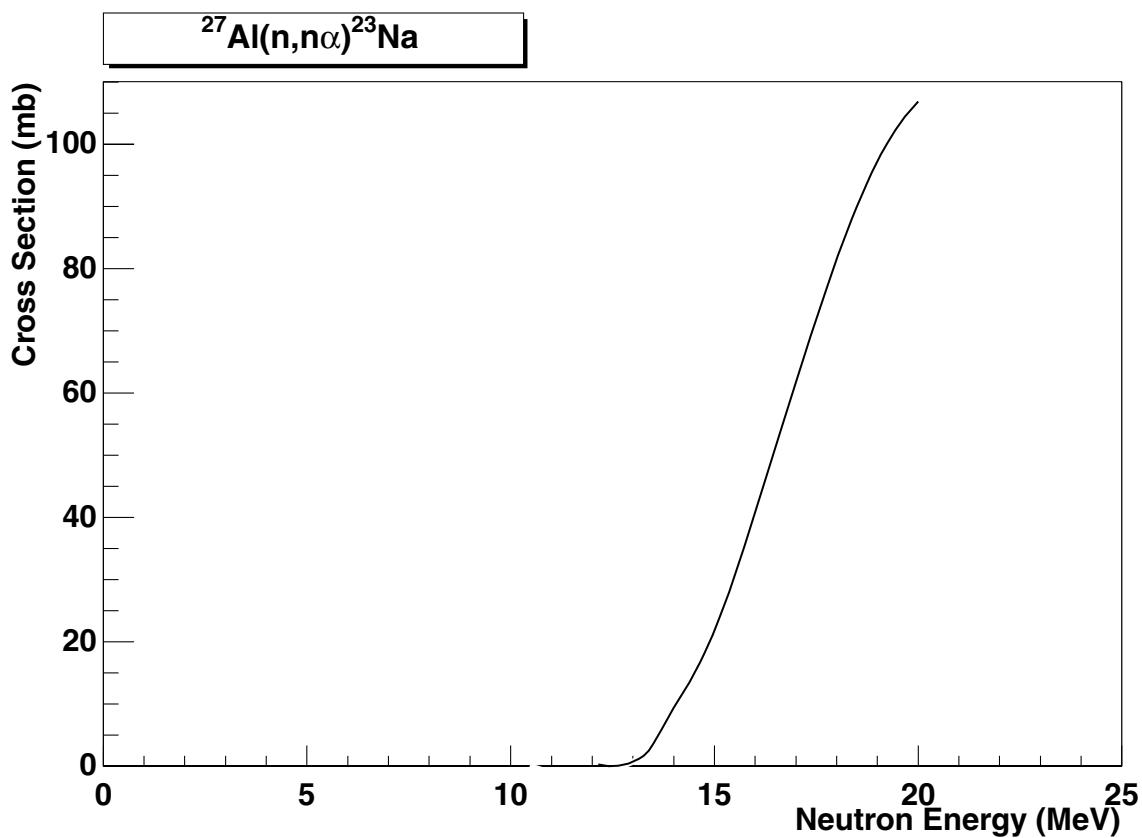
2.15. ^{27}Al (n,nα) ^{23}Na

final state: total
source: ADL-3

No EXFOR data are available. The evaluation results from the calculation with the STAPRE code, results of which are usually reliable.

The legend in the figure reads:

+	BUDNAR	79
·	RIGAUD	74
×	HOLUB	72
✳	MALIK	70
○	RYVES	70
□	COLDITZ	68
△	HASAN	68
◇	OKAZAKI	68
✚	PETO	67
★	CARRE	66
●	CSIKAI	63
▲	CALVI	62
▼	SHER	62
■	GIBBONS	61
	STEFANESCU	61
◎	BROSE	60
⊞	FUKETA	60
△	TATTERSALL	60
◈	VERVIER	59
✚	KONONOV	58
⊛	LEIPUNSKIJ	58
⊠	PERKIN	58
⊗	MACKLIN	57
⊞	HENKEL	53
⊞	BENOIST	51
▲	HUMMEL	51
✚	HENKEL	50
	BEGHIAN	49
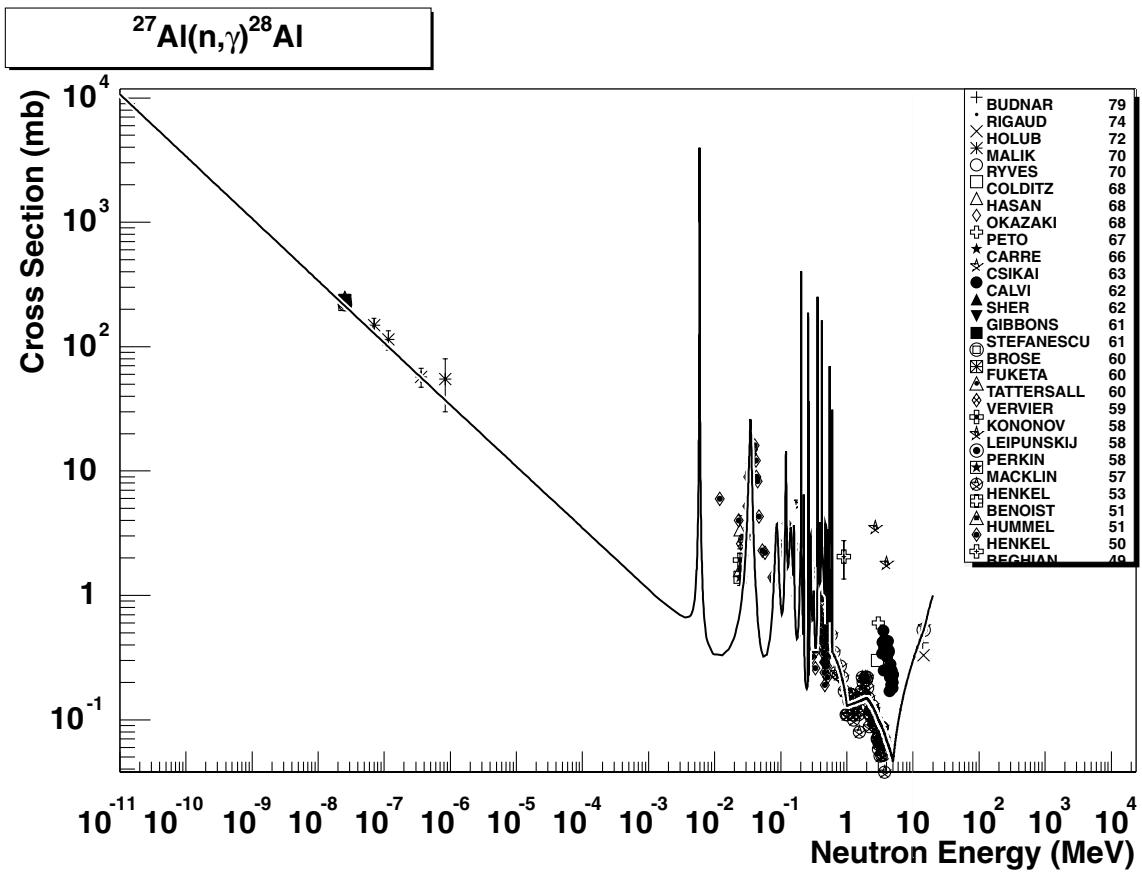
2.16. ^{27}Al (n,γ) ^{28}Al

final state: total
source: EAF-4.1 (JEF-2.2)

ENDF/B-V evaluation was adopted in JEF-2.2 and reproduces reasonably the majority of experimental information. Several old measurements (Beghian49, Leipunskij58, Calvi62 and Peto67) between 1-4 MeV seem to be too large, compared to the trend of other data.

^{27}Al(n,p)^{27}Mg

●	FILATENKOV	97
■	IKEDA	93
▲	GARLEA	92
▼	KLOCHKOVA	92
★	IKEDA	88
□	KOBAYASHI	88
△	KUDO	88
◇	KLOCHKOVA	87
⊕	MEADOWS	87
○	CHIMOYE	86
✩	CSIKAI	86
+	BRADLEY	85
×	ENZ	85
✳	GARLEA	85
·	GUPTA	85
◎	KOBAYASHI	85
⊠	TAHIR	85
△	HUSAIN	83
◇	SHCHEBOLEV	83
⊞	CSIKAI	82
✩	HARPER	82
⊙	QAIM	82
⊠	WELCH	81
⊗	NGOC	79
⊞	ANDERSSON	78
△	GHOSE	78
◆	JARJIS	78
⊕	LAKSHMANA	78
✳	MELENTIEV	78
◎	RYVES	78
⊞	AI	77
△	MOSTAFA	76
◇	SIGG	76
⊕	ALEKSANDROV	75
✩	SMITH	75

44

● DRESLER	73
■ ROBERTSON	73
▲ MOGHARRAB	72
▼ NEMILOV	72
★ ROBERTSON	72
□ PRASAD	71
△ SALAITA	71
◇ HUSAIN	70
⊕ SCHANTL	70
○ RAMA PRASAD	69
✬ CUZZOCREA	68
+ RANAKUMAR	68
× TIWARI	68
✳ FERGUSON	67
· GRUNDL	67
◎ BASS	66
⊠ MITRA	66
⬩ STRAIN	65
◈ BONAZZOLA	64
⊞ CALVI	62
✭ GABBARD	62
◉ HASSLER	62
⊞ KANTELE	62
⊛ LANGMANN	62
⊞ MUKHERJEE	61
⬭ POLLEHN	61
◆ SAKISAKA	61
⊕ DEPRAZ	60
✭ KHURANA	60
◎ MANI	60
⊞ HUDSON JR	59
△ POULARIKAS	59
◇ ALLAN	57
⊕ BROWN	57
✭ YASUMI	57
◉ HENKEL	54
▣ PAUL	53
△ FORBES	52

2.17. ^{27}Al (n,p) ^{27}Mg

final state: total
source: RRDF-98

A very extensive data base is available, covering the period from 1952 to 1997, which shows a large data scatter in particular above 12 MeV. RRDF-98 evaluation runs intermediate to the scatter of data and around 13-15 MeV fits nicely the latest reliable data of Ikeda93 and Filatenkov97.

^{27}Al(n,α)^{24}Na

●	FILATENKOV	97
■	IKEDA	93
▲	ZONGYU	93
▼	GARLEA	92
★	GERALDO	89
□	HAN-LIN	89
△	KORNILOV	89
◇	MOISEEV	89
✢	GREENWOOD	87
○	MEADOWS	87
☆	MUYAO	87
+	CHIMOYE	86
×	CSIKAI	86
✳	CSIKAI	86
·	GARLEA	84
◎	KUDO	84
⊠	ENZ	83
△	FIRKIN	83
◇	CSIKAI	82
✠	FRIEDMANN	81
✶	WELCH	81
◉	GARUSKA	80
⊠	SWINHOE	79
✷	ANDERSSON	78
⊞	NORDBORG	78
▲	RYVES	78
◆	MOSTAFA	76
✠	ROBERTSON	73
✩	TR	72
◎	SALAITA	71
⊞	LEBOWITZ	70
△	VONACH	70
◇	ARON	64

46

^{27}Al(n,α)^{24}Na

● BARRALL	69
■ CRUMPTON	69
▲ BOSCHUNG	68
▼ CUZZOCREA	68
★ FERGUSON	67
□ GRUNDL	67
△ MENLOVE	67
◇ MINETTI	67
✠ HEMINGWAY	66
○ LISKIEN	66
✫ BORMANN	65
＋ PAULSEN	65
✕ SEEBECK	65
✳ STRAIN	65
・ ARON	64
◎ BONAZZOLA	64
⊞ IMHOF	64
◮ BUTLER	63
◈ JERONYMO	63
⊕ GABBARD	62
✶ LANGMANN	62
◉ STROHAL	62
⊠ BAYHURST	61
⊗ BORMANN	61
⊟ SCHMITT	61
◮ DEPRAZ	60
◆ KHURANA	60
✠ MANI	60
✫ TEWES	60
◎ KERN	59
⊞ POULARIKAS	59
△ GRUNDL	58
◇ KUMABE	58
✠ YASUMI	57
✫ PAUL	53
◉ FORBES	52

2.18. ^{27}Al (n,α) ^{24}Na

final states: g.s., meta
source: IRDF-90.2

The IRDF-90.2 evaluation of the total cross-section correctly describes all recent experimental data. Some of the older data (e.g. Tewes60) may be disregarded, they are in significant disagreement with the latest experiments. The branching ratio systematics has been applied to obtain the g.s. and metastable cross sections.

28Si(n,p)28Al

● KLOCHKOVA	92
■ KAWADE	90
▲ KLOCHKOVA	90
▼ IKEDA	88
○ CHIMOYE	86
□ CSIKAI	86
△ CSIKAI	86
◇ BRADLEY	85
⊕ PEPELNIK	85
★ NGOC	80
☆ GHOSE	78
+ SHCHEBOLEV	77
✳ ALEKSANDROV	75
✕ DRESLER	73
· ROBERTSON	73
◎ PRASAD	71
⊠ SINGH	70
⧍ CRUMPTON	69
◈ RANAKUMAR	68
⊞ PASQUARELLI	67
✶ BASS	66
◉ MITRA	66
⊠ KHURANA	65
⊛ STRAIN	65
⊟ BIRK	63
⧍ JERONYMO	63
◆ MAINSBRIDGE	63
⊕ KHURANA	60
✰ KERN	59
◎ COHEN	56
⊞ MARION	56
⧍ PAUL	53
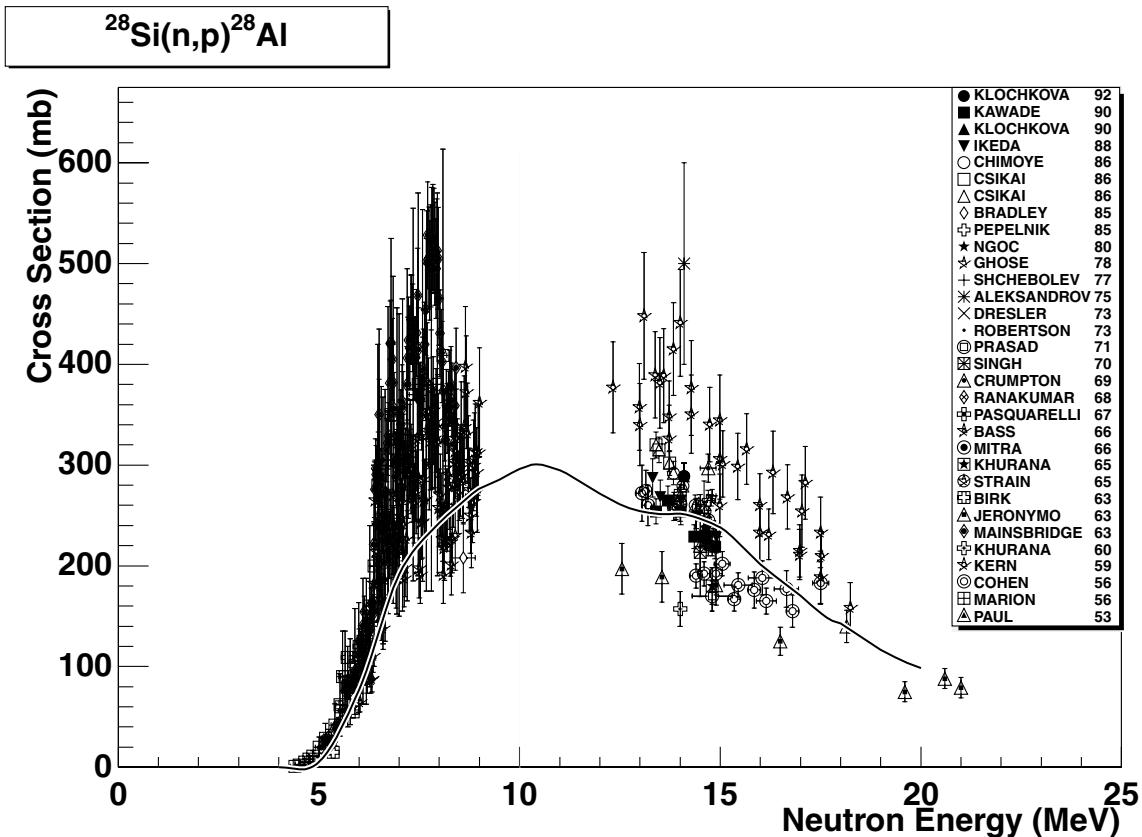
2.19. ^{28}Si (n,p) ^{28}Al

final state: total
source: JENDL-Act96

Experimental data, existing in two energy regions (4-9 MeV and 13-20 MeV), have a very broad distribution due to a large number of old data with inferior quality. The adopted JENDL-Act96 evaluation fits the recent experimental data of Klochkova92,90, Kawade90 and Ikeda88 between 13-15 MeV very well. The low energy part of the excitation curve (below 10 MeV) lies at the lower part of the experimental data band, however, this is still probably a good representation.

^{28}Si(n,np)^{27}Al + ^{28}Si(n,d)^{27}Al
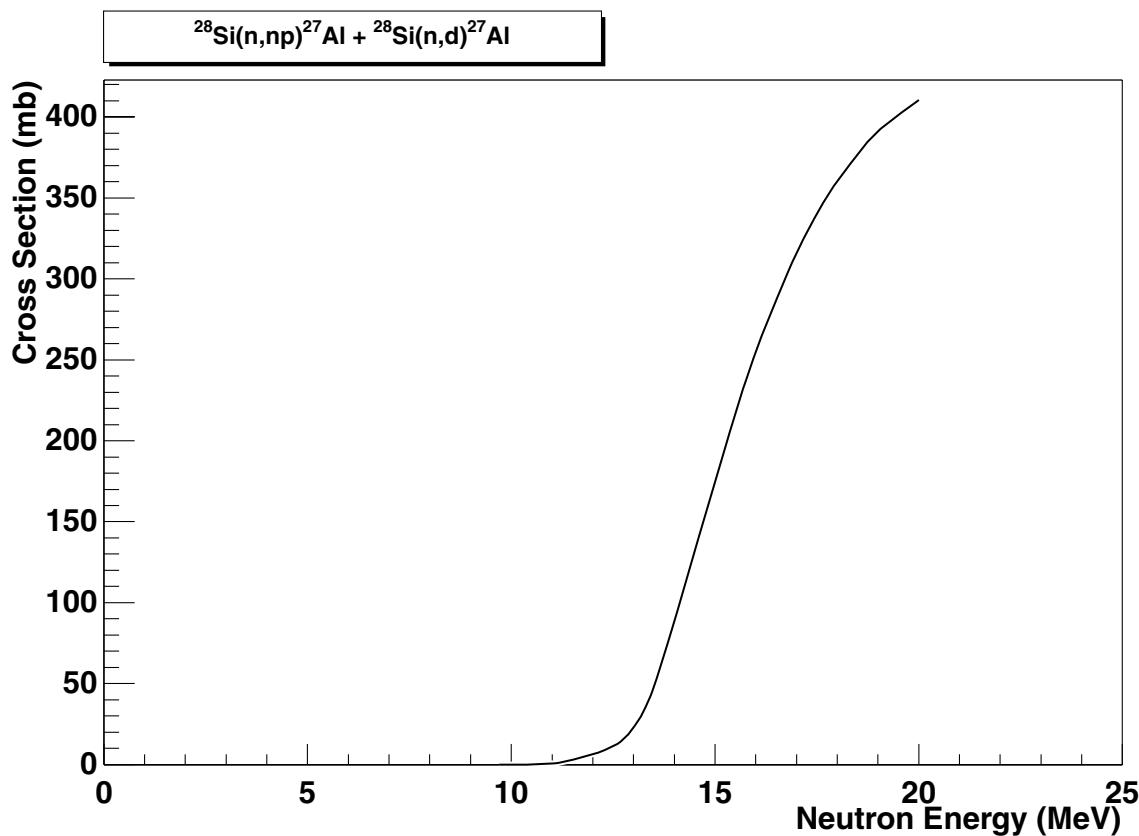
2.20. ^{28}Si (n,d+np) ^{27}Al

final state: total
source: JENDL-Act96

No experimental results are available. The data are stored separately for (n,d) and (n,np) reaction channels.

²⁹Si(n,p)²⁹Al

Legend:
- ● KAWADE 92
- ■ DIGHE 91
- ▲ KOBAYASHI 91
- ▼ GOPYCH 90
- ○ IKEDA 88
- □ PEPELNIK 85
- △ NGOC 80
- ◇ SHCHEBOLEV 77
- ✛ ROBERTSON 73
- ★ PRASAD 71
- ✩ SINGH 70
- + RANAKUMAR 68
- ✳ PASQUARELLI 67
- × STRAIN 65
- · PAUL 53

Cross Section (mb) vs Neutron Energy (MeV)
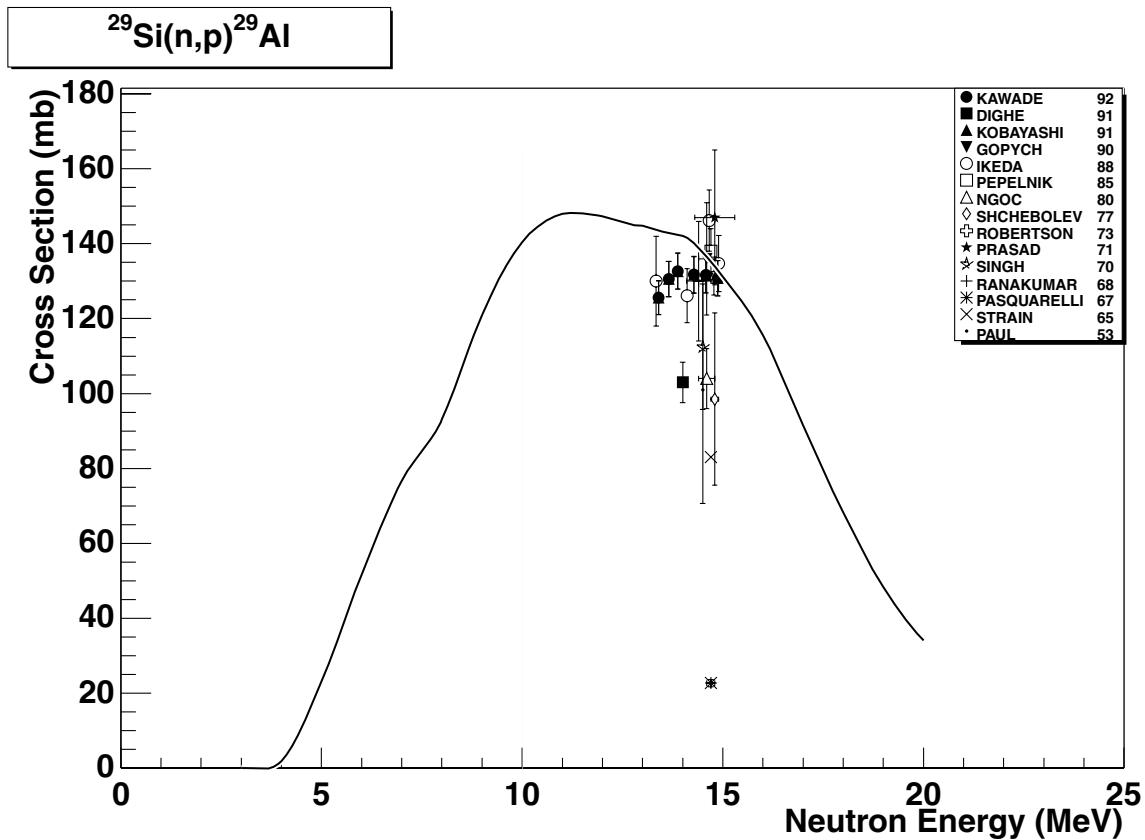
2.21. ^{29}Si (n,p) ^{29}Al

final state: total
source: JENDL-Act96

JENDL-Act96 evaluation slightly overestimates experimental data of Kawade96 but agrees with data of Gopycs90 and lies between the data of Ikeda88. As for the remaining (older) data around 14-15 MeV, the excitation curve runs in the middle of them. A slight decrease (10-15%) of the flat part of the excitation curve may be considered.
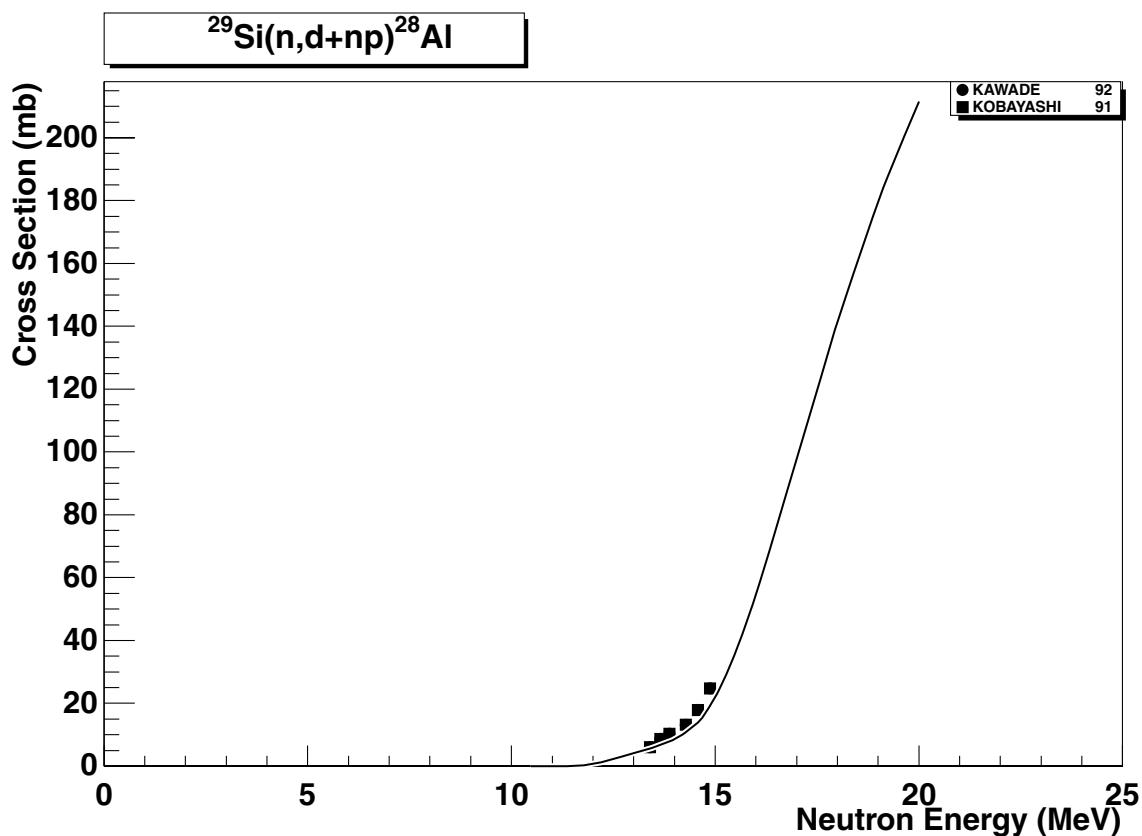
^{29}Si(n,d+np)^{28}Al

2.22. ^{29}Si (n,d+np) ^{28}Al

final state: total
source: JENDL-3.1 [(n,np)], ADL-3 [(n,d)]

Two measurements, up to 15 MeV only, are reported in EXFOR. The evaluated cross-sections reproduce these experiments very well. The data are stored separately for (n,d) and (n,np) reaction channels.
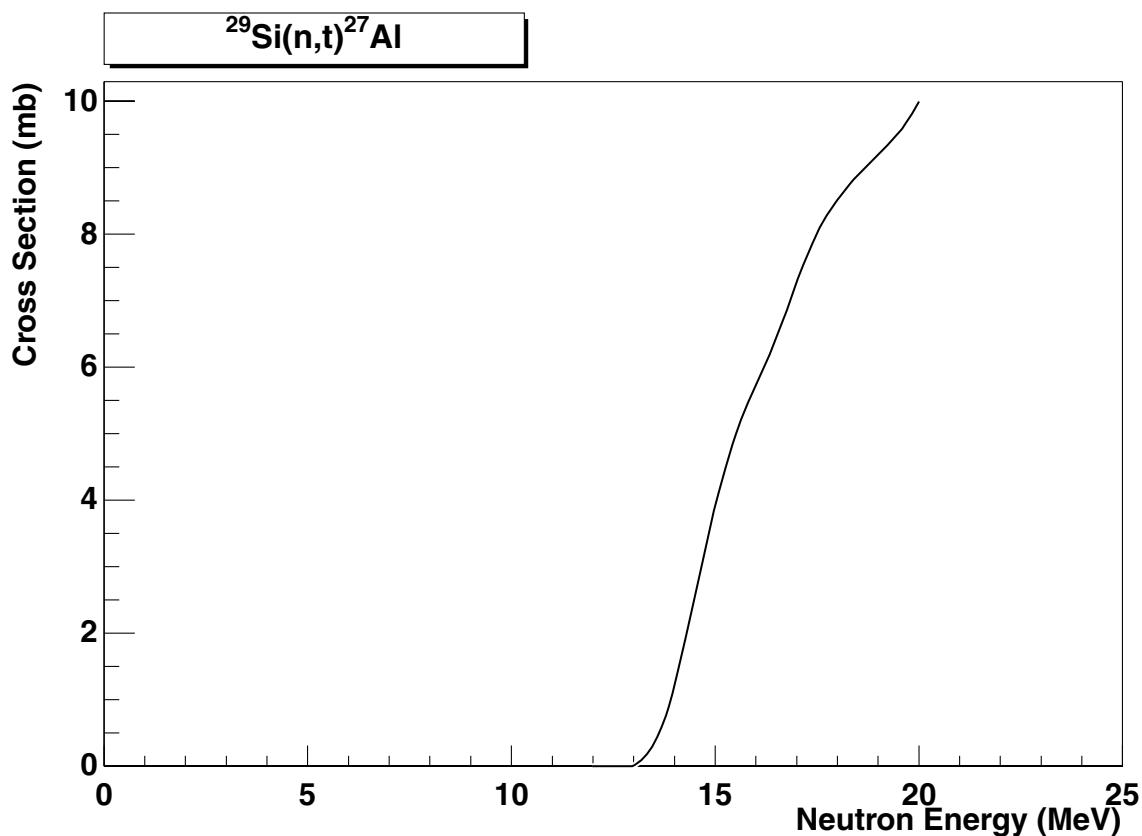
^{29}Si(n,t)^{27}Al

2.23. ^{29}Si (n,t) ^{27}Al

final state: total
source: ADL-3

No EXFOR data are available. The evaluation results from the calculation with the STAPRE code. The evaluation is supported by a reasonable value (C/S= 1.18) against the systematics (see Ref. [2]).

Figure: ^{30}Si(n,α)^{27}Mg

Legend:
- ● BONDAR´KOV 95
- ■ GOPYCH 90
- ▲ KAWADE 89
- ▼ IKEDA 88
- ★ JANCZYSZYN 82
- □ JANCZYSZYN 82
- △ GARUSKA 80
- ◇ HERMAN 80
- ⛊ SHCHEBOLEV 77
- ○ ROBERTSON 73
- ✫ SINGH 70
- + RANAKUMAR 68
- × PASQUARELLI 67
- ✳ KHURANA 65
- · KHURANA 60
- ◎ PAUL 53
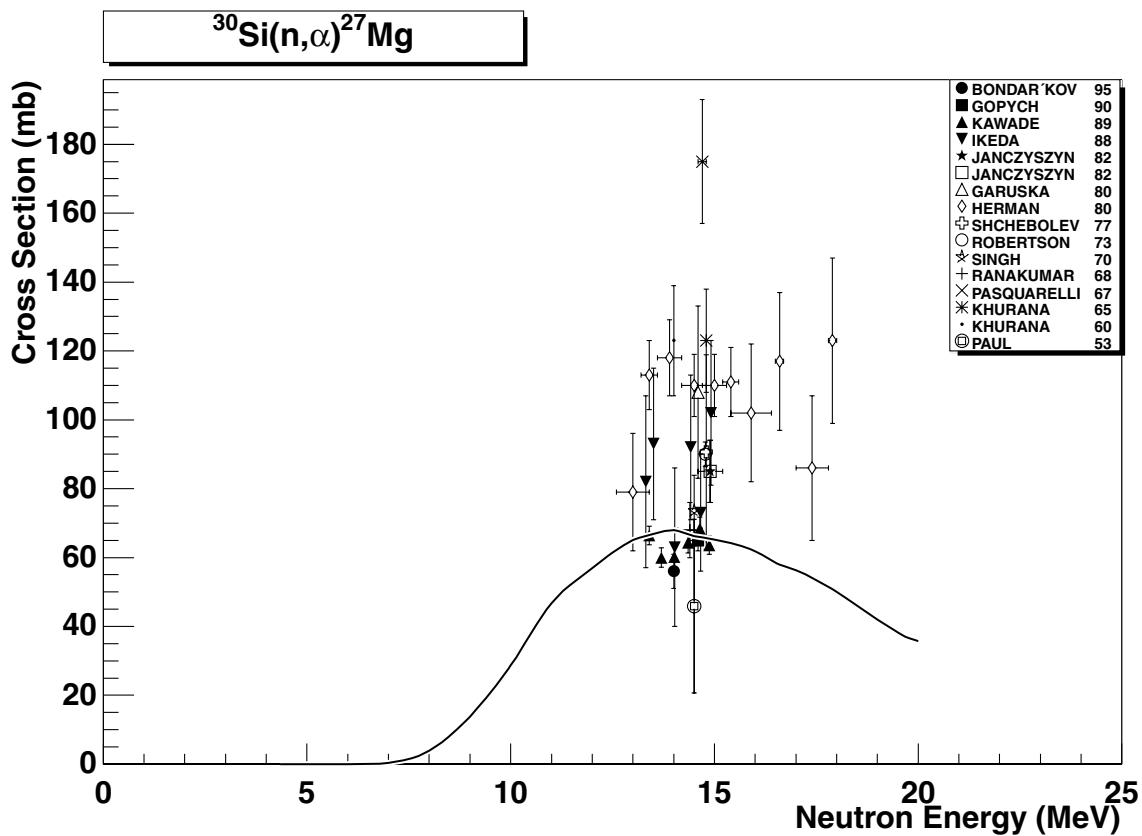
2.24. ^{30}Si (n, α) ^{27}Mg

final state: total
source: JENDL-3.1

The JENDL-3.1 evaluation fits the latest experimental data (Bondarkov95, Gopych90, Kawade89 and Ikeda88) at about 14 MeV. The older data (too large compared to the recent ones) can be disregarded.

53
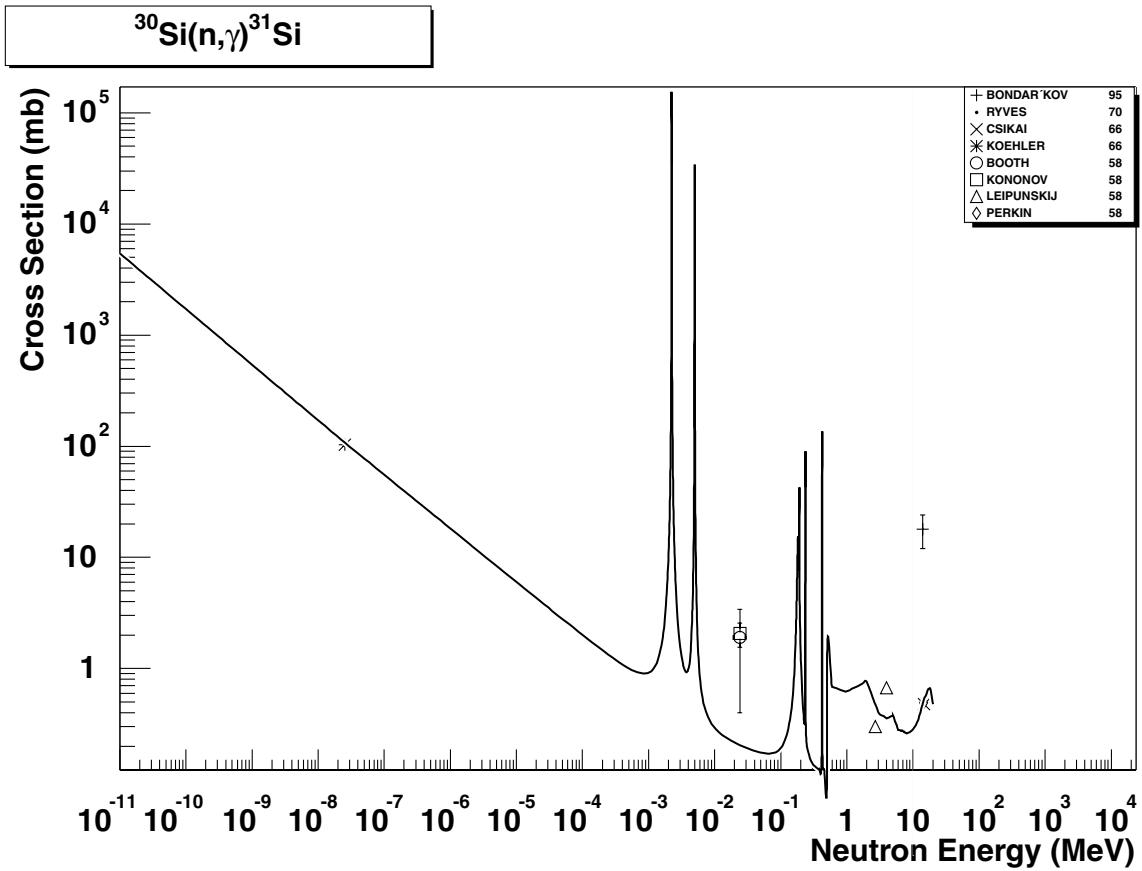
2.25. ^{30}Si (n,γ) ^{31}Si

final state: total
source: EAF-4.1 (JENDL-3.1)

The JENDL-3.1 evaluation fits the thermal cross-section value and reasonably reproduces the few experimental points above 1 MeV. Booth58 and Kononov58 at 30 keV are averaged values, the 14 MeV experimental point of Bondarkov95 is ignored. A value of about 20 mb at this energy is excluded. The pre-equilibrium component was missing in the original JENDL-3.1 evaluation and was added during the EAF-4.1 revision and is based on the PEQ- systematics (for details see Refs. [3] and [35].

The plot shows the cross section (b) versus Neutron Energy (keV) for $^{31}P(n,\gamma)^{32}P$. Legend entries: HOLDEN 94, BUDNAR 79, CSIKAI 67, MACKLIN 63.

2.26. ^{31}P (n,γ) ^{32}P
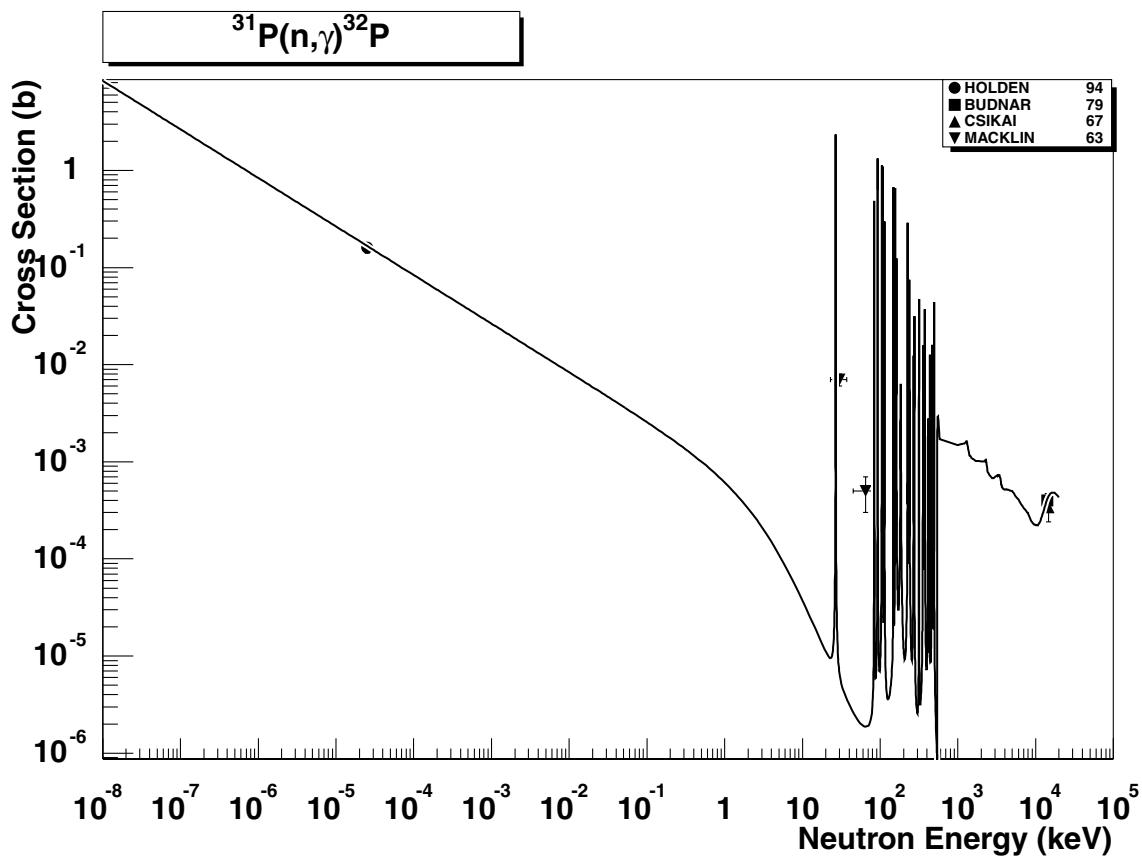
final state: total
source: EAF-4.1 (JEF-2.2)

JENDL-3.1 evaluation has been adopted in JEF-2.2 and reproduces well two experimental values at about 15 MeV. The excitation curve nicely reproduces the thermal cross section value of Holden94 [32] with C/E=1.04.

^{31}P(n,p)^{31}Si

●	ALEKSANDROV	75
■	ROBERTSON	73
▲	PRASAD	71
▼	SCHANTL	70
○	GRUNDL	67
□	PASQUARELLI	67
△	PAULSEN	66
◇	GRIMELAND	65
✛	HASSLER	62
★	KANTELE	62
✪	CUZZOCREA	60
+	GRUNDL	58
✳	MORITA	58
✕	PAUL	53
·	FORBES	52
◉	RICAMO	51
⊠	METZGER	48
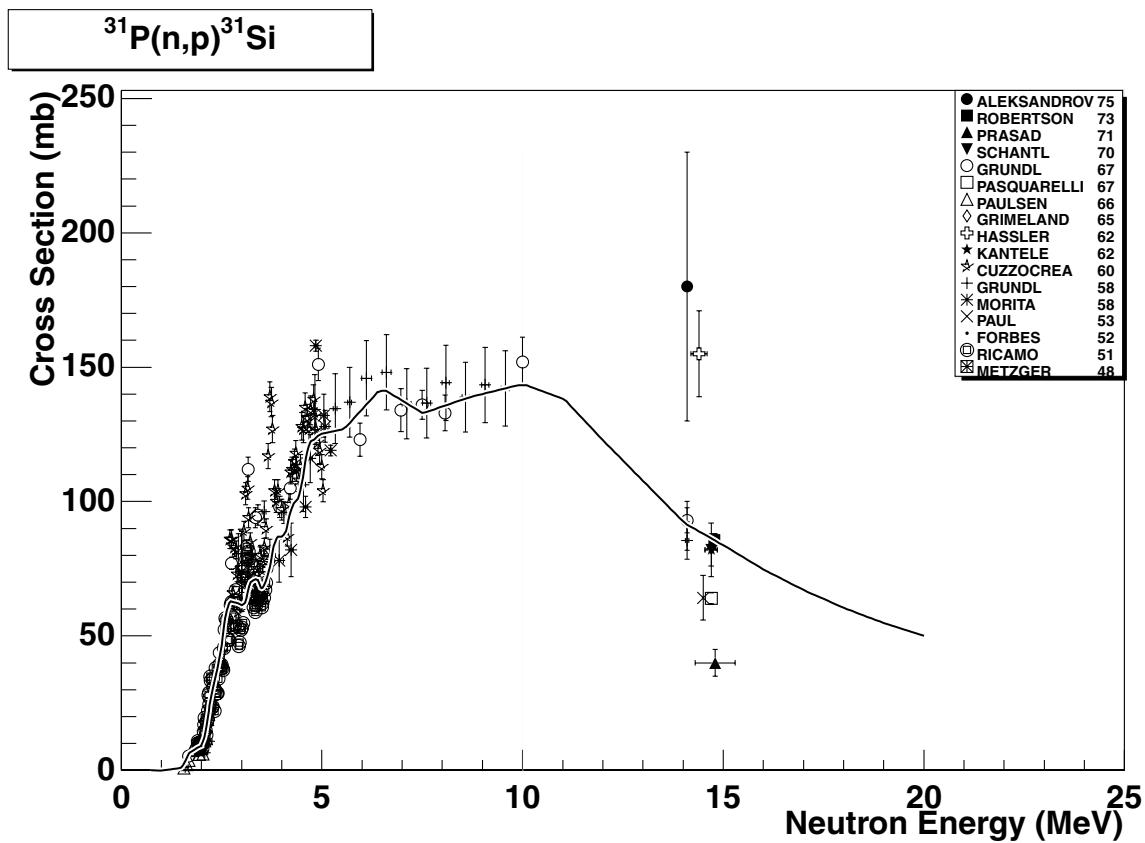
2.27. ^{31}P (n,p) ^{31}Si

final state: total
source: EAF-4.1 (IRDF-90.2)

IRDF-90.2 is in a good agreement with the experimental information in the whole energy range covered by the evaluation. Experimental data of Hassler62, Pasquarelli67 and Prasad71 at 14-15 MeV have been disregarded, they are very different from the recent values and also from the value based on the systematics.

^{31}P(n,α)^{28}Al

●	GOPYCH	90
■	KATOH	89
▲	JANCZYSZYN	82
▼	JANCZYSZYN	82
★	GARUSKA	80
□	ZUPRANSKA	80
△	HANNAPEL	79
◇	HOLMBERG	78
✚	SIGG	76
○	PASQUARELLI	67
✶	BASS	66
+	GRIMELAND	65
✕	PEIL	65
✳	STRAIN	65
·	BORMANN	63
◎	CUZZOCREA	63
✖	GABBARD	62
△	KANTELE	62
◇	PAUL	53

2.28. ^{31}P (n,α) ^{28}Al
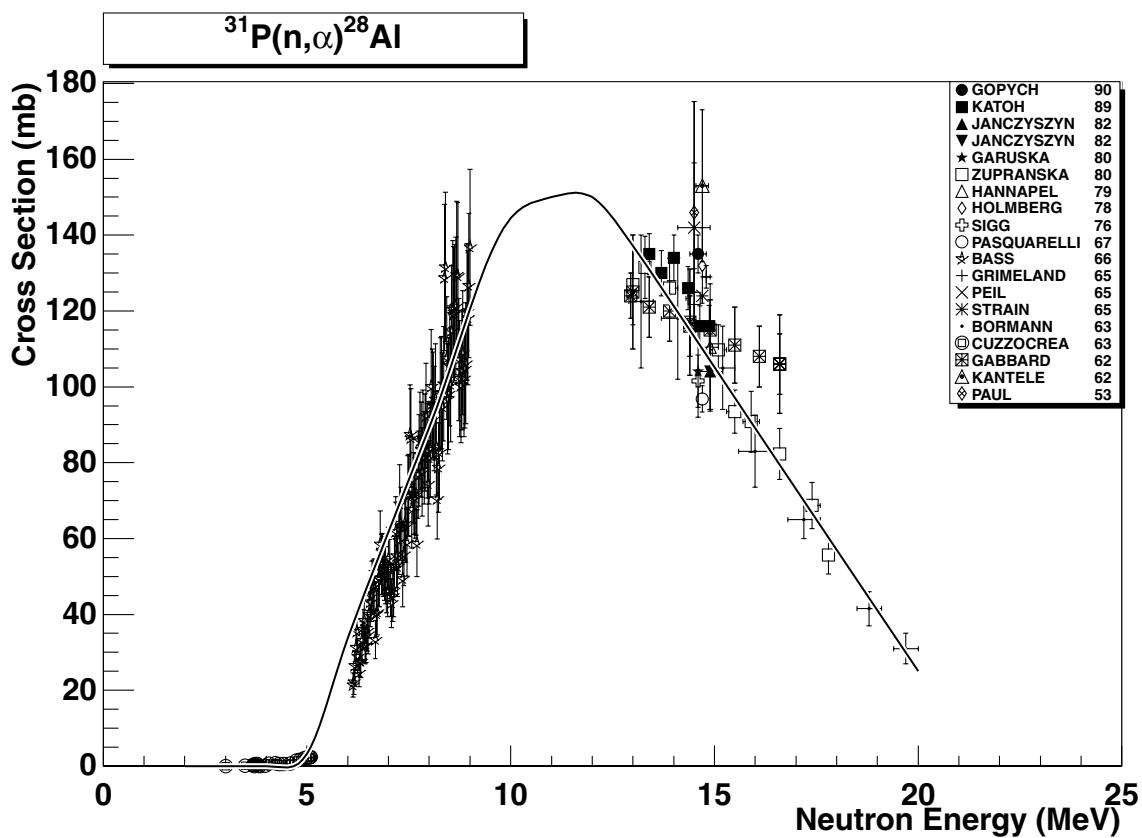
final state: total
source: JENDL-Act96

A very good agreement of the JENDL-Act96 evaluation against the large set of experimental data in the whole energy range.

^{32}S(n,p)^{32}P

● ROBERTSON	73
■ BARRALL	69
▲ LEVKOVSKIJ	68
▼ PASQUARELLI	67
★ PAULSEN	66
□ KHURANA	65
△ LEVKOVSKIJ	63
◇ SANTRY	63
⊕ KHURANA	60
○ ALLEN JR	57
✩ PAUL	53
+ RICAMO	51
✕ KLEMA	48
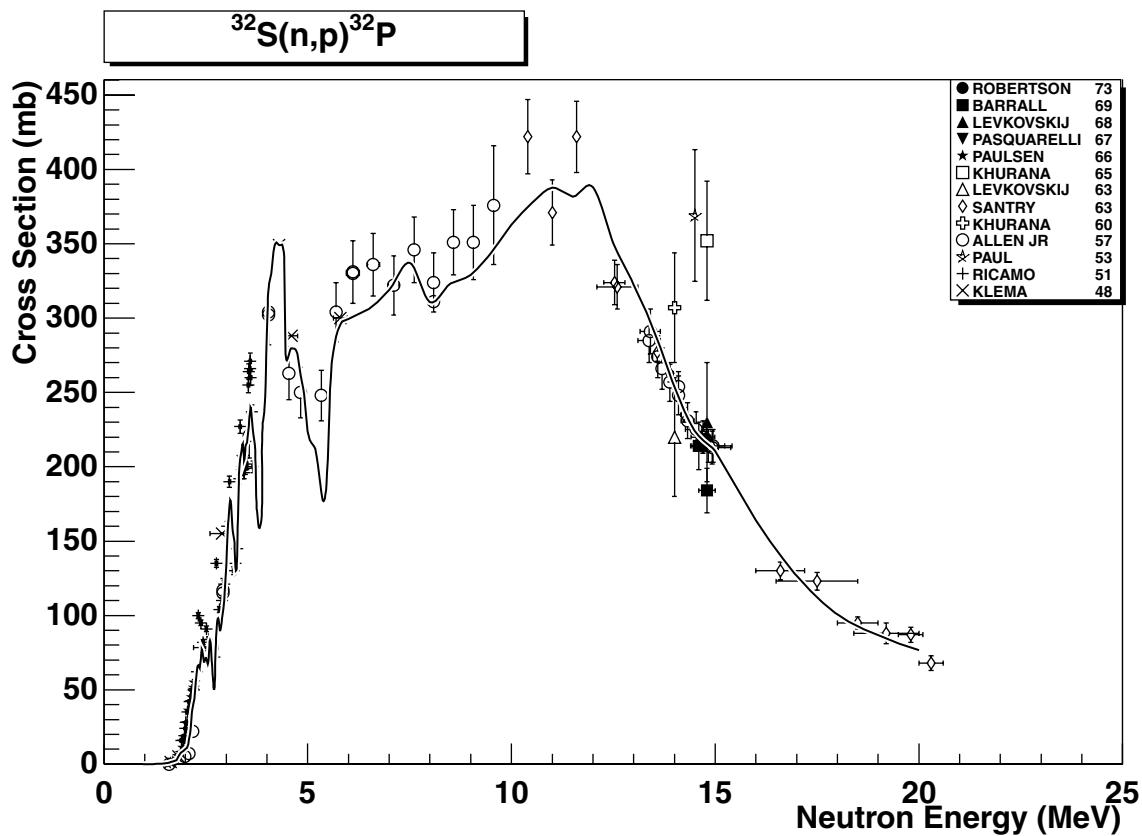
2.29. ^{32}S (n,p) ^{32}P

final state: total
source: IRDF-90.2

A good reproduction of the experimental information in the whole energy range by the IRDF-90.2 evaluation.

58
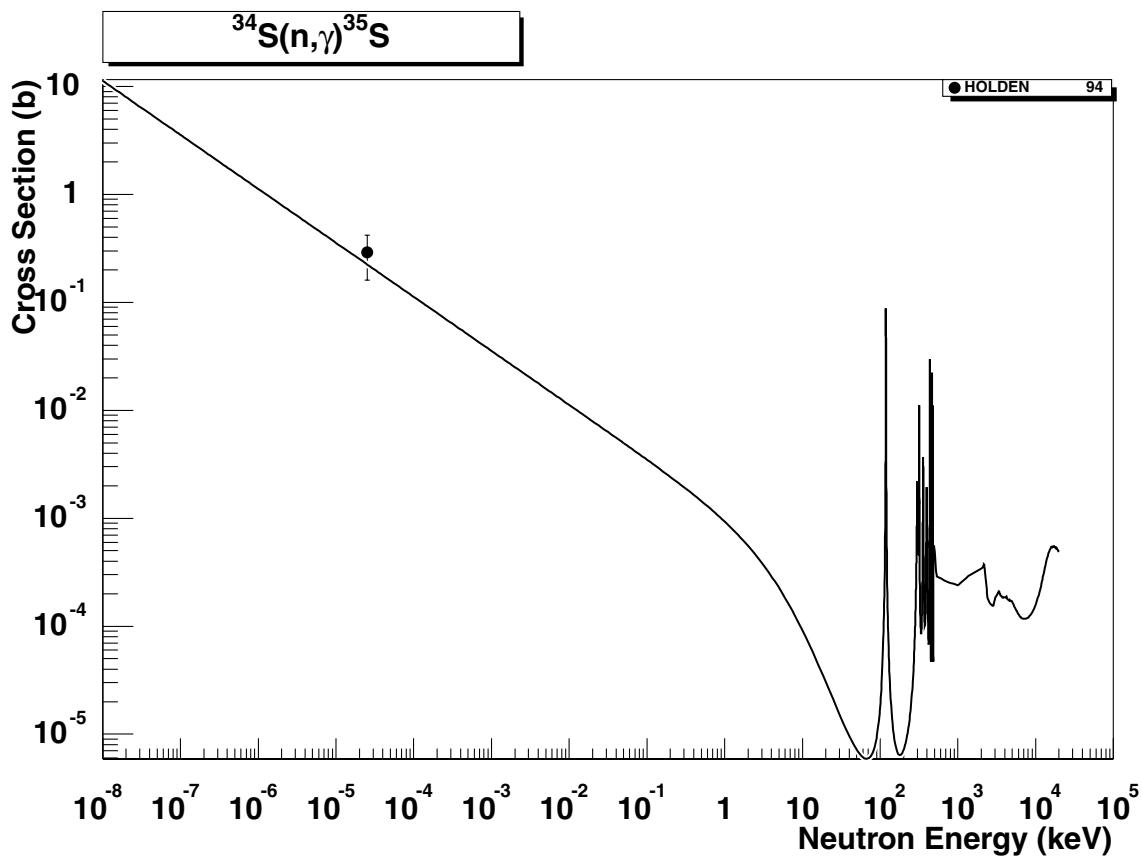
2.30. ^{34}S (n,γ) ^{35}S

final state: total
source: EAF-4.1 (JEF-2.2)

JENDL-3.2 data have been chosen for JEF-2.2. No experimental data outside resonance region are included in EXFOR, however, the value of thermal cross-section of Holden94 [32] is reproduced with C/E=0.77. The missing pre-equilibrium component was added based on the PEQ-systematics (for details see Refs. [3] and [35]).

^{34}S(n,p)^{34}P

● GUPTA	85	
■ NGOC	80	
▲ PRASAD	71	
▼ SCHANTL	70	
★ BORMANN	67	
□ PAUL	53	
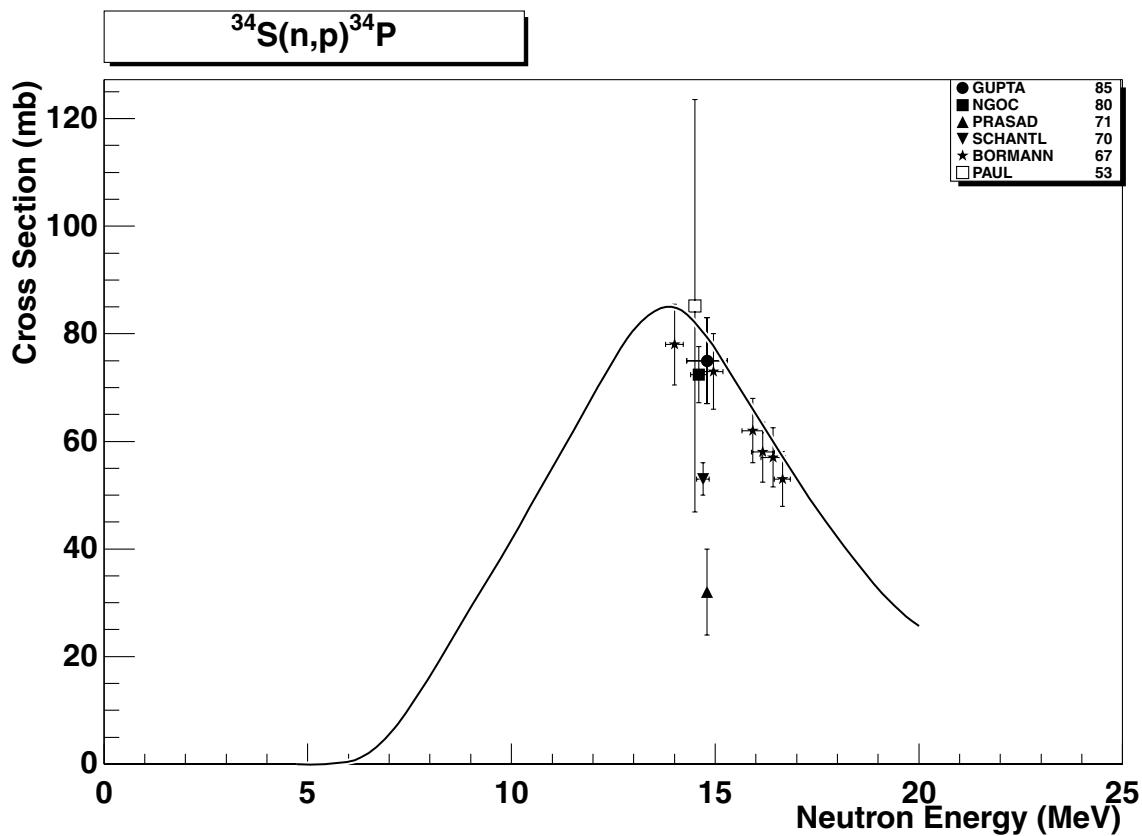
2.31. ^{34}S (n,p) ^{34}P

final state: total
source: ADL-3

ADL-3 evaluation slightly overestimates the experimental data. The renormalization of the whole excitation curve by a decrease of about 5% is recommended.

2.32. ^{36}S (n,γ) ^{37}S
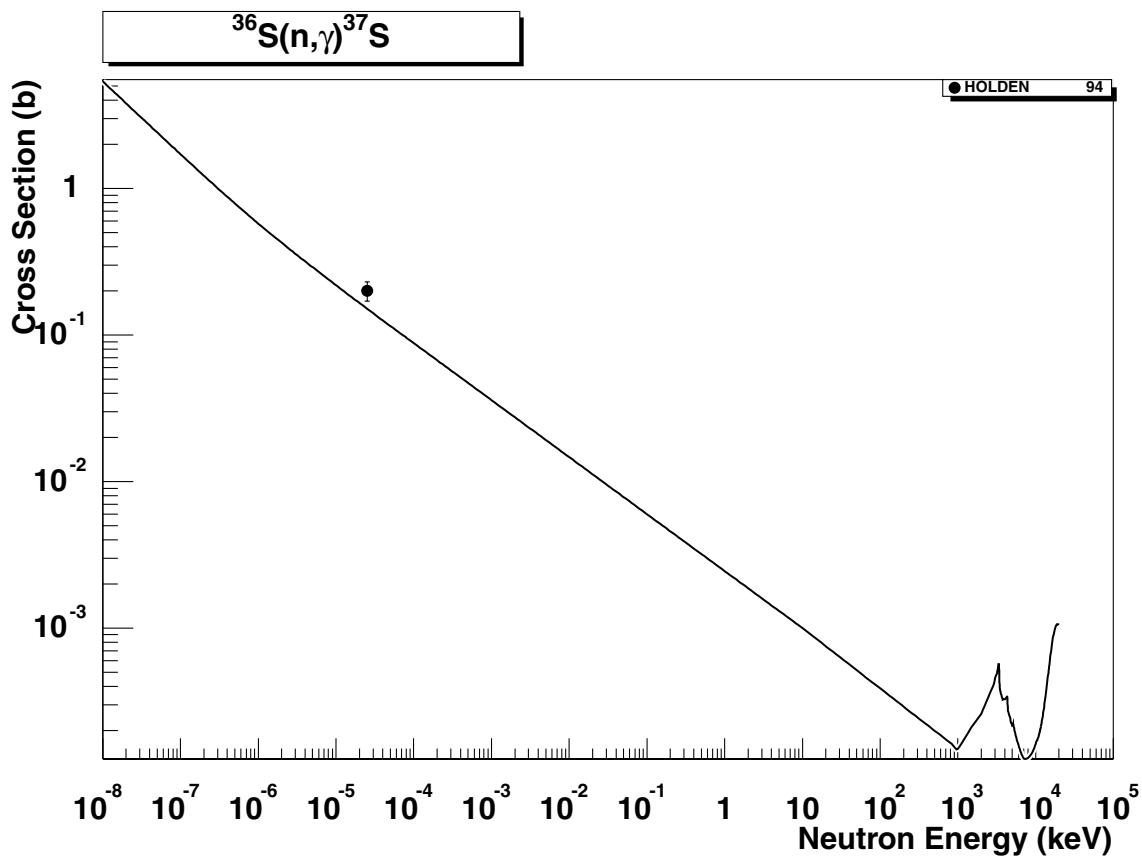
final state: total
source: EAF-4.1 (JEF-2.2)

JENDL-3.2 evaluation was adopted as a basis in JEF-2.2. For the adoption in EAF-4.1, the missing pre-equilibrium component was added based on the PEQ-systematics (for details see Refs. [3] and [35]). No experimental data have been found in the EXFOR data base. The thermal cross-section of Holden94 from Ref. [32] is slightly underestimated with C/E=0.76.

^{35}Cl(n,2n)^{34m}Cl

●	IKEDA	88
■	PEPELNIK	85
▲	HYVOENEN	78
▼	SRINIVASA	78
★	ARAMINOWICZ	73
□	PASQUARELLI	67
△	PRASAD	67
◇	STRAIN	65
⊕	KHURANA	61
○	RAYBURN	61
✰	MANI	60
+	SCALAN	58
×	PAUL	53
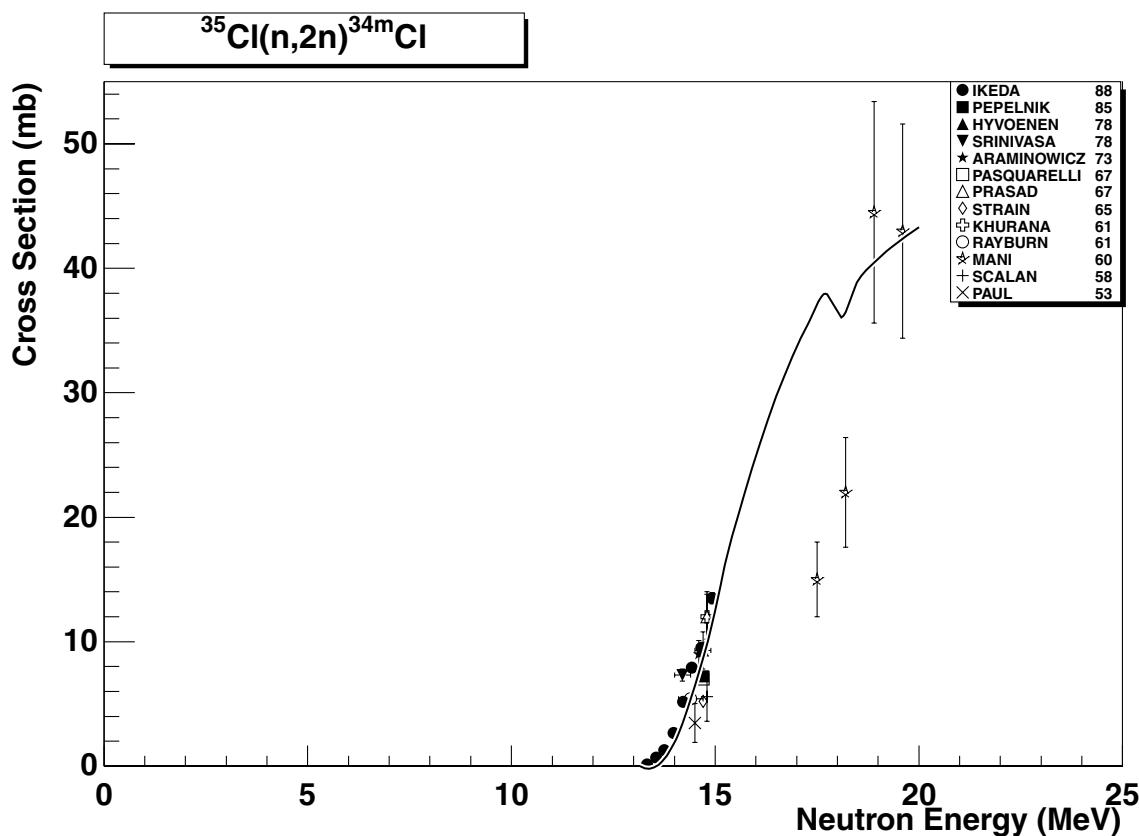
2.33. ^{35}Cl (n,2n) ^{34m}Cl

final states: g.s., meta
source: EAF-4.1

The reaction leading to the first isomeric state is the reference reaction. Branching ratio for cross-sections to the g.s. and meta state result from model calculations. The calculated excitation curve to metastable state is in good agreement with the experimental data. First two data points of Mani60 are wrong.

^{35}Cl(n,γ)^{36}Cl
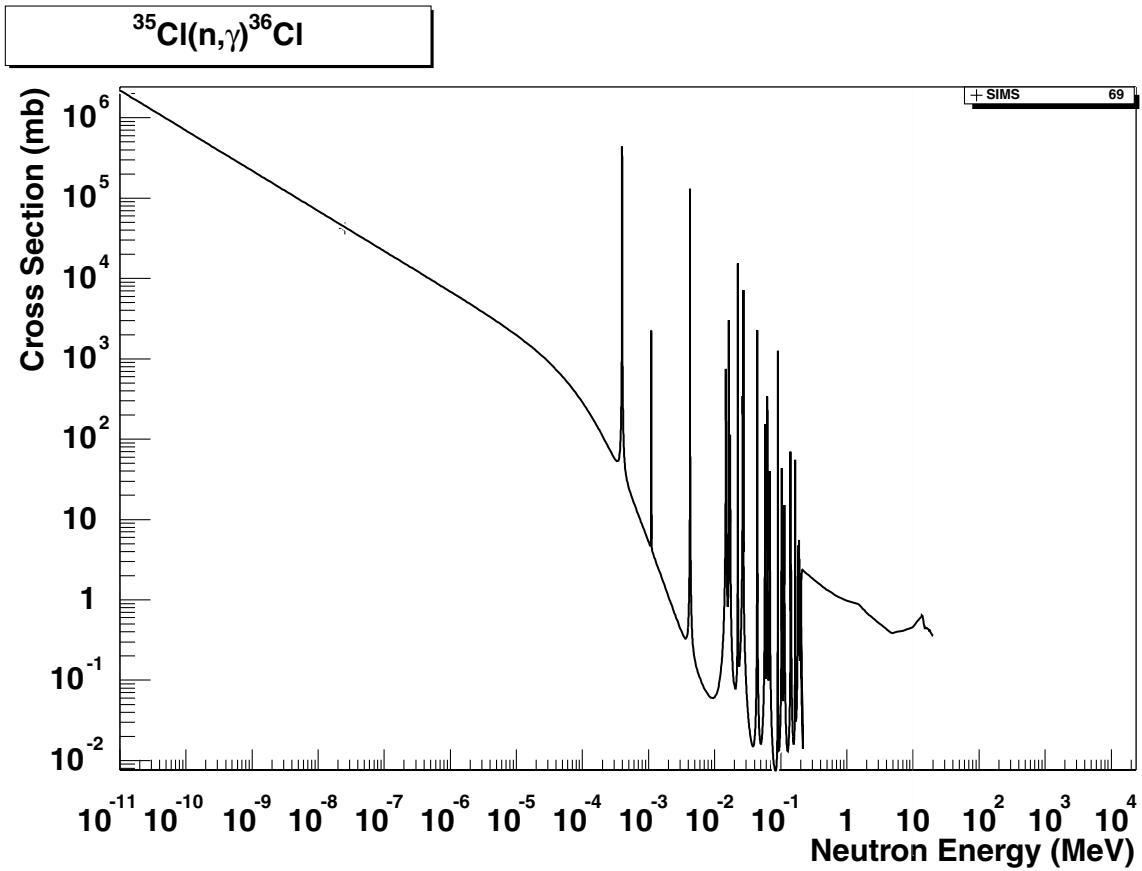
2.34. ^{35}Cl (n,γ) ^{36}Cl

final state: total
source: EAF-4.1

This is the EAF-4.1 evaluation calculated with the code SIGECN-MASGAM. Full MLBW resonance treatment is included. MASGAM is a statistical (Hauser-Feshbach) code with the pre-equilibrium component based on the D-SD model (for details see Ref. [35]). The global parameters are applied for optical model, level densities and gamma-ray strength functions. The thermal cross-section of Sims69 is well reproduced.
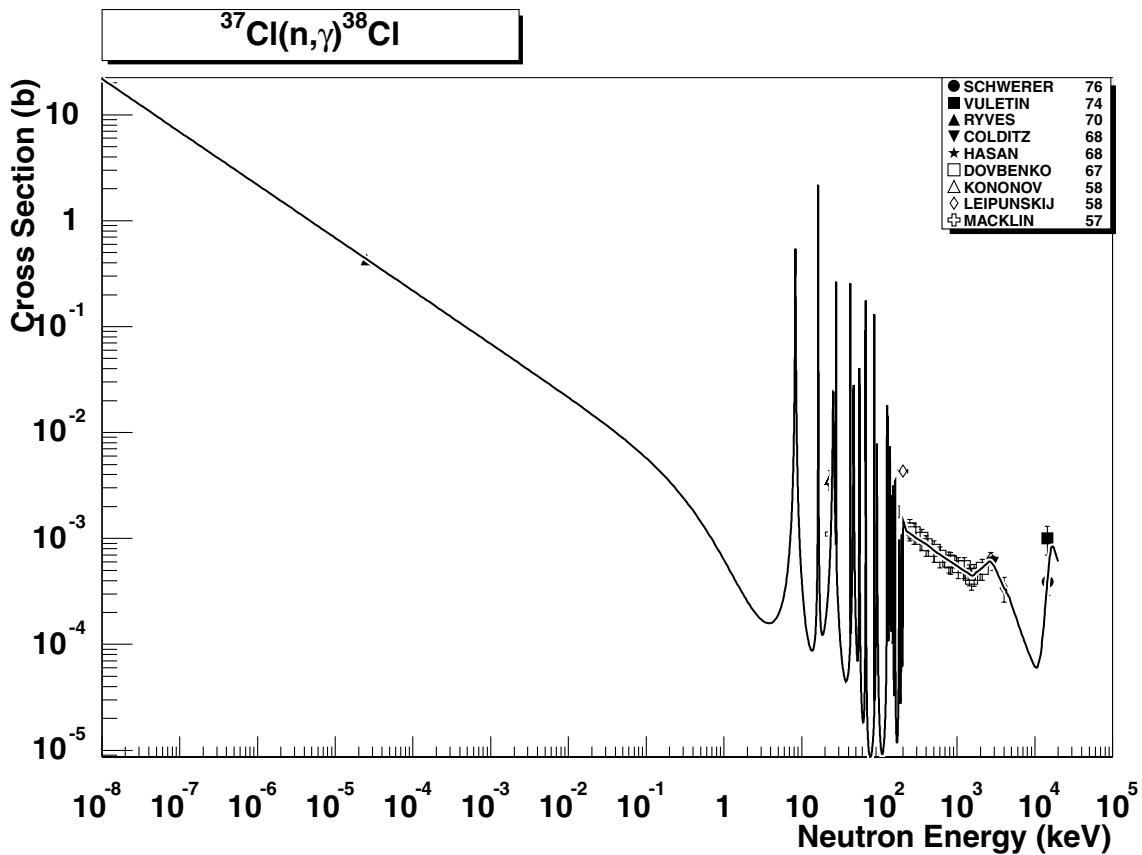
2.35. ^{37}Cl (n,γ) ^{38}Cl

final states: g.s., meta
source: JENDL-3.2

JENDL-3.2 agrees very well with the experimental data, especially in the thermal and high energy regions.

^{37}Cl(n,p)^{37}S

+	KAWADE	90
·	GUPTA	85
×	NGOC	80
✳	HYVOENEN-DABEK	
○	PRASAD	71
□	SCHANTL	70
△	PASQUARELLI	67
◇	MATHUR	66
✣	KHURANA	65
★	STRAIN	65
✰	KHURANA	60
●	MANI	60
▲	SCALAN	58
▼	COHEN	56
■	PAUL	53
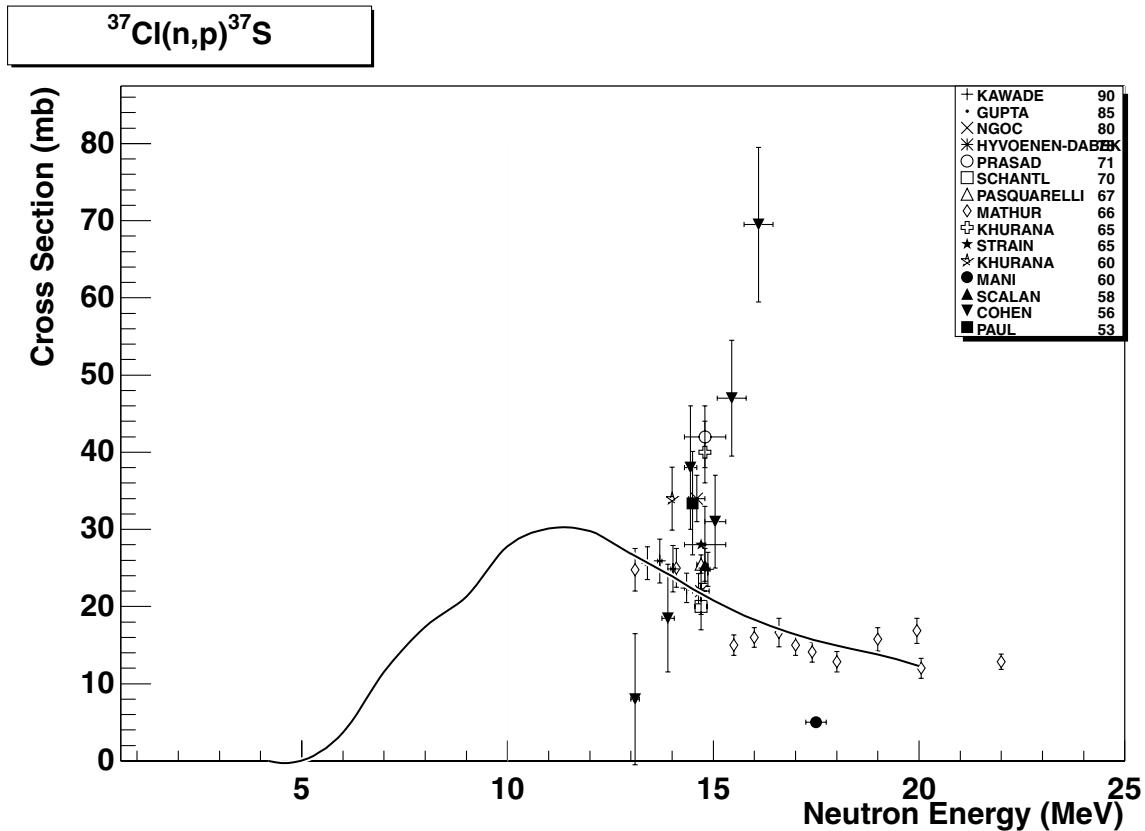
2.36. ^{37}Cl (n,p) ^{37}S

final state: total
source: JENDL-Act96

JENDL-Act96 evaluation reproduces the recent data of Kawade 90 between 13-15 MeV and fits nicely also data of Mathur66 up to 20 MeV. The large scatter of data around 14 MeV is primarily due to very old data (Cohen56, Scalan58) and they seem to be unreliable. They also deviate strongly from the value based on the 14.5 MeV systematics.

2.37. ^{37}Cl (n,α) ^{34}P
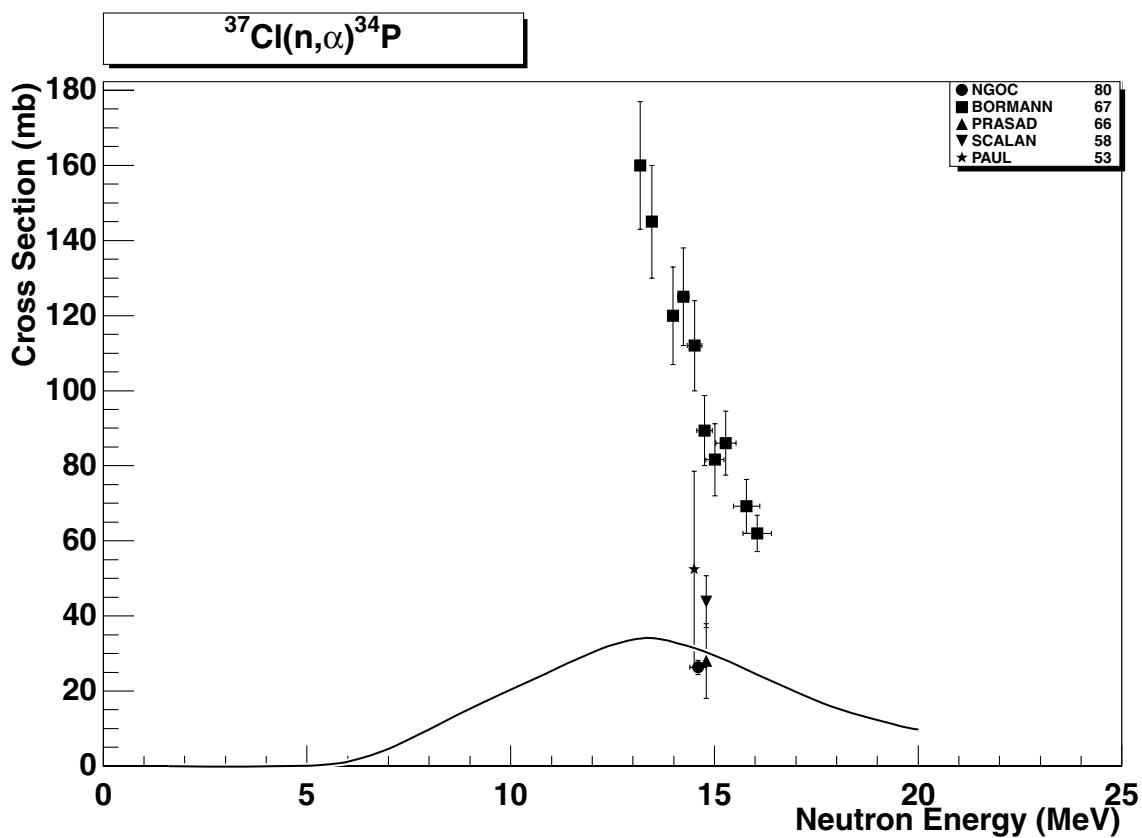
final state: total
source: ADL-3

ADL-3 evaluation fits reasonably four data points around 15 MeV except the data of Botmann67, which are probably wrong (shape as well as values above 120 mb) and can be disregarded.
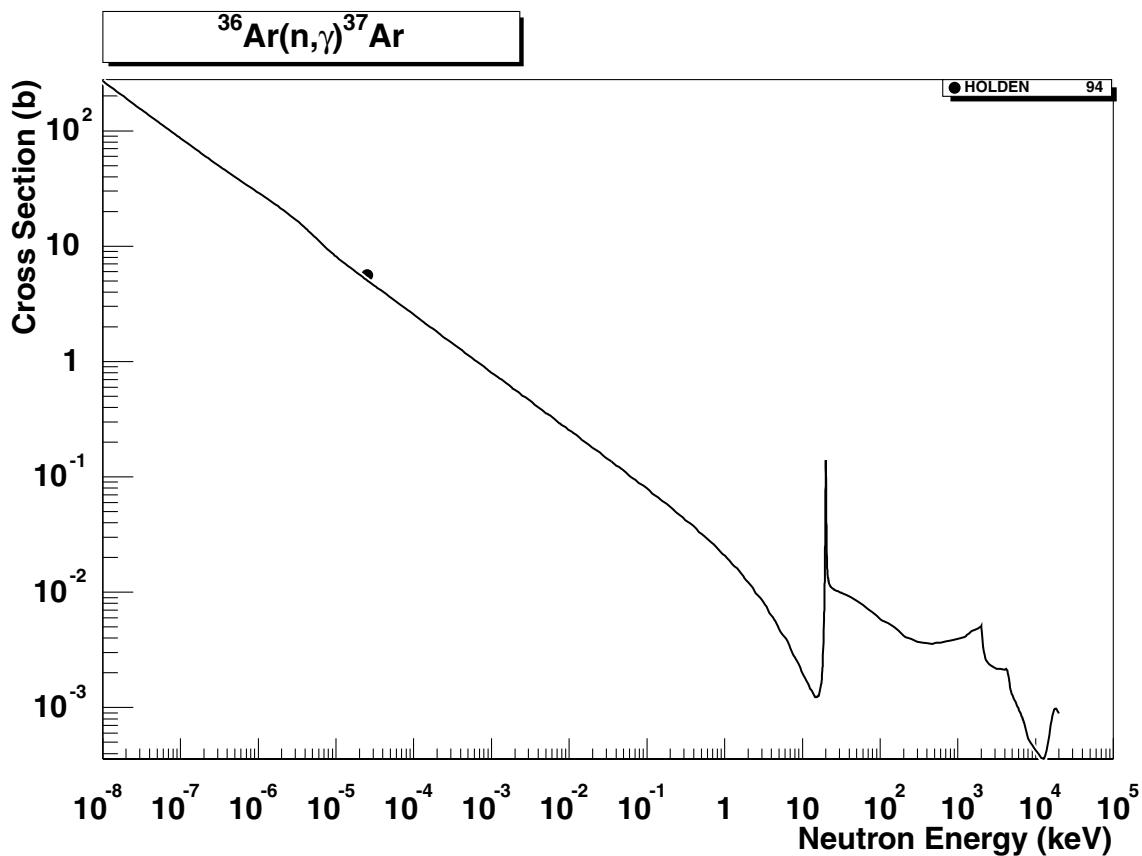
2.38. ^{36}Ar (n,γ) ^{37}Ar

final state: total
source: EAF-4.1 (JEF-2.2)

Original JEF-2.2 evaluation with no resonance parameters is available. No EXFOR data has been found. The thermal cross-section of Holden94 [32] is well reproduced (C/E=0.97). The resonance-like shape at 20 keV is not real and is generated due to an incorrect interpolation law during the linearization procedure in NJOY.
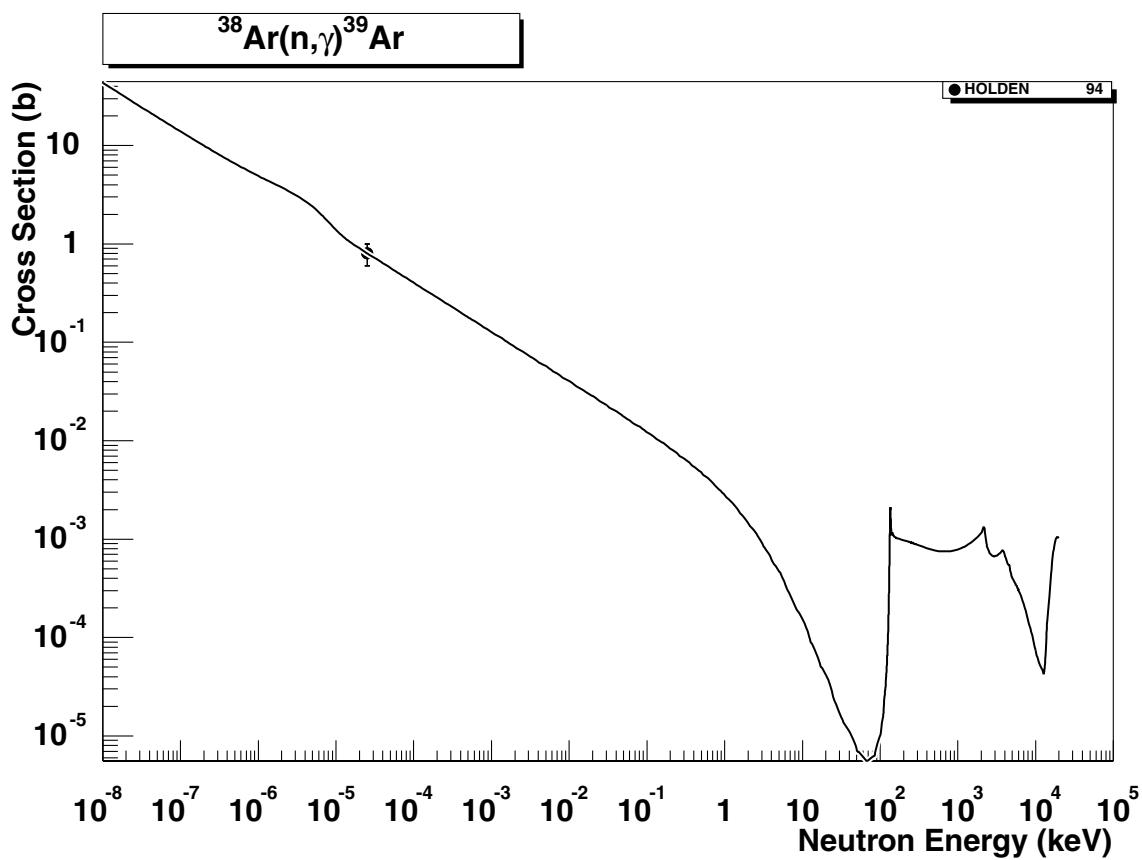
2.39. ^{38}Ar (n,γ) ^{39}Ar

final state: total
source: EAF-4.1 (JEF-2.2)

Original JEF-2.2 evaluation with no resonance parameters is available. The thermal cross-section of Holden94 [32] is well reproduced (C/E=1.00).
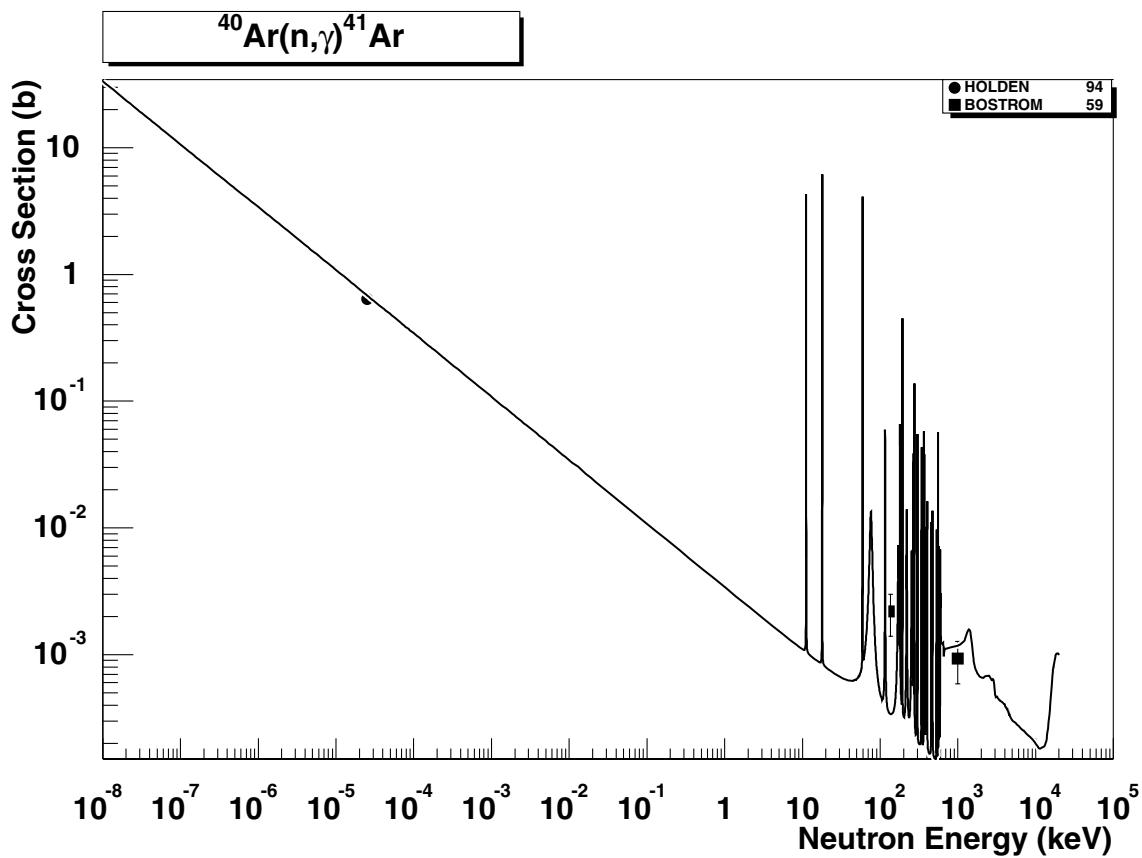
2.40. ^{40}Ar (n,γ) ^{41}Ar

final state: total
source: EAF-4.1 (JEF-2.2)

The original JEF-2.2 evaluation includes the MLBW treatment of resonance parameters. Only two single experimental cross-sections are available in EXFOR. The thermal cross section of Holden94 [32] is well reproduced with C/E=1.03.

39K(n,p)39Ar

● FOLAND	87
■ ALEKSANDROV	75
▲ SCHANTL	70
▼ JOHNSON	67
★ BASS	64
□ DIXON	61
△ BORMANN	60
◇ LINDSTROEM	58
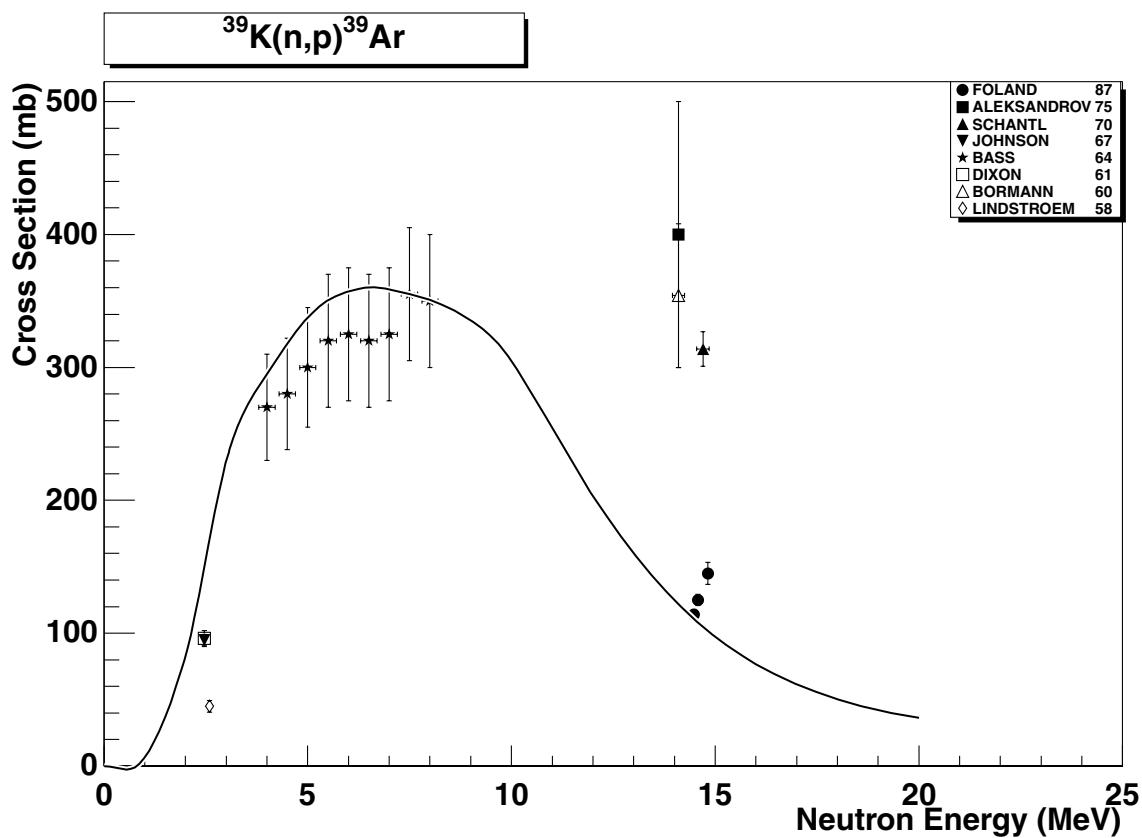
2.41. ^{39}K (n,p) ^{39}Ar

final state: total
source: ADL-3

The available data are reasonably reproduced by the ADL-3 evaluation. Three data points around 15 MeV with values between 300-400 mb are too large (also compared to systematics) and can be disregarded.
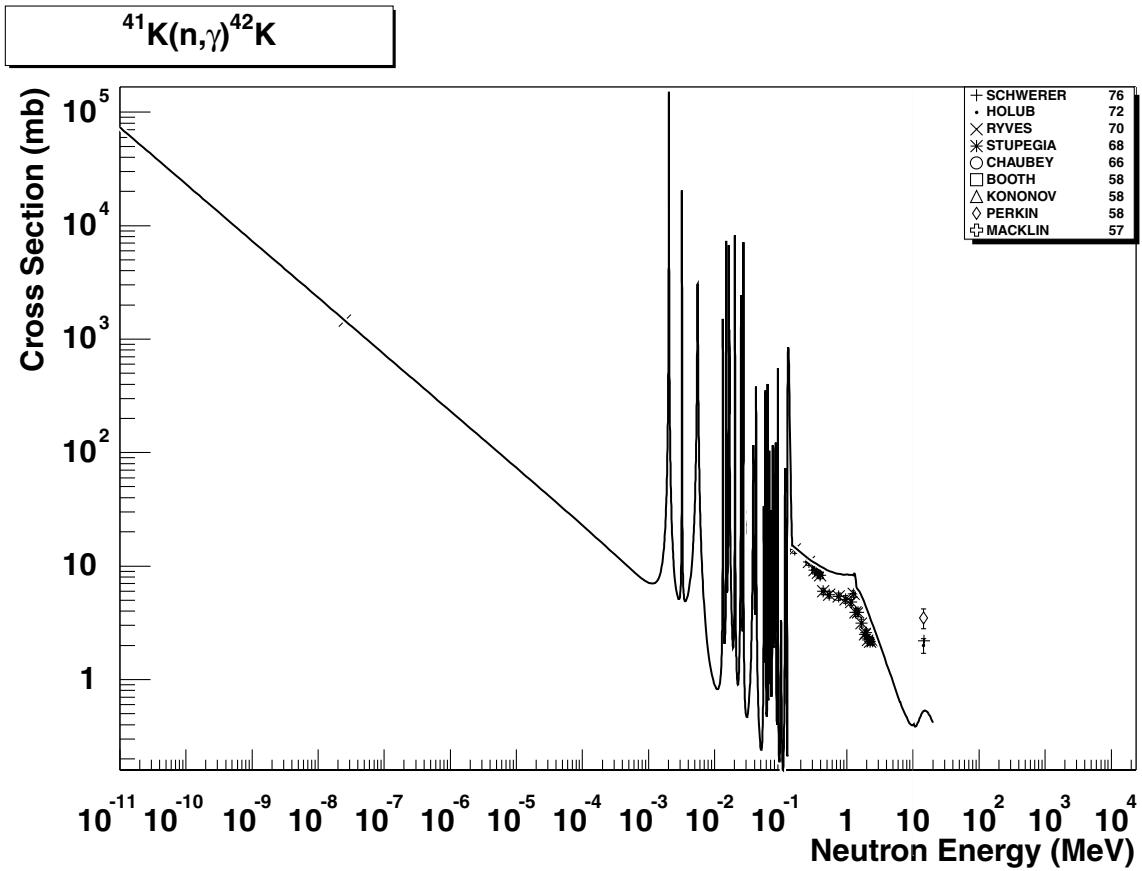
2.42. ^{41}K (n,γ) ^{42}K

final state: total
source: EAF-4.1 (JENDL-3.1)

JENDL-3.1 agrees with the thermal cross-section experimental value of Ryves70 and follows the shape but slightly overestimates data between 400 keV and 2 MeV. The 14 MeV data of Perkin58, Holub72 and Schwerer76 with values above 20 mb are wrong (much too large) and can be disregarded. The pre-equilibrium component was missing in the original JENDL-3.1 evaluation and was added during the EAF-4.1 revision based on the PEQ-systematics [3] and [35].

2.43. ^{41}K (n,α) ^{38}Cl
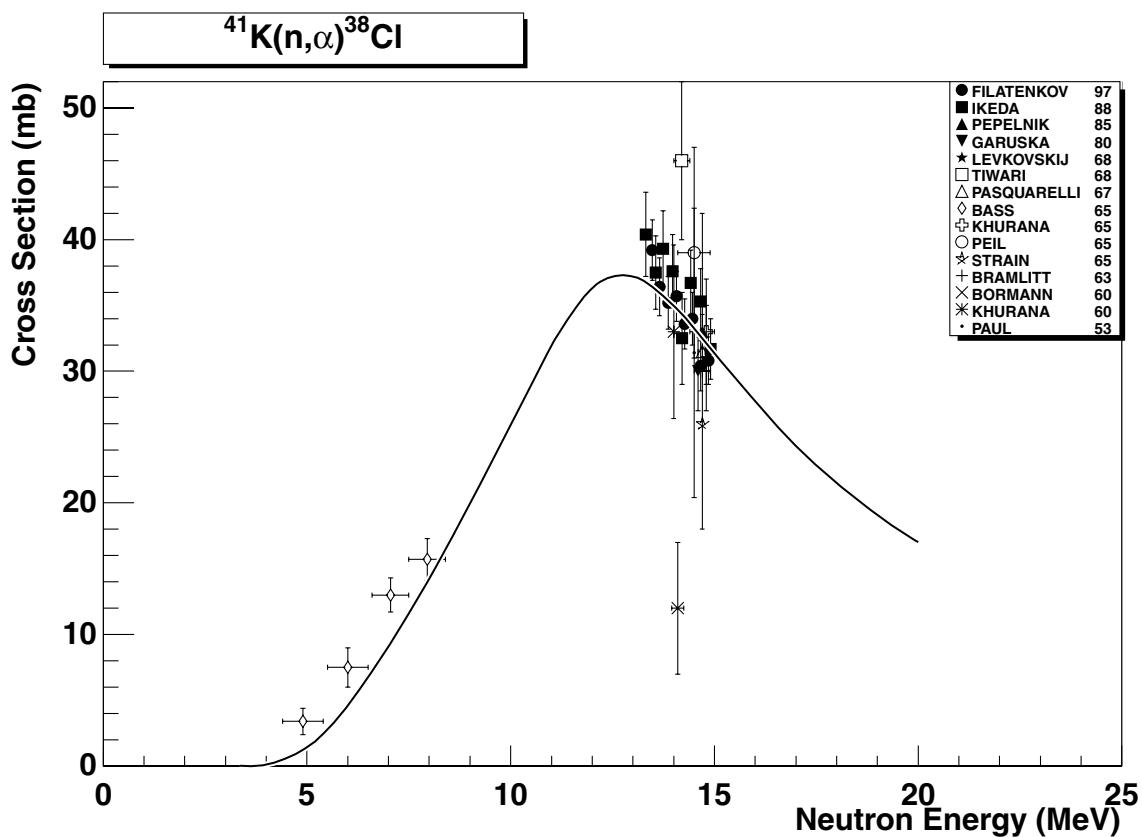
final states: g.s., meta
source: ADL-3

A slight increase of ADL-3 evaluation (by about 5%) may still improve a reasonable agreement with all experimental data. Partial cross-sections to the g.s. and meta state result from model calculations.

^{40}Ca(n,γ)^{41}Ca
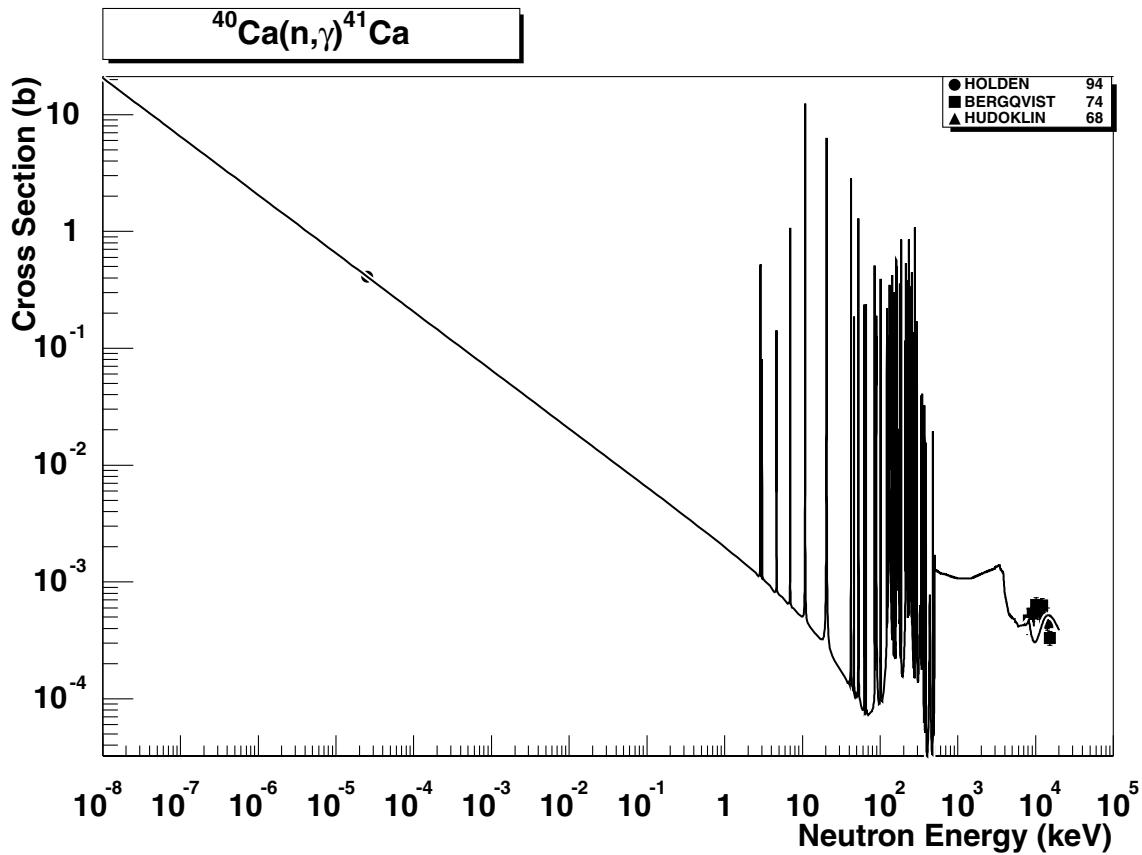
2.44. ^{40}Ca (n,γ) ^{41}Ca

final state: total
source: EAF-4.1 (JENDL-3.1)

JENDL-3.1 evaluation reasonably agrees with the EXFOR data above 10 MeV. The thermal cross-section of Holden94 from Ref. [32] is well reproduced (C/E=1.00). The preequilibrium component was missing in the original JENDL-3.1 evaluation and was added during the EAF-4.1 revision based on the PEQ-systematics [3] and [35].

²⁸⁴⁴Ca(n,p)⁴⁴K

Legend:
- ● IKEDA 88
- ■ PEPELNIK 85
- ▲ HOLMBERG 78
- ▼ QAIM 77
- ★ SCHANTL 70
- □ BRAUN 68
- △ LEVKOVSKIJ 68
- ◇ TIWARI 68
- ⊕ CSIKAI 67
- ○ MINETTI 66
- ✶ BASS 65
- + KHURANA 65
- × LEVKOVSKIJ 63
- ✳ HILLE 61
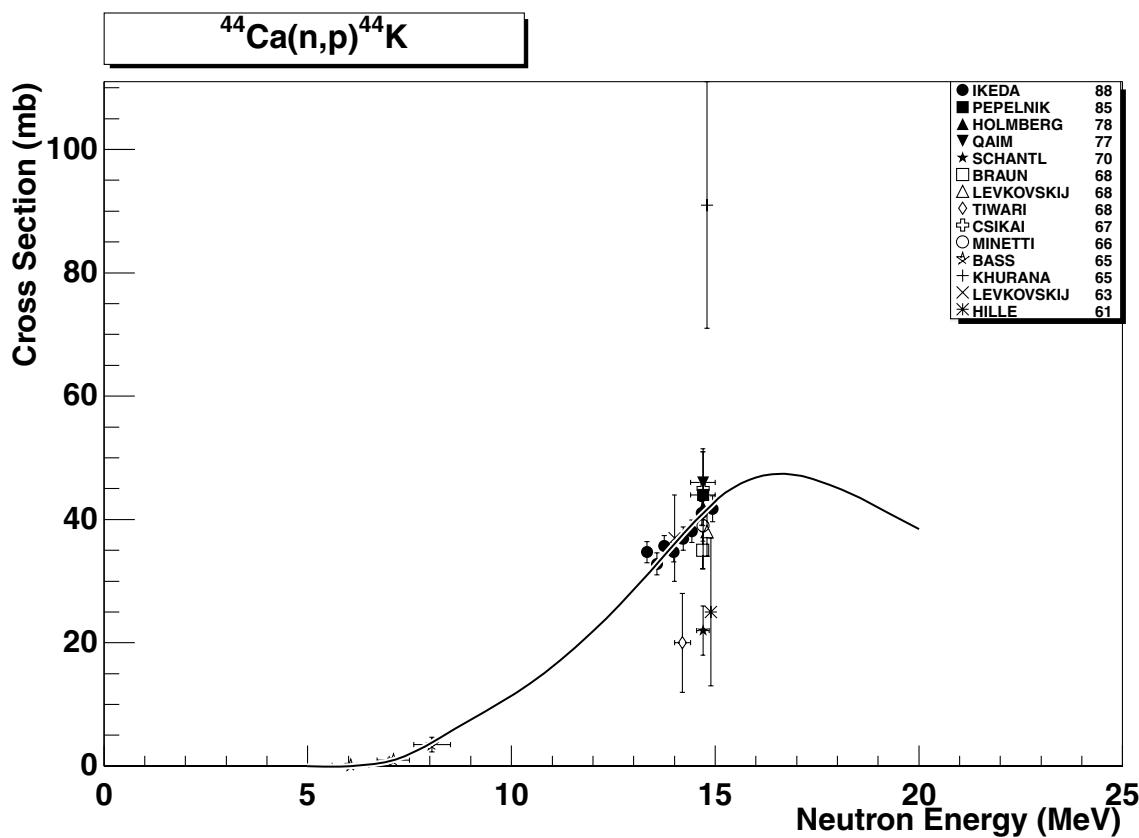
2.45. ^{44}Ca (n,p) ^{44}K

final state: total
source: ADL-3

The shape and absolute values of the ADL-3 evaluation are supported by a number of recent data around 6-8 MeV and 13-15 MeV. Some deviating experimental points can be excluded (in particular Khuvana65 and probably also Hille61, Tivari68, Schantel70).
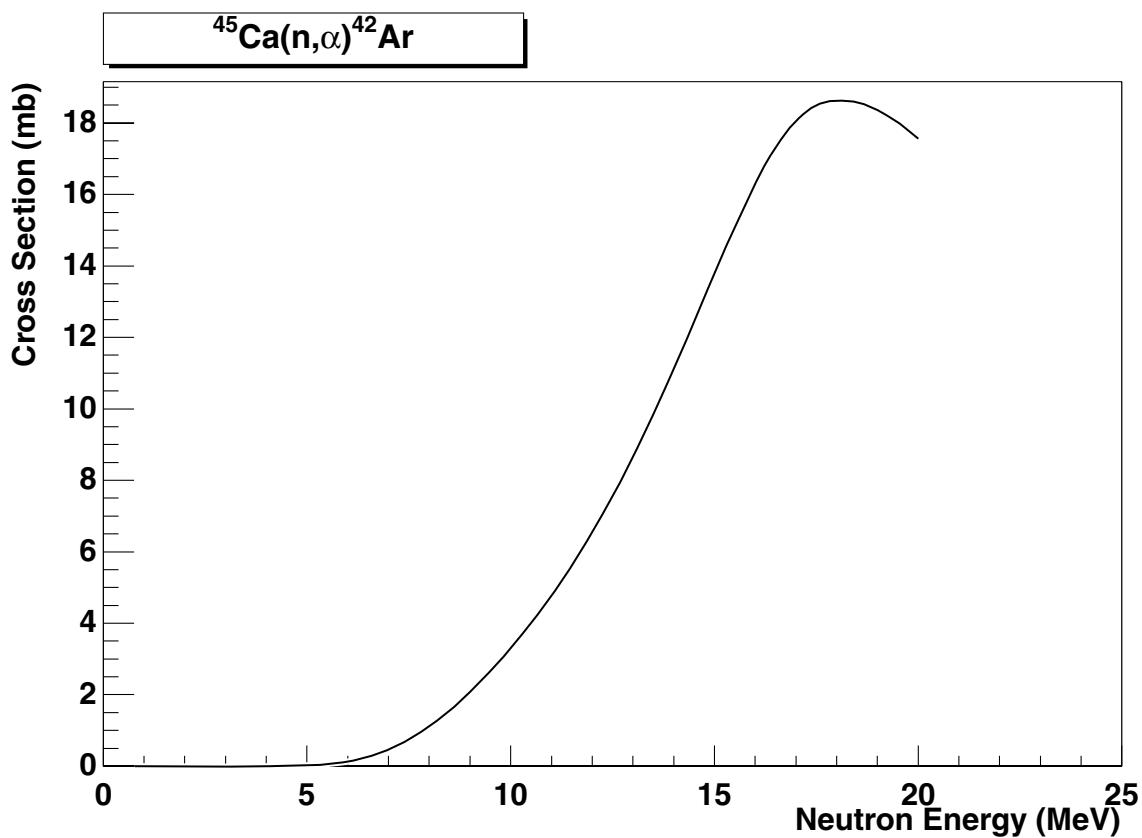
2.46. ^{45}Ca (n,α) ^{42}Ar

final state: total
source: ADL-3

This is a STAPRE calculation for the ADL-3 evaluation. No EXFOR data are available.
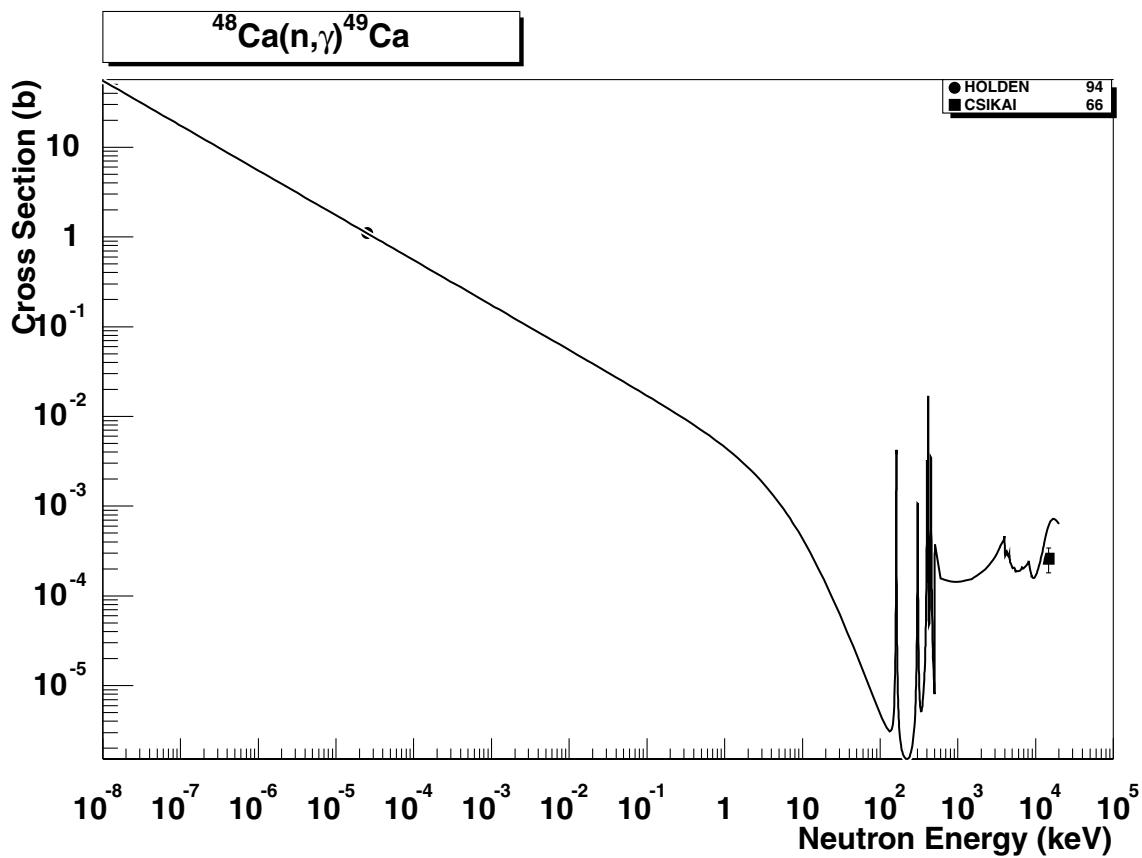
2.47. ^{48}Ca (n,γ) ^{49}Ca

final state: total
source: EAF-4.1 (JENDL-3.1)

JENDL-3.1 evaluation is in acceptable agreement with the single point of Csikai66 at 14.5 MeV. The pre-equilibrium component was missing in the original JENDL-3.1 evaluation and was added during the EAF-4.1 revision based on the PEQ-systematics [3] and [35]. The thermal cross-section of Holden94 [32] is well reproduced (C/E = 1.0).
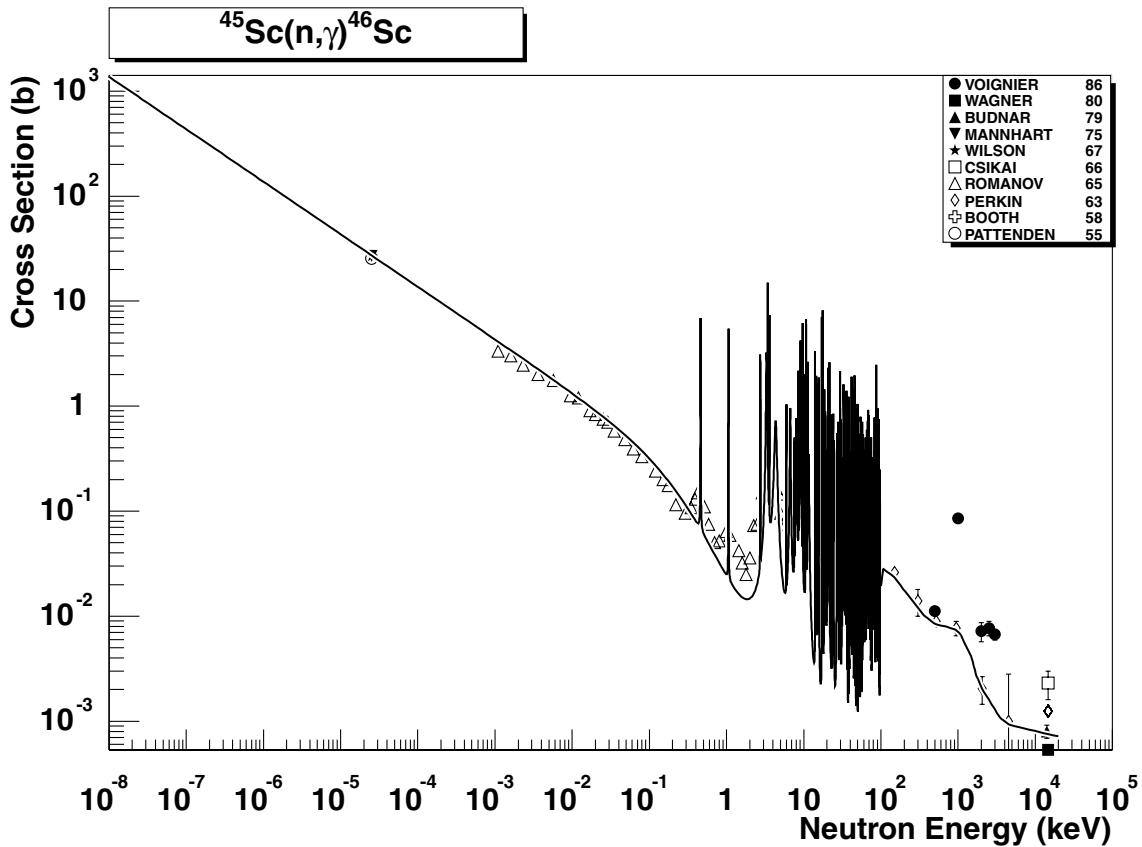
2.48. ^{45}Sc (n,γ) ^{46}Sc

final states: g.s., meta
source: EAF-4.1 (ENDF/B-VI)

The ENDF/B-VI excitation curve agrees well with the experimental data in the whole energy range. The distribution of Voignier86 data is strange, in particular the experimental point at 1 MeV. The 14.5 MeV value is correct, Csikai66 and Perkin63 are too large. Branching ratio between the g.s. and meta state is based on the thermal cross-sections [26] applied up to the end of resolved resonance region, and on the energy dependent systematics [2] for the high energy region. The partial thermal cross-sections are reproduced with C/E=1.0.

46Ti(n,2n)45Ti

● DIGHE	91
■ IKEDA	88
▲ MUYAO	87
▼ MOLLA	83
★ CSIKAI	82
□ QAIM	77
△ SIGG	76
◇ PAULSEN	75
⊕ ARAMINOWICZ	73
○ MASLOV	72
☆ PAI	66
+ BORMANN	65
× CSIKAI	65
✳ STRAIN	65
· CEVOLANI	62
◎ PRESTWOOD	61
⊞ RAYBURN	61
△ POULARIKAS	59
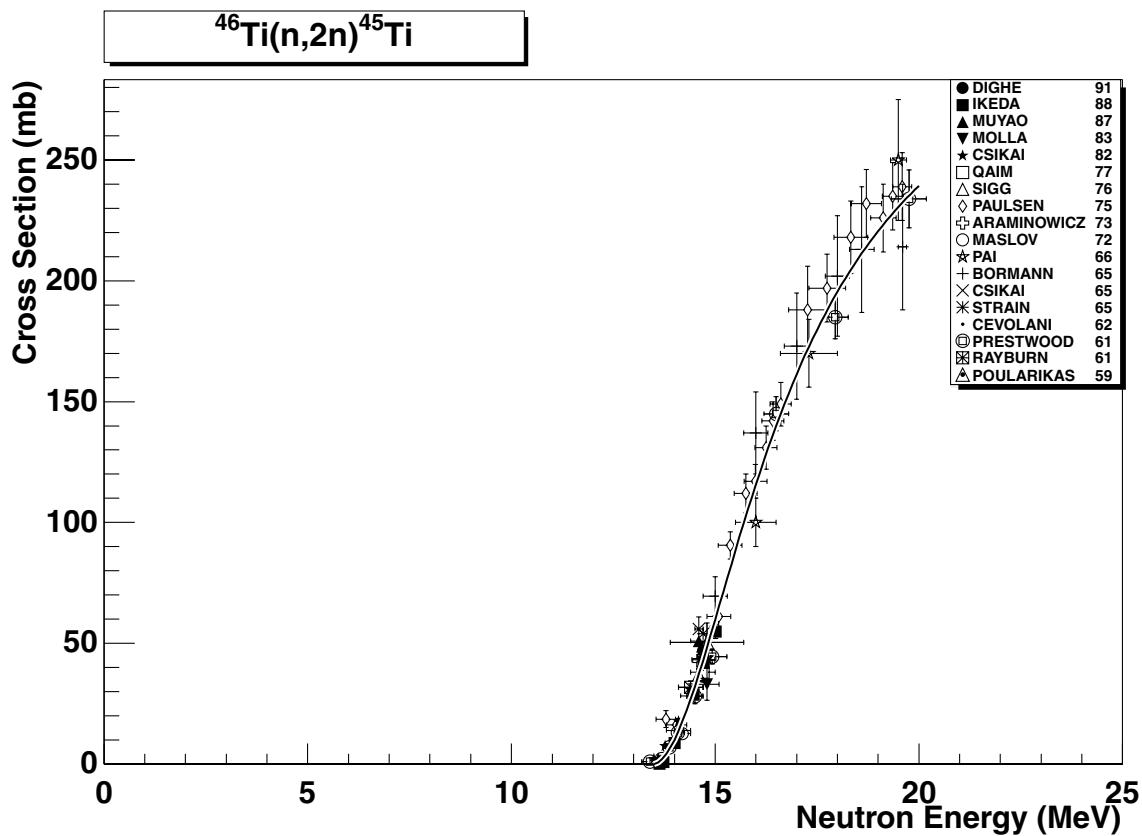
2.49. ^{46}Ti (n,2n) ^{45}Ti

final state: total
source: RRDF-98

A consistent set of experimental data is perfectly reproduced by the recent RRDF-98 evaluation.

^{46}Ti(n,p)^{46}Sc

● OSMAN	96
■ JUNQIAN	92
▲ VIENNOT	91
▼ MOLLA	90
★ HAN-LIN	89
□ HANLIN	89
△ IKEDA	88
◇ KOBAYASHI	88
⊕ MOLLA	86
○ RIBANSKY	83
✭ VIENNOT	82
+ KAYASHIMA	79
× QAIM	77
✳ SMITH	75
· SMITH	75
⊚ SMITH	75
⊠ GHORAI	71
△ LUKIC	71
◈ LUKIC	71
⊞ PAI	66
✩ BORMANN	65
⊙ LISKIEN	65
⊠ KOEHLER	64
⊛ CROSS	63
⊞ POULARIKAS	59
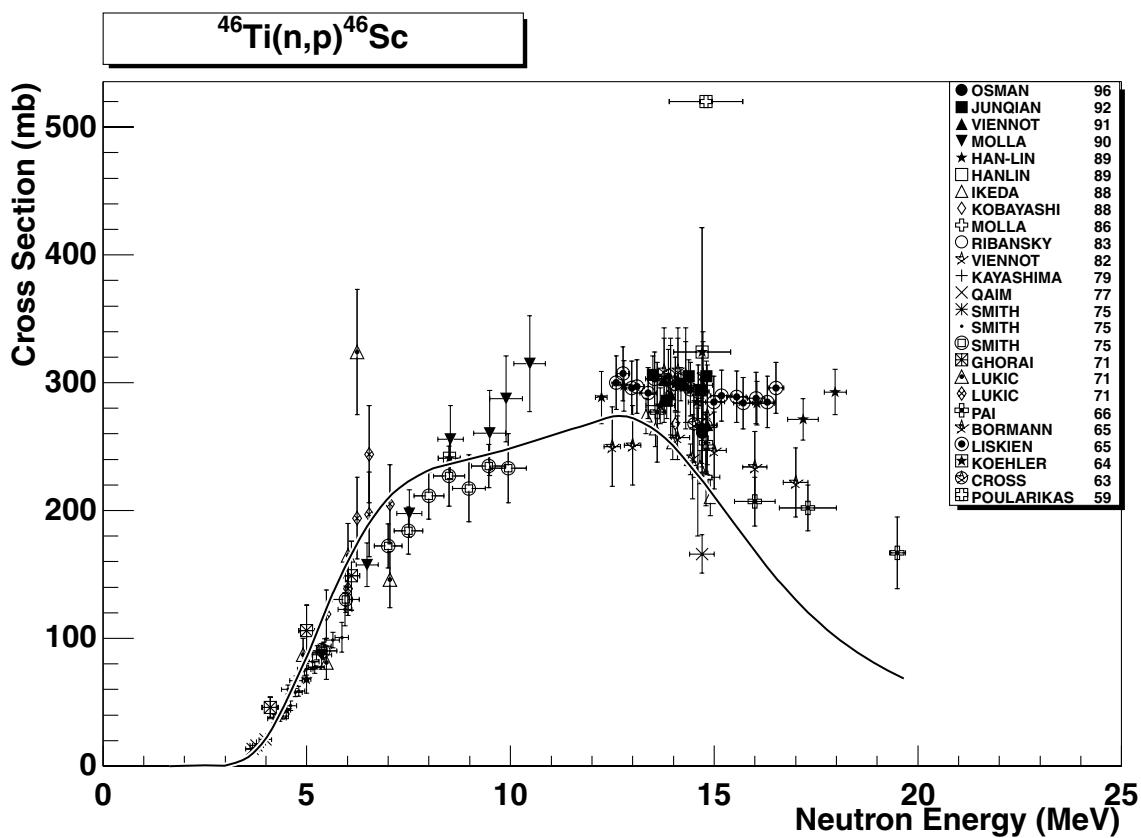
2.50. ^{46}Ti (n,p) ^{46}Sc

final states: g.s., meta
source: ADL-3

ADL-3 evaluation reproduces the experimental data well, however, the maximum of the excitation curve around 15 MeV is slightly below the very recent data.

^{47}Ti(n,p)^{47}Sc

●	OSMAN	96
■	IKEDA	91
▲	QAIM	91
▼	VIENNOT	91
★	IKEDA	90
□	HANLIN	89
△	HECKER	89
◇	MANNHART	89
✛	MANNHART	89
○	IKEDA	88
✫	KOBAYASHI	88
+	DAC LUC	86
×	MOLLA	86
✳	FIRKIN	83
·	HUSAIN	83
◎	RIBANSKY	83
▦	SWINHOE	79
▲	SWINHOE	79
◇	QAIM	77
✦	GOTOH	75
✬	SMITH	75
◉	SMITH	75
▨	SMITH	75
⊛	SPANGLER	75
⊞	TIKKU	72
▲	GHORAI	71
◆	LEVKOVSKIY	69
✛	PAI	66
✶	CROSS	63
◎	GONZALEZ	62
⊞	HILLMAN	62
△	POULARIKAS	59
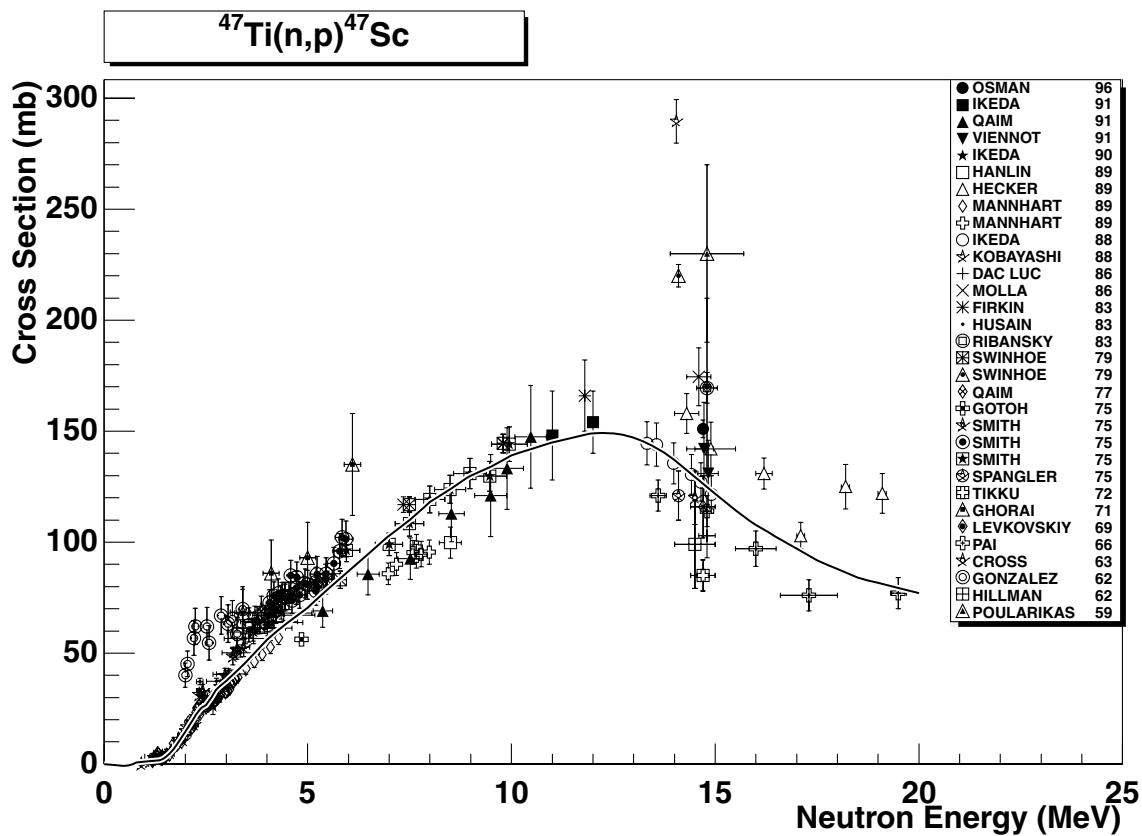
2.51. ^{47}Ti (n,p) ^{47}Sc

final states: total
source: JENDL-Act96

An excellent agreement with all relevant data, some data around 15 MeV can be disregarded (e.g. Kobayashi88).

^{47}Ti(n,np)^{46}Sc + ^{47}Ti(n,d)^{46}Sc

● IKEDA	88
■ MOLLA	86
▲ RIBANSKY	83
▼ PAI	66
★ CROSS	63
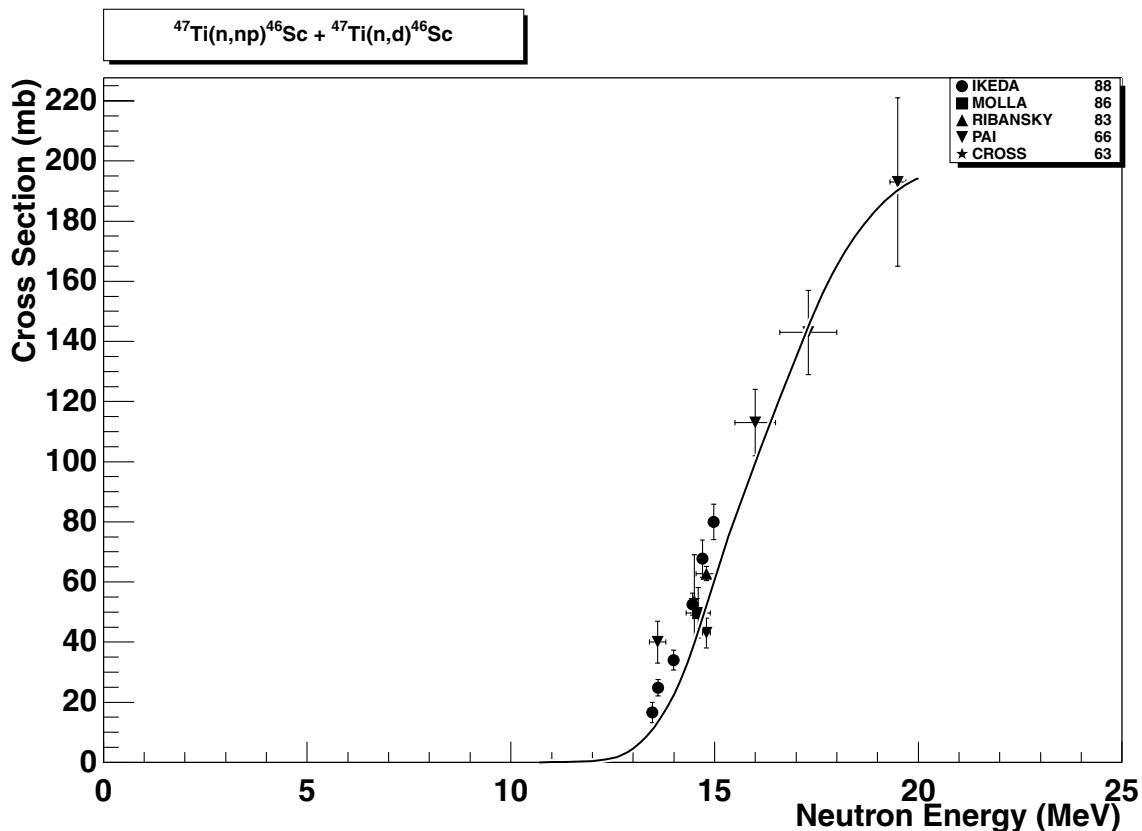
2.52. ^{47}Ti (n,d+np) ^{46}Sc

final states: total
source: RNAL

The evaluation is based on the theoretical calculations with EMPIRE-2.13[36] code. The agreement with experimental data is very good above 15 MeV. Below this energy the recommended cross-sections might be slightly underestimated. The evaluated data are stored in a single file and represent a sum of cross-sections to the g.s. and metastable state resulting from both ((n,d) and (n,np)) reactions.
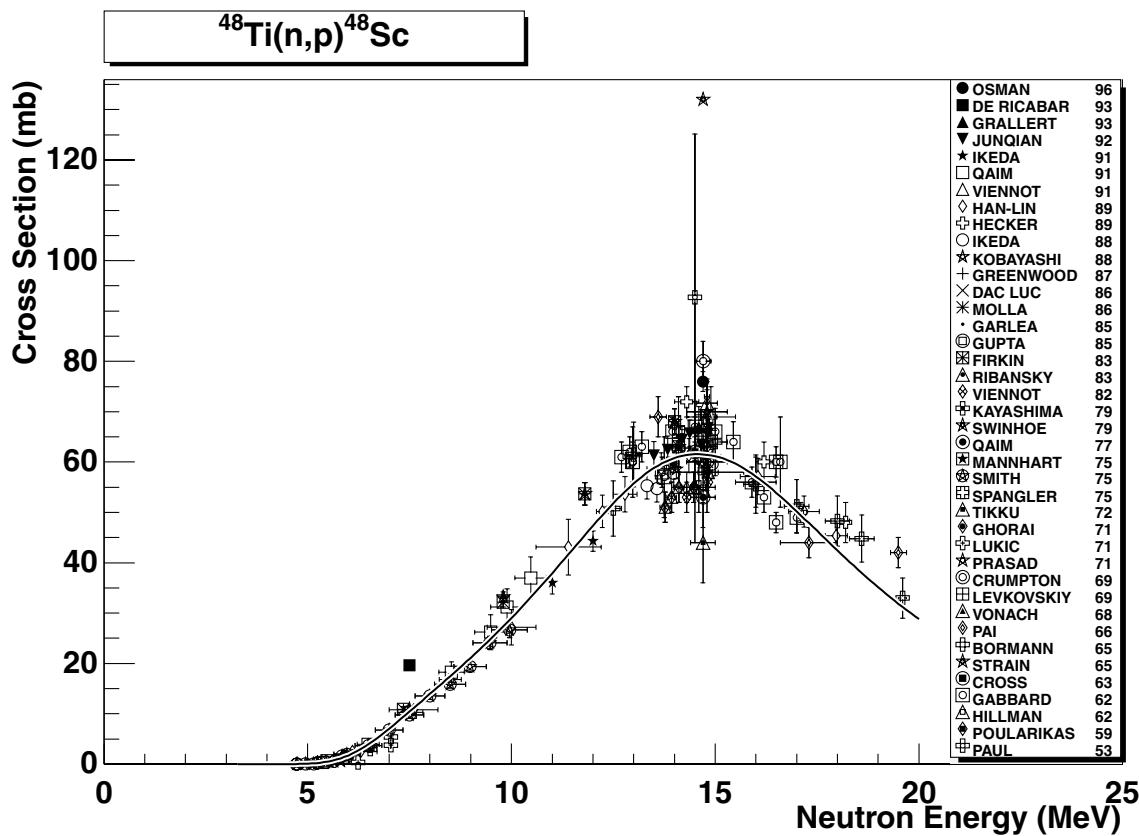
2.53. ^{48}**Ti (n,p)** ^{48}**Sc**

final state: total
source: IRK

An excellent agreement with all relevant data (Strain65 has been disregarded).

48Ti(n,d+np)47Sc

● HECKER		89
■ MOLLA		86
▲ QAIM		77
▼ PAI		66
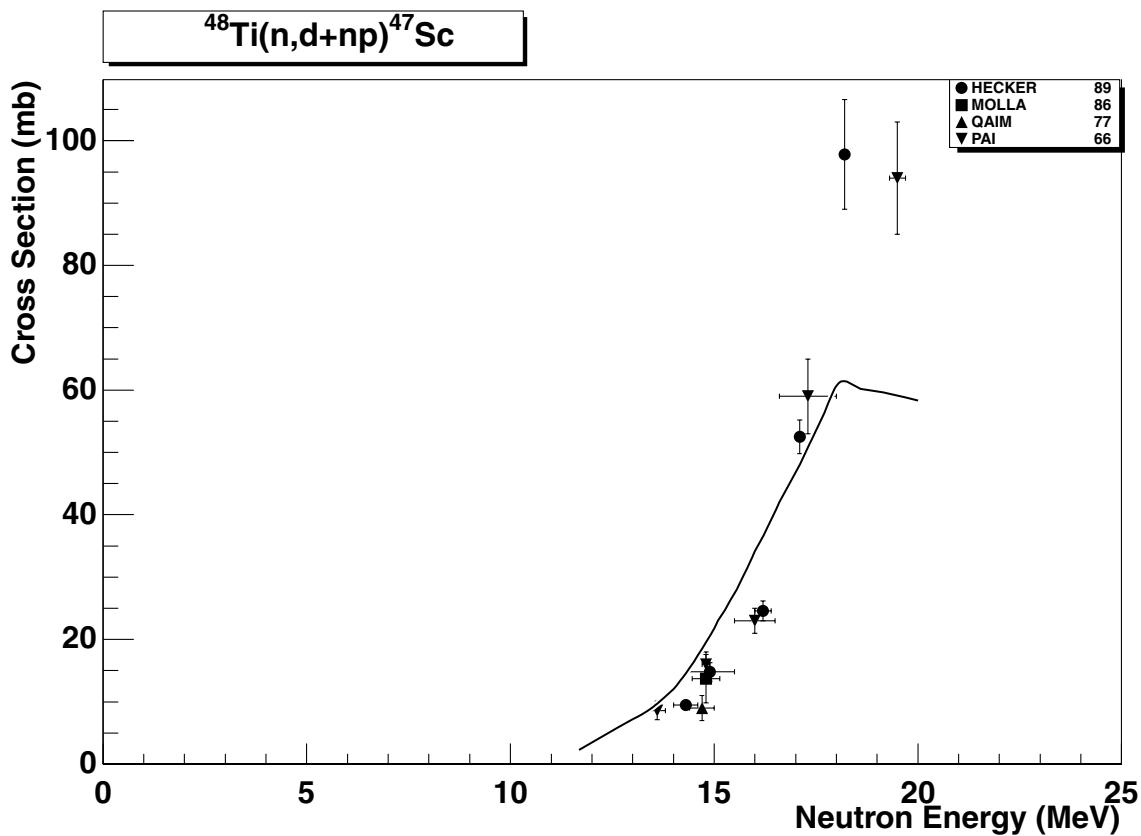
2.54. ^{48}Ti (n,d+np) ^{47}Sc

final state: total
source: FENDL/A-1 [(n,d)], IRDF-90.2 [(n,np)]

The sum of the evaluations reasonably agrees with the (n,d+np) data up to 17 MeV. Two data points above 18 MeV (Heckler89 and Pai60) may indicate, that the shape of the excitation curve above 18 MeV should be revised. The data are stored separately as (n,d) and (n,np) reaction channels.
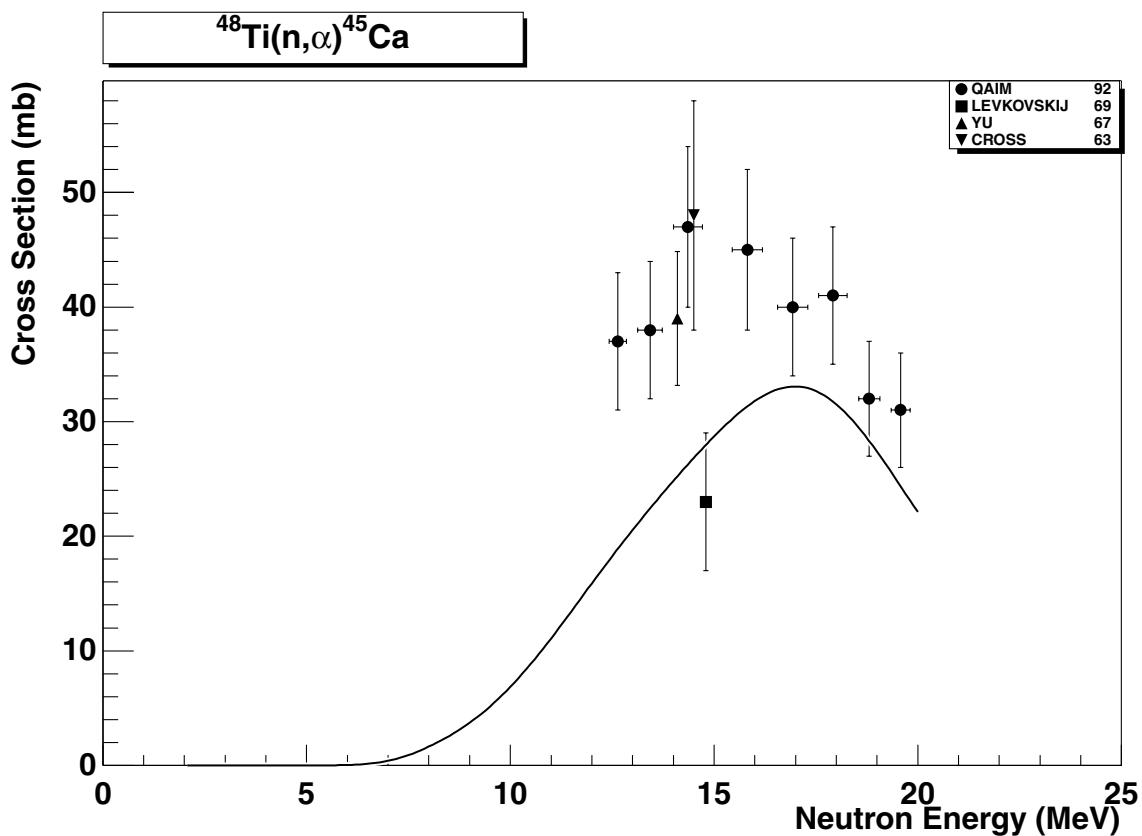
2.55. ^{48}**Ti (n,α)** ^{45}**Ca**

final state: total
source: IPPE

The IPPE evaluation [11] underestimates (by about 15%) the experimental data in the energy range between 13-20 MeV. A renormalization of the excitation curve is recommended.

^{50}Ti(n,α)^{47}Ca

●	OSMAN	96
■	DE RICABAR	93
▲	GRALLERT	93
▼	JUNQIAN	92
★	QAIM	92
□	QAIM	91
△	IKEDA	88
◇	PEPELNIK	85
✚	RIBANSKY	83
○	KAYASHIMA	79
✩	QAIM	77
+	LEVKOVSKIY	69
×	YU	67
✳	CROSS	63
·	HILLMAN	62
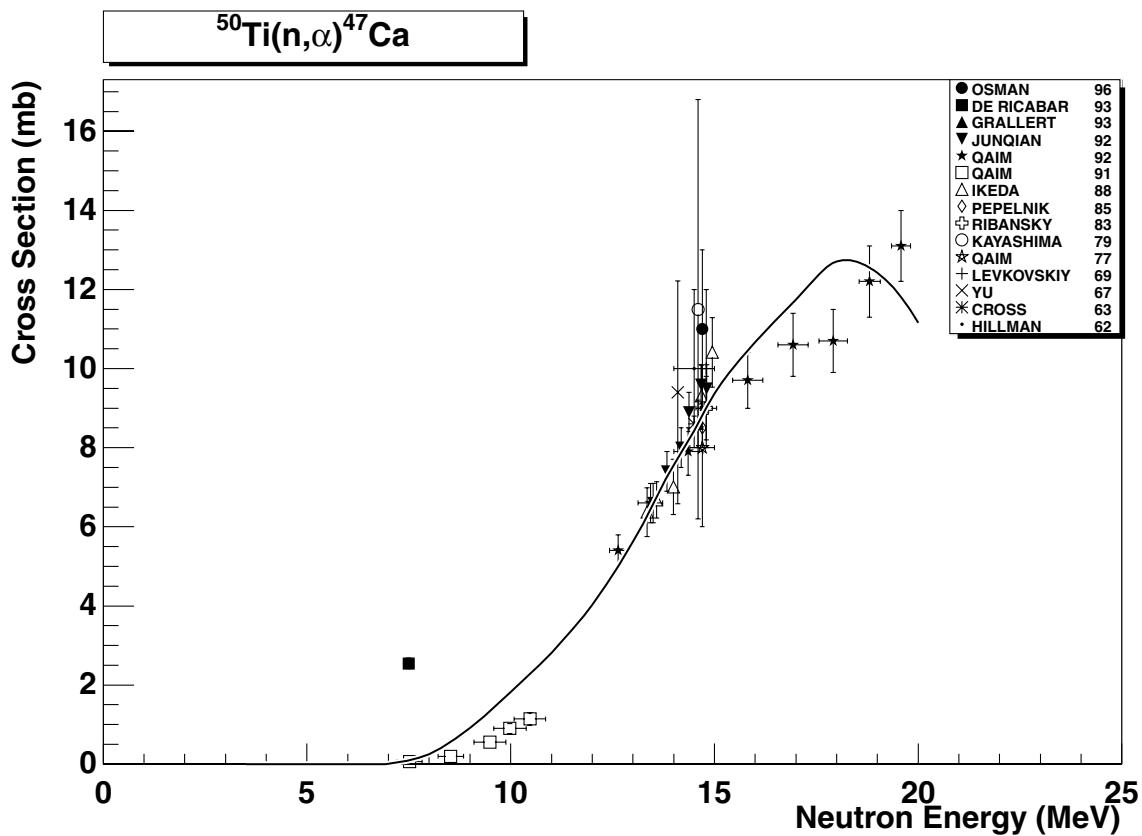
2.56. ^{50}**Ti (n,α)** ^{47}**Ca**

final state: total
source: JENDL-Act96

JENDL-Act96 reproduces the data very well, the single point of De Ricabar93 can be certainly disregarded. There is a small shape discrepancy with Qaim92 data above 15 MeV.

50Ti(n,γ)51Ti

+	RIGAUD	74
·	SCHWERER	74
×	VULETIN	74
✳	RYVES	70
○	DUDEY	69
□	ZAIKIN	67
△	CSIKAI	66
◇	POULARIKAS	59
✛	VERVIER	59
★	PASECHNIK	58
☆	PERKIN	58
●	MACKLIN	57
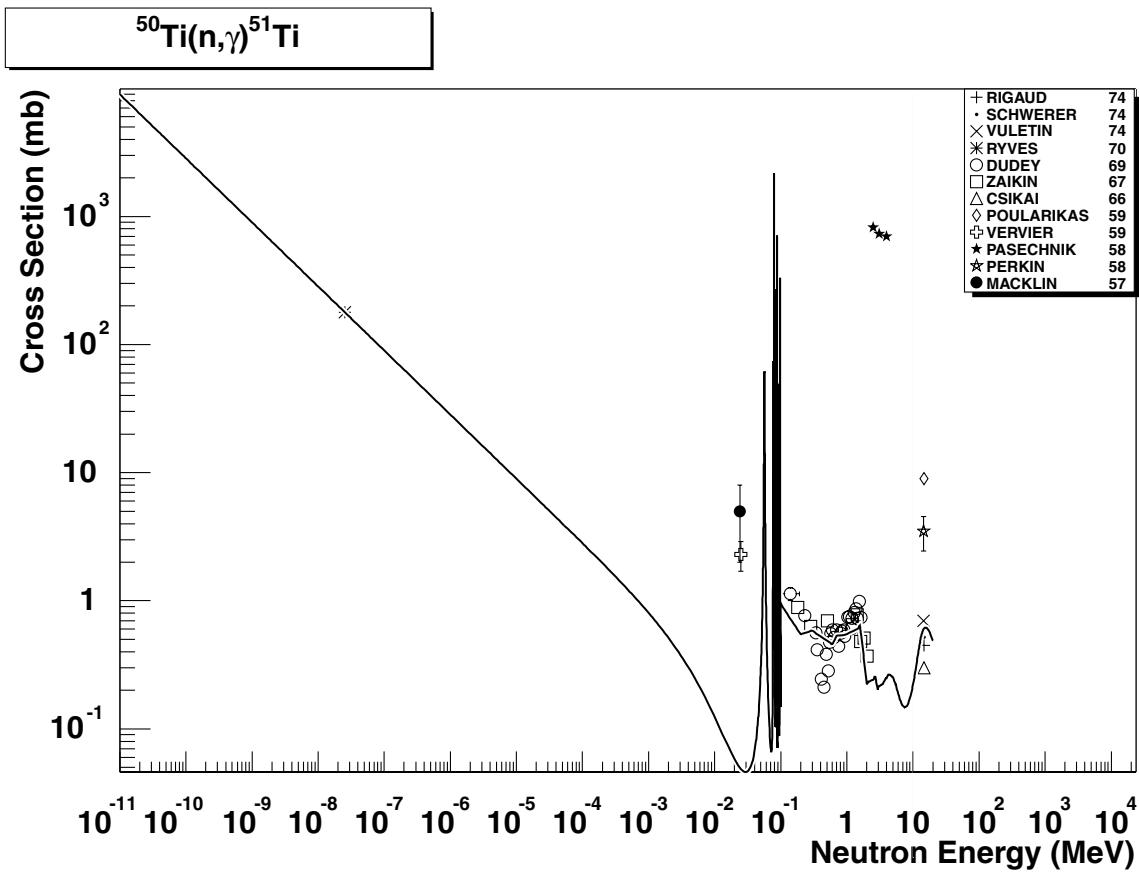
2.57. ^{50}Ti (n,γ) ^{51}Ti

final state: total
source: EAF-4.1 (JENDL-3.1)

JENDL-3.1 evaluation agrees in general with the majority of experimental data. The data of Pasechnik58 at about 3 MeV and of Perkin58 and Poulakiras59 (at 14 MeV) are definitely too large and can be disregarded. The pre-equilibrium component was missing in the original JENDL-3.1 evaluation and was added during the EAF-4.1 revision based on the PEQ-systematics [3] and [35] and agrees with experimental data.

^{50}V(n,2n)^{49}V

● GREENWOOD   89
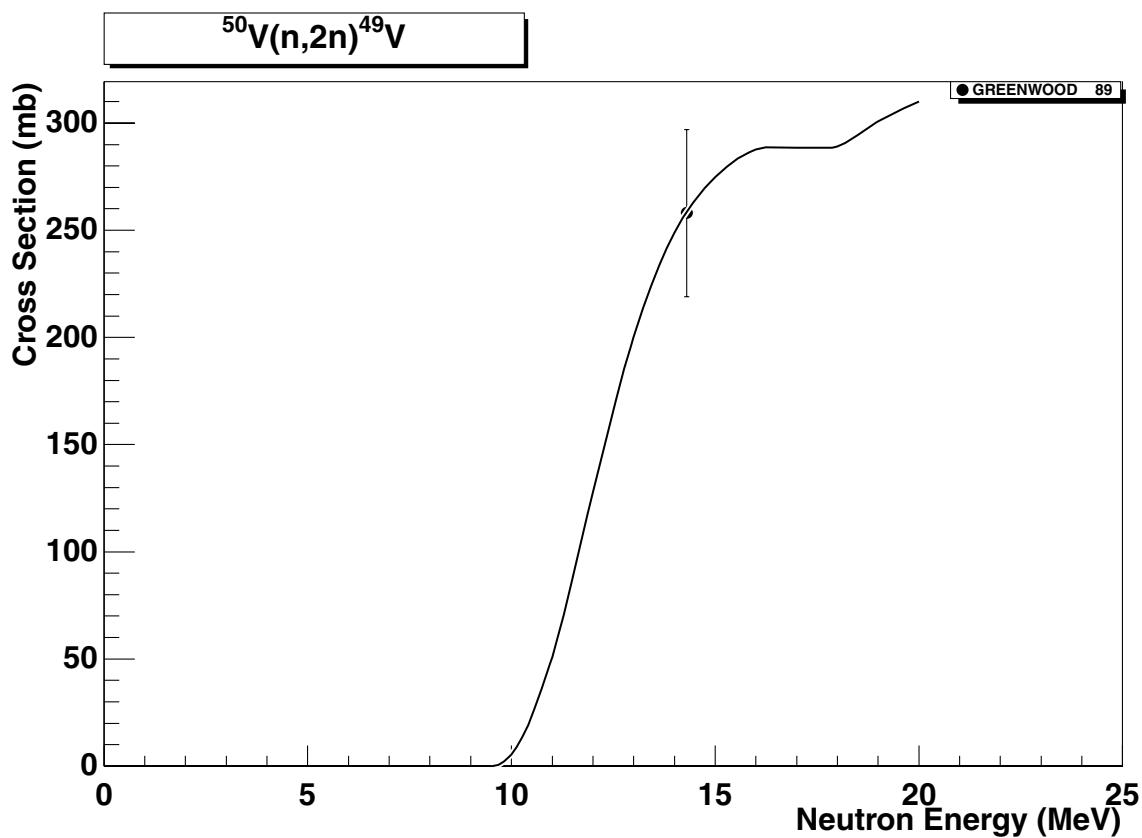
2.58. ^{50}V (n,2n) ^{49}V

final state: total
source: JENDL-Act96

The single experimental point at 14 MeV is in agreement with the JENDL-Act96 evaluation.

^{51}V(n,γ)^{52}V

●	CELENK	91
■	AFZAL ANSARI	86
▲	ANAND	79
▼	BUDNAR	79
★	SCHWERER	76
□	VALKONEN	76
△	PAVLENKO	75
◇	RIGAUD	74
✛	HOLUB	72
○	MAJUMDER	70
✩	RYVES	70
+	DUDEY	69
×	COLDITZ	68
✳	ZAIKIN	67
·	CHAUBEY	66
◎	CSIKAI	66
⊞	GIBBONS	65
▲	KAPCHIGASHEV	65
◈	STRAIN	65
✛	GLICKSTEIN	63
✦	MACKLIN	63
⊙	SHER	62
⊠	STAVISSKII	60
⊛	JOHNSRUD	59
⊞	LYON	59
⬟	KONONOV	58
◆	LEIPUNSKIJ	58
✛	MACKLIN	57
✩	GRIMELAND	52
◎	HUMMEL	51

2.59. ^{51}V (n,γ) ^{52}V
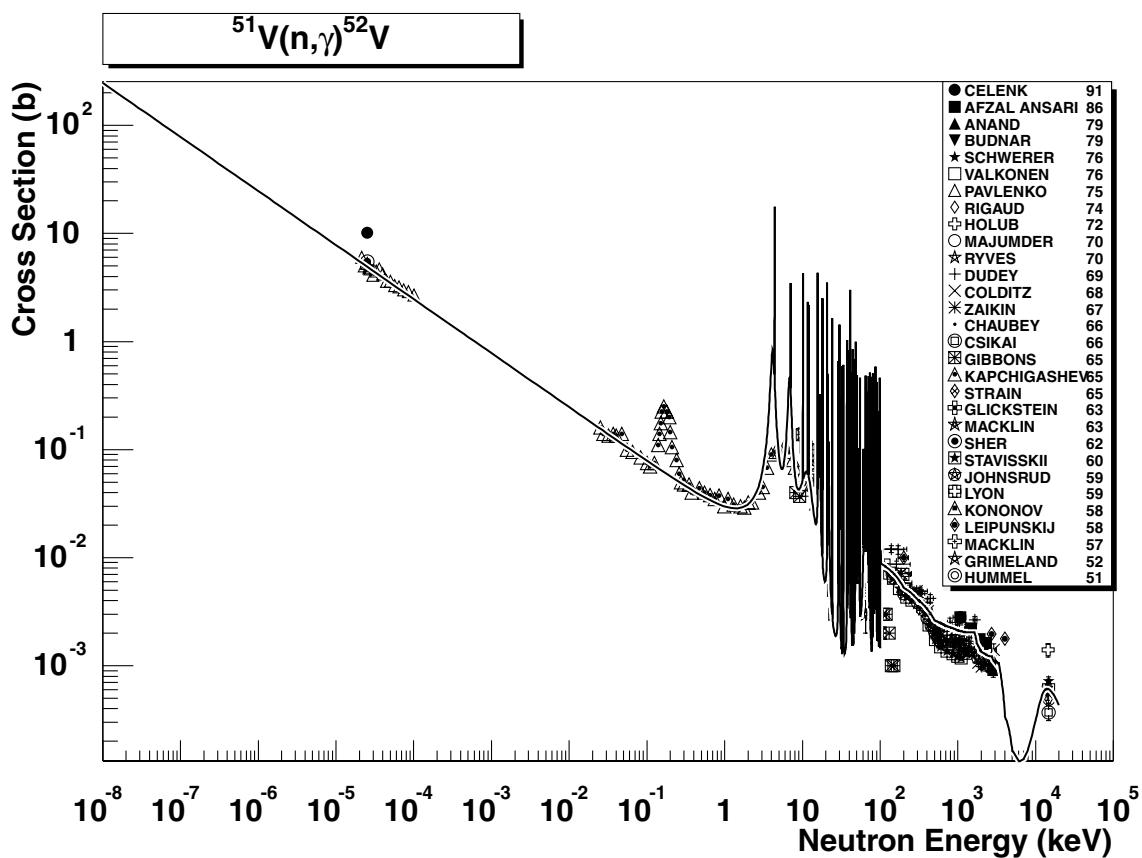
final state: total
source: EAF-4.1 (JENDL-3.1)

There is a good agreement with the experimental information in the whole energy range. A broad resonance like structure in the experimental data at about 200 eV does not belong to the V-51(n,γ) reaction.

88

^{51}V(n,p)^{51}Ti

● KATOH	89
■ IKEDA	88
▲ ALARCON	87
▼ MEADOWS	87
★ GUPTA	85
□ PEPELNIK	85
△ SMITH	84
◇ KHAN	83
✠ ANDERS	82
○ WARREN	82
✩ VAENSKAE	80
+ NGOC	79
× QAIM	77
✳ SCHWERER	76
· SPANGLER	75
◎ DRESLER	73
⊠ ROBERTSON	73
△ TIKKU	72
◇ PRASAD	71
✛ CRUMPTON	69
✦ LEVKOVSKIJ	69
◉ MITRA	66
⊞ WESTERN	66
✪ KHURANA	65
⊞ STRAIN	65
◭ BORMANN	63
◈ BRAMLITT	63
✛ KHURANA	60
✩ POULARIKAS	60
◎ PAUL	53
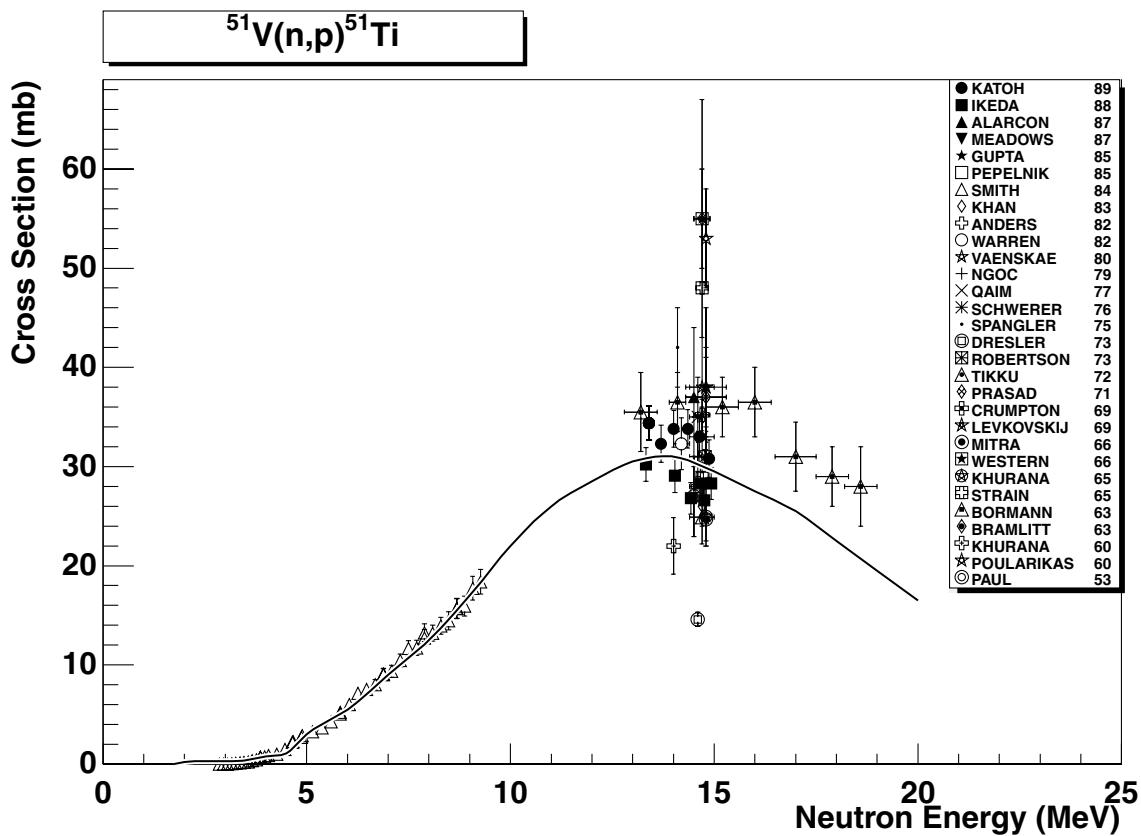
2.60. ^{51}V (n,p) ^{51}Ti

final state: total
source: JENDL-Act96

JENDL-Act96 agrees very well with the data below 10 MeV. The recent data of Katoh89 and Ikeda88 around 14 MeV agree nicely with each other and are assumed to be superior to the rest. The excitation curve runs in the middle between the above mentioned two experiments.

^{51}V(n,α)^{48}Sc

●	FILATENKOV	97
■	MOLLA	94
▲	HAN-LIN	89
▼	HANLIN	89
○	IKEDA	88
□	KOBAYASHI	88
△	GRIGOR´EV	87
◇	MEADOWS	87
⊹	MOLLA	86
★	PEPELNIK	85
☆	HELFER	84
+	KANNO	84
✳	KHAN	83
✕	WARREN	82
·	GARUSKA	80
◎	ZUPRANSKA	80
⊞	DOLYA	77
◭	QAIM	77
◈	SCHWERER	76
⊕	MANNHART	75
★	SPANGLER	75
◉	PAULSEN	74
⊠	ROBERTSON	73
⊛	CRUMPTON	69
⊞	LEVKOVSKIJ	69
◮	VONACH	68
◆	STRAIN	65
⊹	BRAMLITT	63
☆	HILLMAN	62
◎	BORMANN	61
⊞	GABBARD	60
△	POULARIKAS	60
◈	KUMABE	58
⊕	VONACH	58
★	PAUL	53

2.61. ^{51}V (n,α) ^{48}Sc
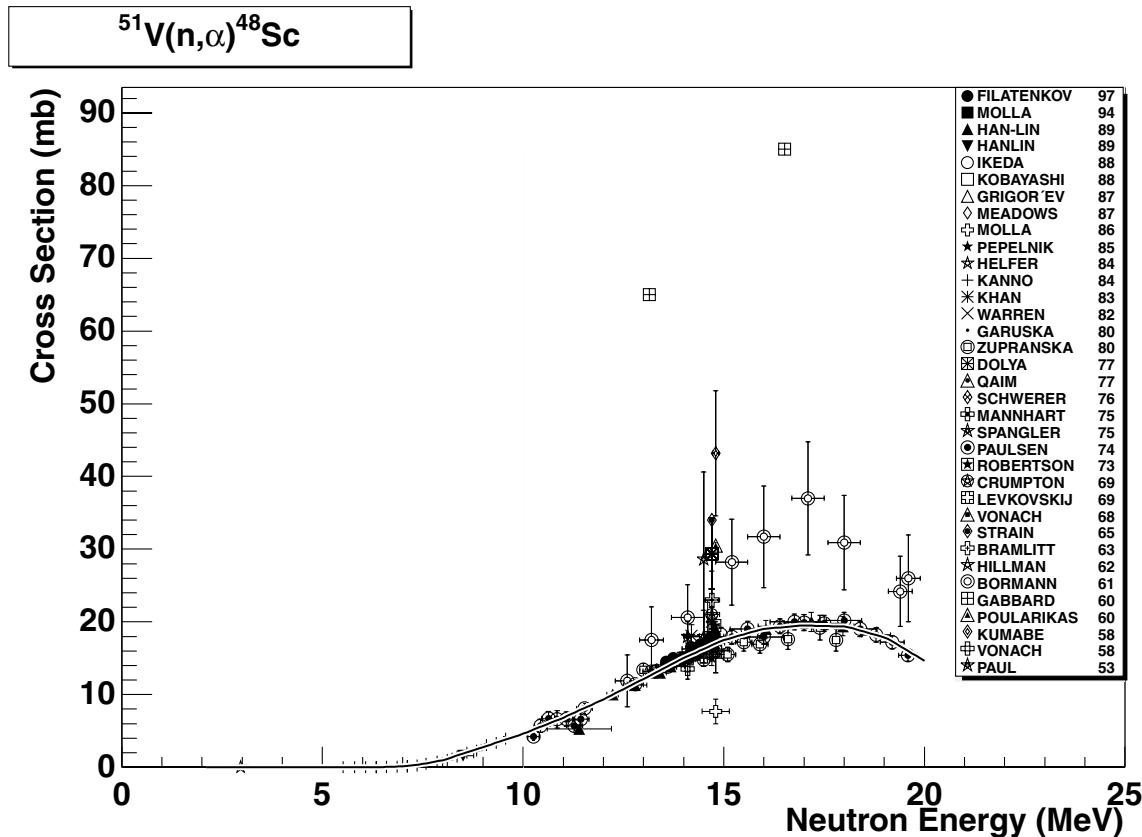
final state: total
source: EAF-4.1 (IRDF-90.2)

IRDF-90.2 shows a good agreement with all major recent data (around 14 MeV). Data of Borman61 and Gabbard60 proved to be wrong during the FENDL selection panel and were disregarded.

^{50}Cr(n,γ)^{51}Cr
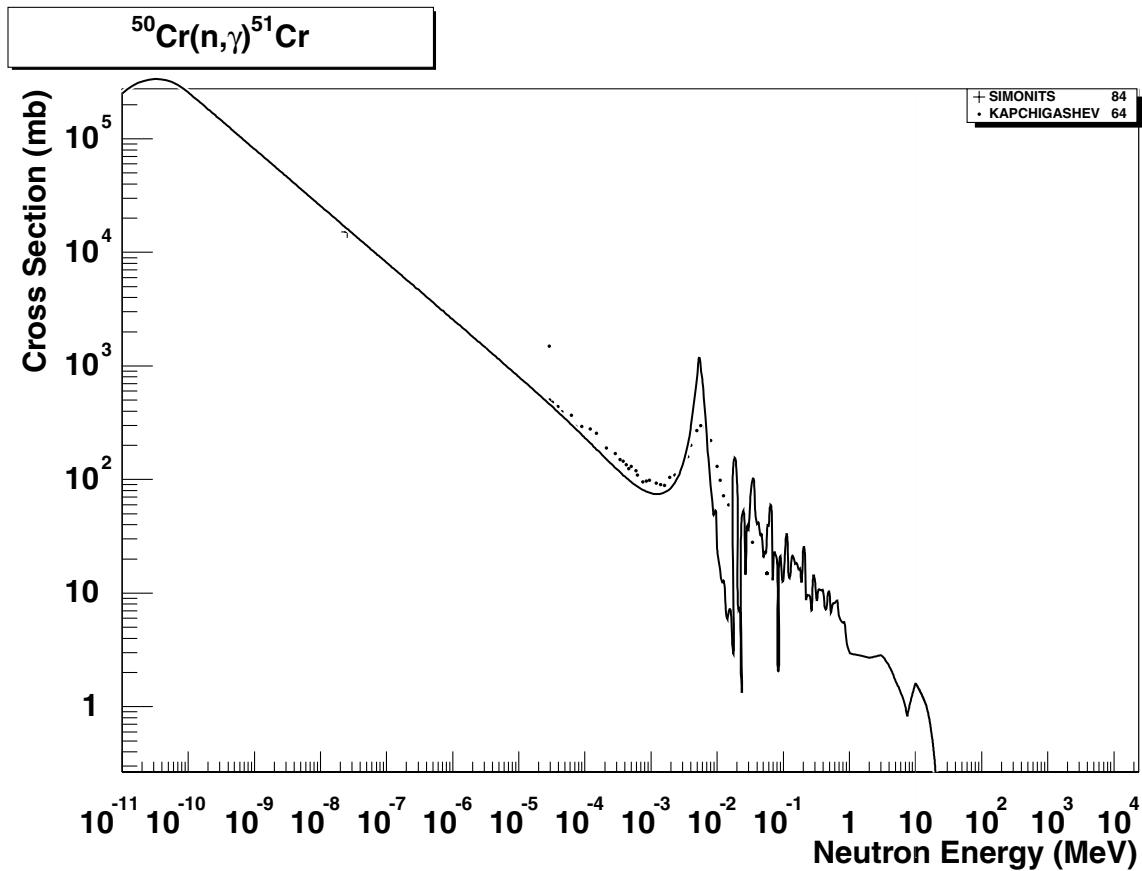
2.62. ^{50}Cr (n,γ) ^{51}Cr

final state: total
source: EAF-4.1(EFF-2.4)

ENEA evaluation (EFF-2.4) is reasonably close to the experimental data at low energies, however, the high energy part of the excitation curve looks strange. A replacement of this data by ENDF/B-VI may be considered. Data are stored in SANDII group structure, the original EFF-2.4 point-wise data include 9519 energy points.
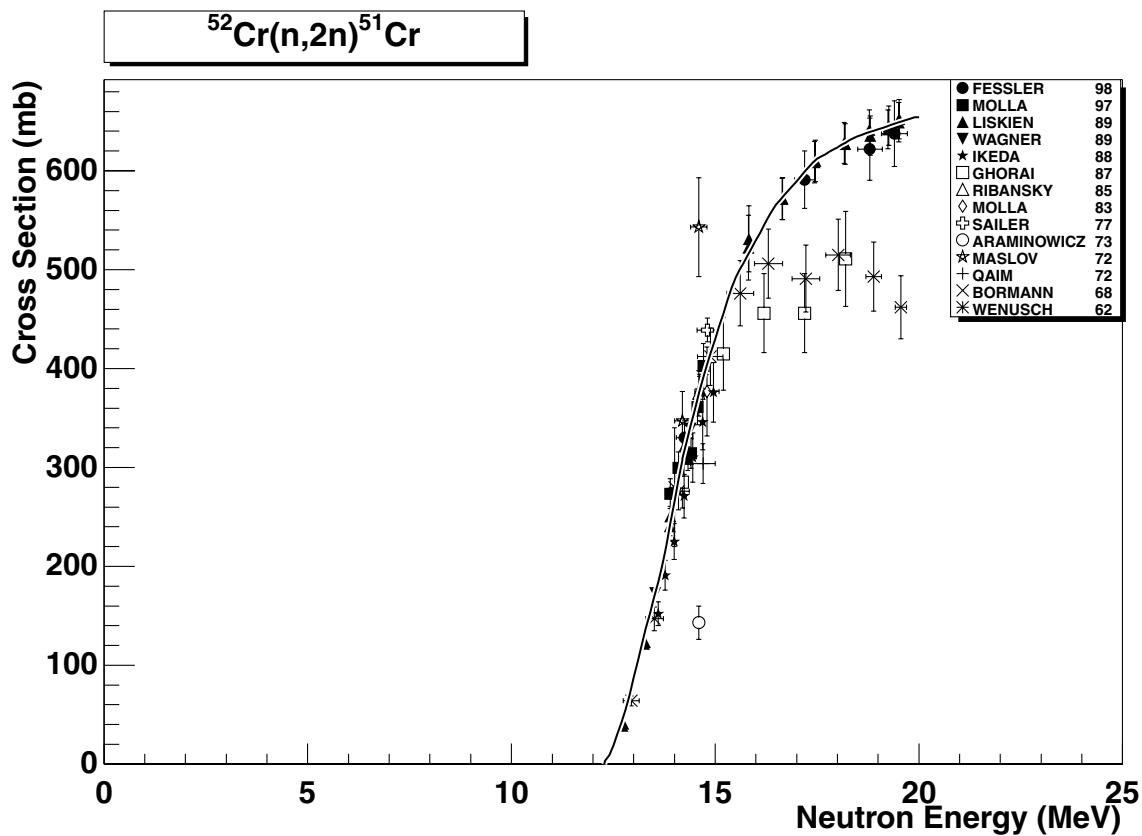
2.63. ^{52}Cr (n,2n) ^{51}Cr

final state: total
source: IRDF-90.2

IRDF-90.2 reproduces the experimental data very well. The experiment of Liskien89 was decisive for the shape above 15 MeV and overruled the previously measured data.

^{52}Cr(n,p)^{52}V

●	FESSLER	98
■	OSMAN	96
▲	VIENNOT	91
▼	KAWADE	90
★	IKEDA	88
□	GHORAI	87
△	DAC LUC	86
◇	GUPTA	85
✛	RIBANSKY	85
○	VIENNOT	82
✭	ARTEM´EV	80
+	SMITH	80
✕	QAIM	77
✳	VALKONEN	76
·	ALEKSANDROV	75
◎	DRESLER	73
▨	PRASAD	71
◮	CLATOR	69
◈	HUSAIN	67
⊞	MITRA	66
✪	KHURANA	65
◉	STRAIN	65
▨	CHITTENDEN	61
⬡	MUKHERJEE	61
⊟	KHURANA	60
◭	KERN	59
◆	PAUL	53
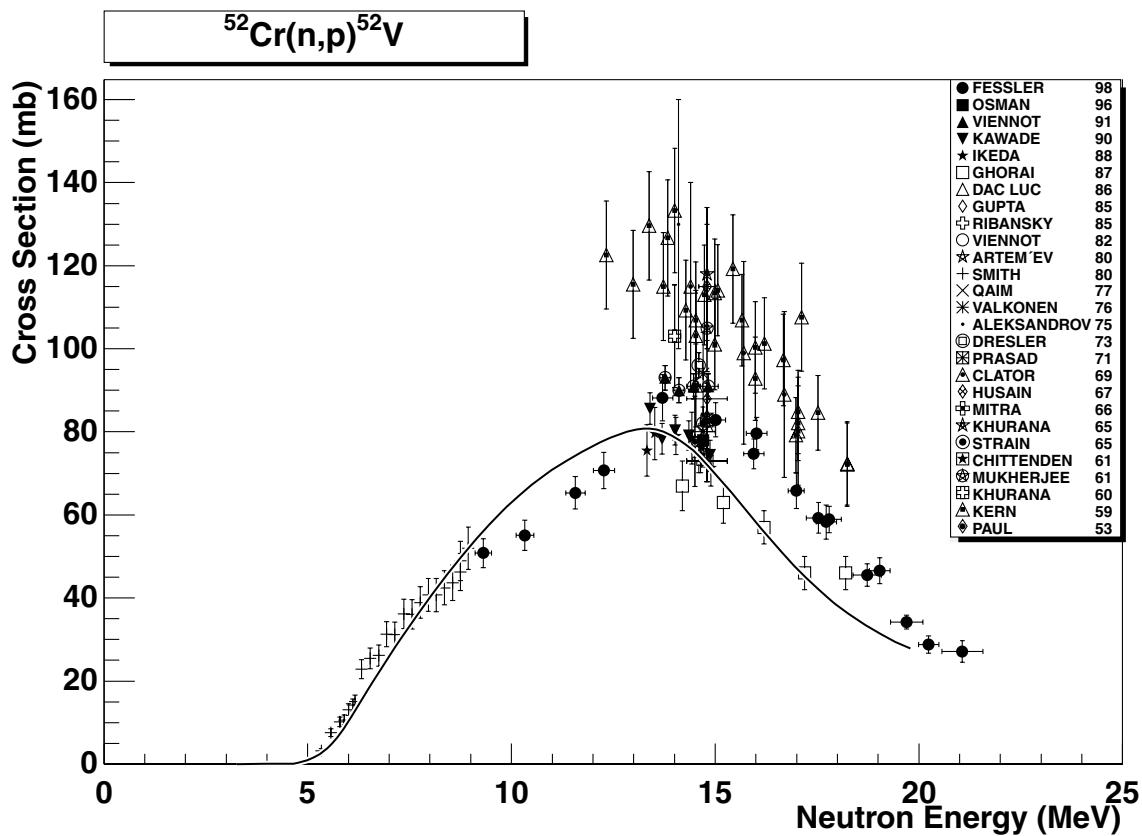
2.64. ^{52}Cr (n,p) ^{52}V

final state: total
source: ADL-3

ADL-3 evaluation agrees nicely with Smith80 below 10 MeV. Around 14 MeV the evaluation runs between the data of Ikeda88 and Kawade90. The slightly larger data of Viennot91 have been shown too large by the very recent measurement of Osman96, which support values of Ikeda88 and Kawade90. Data of Kern59 may be disregarded.

^{53}Cr(n,d+np)^{52}V
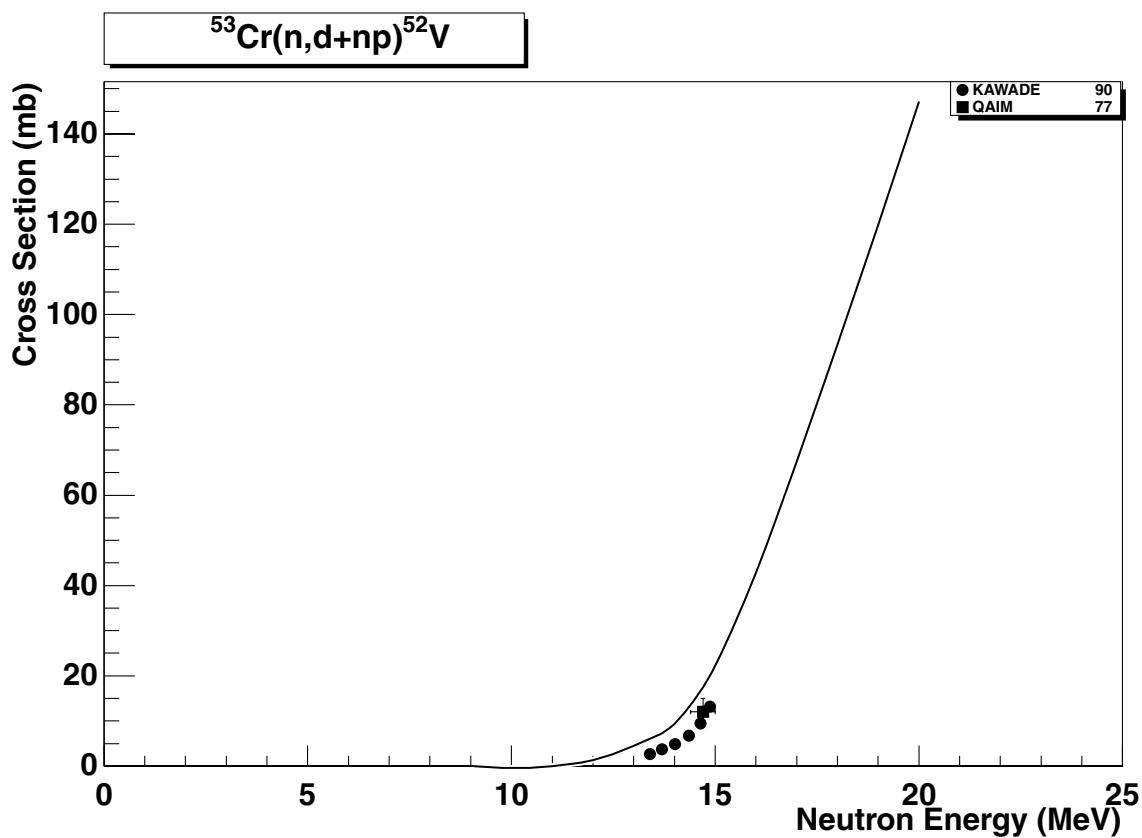
● KAWADE	90
■ QAIM	77

2.65. ^{53}Cr (n,d+np) ^{52}V

final state: total
source: EFF-2.4

EFF-2.4 evaluation is plotted against (n,d+np) data. The 14-15 MeV cross section value lies reasonably close to the experimental data of Qaim77 and Kawade90. The data are stored separately as (n,d) and (n,np) reaction channels.
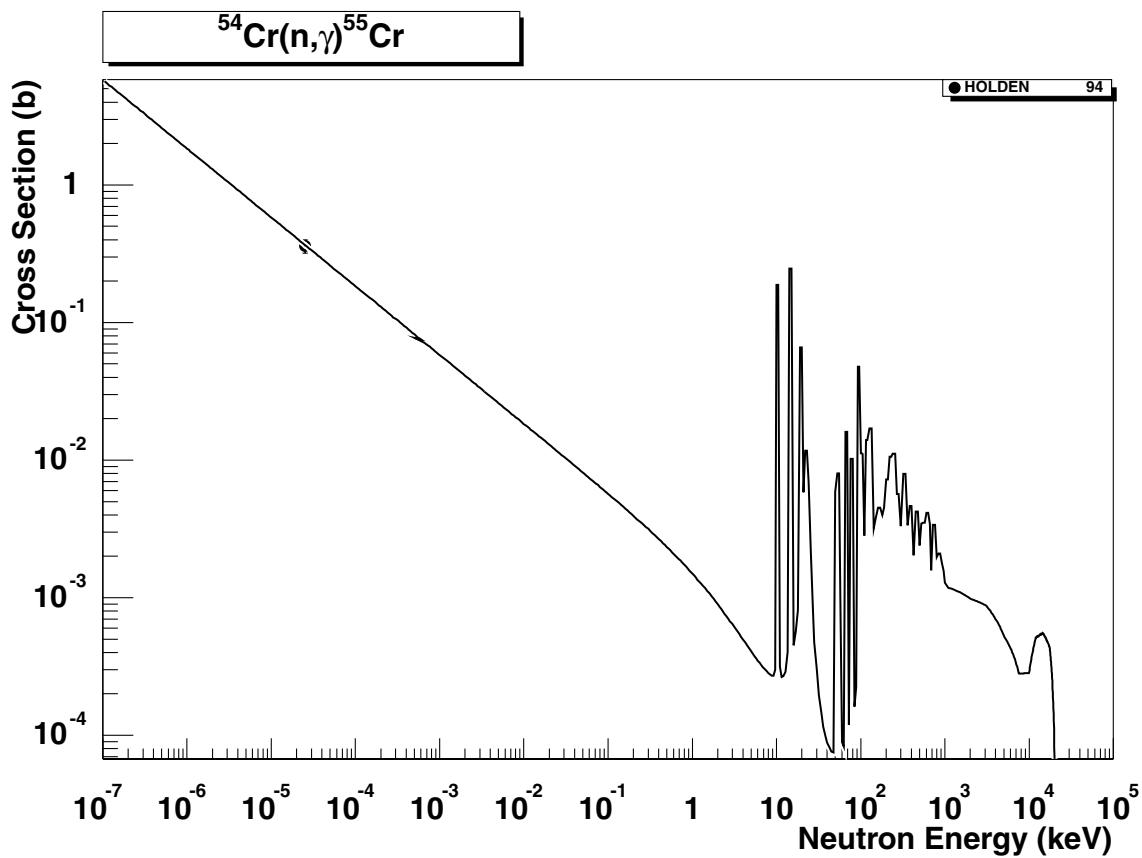
2.66. ^{54}Cr (n,γ) ^{55}Cr

final state: total
source: EAF-4.1 (EFF-2.4)

EFF-2.4 evaluation includes the resolved resonance data. No high energy data is available. The thermal cross-section of Holden [32] is nicely reproduced with C/E=1.01. Data are plotted in the multigroup SANDII structure.
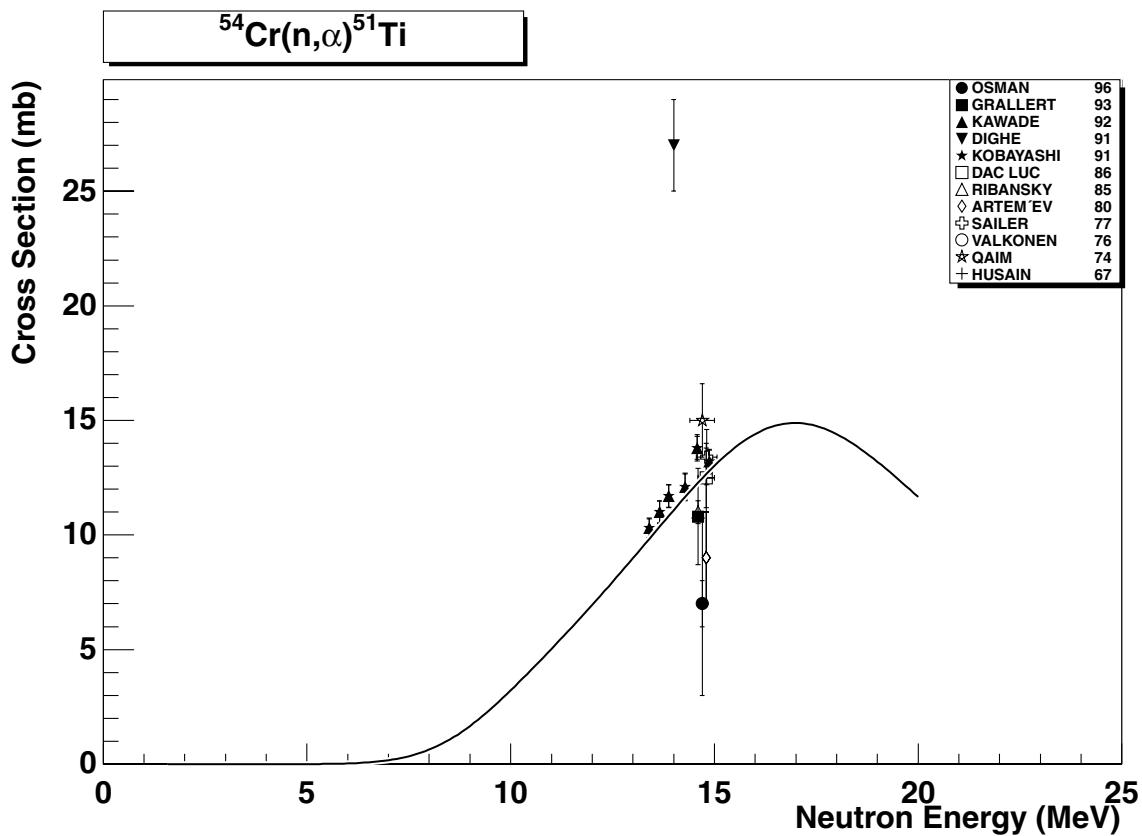
2.67. ^{54}Cr (n,α) ^{51}Ti

final state: total
source: IPPE

Recent IPPE evaluation [11] is close to the Kawade92 data around 14 MeV. Dighe91 is too large and can be disregarded.
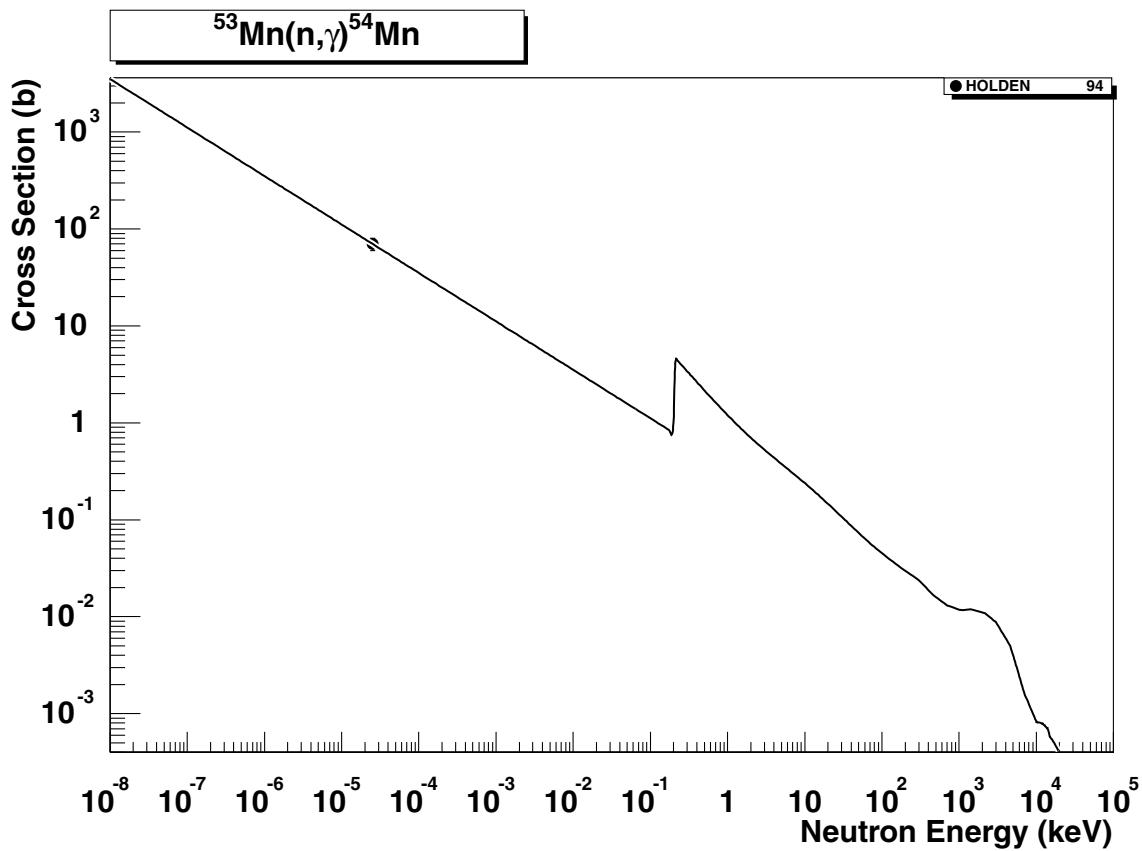
2.68. ^{53}Mn (n,γ) ^{54}Mn

final state: total
source: EAF-4.1

This EAF-4.1 evaluation is based on calculations with the MASGAM code. MASGAM is a statistical (Hauser-Feshbach) code with the pre-equilibrium component based on the D-SD model (for details see Ref. [35]). The global parameters are applied for optical model, level densities and gamma-ray strength functions. The thermal cross-section of Holden94 [32] is well reproduced with C/E=1.0.
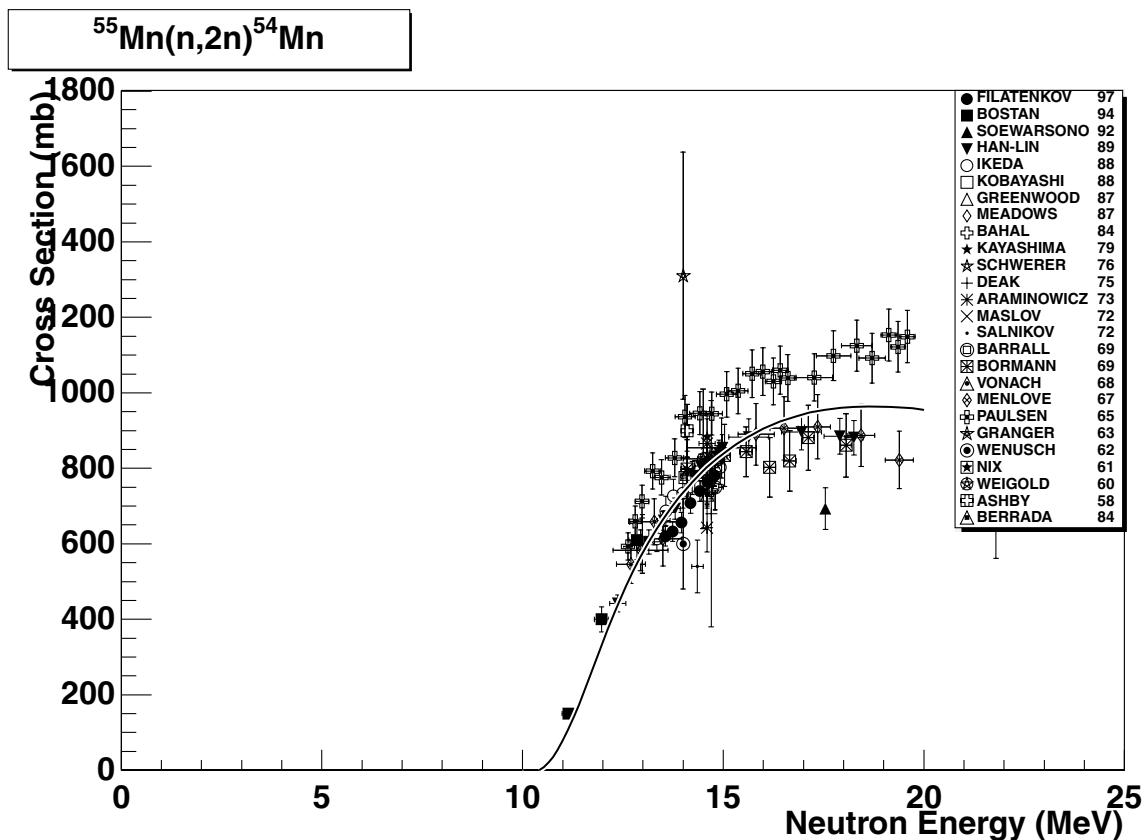
2.69. ^{55}Mn (n,2n) ^{54}Mn

final state: total
source: ADL-3

ADL-3 excitation curve fits the data well up to 15 MeV, in particular the recent data of Filatenkov97 and Bostan94. The shape above 15 MeV is closer to the lower data of Han-Lin89, but in principle lies between the data sets. The excitation curve around 18 MeV starts to be uncertain.

^{55}Mn(n,γ)^{56}Mn

●	GAUTAM	90
■	GAUTAM	88
▲	TROFIMOV	87
▼	ARBILDO	86
★	BAHAL	84
□	MAGNUSSON	80
△	BUDNAR	79
◇	LE RIGOLEUR	76
⊕	SCHWERER	76
○	WIDDER	75
☆	VULETIN	74
+	CHATURVEDI	70
×	DOVBENKO	69
✳	SOKOLOWSKI	69
·	COLDITZ	68
◎	SPITZ	68
⊞	STUPEGIA	68
⧈	MENLOVE	67
◈	PETO	67
⊞	CARRE	66
✬	CSIKAI	66
◉	CHAUBEY	65
⊠	STRAIN	65
⊛	MACKLIN	63
⊞	MEADOWS	61
⧈	STAVISSKIJ	61
◆	TATTERSALL	60
⊕	BOSTROM	59
✩	JOHNSRUD	59
◎	LYON	59
⊞	BOOTH	58
⧈	KONONOV	58
◇	LEIPUNSKIJ	58
⊕	PERKIN	58
★	MACKLIN	57
◉	GRIMELAND	52
◻	HUMMEL	51
△	BEGHIAN	49

2.70. ^{55}Mn (n,γ) ^{56}Mn

final state: total
source: EAF-4.1 (JEF-2.2)

The evaluation originates from ENDF/B-VI and runs well through the experimental data in the whole energy range. Two large data points at 14 MeV (Strain65 and Bahal84) are ignored.

2.71. ^{55}Mn (n,α) ^{52}V
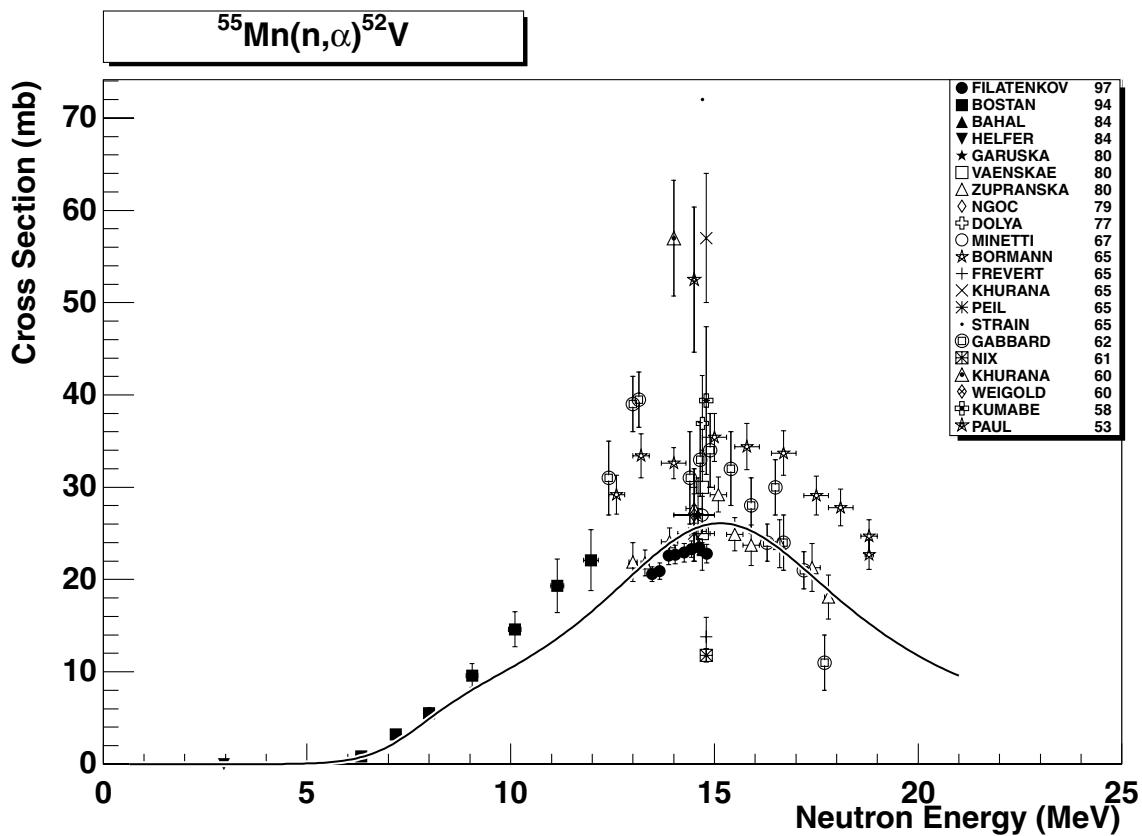
final state: total
source: IPPE

Recent IPPE evaluation[11] runs between the two latest experimental data sets of Bostan94 (below 12 MeV) and Filatenkov97 (between 13-15 MeV). There are a number of the old data (Paul53, Khurana60,65, Gabbard62 and Borman65) which were found too large and not considered in the IPPE evaluation adjustment.

^{54}Fe(n,2n)^{53}Fe

●	FESSLER	98
■	VIENNOT	91
▲	KATOH	89
▼	ZHOU MUY	87
★	GREENWOOD	85
□	BAHAL	84
△	RYVES	78
◇	RYVES	78
✛	BORMANN	76
○	SIGG	75
✭	ARAMINOW	73
+	QUAIM	72
×	ANDREEV	68
✳	CSIKAI	65
·	SALISBURY	65
◎	STRAIN	65
⊞	CARLES	63
△	CROSS	63
◇	CHITTENDEN	61
✛	POLLEHN	61
✭	RAYBURN	61
◉	DEPRAZ	60
⊠	TERRELL	58
✿	ALLAN	56
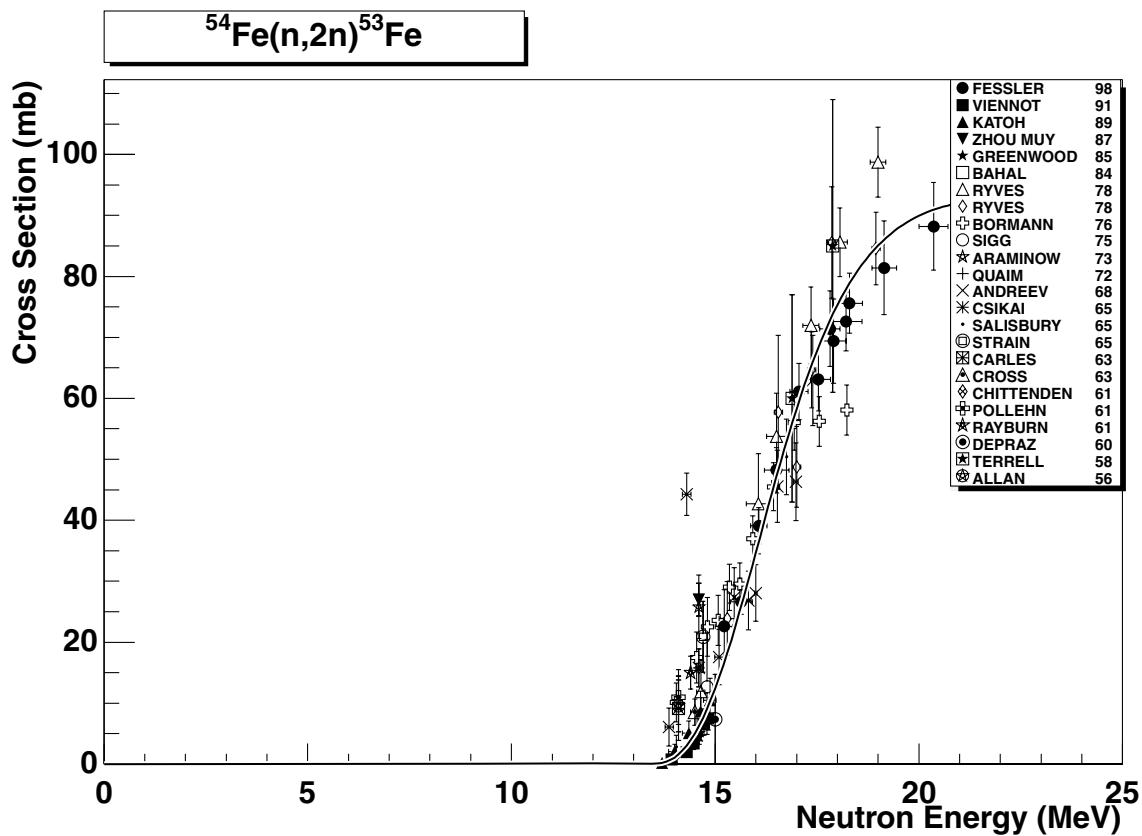
2.72. ^{54}Fe (n,2n) ^{53}Fe

final states: g.s., meta
source: RRDF-98

Experimental data plotted above were renormalized according to the new recommended standards and decay schemes which resulted in a very consistent set. The RRDF-98 evaluation reproduces this set very well.
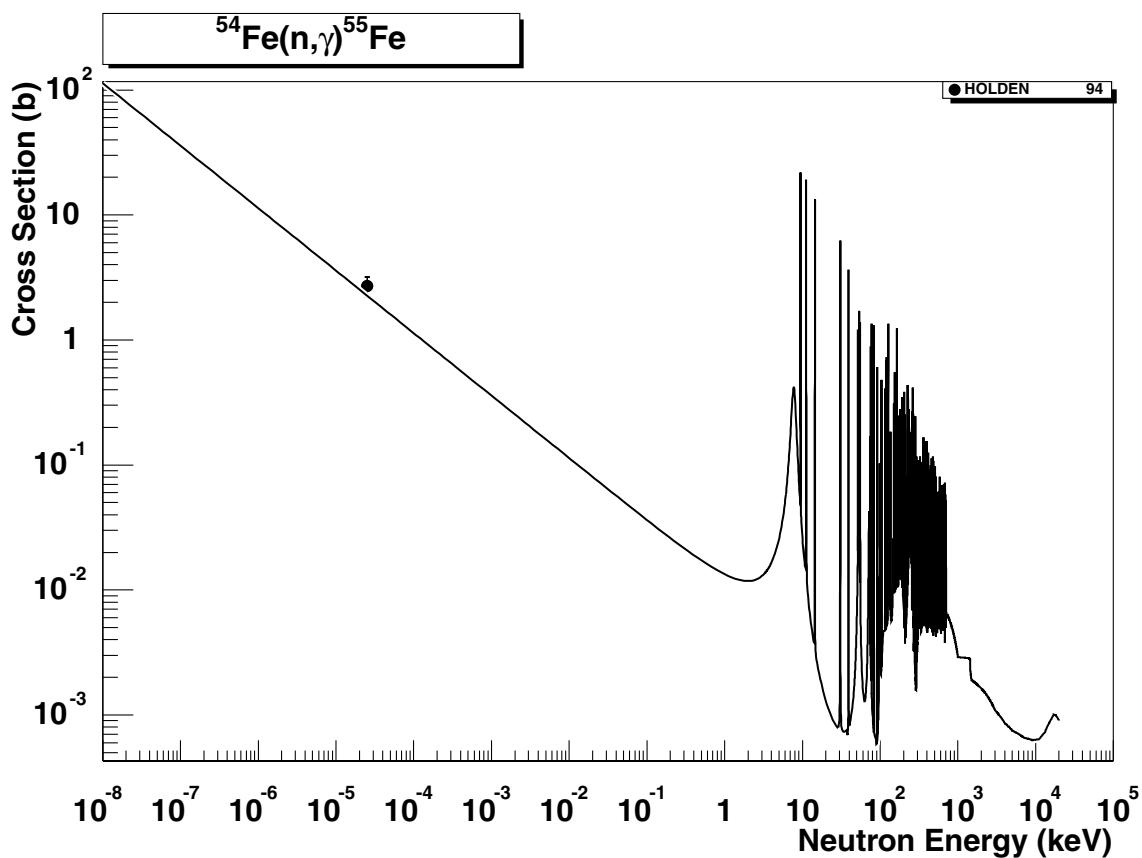
2.73. ^{54}Fe (n,γ) ^{55}Fe

final state: total
source: EAF-4.1 (ENDF/B-VI)

ENDF/B-VI evaluation includes the resolved resonance data. No EXFOR data are available outside the resonance region. The thermal cross-section of Holden94 [32] is reproduced with C/E=0.83.

^{54}Fe(n,p)^{54}Mn

● MEADOWS	96
■ GARLEA	92
▲ KLOCHKOVA	92
▼ SARAF	91
○ VIENNOT	91
□ HAN-LIN	89
△ HANLIN	89
◇ IKEDA	88
✚ KOBAYASHI	88
★ GREENWOOD	87
☆ KLOCHKOVA	87
＋ GARLEA	85
✳ BAHAL	84
✕ VIENNOT	82
· ARTEM´EV	80
◎ PAULSEN	79
⊠ FUKUDA	78
△ AI	77
◇ SMITH	75
⊕ SINGH	72
★ PAULSEN	71
◉ QAIM	71
⊞ BARRALL	69
⊛ VENUGOPALA RAO	70
⊡ CARROLL JR	65
△ LAUBER	65
◆ SALISBURY	65
⊕ CROSS	63
★ POLLEHN	61
◎ ALLAN	59
⊞ ALLAN	57
△ IKEDA	90
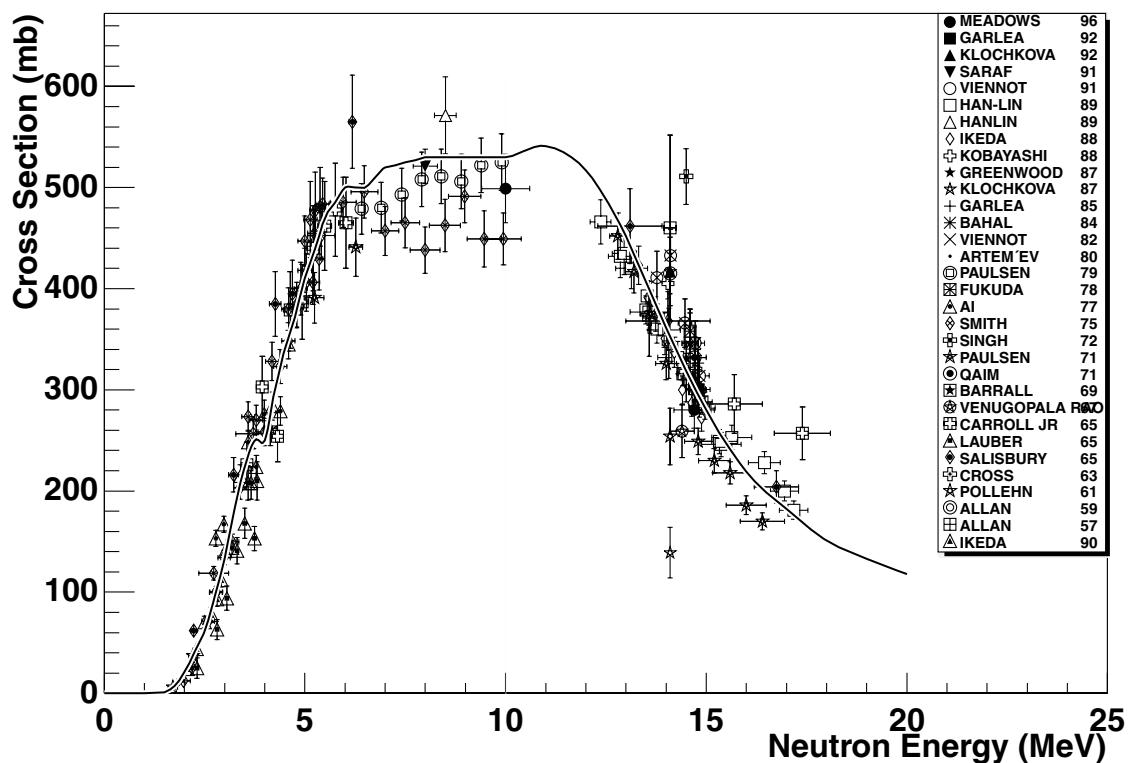
2.74. ^{54}Fe (n,p) ^{54}Mn

final state: total
source: JENDL-Act96

JENDL-Act96 evaluation reproduces the consistent data very well in the whole energy range.
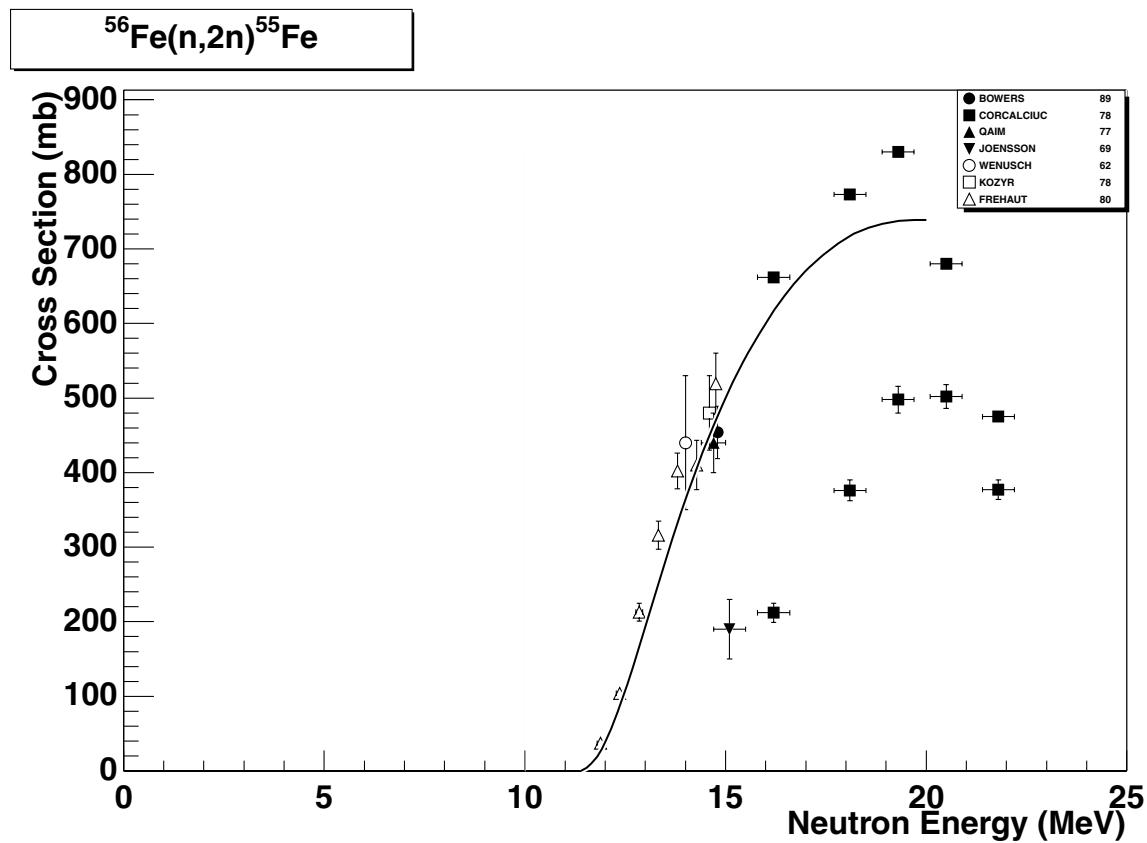
2.75. ^{56}Fe (n,2n) ^{55}Fe

final state: total
source: ADL-3

ADL-3 evaluation agrees reasonably with the data of Frehaut80 and Bowers89. The data of Corcalciuc78 above 15 MeV are a combination of calculations with partial data and may be disregarded.

^{56}Fe(n,γ)^{57}Fe
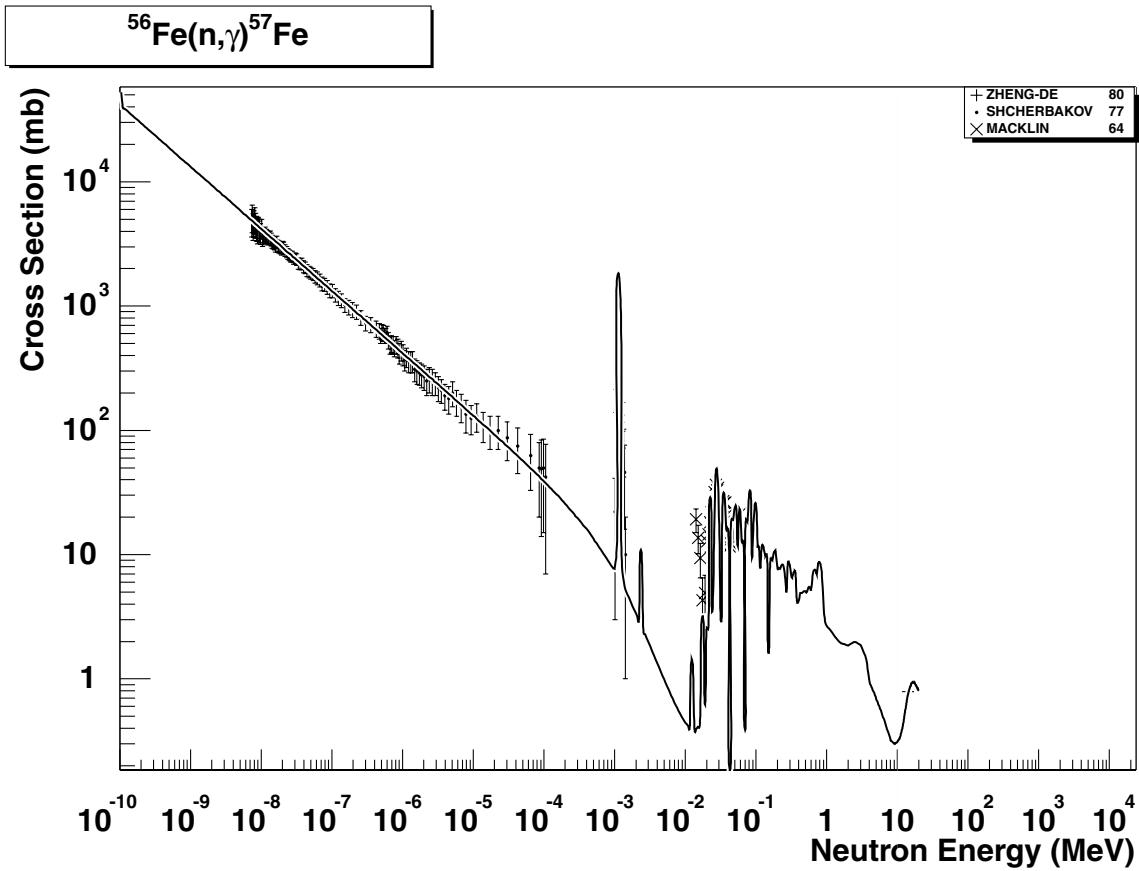
2.76. ^{56}Fe (n,γ) ^{57}Fe

final state: total
source: EAF-4.1 (ENDF/B-VI)

ENDF/B-VI evaluation reproduces well the experimental data in the whole energy range. Data are stored in SANDII group structure, the original ENDF/B-VI evaluation includes 41312 energy points.

^{56}Fe(n,p)^{56}Mn

● SMITH	75
■ SPANGLER	75
▲ ROBERTSON	73
▼ DYER	72
★ SINGH	72
□ QAIM	71
△ BARRALL	69
◇ JOENSSON	69
✚ CUZZOCREA	68
○ LEVKOVSKIJ	68
☆ VONACH	68
+ GRUNDL	67
× HEMINGWAY	66
✳ LISKIEN	66
· BORMANN	65
◉ LISKIEN	65
⊠ STRAIN	65
△ BONAZZOLA	64
◇ SANTRY	64
✚ CROSS	63
★ BORMANN	62
◉ GABBARD	62
⊠ CHITTENDEN II	61
✪ POLLEHN	61
⊞ DEPRAZ	60
▲ KERN	59
◆ TERRELL	58
✚ ALLAN	57
★ BROWN	57
◎ YASUMI	57
⊞ MC CLURE	55
△ PAUL	53
◇ FORBES	52

106

^{56}Fe(n,p)^{56}Mn

● FILATENKOV	97
■ IKEDA	93
▲ ZONGYU	93
▼ KLOCHKOVA	92
★ FUGA	91
□ SARAF	91
△ CHI-CHOU	89
◇ IKEDA	88
✠ KOBAYASHI	88
○ ZHOU-MUYAO	87
☆ GARLEA	85
+ GUPTA	85
✕ GARLEA	84
✳ KUDO	84
· NGOC	84
◎ NHU-NGOC	83
⊞ KUDO	82
◮ VIENNOT	82
◈ NEMILOV	78
✛ RYVES	78
✩ SHARMA	78
◉ KUDO	77
⊠ RAMENDIK	77
✾ SOTHRAS	77
⊞ MOSTAFA	76

2.77. ^{56}Fe (n,p) ^{56}Mn

final state: total
source: EAF-4.1 (IRDF-90.2)

An excellent agreement of the IRDF-90.2 evaluation with all experimental data.
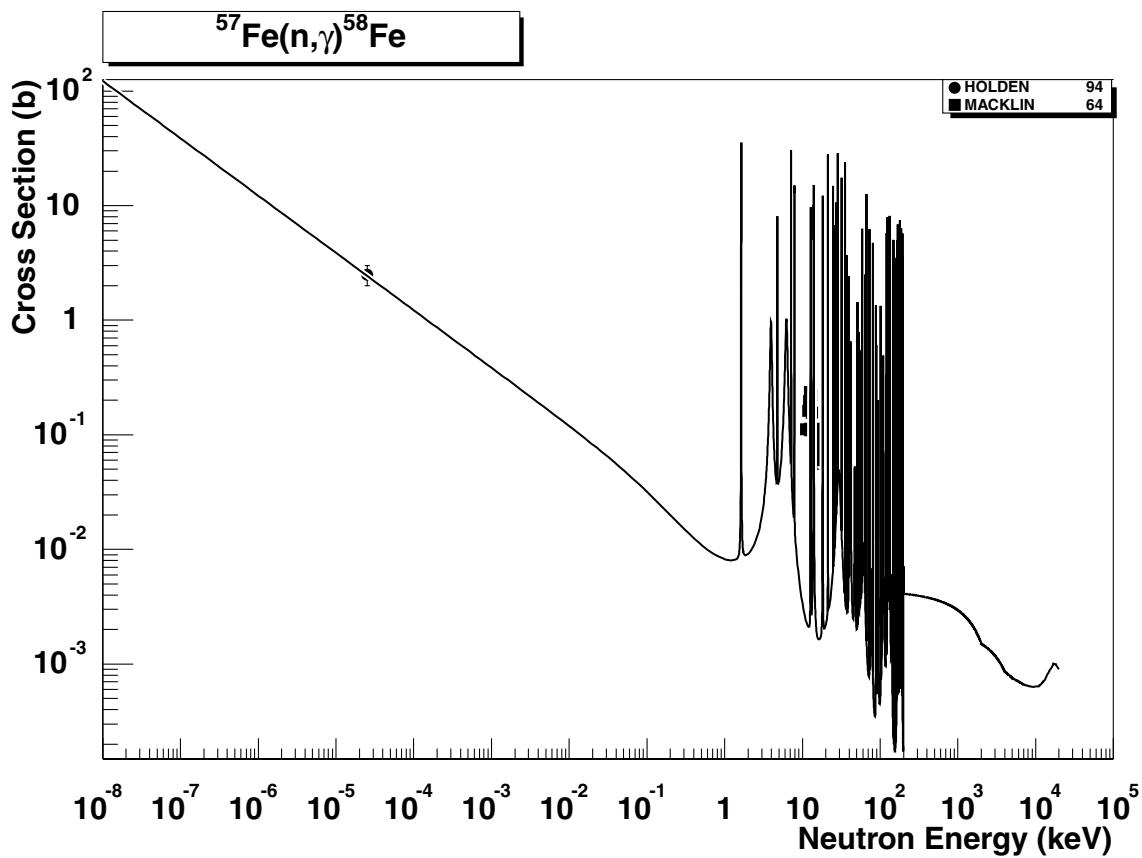
2.78. ^{57}Fe (n,γ) ^{58}Fe

final state: total
source: EAF-4.1 (ENDF/B-VI)

Experimental data are rather scarce, only a few points are available in the resolved reso-
nance region. The thermal cross-section of Holden94 [32] is reproduced with C/E=0.98.
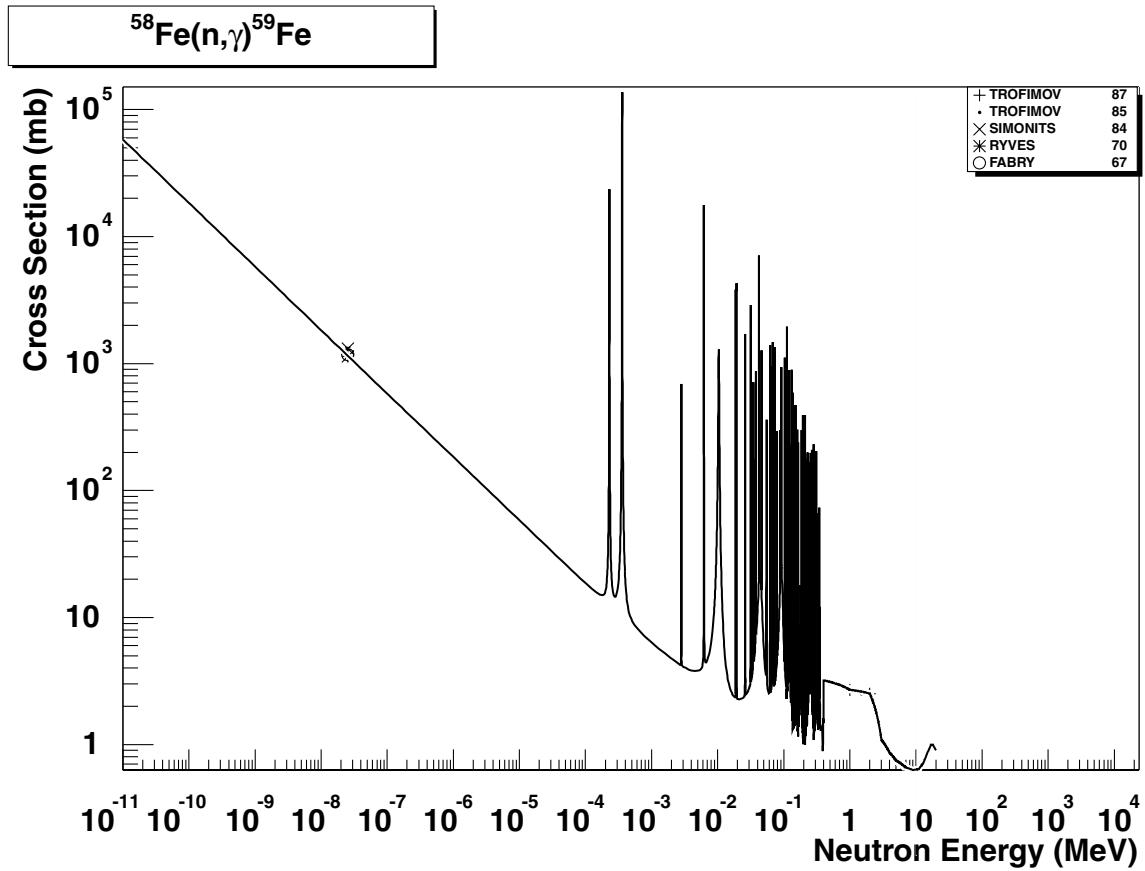
2.79. ^{58}**Fe (n,γ)** ^{59}**Fe**

final state: total
source: EAF-4.1 (ENDF/B-VI)

ENDF/B-VI is in good agreement with experimental data, both in the thermal region
and in the smooth statistical region around 1 MeV (Trofimov85,87).
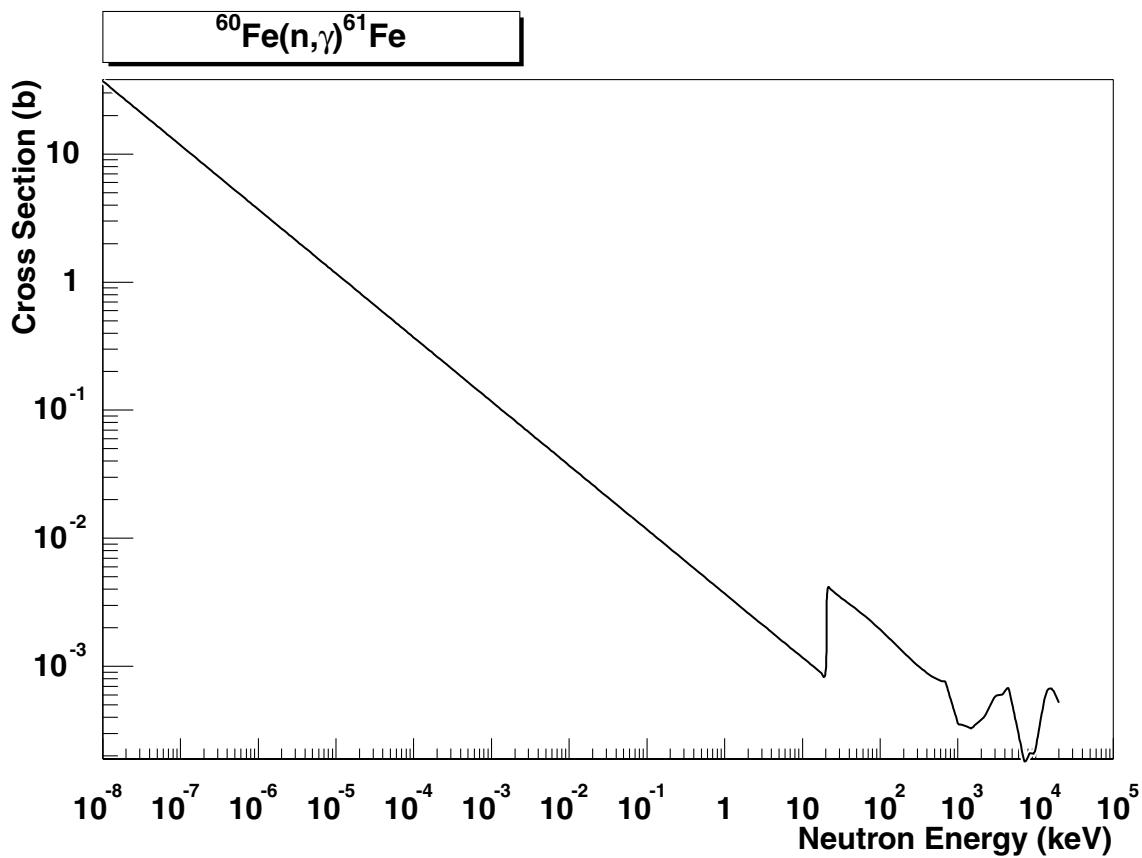
2.80. ^{60}Fe (n,γ) ^{61}Fe

final state: total
source: EAF-4.1

No experimental data are available. The evaluated data are based on the simplified model calculations with the code MASGAM with global parameters (Hauser-Feshbach and DSD model with no resonance region generation, E_H is based on a $D_0/2$ estimate; for details see Ref. [35]).

110

The figure shows a plot titled ^{59}Co(n,2n)^{58}Co, with Cross Section (mb) on the vertical axis and Neutron Energy (MeV) on the horizontal axis.

Legend:

●	FILATENKOV	97
■	OSMAN	96
▲	MOLLA	94
▼	GARLEA	92
★	DIGHE	91
□	FREHAUT	90
△	TINGYAN	90
◇	JIAN-ZHOU	89
✛	IKEDA	88
○	KOBAYASHI	88
✭	RYVES	88
+	GREENWOOD	87
✕	MEADOWS	87
✳	HASAN	86
·	GARLEA	85
◉	IKEDA	84
⊠	MOLLA	83
△	GHORAI	80
◇	PROKOPEC	80
✜	PROKOPETS	80
✭	FUKUDA	78
◉	KOZYR´	78
⊠	KOZYR´	77
✪	VEESER	77
⊞	ARAMINOWICZ	73
△	SALNIKOV	72
◈	BARRALL	69
✛	OKUMURA	67
★	BORMANN	66
◎	PAULSEN	65
⊞	STRAIN	65
△	GRANGER	63
◇	JERONYMO	63
✜	WEIGOLD	62
★	WENUSCH	62
◉	BORMANN	61
▣	KERN	60
△	WEIGOLD	60
◈	ASHBY	58

2.81. ^{59}Co (n,2n) ^{58}Co

final state: total
source: IRDF-90.2 (pointwise)

IRDF-90.2 agrees well with the experimental data below 15 MeV and runs through the data up to 20 MeV. Data set Ikeda88 is wrong and can be disregarded.
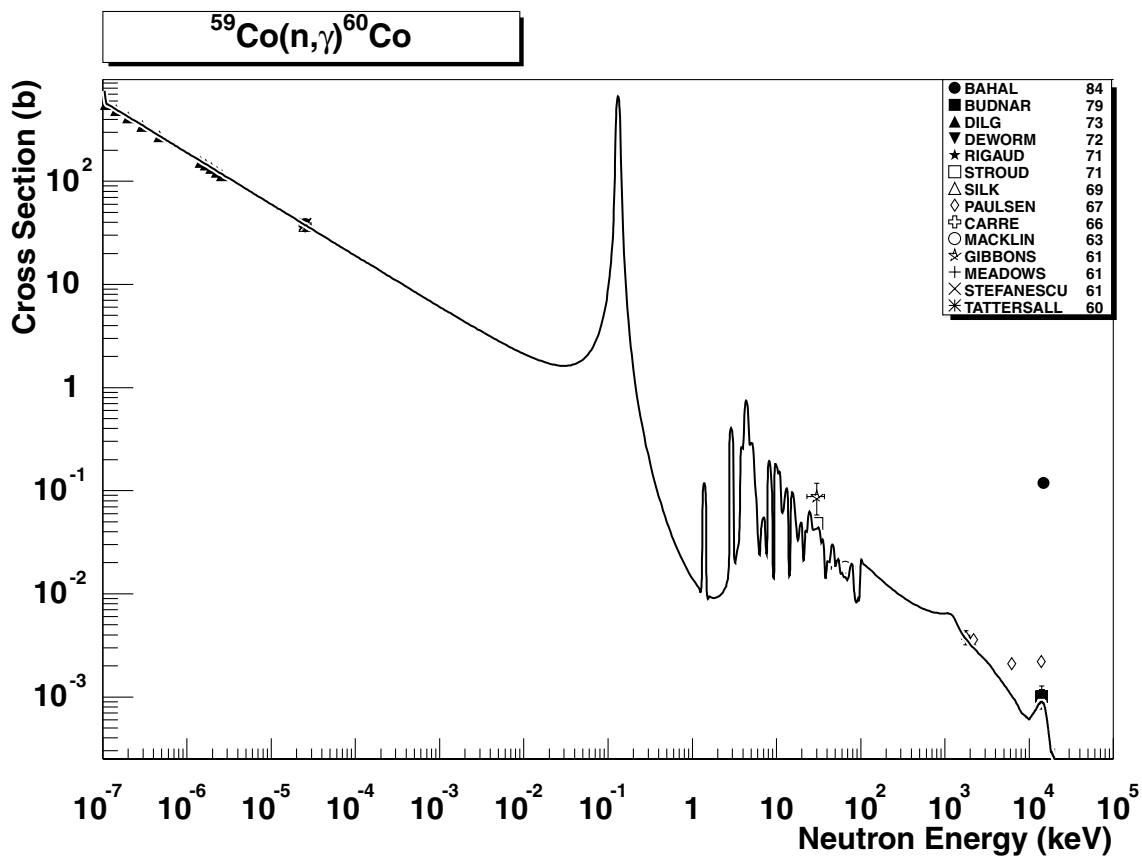
2.82. ^{59}Co (n,γ) ^{60}Co

final state: g.s., meta
source: EAF-4.1 (JEF-2.2)

ENDF/B-VI data are adopted in JEF-2.2. The evaluation agrees well with the data in the 1/v region and is in reasonable agreement to the a scattered data around 10 keV and above 1 MeV. The 14 MeV data point of Bahal84 is ignored.

^{59}Co(n,α)^{56}Mn

●	FILATENKOV	97
■	OSMAN	96
▲	MANNHART	94
▼	MOLLA	94
★	GARLEA	92
□	TINGYAN	90
△	JIAN-ZHOU	89
◇	IKEDA	88
✣	KOBAYASHI	88
○	RYVES	88
✮	MEADOWS	87
+	GARLEA	85
×	AGRAWAL	84
✳	BAHAL	84
·	BERRADA	84
◎	GHORAI	80
▨	ZUPRANSKA	80
△	GARUSKA	78
◇	DOLYA	77
✚	ROBERTSON	73
✬	LEVKOVSKIJ	68
◉	LISKIEN	66
▩	BORMANN	65
⊛	KHURANA	65
⊞	LISKIEN	65
▲	STRAIN	65
◆	SANTRY	64
✢	JERONYMO	63
✩	GABBARD	62
◎	BORMANN	61
⊞	KHURANA	60
△	PREISS	60
◈	WEIGOLD	60
⊕	BLOSSER	58
✪	KUMABE	58
◉	PAUL	53
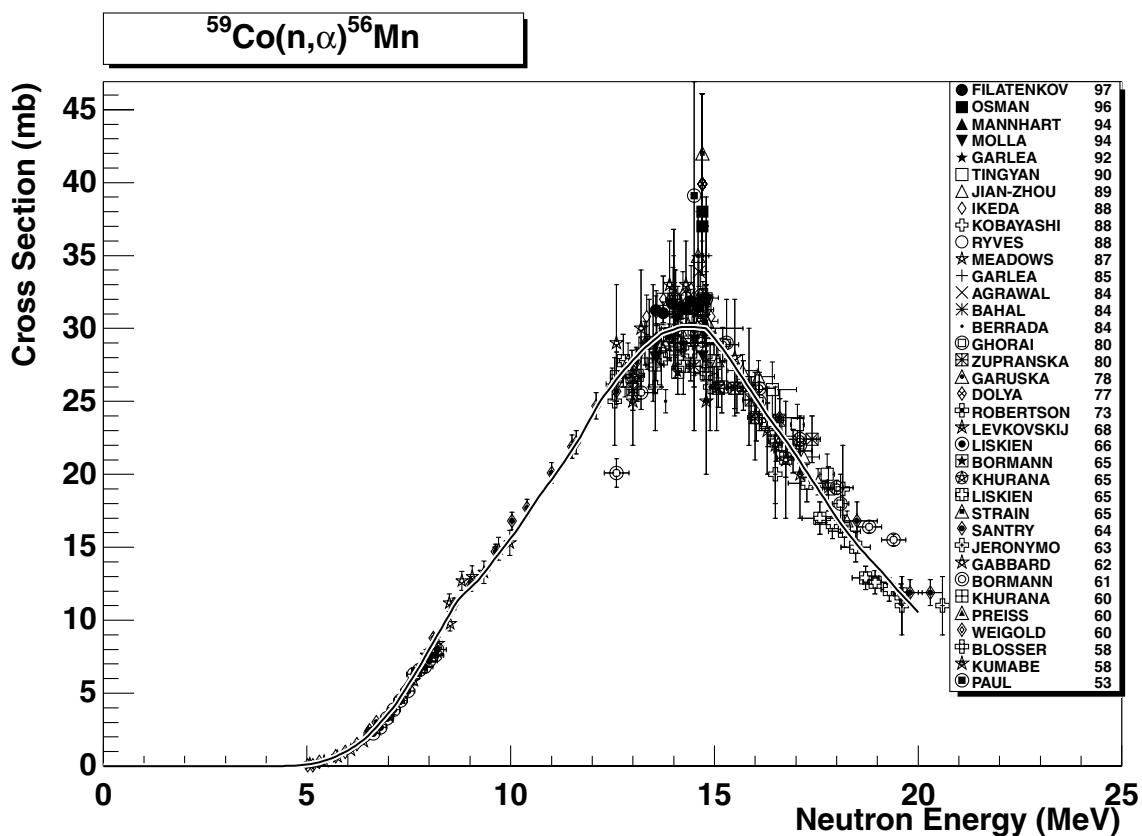
2.83. ^{59}Co (n,α) ^{56}Mn

final state: total
source: EAF-4.1 (IRDF-90.2)

IRDF-90.2 runs through a very consistent set of experimental data in an excellent way.

^{60}Co(n,γ)^{61}Co

HOGG   66
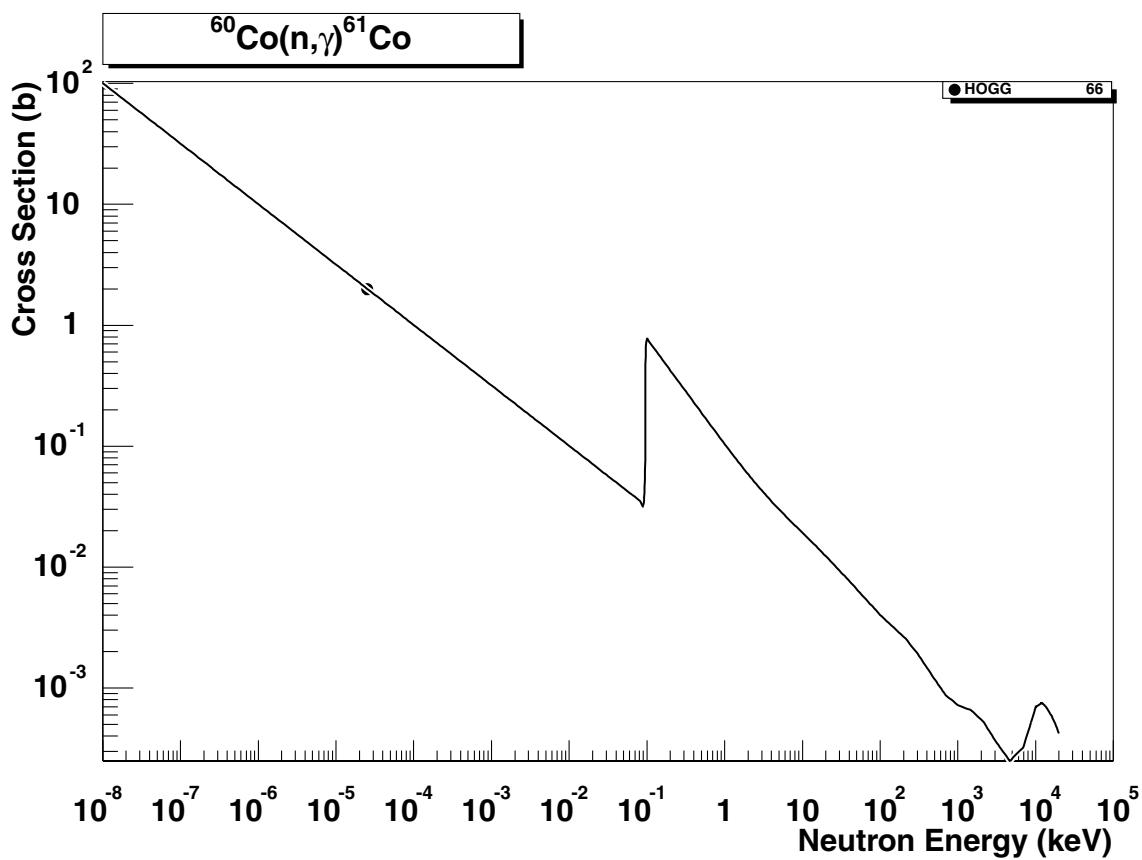
2.84. ^{60}Co (n,γ) ^{61}Co

final state: total
source: EAF-4.1

Data are based on the simplified model calculations with the code MASGAM (Hauser-Feshbach and DSD model with no resonance region generation, E_H is based on $D_0/2$ estimate; for details see Ref. [35]). The 1/v component is adjusted to the experimental value of (2.0 +- 0.2) b [32].
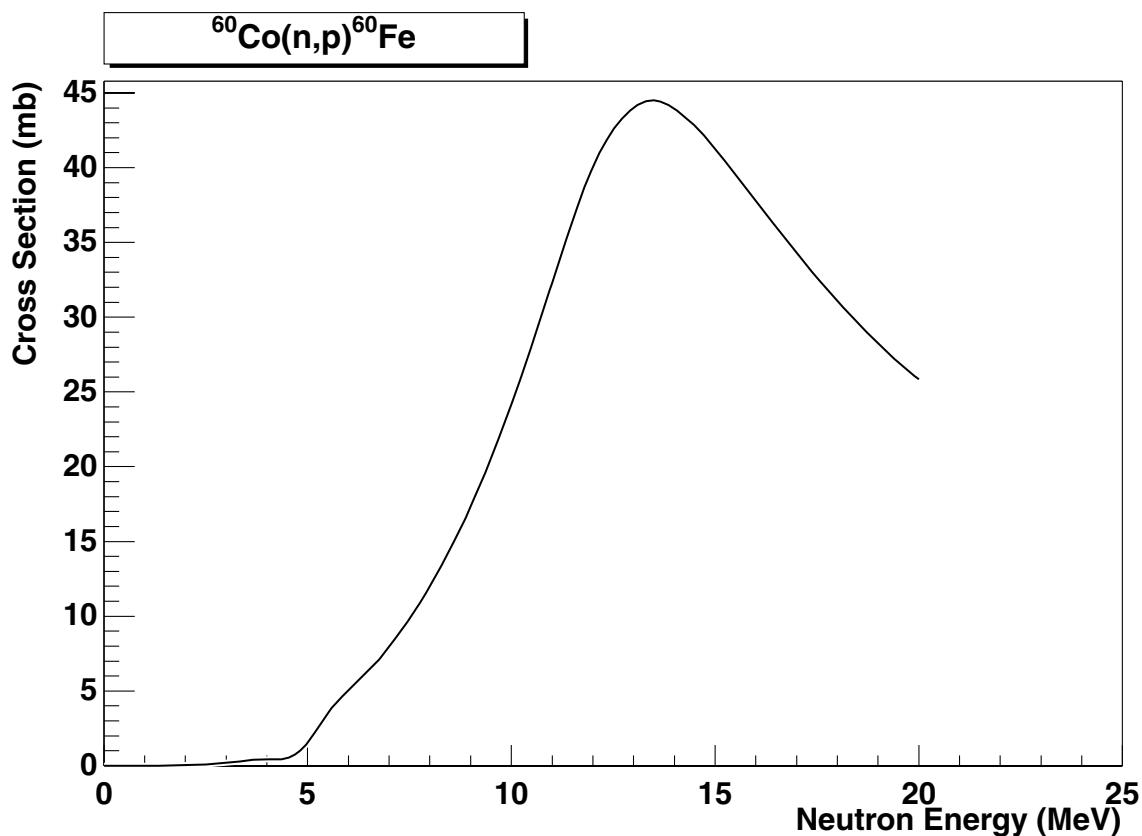
60Co(n,p)60Fe

2.85. ^{60}Co (n,p) ^{60}Fe

final state: total
source: ADL-3

No experimental data in EXFOR, the ADL-3 evaluation adopted.

^{58}Ni(n,2n)^{57}Ni

|		
●	FILATENKOV	97
■	OSMAN	96
▲	GARLEA	92
▼	JUNQIAN	92
○	MOLLA	91
□	VIENNOT	91
△	IKEDA	88
◇	KOBAYASHI	88
⊕	GREENWOOD	87
★	MEADOWS	87
☆	MUYAO	87
+	RAMA RAO	86
✳	GARLEA	85
✕	KOBAYASHI	85
·	PAVLIK	85
⊙	RIBANSKY	85
⊞	BAHAL	84
△	IKEDA	84
◈	NGOC	84
⊕	MOLLA	83
✶	CSIKAI	82
⊙	HARPER	82
⊞	PAVLIK	82
⊗	RAICS	81
⊞	ADAMSKI	80
△	HUDSON	78
◉	HAN-LIN	77
⊕	QAIM	77
★	SIGG	76
⊙	BAYHURST	75
⊞	SPANGLER	75
△	ARAMINOWICZ	73
◇	HEMINGWAY	73
+	FINK	70
★	BARRALL	69
⊙	TEMPERLEY	68
⊡	BORMANN	66
△	CSIKAI	65
◉	PAULSEN	65
⊕	STRAIN	65
★	BRAMLITT	63
⊙	CROSS	63
⊠	JERONYMO	63
△	GLOVER	62
◇	PRESTWOOD	61
⊕	RAYBURN	61
★	PREISS	60
⊙	BURSER	59
⊠	PAUL	53

2.86. ^{58}Ni (n,2n) ^{57}Ni

final state: total
source: EAF-4.1 (IRDF-90.2)

IRDF-90.2 reproduces well the data below 15 MeV and slightly overestimates the data of
Pavlik82 above 16 MeV.
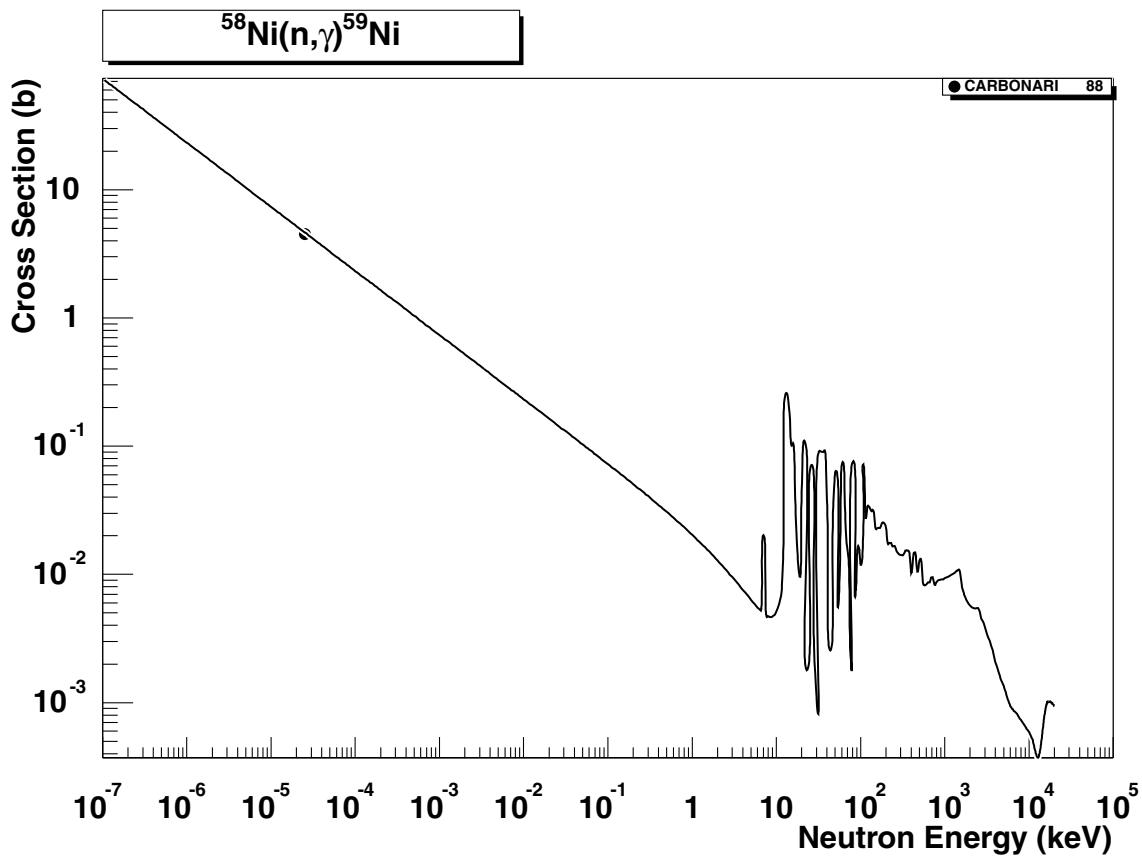
2.87. ^{58}Ni (n,γ) ^{59}Ni

final state: total
source: EAF-4.1 (EFF-2.4)

EFF-2.4 evaluation reproduces well the thermal cross-section of Carbonari88. No other EXFOR data are available outside the resonance region. Data are stored in SANDII group structure, the original evaluation includes 69138 energy points.

^{58}Ni(n,p)^{58}Co

●	SWINHOE	79
■	FUKUDA	78
▲	HUDSON	78
▼	NEMILOV	78
★	JIANZHOU	77
□	WU	77
△	SMITH	75
◇	DRESLER	73
✚	HEMINGWAY	73
○	MASLOV	72
☆	PAULSEN	71
+	FINK	70
✕	BARRALL	69
✳	TEMPERLEY	68
·	BORMANN	67
◎	OKUMURA	67
⊠	BORMANN	66
△	BORMANN	66
◈	PAULSEN	66
✚	DEBERTIN	65
★	STRAIN	65
◉	CROSS	63
⊠	KONIJN	63
⊛	MEADOWS	63
⊞	BARRY	62
△	GLOVER	62
◆	GONZALEZ	60
✚	PURSER	59
☆	ALLAN	57

118

^{58}Ni(n,p)^{58}Co

	FILATENKOV	97
■	BUCZKO	95
▲	GARLEA	92
▼	JUNQIAN	92
★	KLOCHKOVA	92
□	TINGYAN	92
△	DIGHE	91
◇	MOLLA	91
✢	SMITH	91
○	VIENNOT	91
✩	KLOCHKOVA	90
+	HANLIN	89
×	VONACH	89
✳	IKEDA	88
·	IKEDA	88
◎	KOBAYASHI	88
▨	GREENWOOD	87
◬	RONDIO	87
◈	MOLLA	86
⊞	DAROCZY	85
✭	GARLEA	85
◉	KOBAYASHI	85
▩	KORNILOV	85
⊛	RIBANSKY	85
⊞	RONDIO	85
◭	NGOC	84
◆	HUSAIN	83
✢	VIENNOT	82
✰	RAICS	81

2.88. ^{58}Ni (n,p) ^{58}Co

final state: total
source: IPPE

The IPPE evaluation [12] reproduces very well all consistent experimental data. The remaining discrepant results can be disregarded.

^{58}Ni(n,d+np)^{57}Co

●	HANLIN	94
■	MOLLA	86
▲	PAVLIK	85
▼	RAICS	81
★	QAIM	74
□	HEMINGWAY	73
△	MASLOV	72
◇	FINK	70
✚	BARRALL	69
○	TEMPERLEY	68
✫	BRAMLITT	63
+	CROSS	63
×	GLOVER	62
✳	PURSER	59
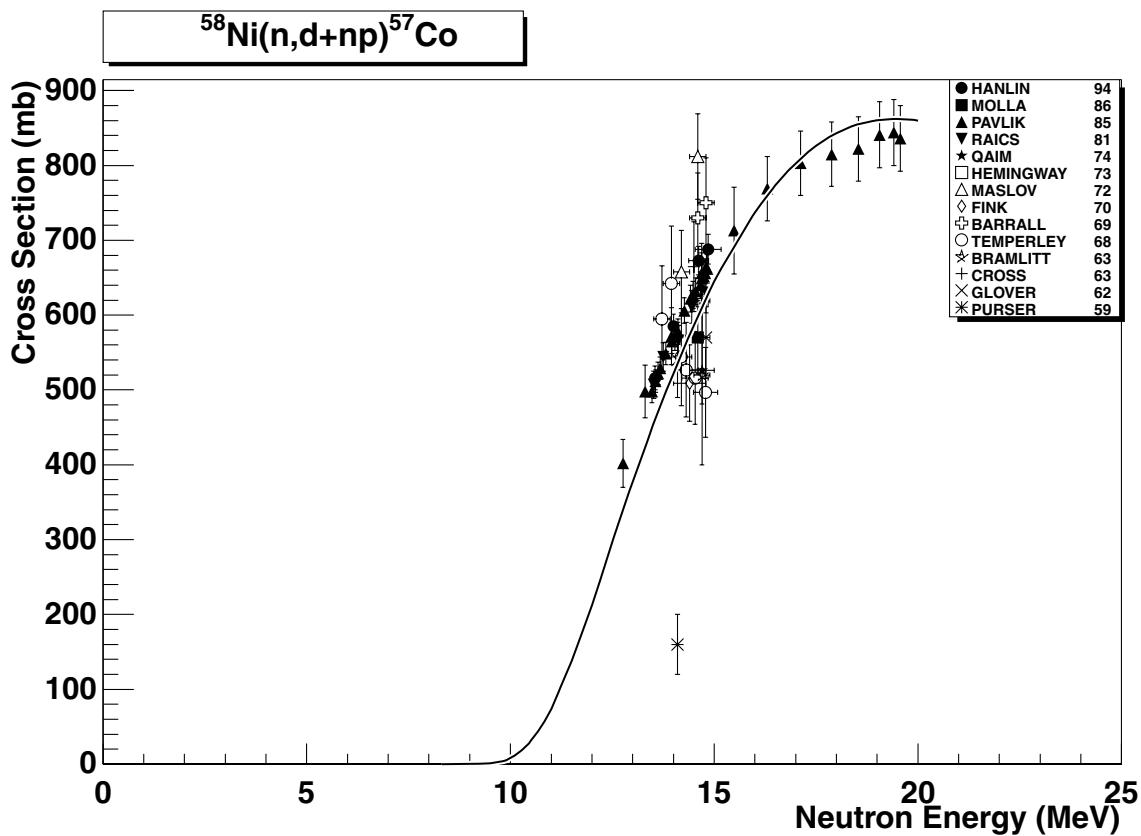
2.89. ^{58}Ni (n,d+np) ^{57}Co

final state: total
source: EAF-4.1 (JEF-2.2)

The combined JEF-2.2 and EFF-2.4 evaluation is plotted against (n,d+np) data. The agreement with the experimental data is very good. The data are stored separately as (n,d) and (n,np) reaction channels, adopted from JEF-2.2 and EFF-2.4, respectively.
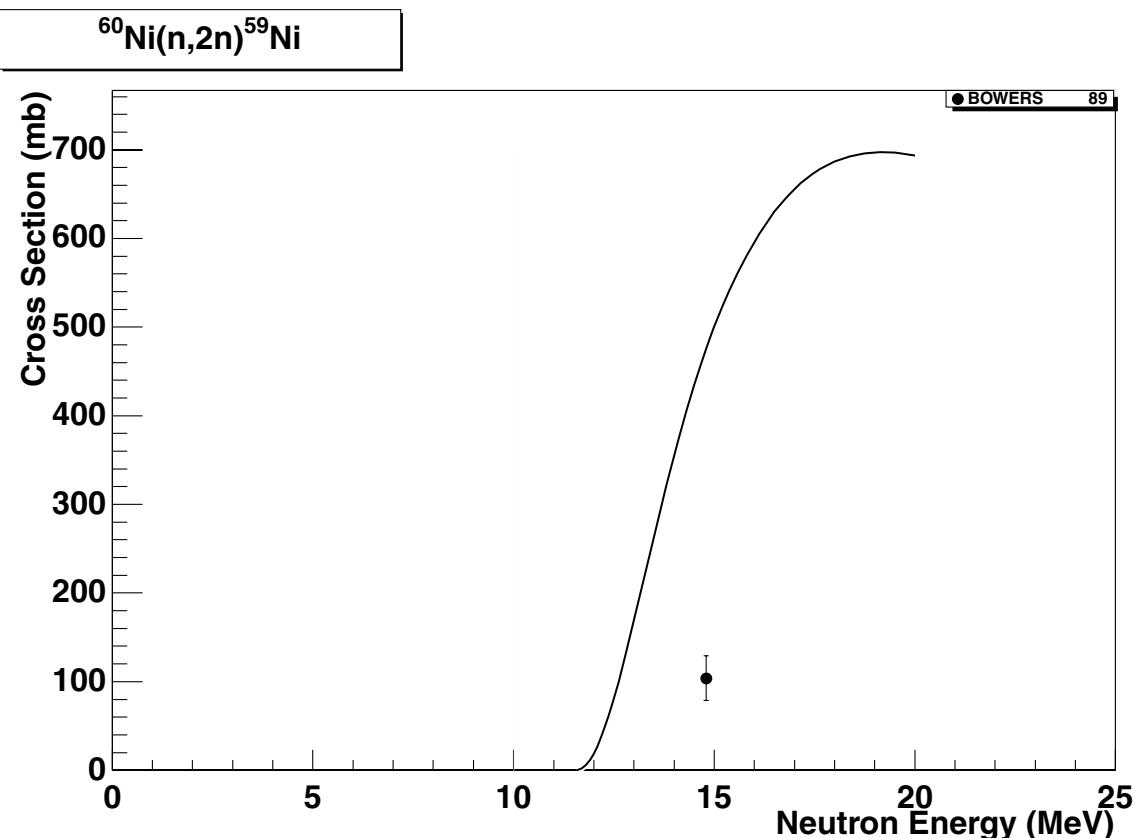
2.90. ^{60}Ni (n,2n) ^{59}Ni

final state: total
source: ADL-3

The single experimental point (at about 15 MeV) extracted from EXFOR is wrong. It is considerably smaller than values of (311 +- 55) mb and (309 +- 83) mb from references [37] and [38], respectively. These values are reasonably reproduced by the adopted ADL-3 evaluation.

^{60}Ni(n,p)^{60}Co

● FILATENKOV	97
■ OSMAN	96
▲ HANLIN	94
▼ TINGYAN	92
★ SUDAR	91
□ VIENNOT	91
△ WAGNER	91
◇ YONGCHANG	90
✛ VONACH	89
○ GREENWOOD	87
✩ MOLLA	86
+ BAHAL	84
✕ LEES	79
✳ QAIM	77
· HEMINGWAY	73
◎ MASLOV	72
⊠ LEVKOVSKIJ	69
▲ PAULSEN	67
◇ CROSS	63
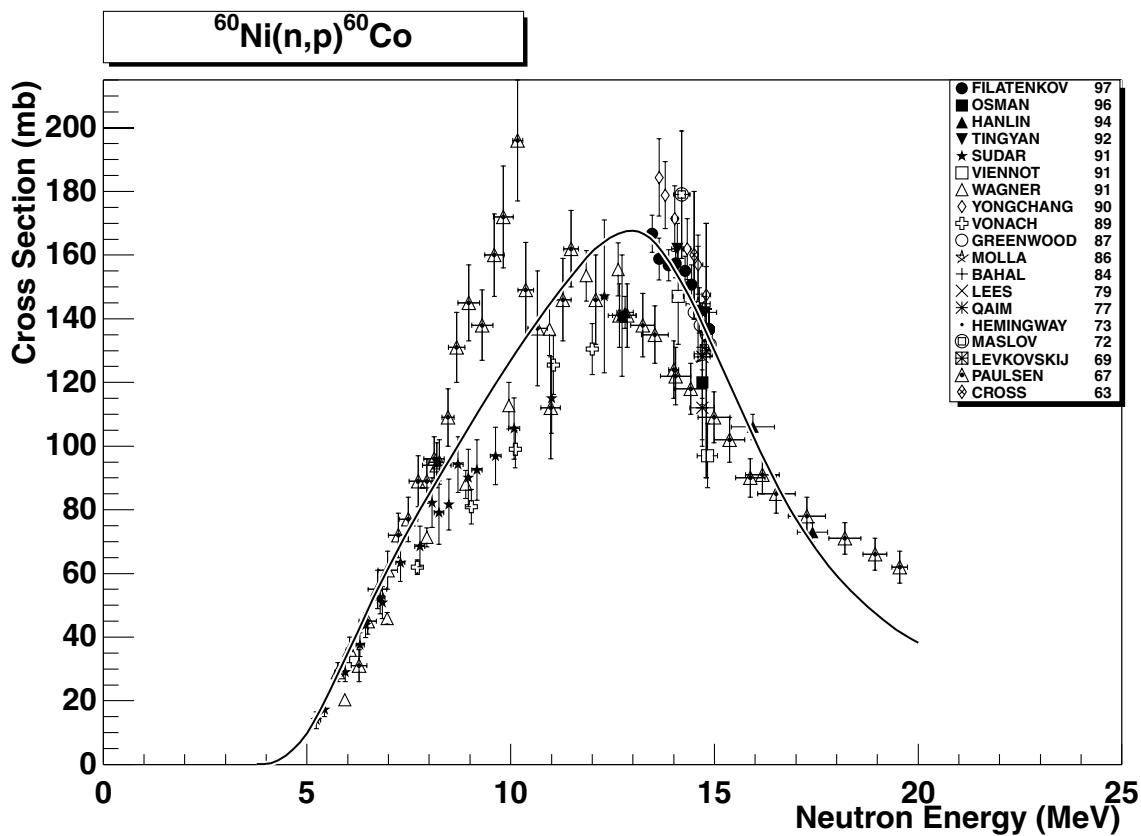
2.91. ^{60}Ni (n,p) ^{60}Co

final states: g.s., meta
source: ADL-3

ADL-3 runs in the middle of the experimental data, fitting well the very recent experiment of Filatenkov97 between in the 13-15 MeV range. The branching ratio between the g.s. and meta state is based on model calculations.

61Ni(n,γ)62Ni ● HOLDEN 94
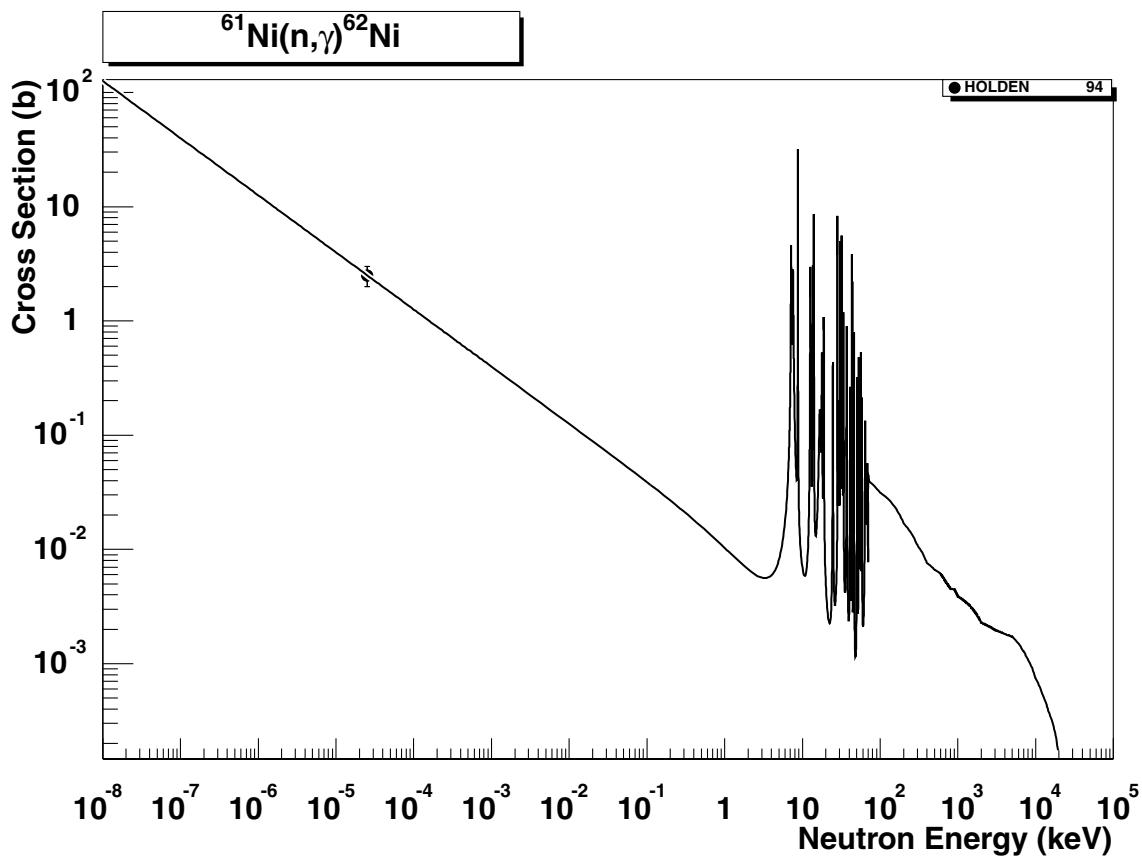
2.92. ^{61}**Ni (n,γ)** ^{62}**Ni**

final state: total
source: EAF-4.1 (EFF-2.4)

ENDF/B-VI was chosen for EFF-2.4. No EXFOR data are available outside the resonance region. The thermal cross-section of Holden94 [32] is reproduced with C/E=1.00.
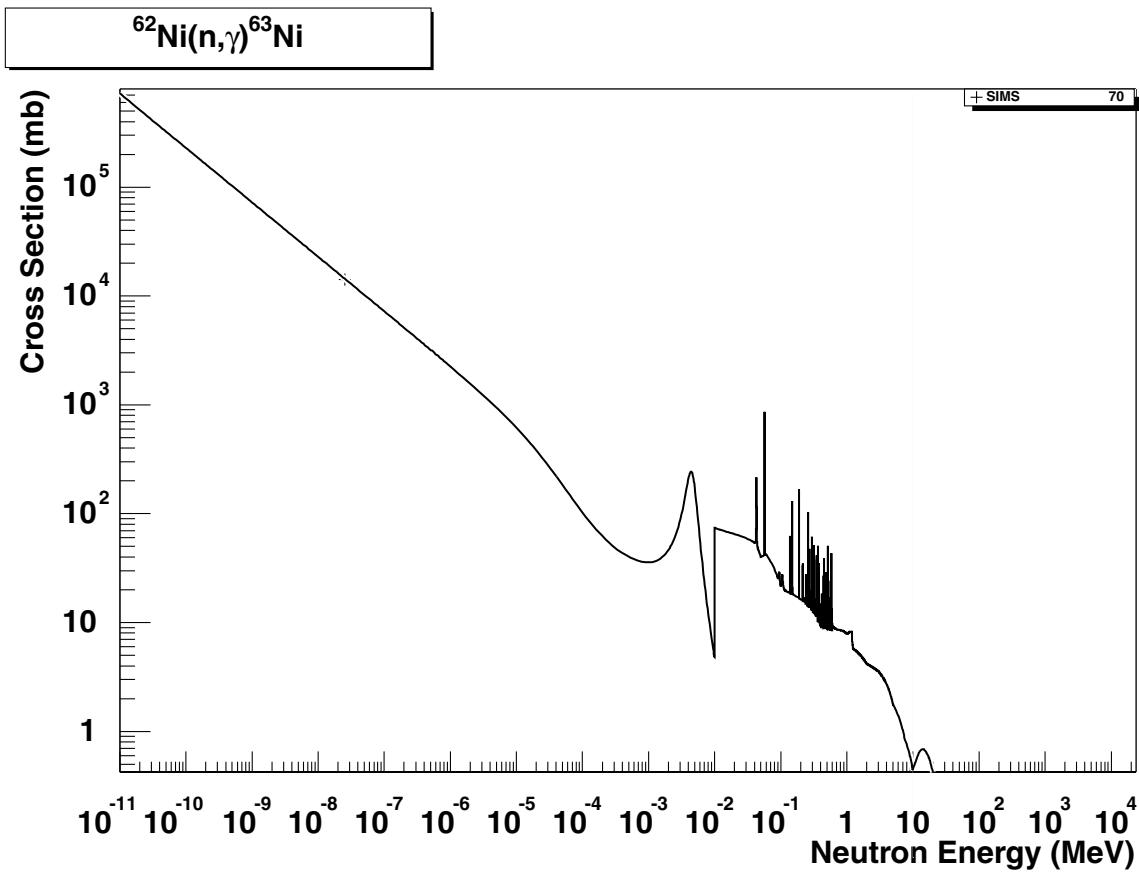
2.93. ^{62}Ni (n,γ) ^{63}Ni

final state: total
source: EAF-4.1 (EFF-2.4)

ENDF/B-VI was chosen for EFF-2.4. The only experimental point of Sims70 at 0.0253 eV is well reproduced.
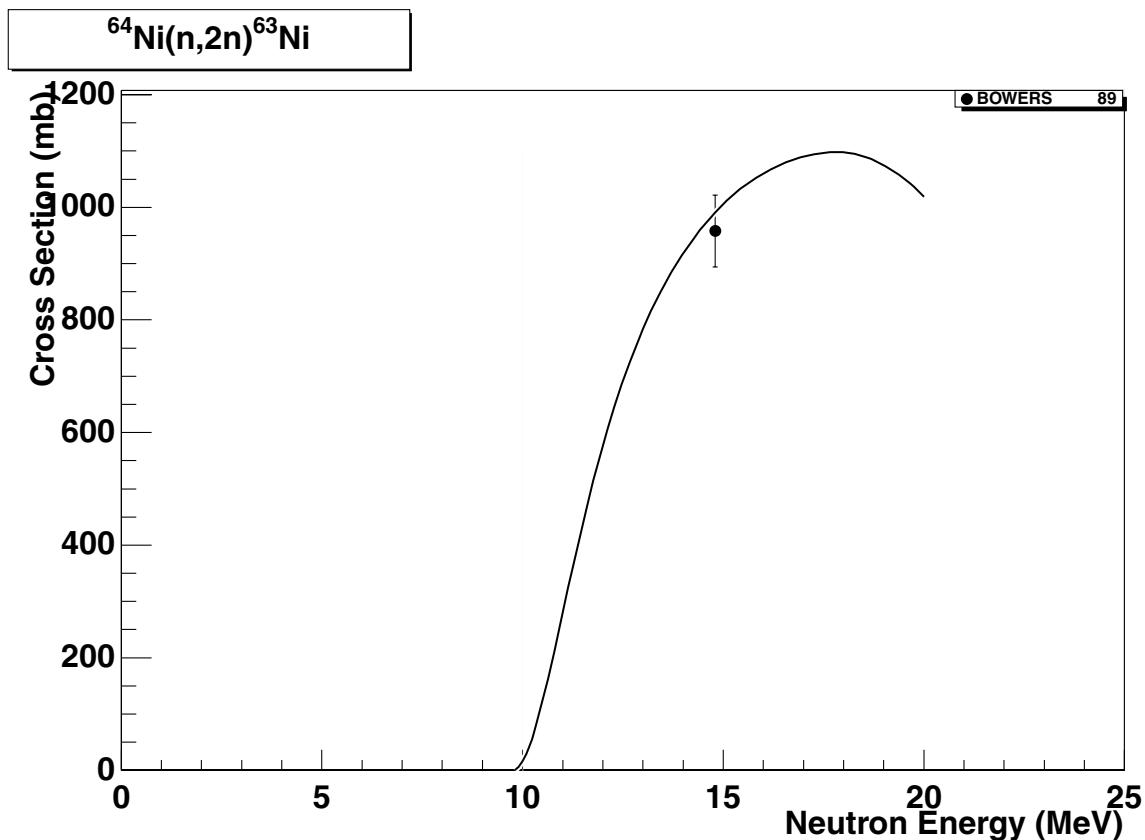
^{64}Ni(n,2n)^{63}Ni

2.94. ^{64}Ni (n,2n) ^{63}Ni

final state: total
source: ADL-3

ADL-3 is close to the single experimental point of Bowers89 around 15 MeV.

^{64}Ni(n,γ)^{65}Ni

● RYVES	70
■ GRENCH	65
▲ BOOTH	58
▼ KONONOV	58
★ LEIPUNSKIJ	58
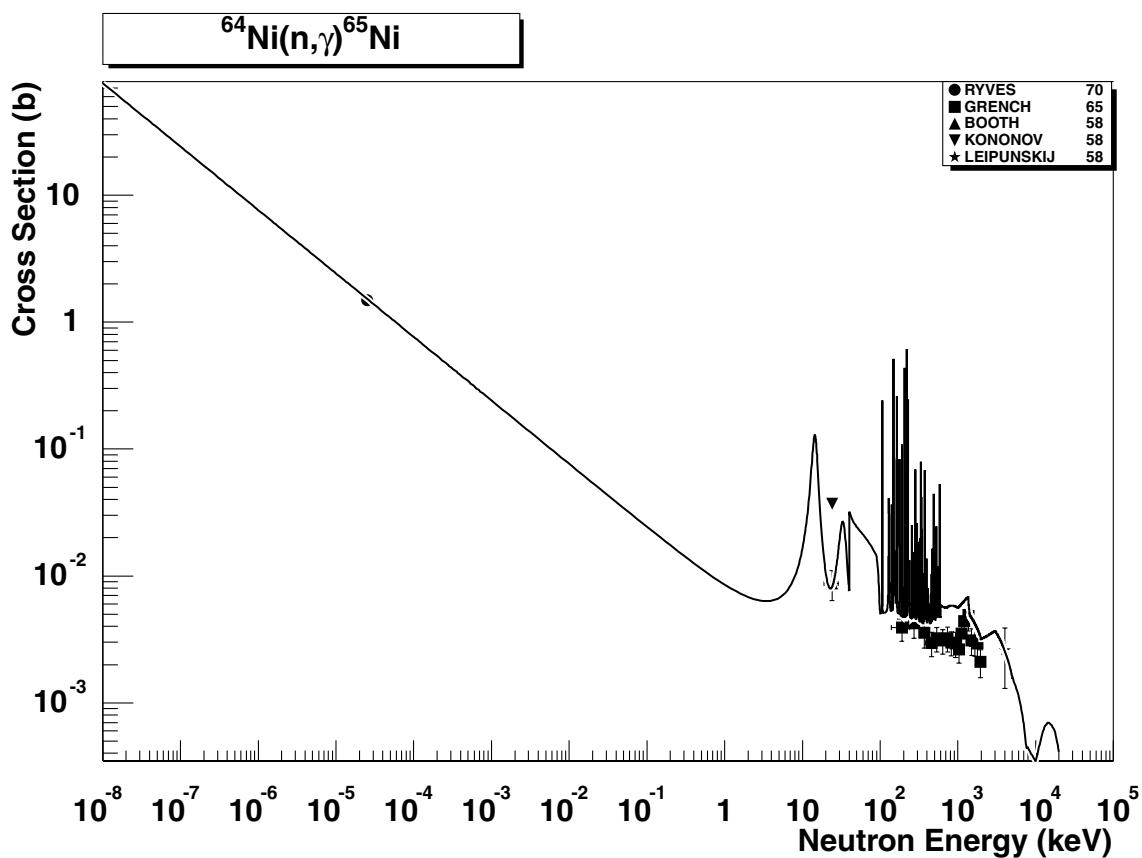
2.95. ^{64}**Ni (n,γ)** ^{65}**Ni**

final state: total
source: EAF-4.1 (EFF-2.4)

ENDF/B-VI was adopted for EFF-2.4. The experimental point of Ryves70 at 0.0253 eV
is well reproduced. The smooth statistical component above 50 keV slightly overestimates
the averaged data of Greench65.
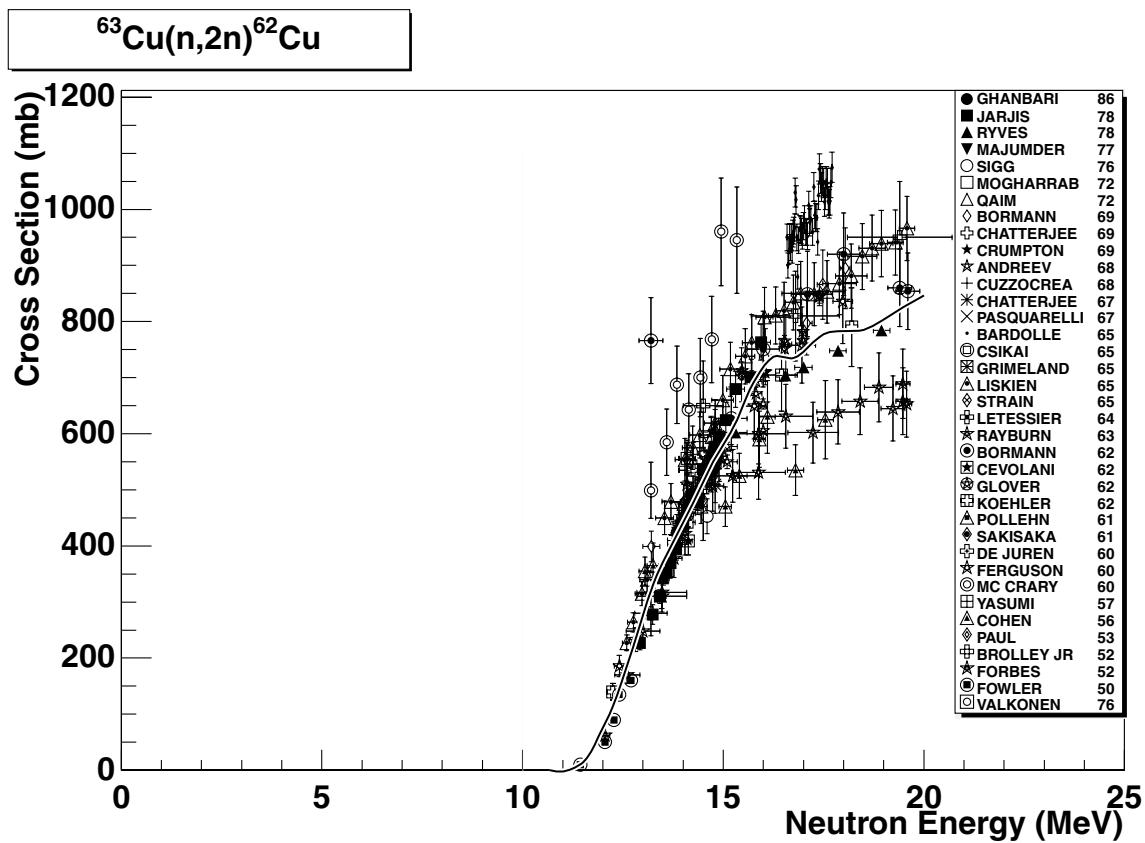
2.96. ^{63}Cu (n,2n) ^{62}Cu

final state: total
source: EAF-4.1 (IRDF-90.2)

IRDF-90.2 fits well the data below 15 MeV and runs in the middle of the data above 15 MeV (close to the data of Ryves78).

Figure: ^{63}Cu(n,γ)^{64}Cu cross section plot. Legend: CELENK 91, VOIGNIER 86, ANAND 79, RYVES 74, CHATURVEDI 70, DIKSIC 70, RYVES 70, DOVBENKO 69, HASAN 68, ZAIKIN 68, PINONCELLI 67, TOLSTIKOV 66, LYON 59, VERVIER 59, BOOTH 58, PERKIN 58, MACKLIN 57, BLAIR 44, GLEASON 77.
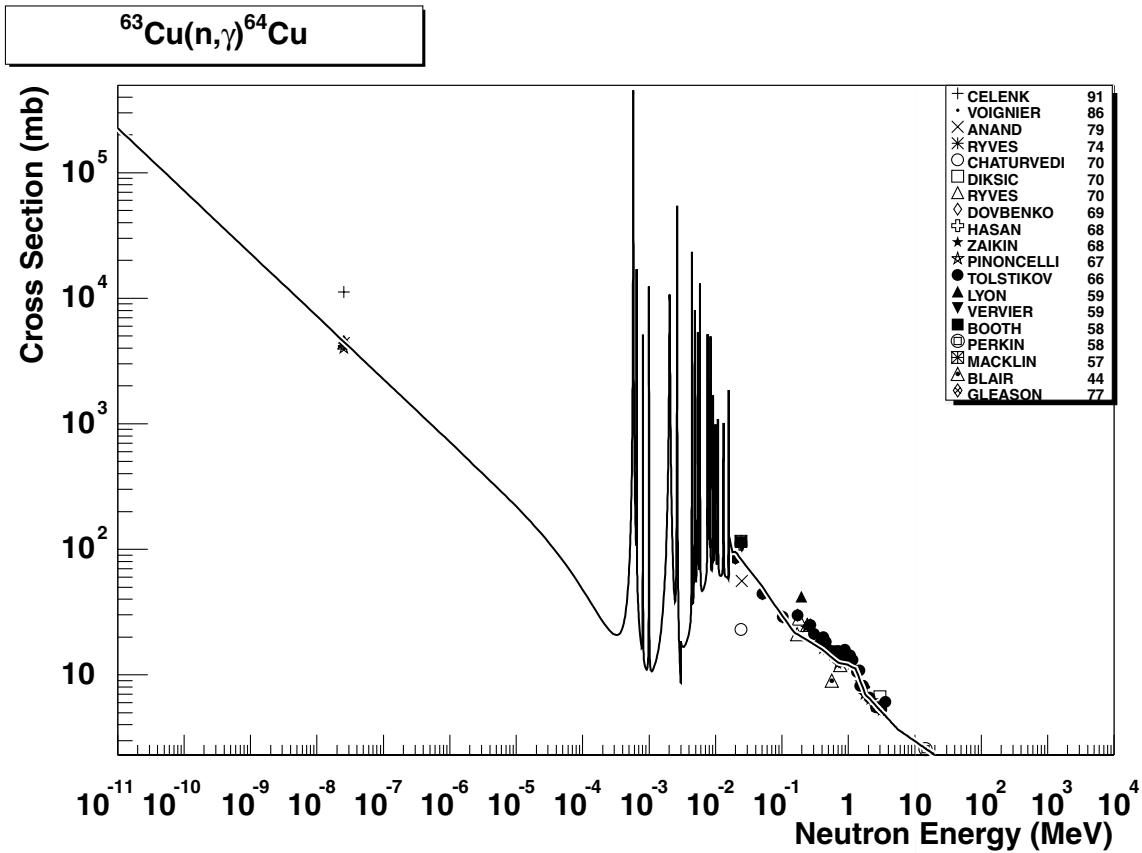
2.97. ^{63}Cu (n,γ) ^{64}Cu

final state: total
source: EAF-4.1 (ENDF/B-VI)

ENDF/B-VI evaluation is very close to all experimental data, both in the thermal range and the smooth statistical region above 20 keV. The thermal value of Celenk91 contradicts the other measurements and the value of 4.5 ± 0.02 b recommended in [26] by more than a factor of two. This point can be disregarded.
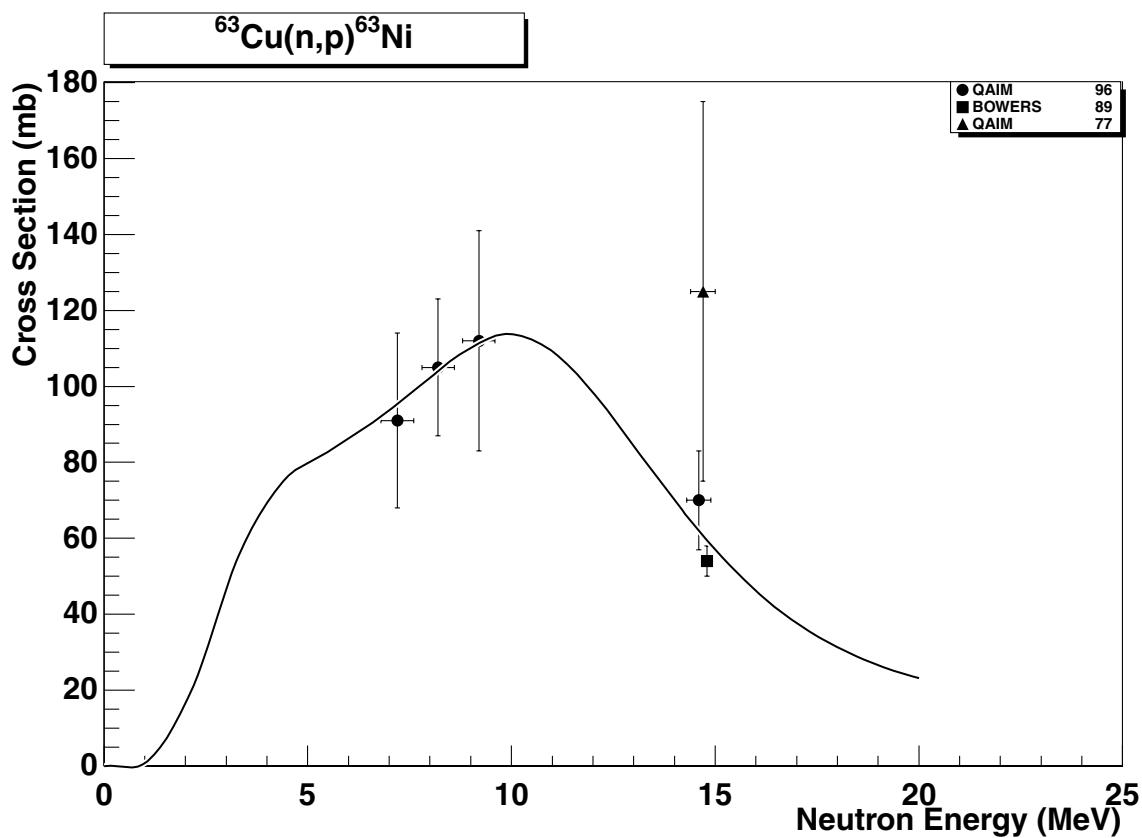
**2.98.** ^{63}**Cu (n,p)** ^{63}**Ni**

final state: total
source: ADL-3

ADL-3 agrees with all experimental data. The point by Qaim77 is consistent with the recommended evaluation considering its large error.

^{63}Cu(n,α)^{60}Co

●	FILATENKOV	97
■	MEADOWS	96
▲	HANLIN	90
▼	YONGCHANG	90
★	GREENWOOD	87
□	ARTEM´EV	80
△	GARUSKA	80
◇	WINKLER	80
✧	KAYASHIMA	79
○	WINKLER	78
✩	BORMANN	72
+	MASLOV	72
×	BARRALL	69
✳	PAULSEN	67
·	CZAPP	60
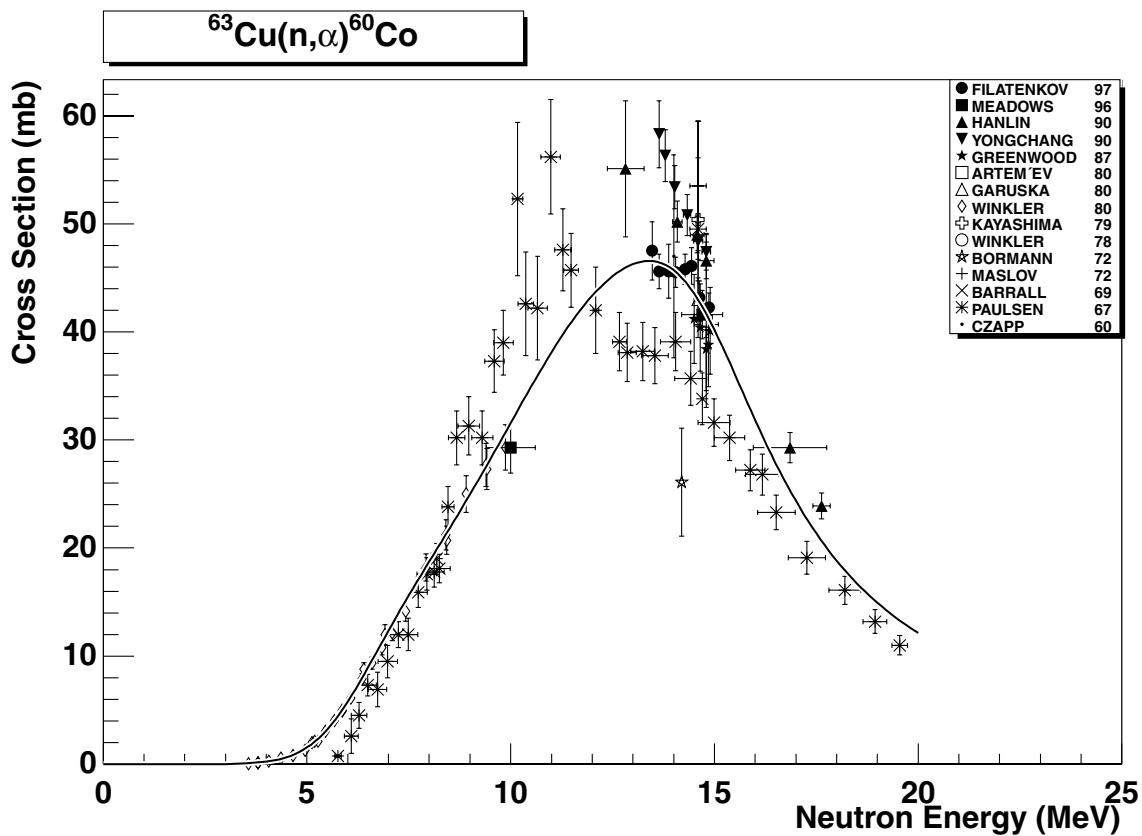
2.99. ^{63}Cu (n,α) ^{60}Co

final state: total
source: RRDF-98

RRDF-98 has been adopted. The total cross-section data are not very consistent. RRDF-98 is a reasonable representation. It runs in the middle of the data around 14 MeV and overestimates high energy data of Barrall69 to account for the more recent and reliable data by Hanlin90.

●	FILATENKOV	97
■	MOLLA	94
▲	IKEDA	88
▼	MEADOWS	87
★	GHANBARI	86
□	NGOC	84
△	WINKLER	83
◇	CSIKAI	82
✛	RYVES	78
○	SIGG	76
✬	MANNHART	75
+	SPANGLER	75
✕	ARAMINOWICZ	73
✱	ROBERTSON	73
·	MOGHARRAB	72
◎	QAIM	72
⊠	BARRALL	69
⧋	BORMANN	69
◇	CHATTERJEE	69
⊞	CLATOR	69
✩	CRUMPTON	69
◉	CUZZOCREA	68
⊠	VONACH	68
⊛	NAGEL	66
⊞	CSIKAI	65
⧋	PAULSEN	65
◈	SANTRY	65
✛	STRAIN	65
★	BONAZZOLA	64
◎	BORMANN	63
⊞	GLOVER	62
△	RAYBURN	62
◈	POLLEHN	61
⊕	PRESTWOOD	61
✬	RAYBURN	61
◉	DEPRAZ	60
▣	MC CRARY	60
⧋	WEIGOLD	60
◈	POULARIKAS	59
⊕	PAUL	53
✬	FORBES	52

2.100. ^{65}Cu (n,2n) ^{64}Cu

final state: total
source: JENDL-Act96

JENDL-Act96 reproduces the relevant and recent data in the whole energy range very
well. The data of Mc Crary60 are obviously wrong and can be disregarded.

^{65}Cu(n,γ)^{66}Cu

+	VOIGNIER	86
·	RYVES	74
×	RYVES	70
✳	COLDITZ	68
○	ZAIKIN	68
□	PETO	67
△	CHAUBEY	66
◇	TOLSTIKOV	64
✚	STAVISSKIJ	61
★	JOHNSRUD	59
✩	LYON	59
●	VERVIER	59
▲	BOOTH	58
▼	KONONOV	58
■	LEIPUNSKIJ	58
◎	PASECHNIK	58
⊞	PERKIN	58
△	MACKLIN	57
◇	HUMMEL	51
⊕	BEGHIAN	49
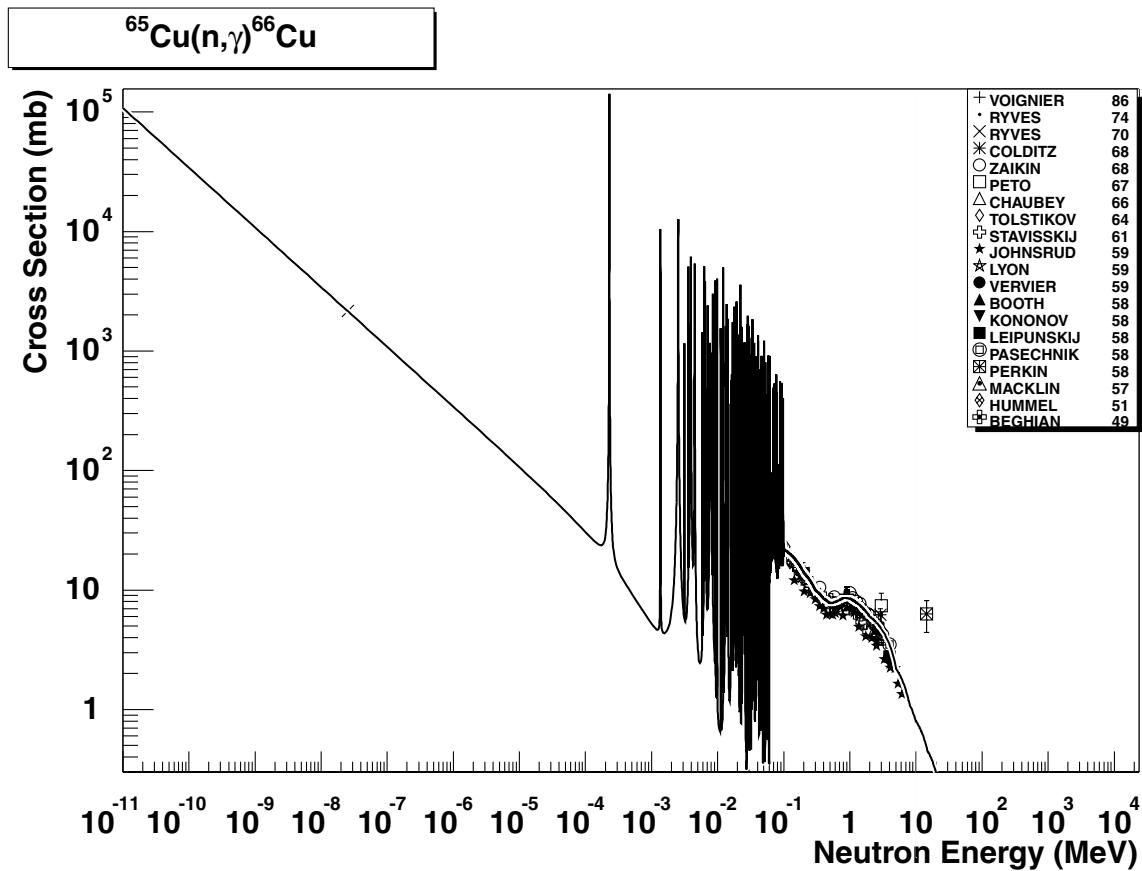
2.101. ^{65}Cu (n,γ) ^{66}Cu

final state: total
source: EAF-4.1 (ENDF/B-VI)

ENDF/B-VI evaluation is in good agreement with all experimental data, both in the thermal range and in the smooth statistical region above 100 keV. The single point at about 15 MeV of Perkin58 is about ten times higher than the value resulting from the 14.5 MeV systematics and can be disregarded.
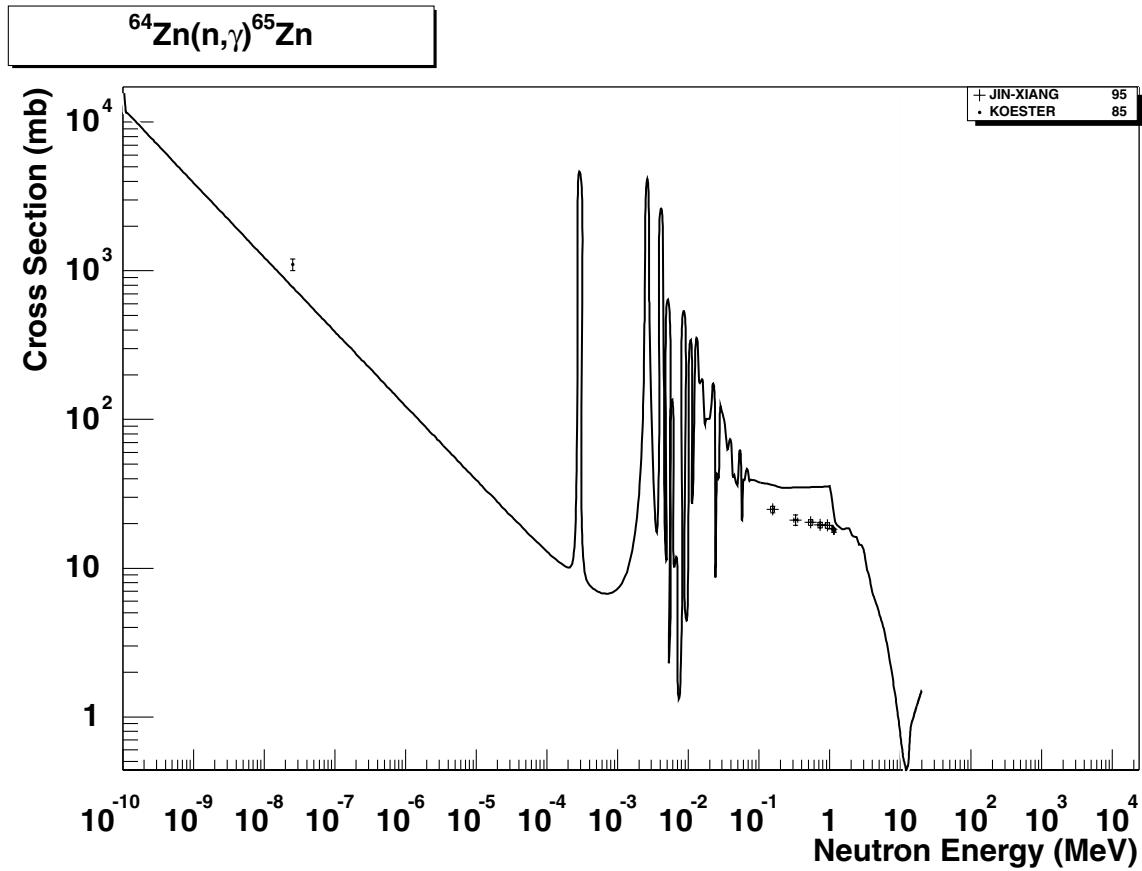
2.102. ^{64}**Zn (n,γ)** ^{65}**Zn**

final state: total
source: EAF-4.1 (JEF-2.2)

This is the original JEF-2.2 evaluation (from RCN fission products subfile) given in the multigroup structure. The thermal cross-section of Koester85 is slightly underestimated, however, the evaluation is in agreement with the recommended value of (740+-50) mb from Ref. [26] with C/E=1.02. The statistical component between 0.1 MeV and 1 MeV overestimates the recent data of Jin-Xian95 by about a factor of two. Re-evaluation of this component is recommended.

^{64}Zn(n,p)^{64}Cu

+		
.	GHORAI	95
×	KIELAN	95
✳	MOLLA	94
○	GARLEA	92
□	IKEDA	91
△	VIENNOT	91
◇	IKEDA	90
⊕	GRIGORIEV	89
★	KOBAYASHI	88
✭	RUTHERFORD	88
●	GARLEA	85
▲	GUPTA	85
▼	GUPTA	85
■	HUSAIN	83
◎	VIENNOT	82
⊠	KING	79
△	NEMILOV	78
◇	QAIM	77
⊕	CASANOVA	76
★	SIGG	76
⊙	SMITH	75
⊠	SPANGLER	75
⊛	DRESLER	73
⊞	SANTRY	72
△	PRASAD	71
◆	BARRALL	69
⊕	BORMANN	69
★	RANAKUMAR	68
◎	VINITSKAYA	67
⊞	KJELBERG	66
△	PAULSEN	66
◇	STRAIN	65
⊕	BORMANN	63
★	BRAMLITT	63
◉	LEVKOVSKIJ	63
▣	GABBARD	62
△	NAKAI	62
◆	WEIGOLD	62
⊕	ARMSTRONG	60
★	PREISS	60
⊕	RAPAPORT	59
⊠	PAUL	53

Neutron Energy (MeV)

Cross Section (mb)

2.103. ^{64}Zn (n,p) ^{64}Cu

final state: total
source: JENDL-Act96

An very good agreement of JENDL-Act96 excitation curve with the relevant and recent experiments. Some of the data (deviating from the main experimental trend) may be disregarded, in particular Smith75 between 5-10 MeV and a few points above 300 mb around 15 MeV.

134

^{66}Zn(n,p)^{66}Cu

+	GHORAI	95
·	KIELAN	95
×	VIENNOT	91
✳	KAWADE	90
○	GUPTA	85
□	SRINIVASA RAO	82
△	VIENNOT	82
◇	SMITH	80
✧	QAIM	77
★	CASANOVA	76
☆	SIGG	76
●	VALKONEN	76
▲	DRESLER	73
▼	PRASAD	71
■	CLATOR	69
◎	RANAKUMAR	68
⊠	VINITSKAYA	67
△	BORMANN	65
◇	STRAIN	65
✛	LEVKOVSKIJ	63
✦	PREISS	60
◉	YASUMI	57
✺	PAUL	53
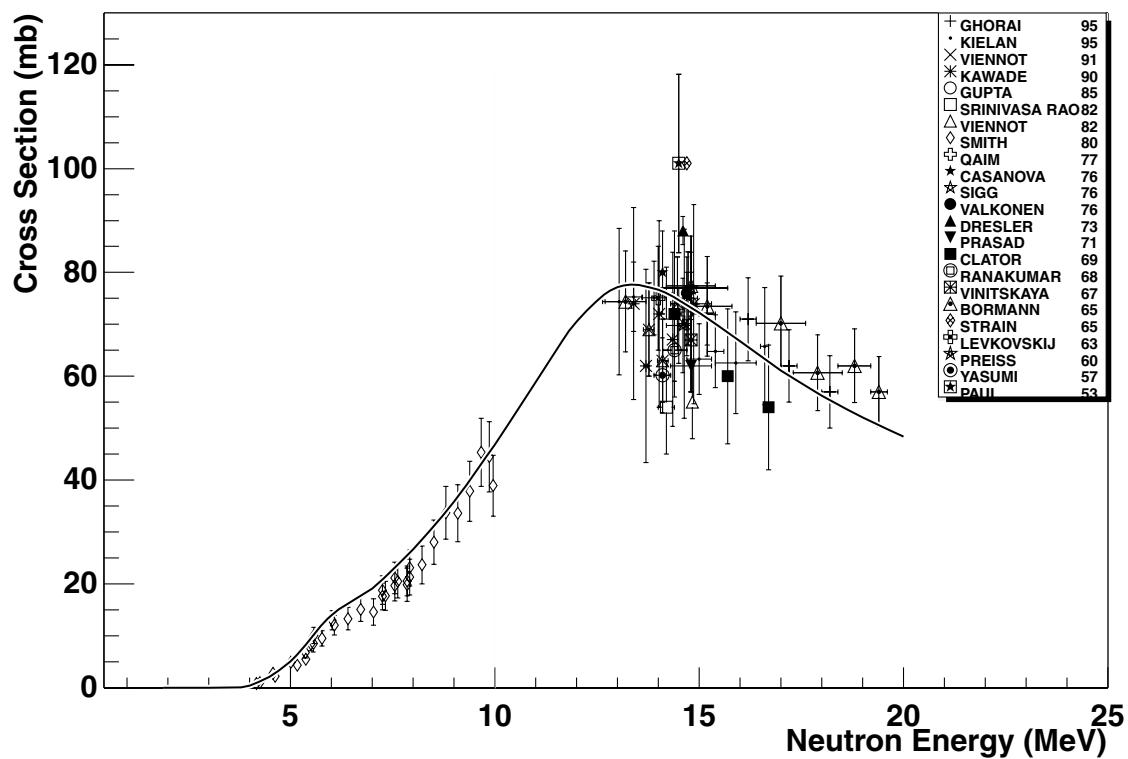
2.104. ^{66}Zn (n,p) ^{66}Cu

final state: total
source: JENDL-Act96

JENDL-Act96 reproduces very well almost all data, except two single, and highly uncertain, points at 15 MeV with values around 100 mb (Paul53 and Strain65).
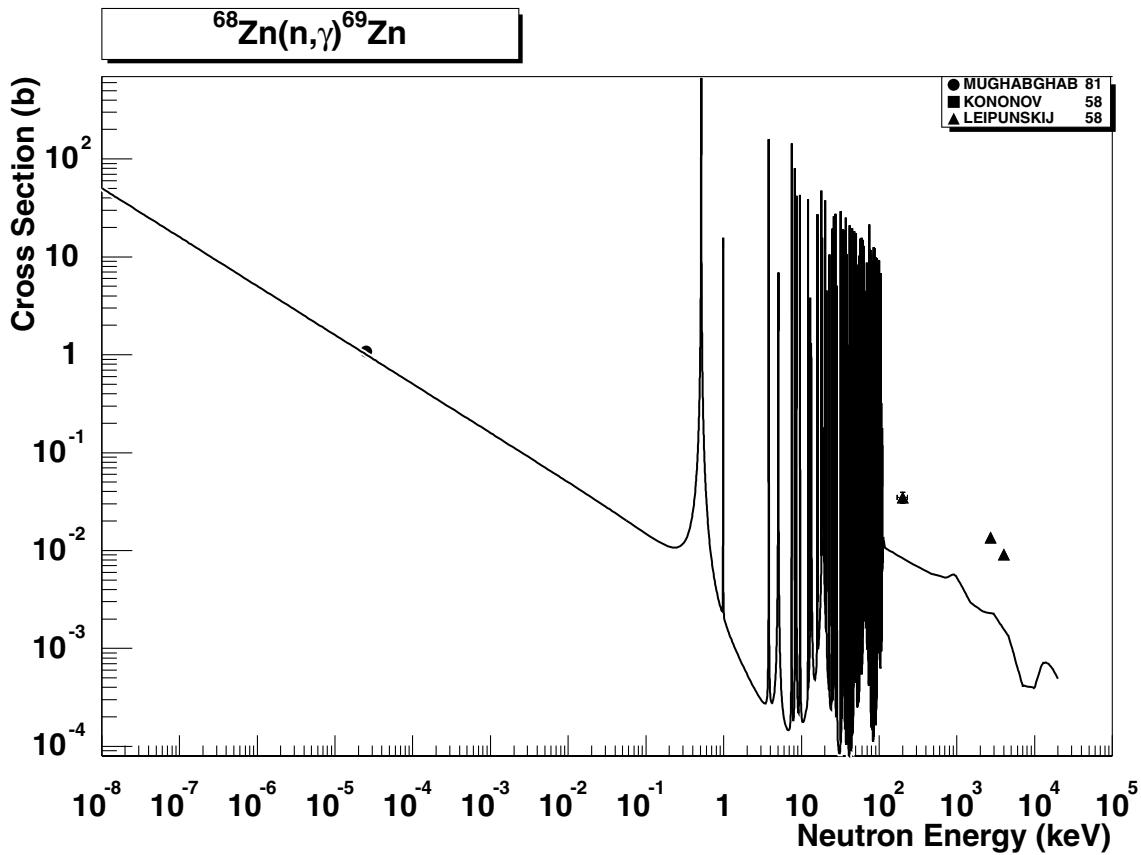
2.105. ^{68}Zn (n,γ) ^{69}Zn

final states: g.s., meta
source: EAF-4.1

This is the original EAF-4.1 evaluation calculated with the code SIGECN-MASGAM. Branching ratio between the g.s. and meta state is based on experimental data (thermal cross-sections) and applied up to the end of the resolved resonance region, and on the energy dependent branching ratio systematics [2] for the high energy region. Full MLBW resonance treatment is included and the total and partial thermal cross-sections [26] are reproduced with C/E=0.93. However, the smooth statistical component between 100 keV and 4 MeV severely underestimates three experimental data points of Leipunskij58. Since the statistical component is based on simplified calculations with the code MASGAM (using global parameters), it might be recommended to repeat these calculations in a more rigorous way. However, the pre-equilibrium part of the excitation curve looks reasonable.
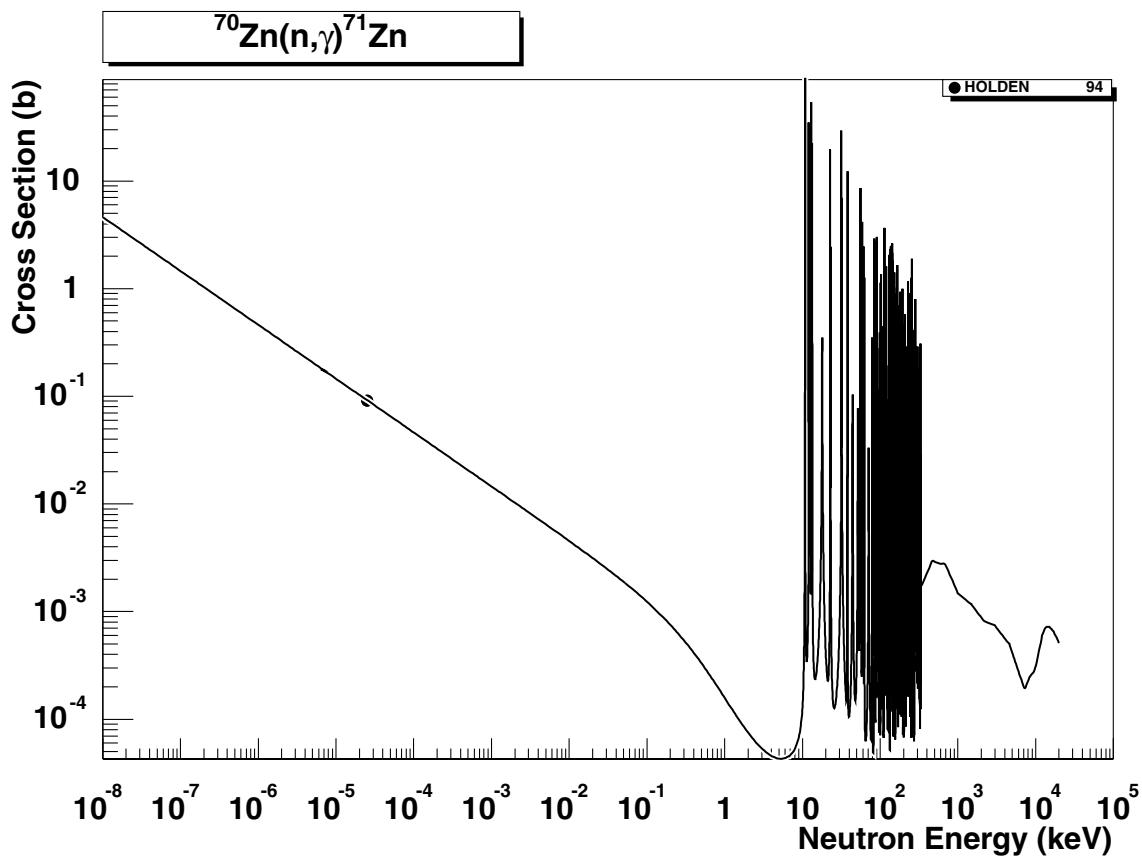
2.106. ^{70}Zn (n,γ) ^{71}Zn

final state: g.s., meta
source: EAF-4.1

This is the EAF-4.1 evaluation calculated with the code SIGECN-MASGAM. Branching ratio between the g.s. and meta state is based on the experimental data (thermal cross-sections) applied up to the end of the resolved resonance region, and on the energy dependent branching ratio systematics [2] for the high energy region. Full MLBW resonance treatment is included and the total and partial thermal cross-sections [26] are well reproduced (C/E=1.0). The statistical component is based on simplified calculations with the code MASGAM using global parameters.

^{69}Ga(n,γ)^{70}Ga

+	KOESTER	84
·	RYVES	71
×	ZAIKIN	71
✳	DOVBENKO	69
○	DOVBENKO	69
□	PETO	67
△	CHAUBEY	65
◇	STAVISSKII	59
✚	KONONOV	58
★	PASECHNIK	58
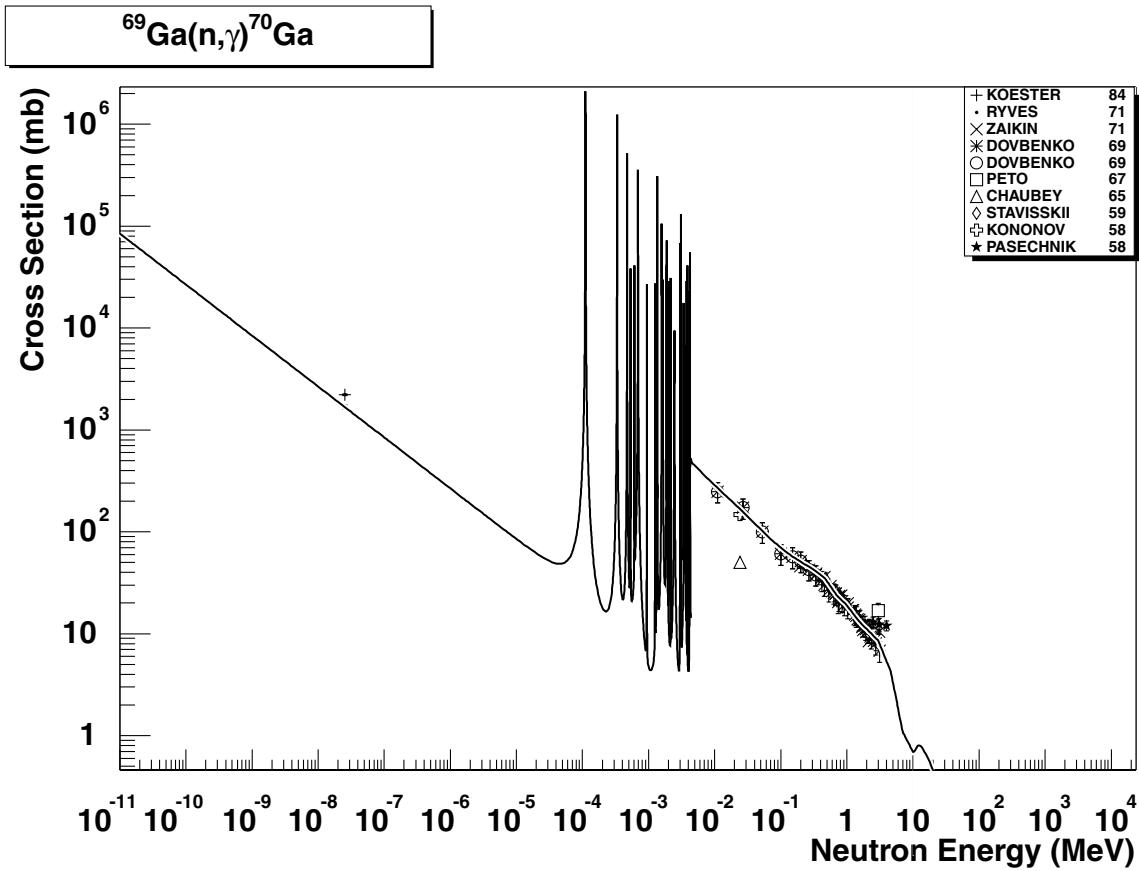
2.107. ^{69}**Ga (n,γ)** ^{70}**Ga**

final state: total
source: EAF-4.1

This is the EAF-4.1 evaluation calculated with the code SIGECN-MASGAM. Full MLBW resonance treatment is included and the total thermal cross-section [26] is well reproduced (C/E=1.0). The statistical component is based on simplified calculations with the code MASGAM (using global parameters) and agrees very well with experimental data between 10 keV and 4 MeV.
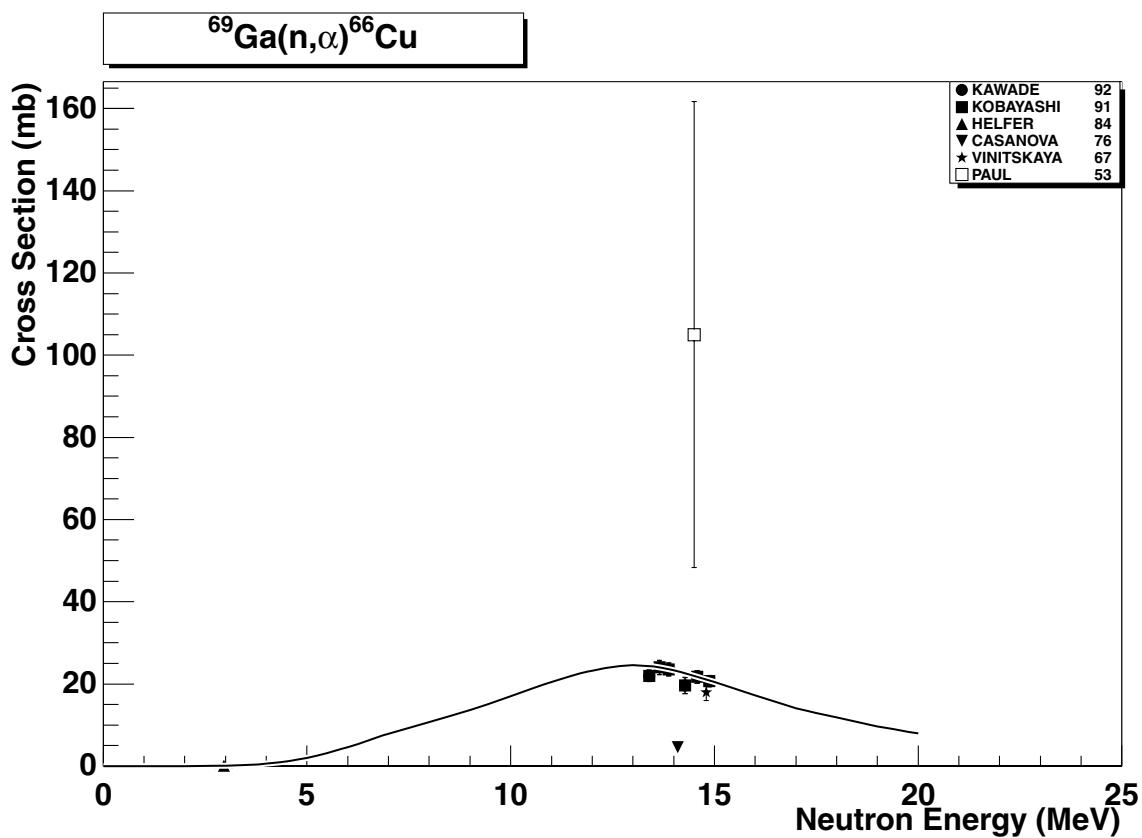
2.108. ^{69}**Ga (n,α)** ^{66}**Cu**

final state: total
source: JENDL-Act96

JENDL-Act96 agrees very well with the experimental data between 13-15 MeV, except Casanova76, which is obviously too low.

71Ga(n,γ)72Ga

+	TROFIMOV	87
·	KOESTER	84
×	ANAND	79
✳	SCHWERER	76
○	RYVES	71
□	ZAIKIN	71
△	MAJUMDER	70
◇	DOVBENKO	69
⊕	DOVBENKO	69
★	PETO	67
✧	CHAUBEY	65
●	JOHNSRUD	59
▲	LYON	59
▼	MACKLIN	59
■	STAVISSKII	59
⊙	PERKIN	58
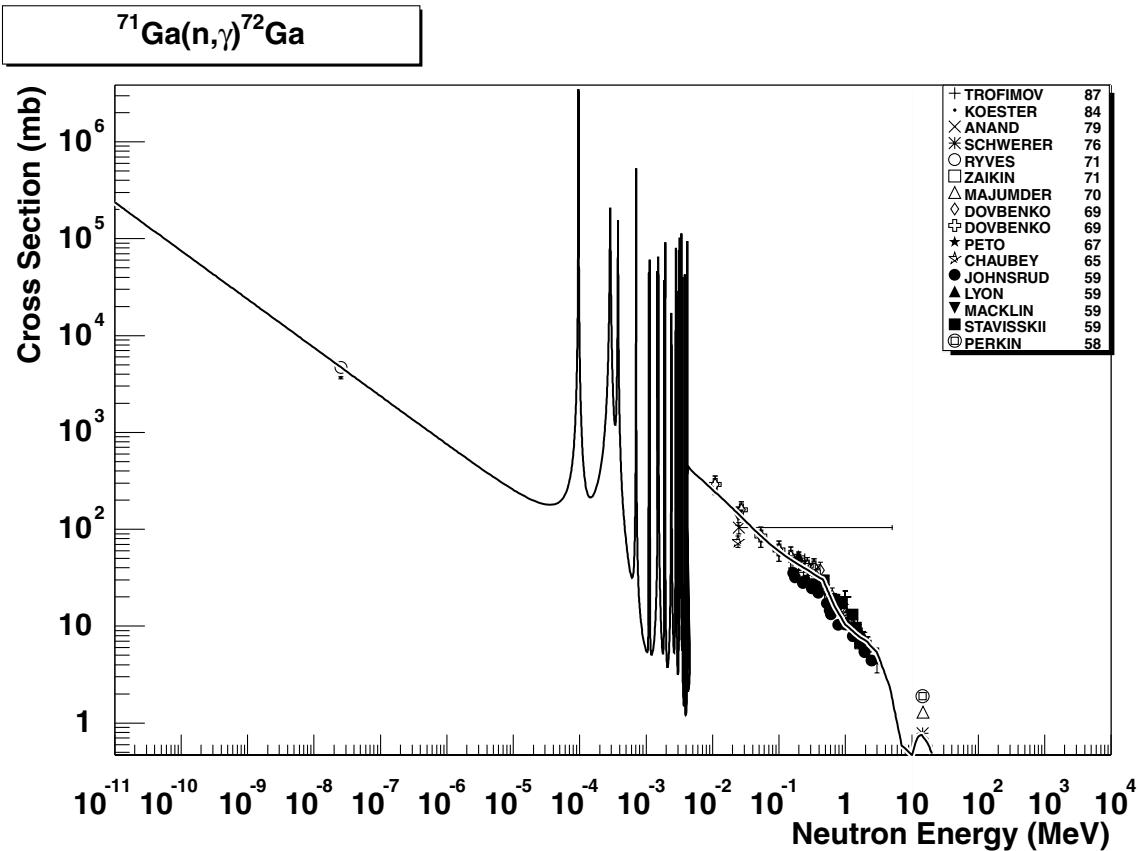
2.109. ^{71}**Ga (n,**γ**)** ^{72}**Ga**

final state: total
source: EAF-4.1

This is the EAF-4.1 evaluation calculated with the code SIGECN-MASGAM. Full MLBW resonance treatment is included and the total thermal cross-section [26] is well reproduced (C/E=1.0). The statistical component is based on simplified calculations with the code MASGAM using global parameters and agrees very well with experimental data between 10 keV and 3 MeV. The 14 MeV value agrees with Schwerer76, Majumder70 and the 14.5 MeV systematics. The value of Perkin58 is too large.

^{74}Se(n,γ)^{75}Se

● HOLDEN	94
■ TROFIMOV	89
▲ SIDDAPPA	72
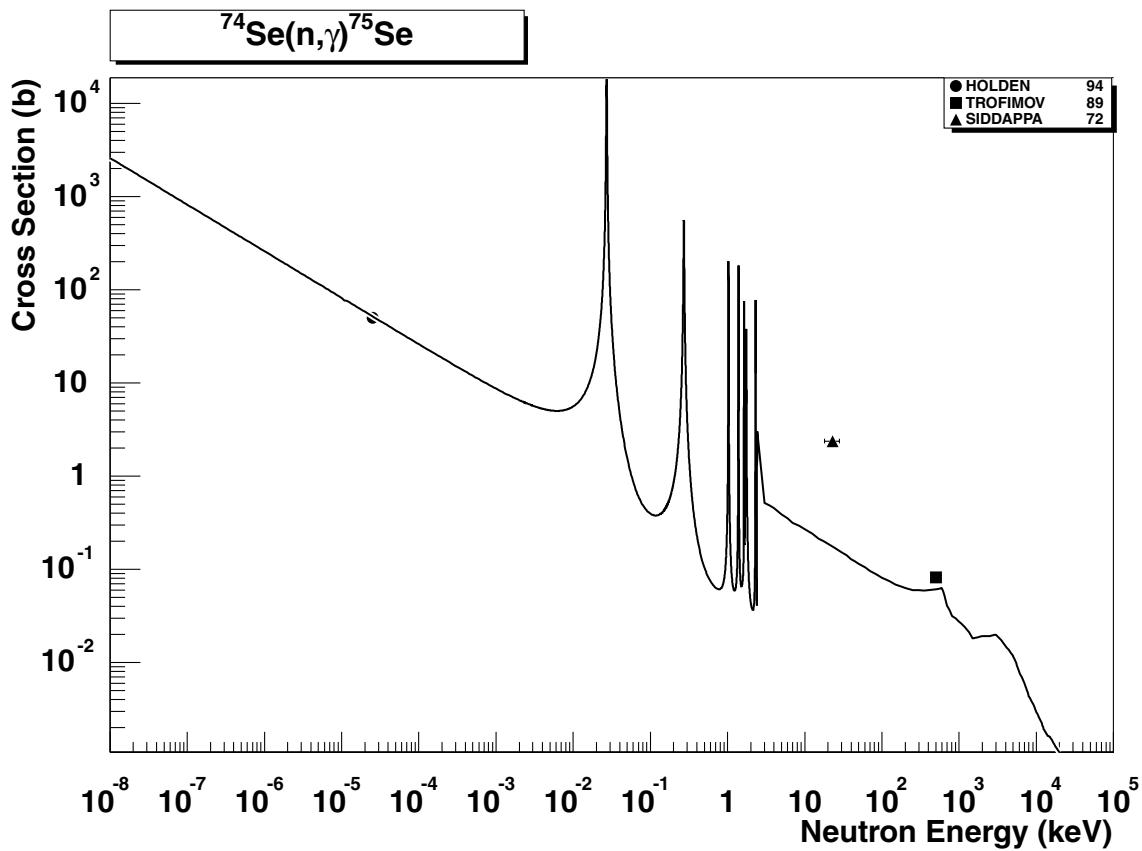
2.110. ^{74}Se (n,γ) ^{75}Se

final state: total
source: EAF-4.1 (JEF-2.2)

Data originate from the upgraded ENDF/B-V evaluation. The thermal cross-section of
(50 ± 4) b from [32] is reproduced with C/E=1.12. The single experimental point of
Siddappa72 seems to be too large and is also contradicted by the recommended 30 keV
value of 0.24 b from [27]. The evaluation is close to Tromifov89 at about 500 keV.
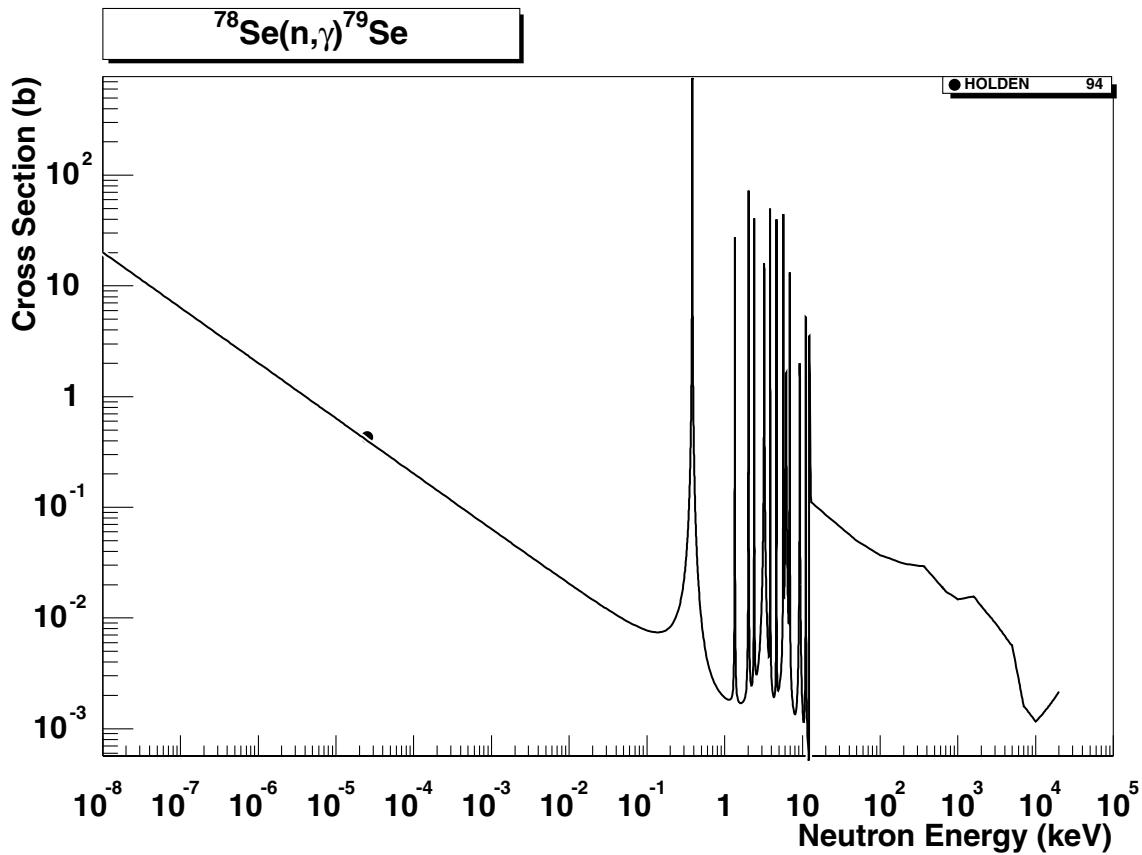
2.111. ^{78}Se (n,γ) ^{79}Se

final states: g.s., meta
source: EAF-4.1 (JEF-2.2)

This is the EAF-4.1 evaluation calculated with the code SIGECN-MASGAM. Branching ratio between the g.s. and meta state is based on experimental data (thermal cross-sections [31]) applied up to the end of the resolved resonance region, and on the energy dependent branching ratio systematics [2] for the high energy region. Full MLBW resonance treatment is included and the total and partial thermal cross-sections [26] are reproduced with C/E=0.93. The statistical component is based on simplified calculations with the code MASGAM using global parameters and is supported by the adopted 30 keV cross-section [26].
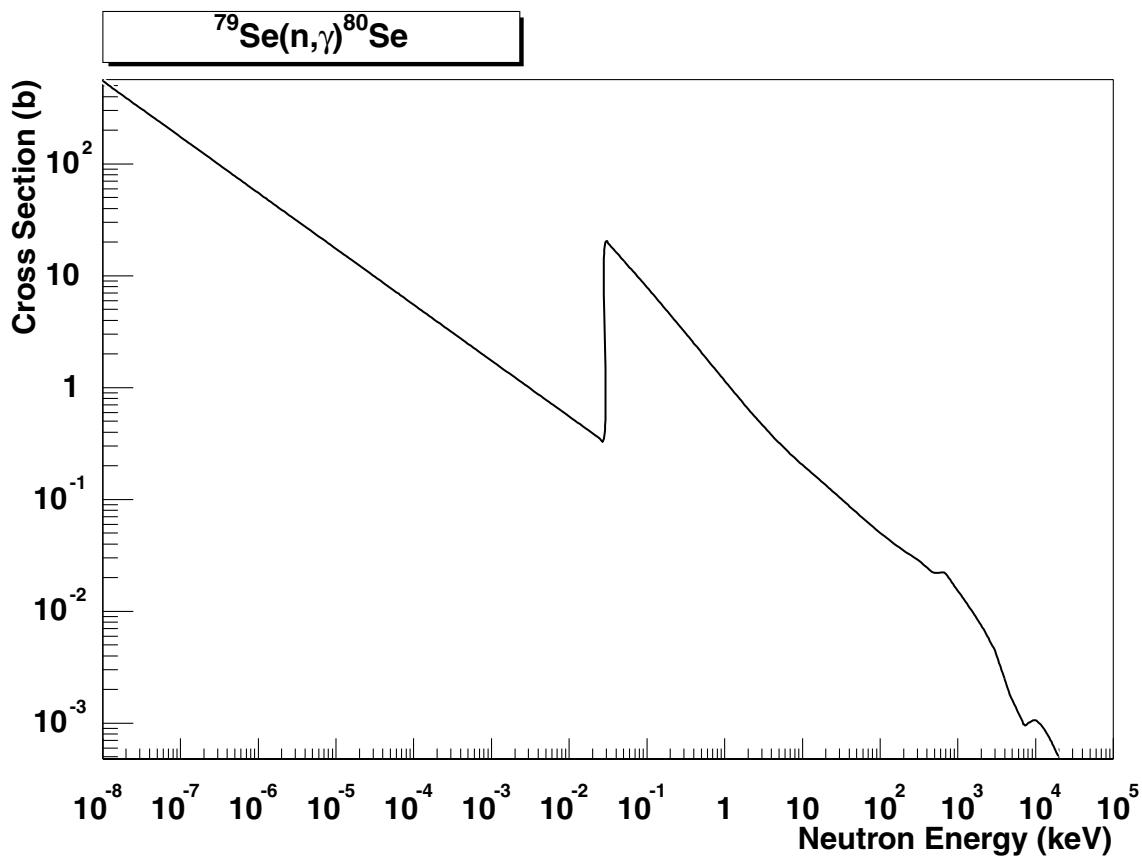
2.112. ^{79}Se (n,γ) ^{80}Se

final state: total
source: EAF-4.1

No experimental data is available. The evaluation is based on the simplified model calculations with the code MASGAM and the global parameters (Hauser-Feshbach and DSD model with no resonance region generation, E_H is based on a $D_0/2$ estimate; for details see Ref. [35]). The statistical component is supported by the adopted 30 keV cross-section [26].
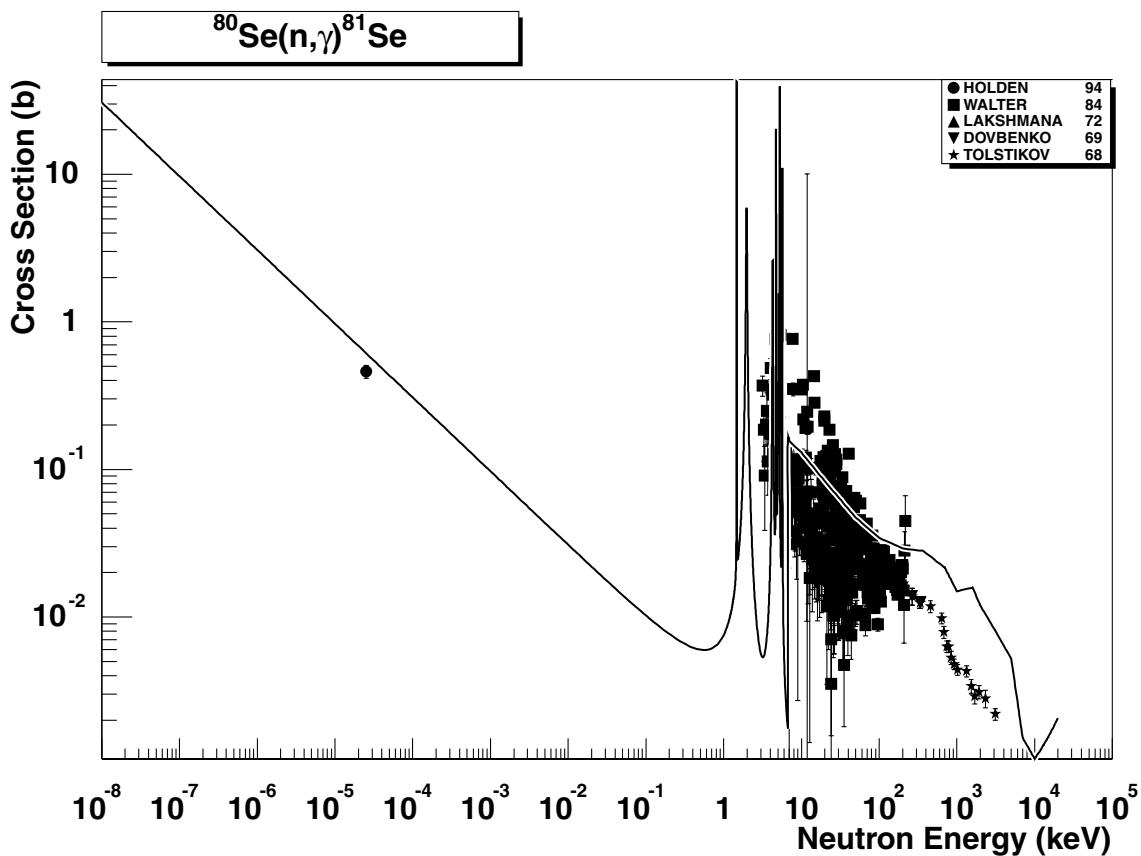
2.113. ^{80}Se (n,γ) ^{81}Se

final states: g.s., meta
source: EAF-4.1 (JEF-2.2)

Data originate from the upgraded ENDF/B-V evaluation. Branching ratio between the g.s. and meta state is based on experimental data (thermal cross-sections [26]) applied up to the end of the resolved resonance region, and on the energy dependent branching ratio systematics [2] for the high energy region. The total and partial thermal cross-sections [26] are well reproduced (C/E=1.0). The smooth statistical part severely overestimates the experimental data of Tolstikov68 above 100 keV. A revision of this component is recommended together with the check for the validity of Tolstikov68 data.
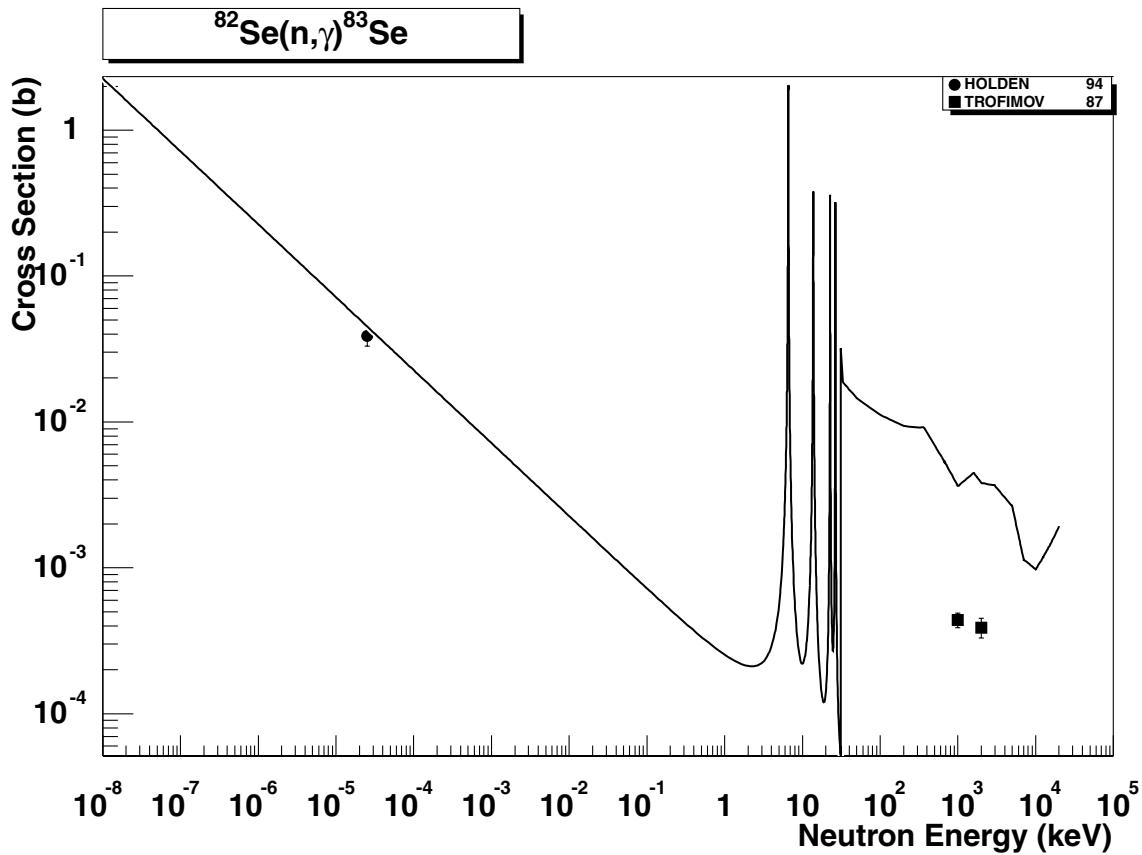
2.114. ^{82}Se (n,γ) ^{83}Se

final states: g.s., meta
source: EAF-4.1 (JEF-2.2)

Data originate from the upgraded ENDF/B-V evaluation. Branching ratio between the g.s. and meta state is based on experimental data (thermal cross-sections [26]) applied up to the end of the resolved resonance region, and on the energy dependent branching ratio systematics [2] for the high energy region. The total and partial thermal cross-sections [26] are well reproduced (C/E=1.2). Also, the averaged cross-section at 30 keV [27] supports the evaluation. The smooth statistical part overestimates two experimental data points of Trofimov87 at 1 and 2 MeV, which, however, seem to be too small. A revision of this component is recommended together with the check of the experimental information.

^{80}Kr(n,γ)^{81}Kr
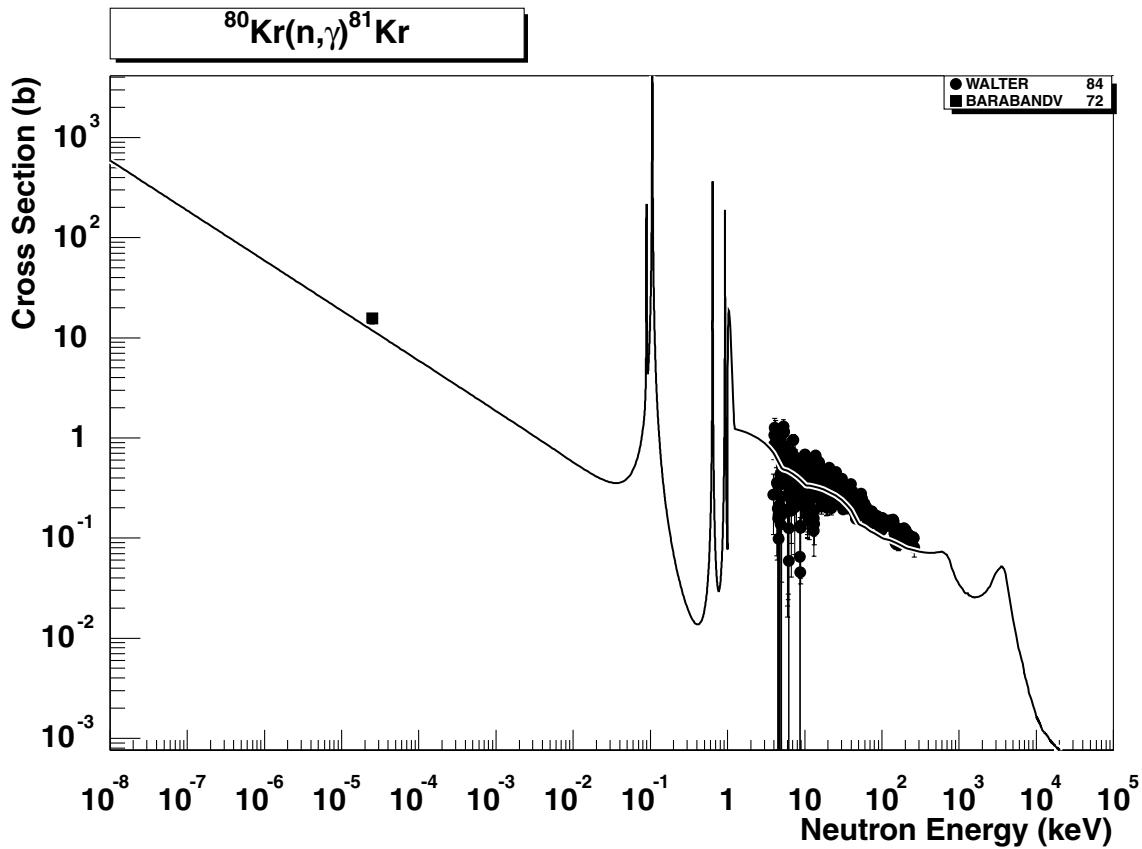
2.115. ^{80}Kr (n,γ) ^{81}Kr

final states: g.s., meta
source: EAF-4.1 (JEF-2.2)

Data originate from the upgraded ENDF/B-V evaluation. Branching ratio between the g.s. and meta state is based on experimental data (thermal cross-sections [26]) applied up to the end of the resolved resonance region, and on the energy dependent branching ratio systematics [2] for the high energy region. The total thermal cross-sections of Barabanov72 is slightly underestimated, the partial cross-sections (g.s. and meta state) are reproduced with C/E=0.94. The smooth statistical part runs reasonably through the experimental data between 4 and 300 keV.
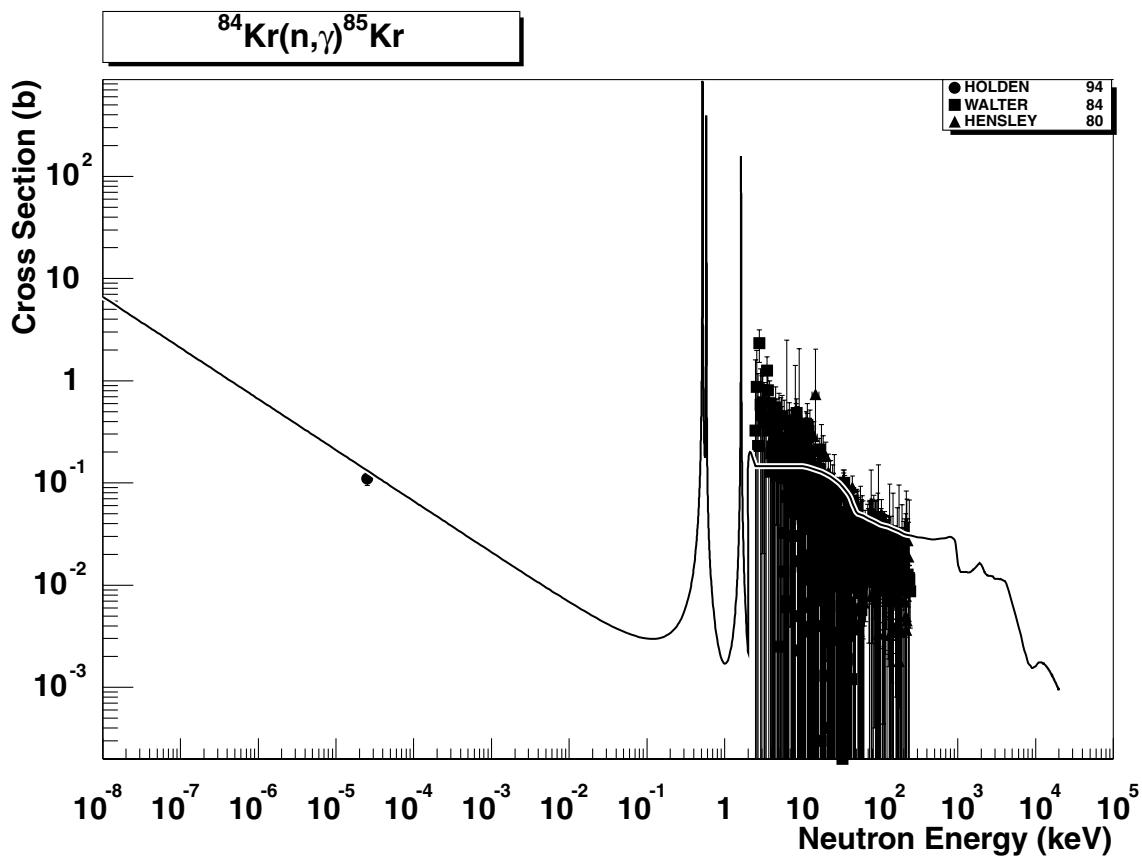
2.116. ^{84}**Kr (n,γ)** ^{85}**Kr**

final states: g.s., meta
source: EAF-4.1 (JEF-2.2)

Data originate from the upgraded ENDF/B-V evaluation. Branching ratio between the g.s. and meta state is based on experimental data (thermal cross-sections [26]) applied up to the end of the resolved resonance region, and on the energy dependent branching ratio systematics [2] for the high energy region. The total and partial thermal cross-sections [26] are well reproduced (C/E=1.0). The smooth statistical part runs within the scattered data between 2 and 200 keV, however, the shape of the excitation curve could be improved.
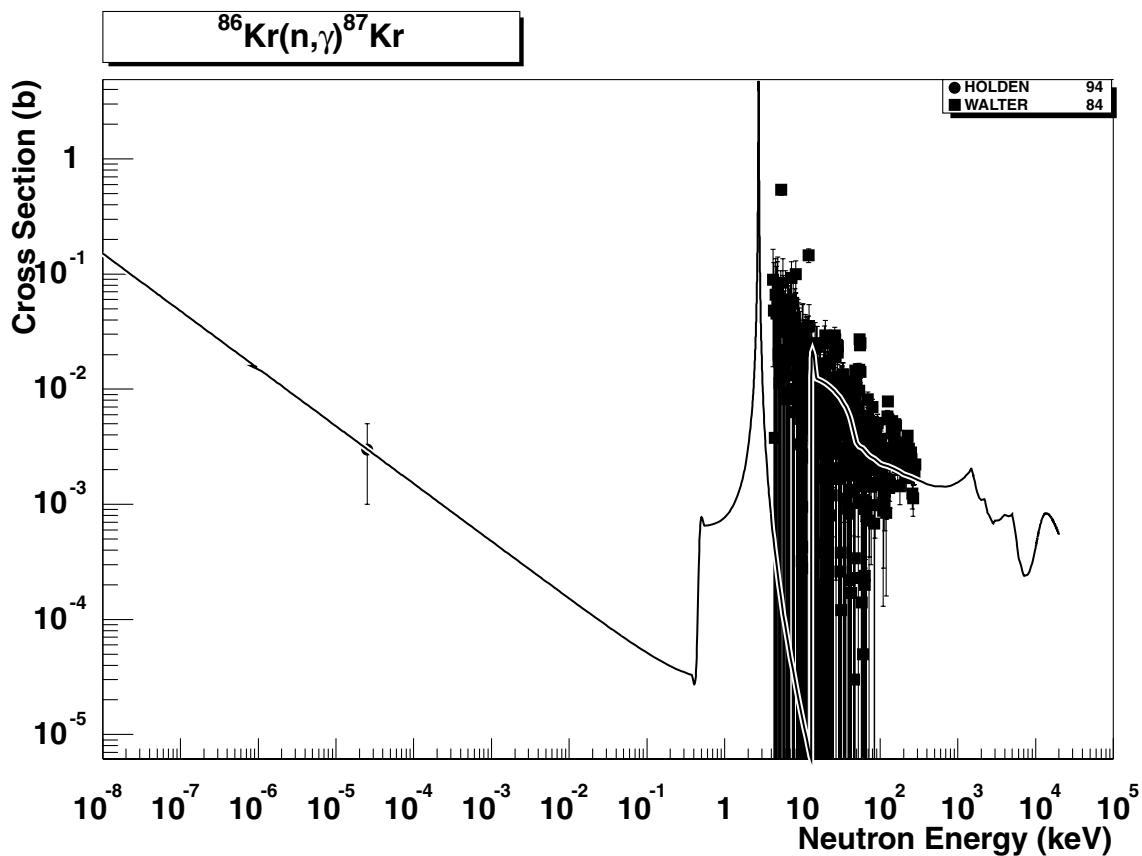
2.117. ^{86}Kr (n,γ) ^{87}Kr

final state: total
source: EAF-4.1 (JEF-2.2)

Data originate from the upgraded ENDF/B-V evaluation. The 1/v component has been adjusted to the thermal cross-section of 3 ± 2 mb [26], which resulted in a non-physical shape of the excitation curve between 0.1 and 1 keV (just below the only included resonance). The better treatment would call for a new adjustment of the 'averaged' resonance parameters or an introduction of a destructively interfering negative resonance. The statistical component reproduces reasonably the data of Walter84 up to 300 keV.
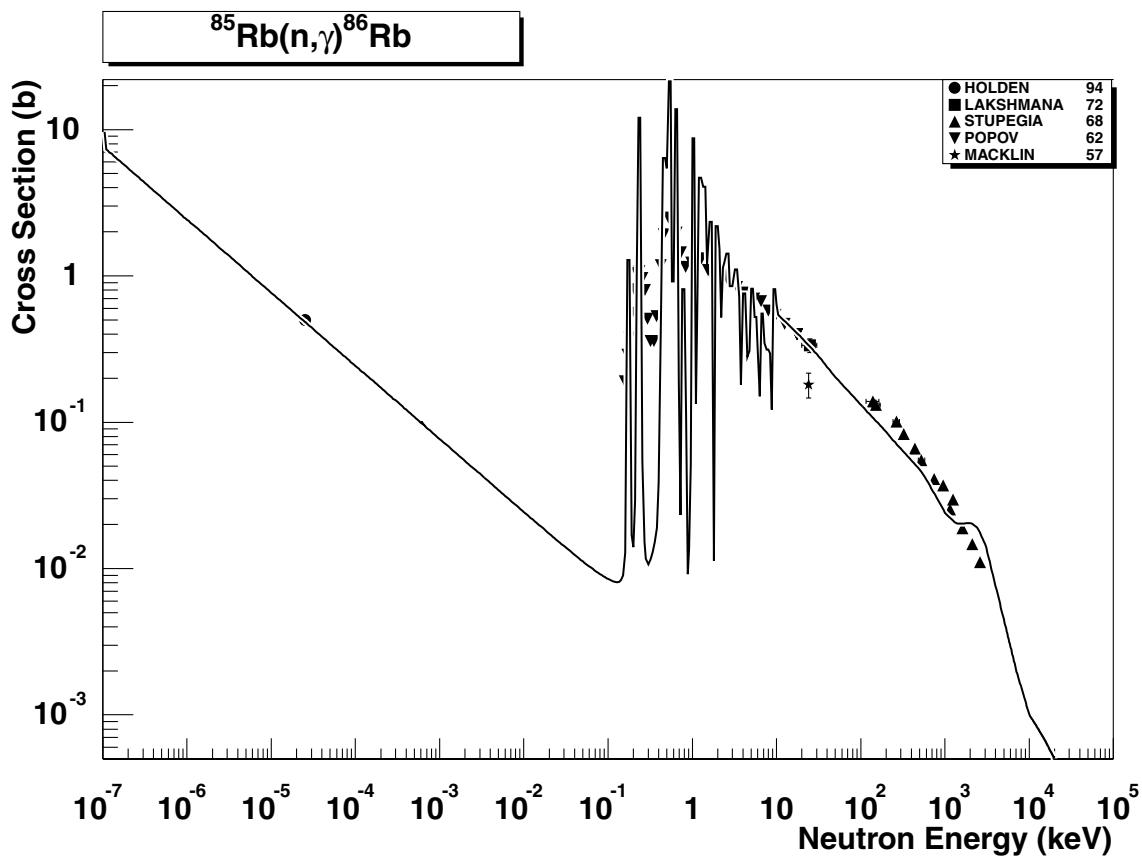
2.118. ^{85}Rb (n,γ) ^{86}Rb

final states: g.s., meta
source: EAF-4.1 (JEF-2.2)

Data originate from the upgraded ENDF/B-V evaluation. Branching between the g.s. and meta state is based on experimental data (thermal cross-sections [26]) applied up to the end of the resolved resonance region, and on the energy dependent branching ratio systematics [2] for the high energy region. The total and partial thermal cross-sections [26] are well reproduced (C/E=0.99). The smooth statistical part agrees very well with the data up to 2 MeV.
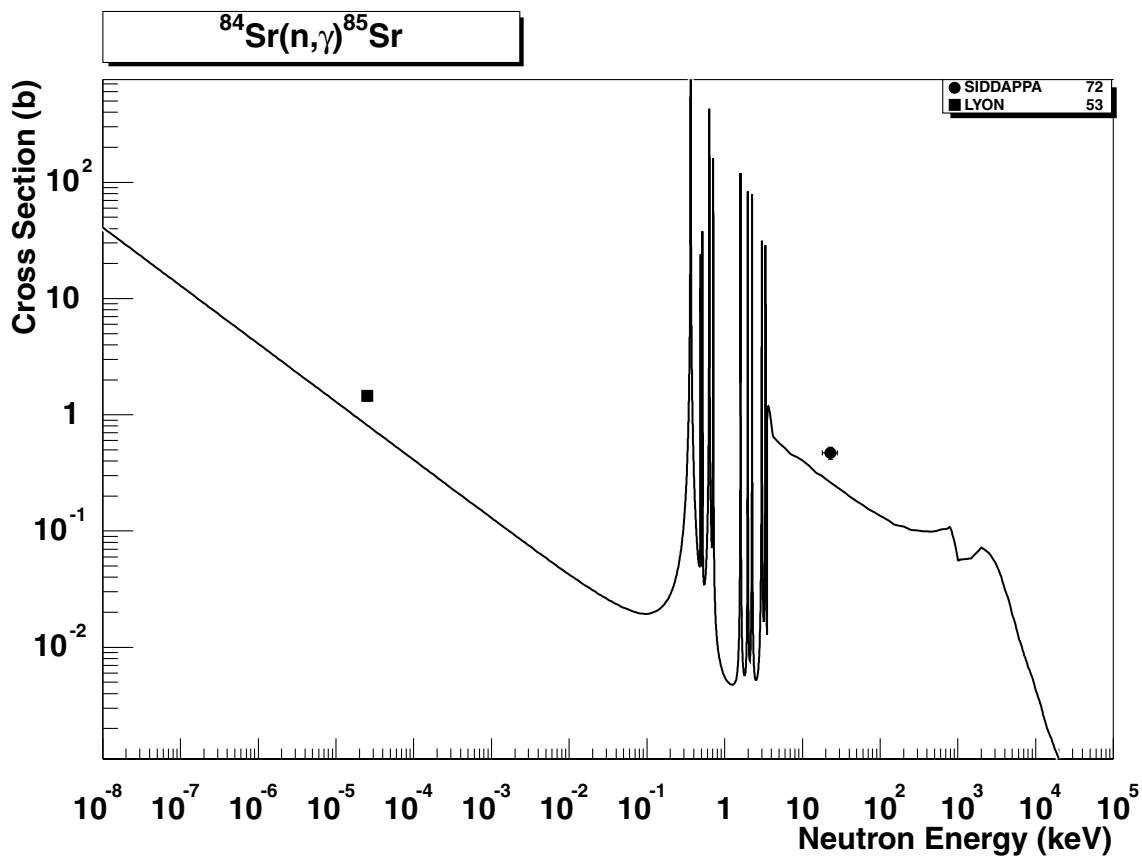
2.119. ^{84}Sr (n,γ) ^{85}Sr

final states: g.s., meta
source: EAF-4.1

Data originate from the upgraded ENDF/B-V evaluation. Branching ratio between the g.s. and meta state is based on experimental data (thermal cross-sections [26]) applied up to the end of the resolved resonance region, and on the energy dependent branching ratio systematics [2] for the high energy region. The total and partial thermal cross-sections [26] are reproduced with C/E=0.86, similar as the old measurement of Lyon53. The statistical component slightly underestimates the single experimental point of Siddapa72 at about 30 keV.